



O'Rourke, Kerry M. (2018) The synthesis of novel PET and SPECT imaging agents and the development of new radioiododeboronation procedures. PhD thesis.

<https://theses.gla.ac.uk/39012/>

Copyright and moral rights for this work are retained by the author

A copy can be downloaded for personal non-commercial research or study, without prior permission or charge

This work cannot be reproduced or quoted extensively from without first obtaining permission in writing from the author

The content must not be changed in any way or sold commercially in any format or medium without the formal permission of the author

When referring to this work, full bibliographic details including the author, title, awarding institution and date of the thesis must be given

Enlighten: Theses

<https://theses.gla.ac.uk/>
research-enlighten@glasgow.ac.uk

The Synthesis of Novel PET and SPECT Imaging Agents and the Development of New Radioiododeboronation Procedures

Kerry M O'Rourke, MChem

A thesis submitted in part fulfilment of the requirements
of the degree of Doctor of Philosophy



University of Glasgow | School of
Chemistry

School of Chemistry

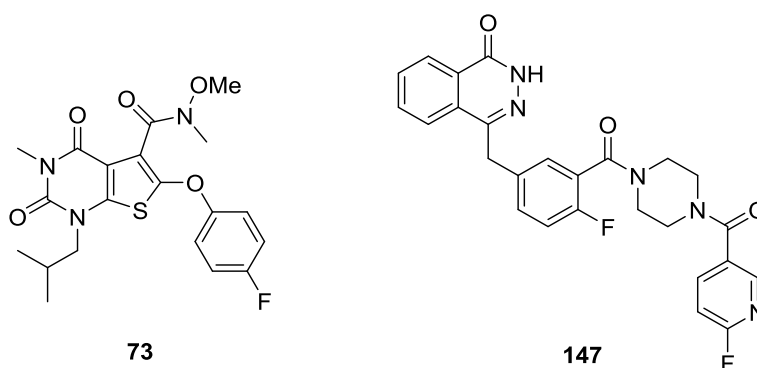
College of Science and Engineering

University of Glasgow

September 2018

Abstract

During the course of this PhD, a number of potential PET and SPECT imaging agents were synthesised for particular *in vivo* targets. The first targets were monocarboxylate transporters 1 and 2 (MCT 1 and 2) which are responsible for the transport of monocarboxylates such as lactate and pyruvate across plasma membranes. The generation of imaging agents which bind to these MCTs could lead to the effective molecular imaging of epileptogenic regions of the brain. A potent and selective inhibitor of MCT 1 and 2 was previously synthesised by AstraZeneca (AR-C155858). In this project, a library of analogues of this compound was synthesised, containing potential sites for radiolabelling. A group of these compounds underwent preliminary biological evaluation to determine the inhibitory effect on lactate uptake against MCT 1, 2 and 4 (the most active being thienopyrimidine **73**). The second target was poly(ADP-ribose) polymerase-1 (PARP-1), an enzyme used in the repair of DNA. Targeting PARP-1 with radiotracers could aid the diagnosis and monitoring of various tumours. A small library of potential PET imaging agents, which have the potential to undergo facile radiofluorination, were synthesised based on the PARP-1 inhibitor olaparib. This series of compounds were subject to a PARP-1 immunofluorescence assay and the most potent compound in the series was found to be phthalazinone **147**.



The second part of this thesis describes the development of novel radioiododeboronation methods using both gold(I) and potassium acetate catalysis. These methods were used in the radiosynthesis of a number of aromatic iodides, giving the radiolabelled products in high radiochemical yields. SPECT imaging agents [¹²⁵I]MIBG and a PARP-1 tracer were also generated under these conditions.

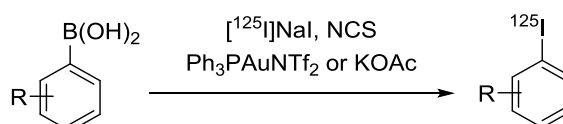


Table of contents

Abstract	2
Acknowledgements	6
Authors declaration	7
Abbreviations	8
1. Introduction to PET and SPECT imaging	13
1.1 Molecular Imaging	13
1.2 PET imaging	13
1.2.1 Radiolabelling techniques for the production of PET imaging agents	15
1.3 SPECT imaging	19
1.3.1 Radiolabelling techniques for the production of SPECT imaging agents	19
1.4 PET and SPECT imaging of neurological disorders	21
2. The synthesis of novel PET and SPECT imaging agents for MCT 1 and 2	23
2.1 Introduction	23
2.1.1 Epilepsy- Current treatments and the need for advanced imaging techniques	23
2.1.2 Monocarboxylate transporters 1 and 2 and their role in epilepsy	26
2.1.3 MCT 1 and 2 inhibitors	27
2.1.4 Proposed research	30
2.2 Results and discussion	31
2.2.1 Synthesis and optimisation of the thienopyrimidinedione core	31
2.2.2 Synthesis of potential imaging agents	35
2.2.2.1 Synthesis of benzyl amide derivatives	35
2.2.2.2 Synthesis of halogenated phenoxy derivatives	38
2.2.2.3 Synthesis of phenyl derivatives	41
2.2.3 Synthesis of a known inhibitor of MCT 1	46

2.2.4 Assessment of physiochemical properties	47
2.2.5 Biological evaluation	52
2.2.6 Second generation compounds	54
2.3 Conclusions and future work	57
3. The synthesis of novel PET imaging agents based on PARP-1 inhibitors	58
3.1 Introduction	58
3.1.1 PARP-1 and its function in DNA repair	58
3.1.2 PARP-1 inhibitors in cancer treatment	59
3.1.3 Imaging agents targeting PARP-1	60
3.1.4 Previous work and proposed research	62
3.2 Results and discussion	66
3.2.1 Synthesis of the olaparib core structure	66
3.2.2 Synthesis of potential PARP-1 imaging agents	69
3.2.3 Physiochemical testing and biological evaluation of potential PARP-1 imaging agents	70
3.2.4 Synthesis of a novel olaparib based scaffold	72
3.3 Conclusions and future work	74
4. Gold catalysed radioiododeboronation	77
4.1 Introduction	77
4.1.1 Modern radioiodination methods	77
4.1.2 Previous work and proposed research	78
4.2 Results and discussion	79
4.2.1 The development of a gold-catalysed radioiododeboronation procedure and the synthesis of radiolabelled aryl iodides	79
4.2.2 Synthesis of SPECT imaging agents	82
4.3 Conclusions and future work	86

5. Base catalysed radioiododeboronation for the development of SPECT tracers	87
5.1 Introduction	87
5.1.1 Transition metal-free halodeboronations	87
5.1.2 Previous work and proposed research	88
5.2 Results and discussion	89
5.2.1 Development of a radioiododeboronation procedure	89
5.2.2 Radiosynthesis of labelled aryl iodides	90
5.2.3 Synthesis of SPECT imaging agents	91
5.3 Conclusions and future work	93
6. Experimental	94
6.1 General Experimental	94
6.2 MCT 1 and 2 experimental	94
6.3 HPLC methods for physicochemical analysis	136
6.4 PARP-1 experimental	139
6.5 Radioiododeboronation experiemental	153
7. References	171
8. Appendix	179
8.1 Radio-HPLC and UV/Vis HPLC chromatograms	179

Acknowledgments

I would like to dedicate this thesis to my beautiful gran/best friend Marjory McCorrie. I miss you millions and I hope this would make you proud.

Thank you to my supervisor Dr Andrew Sutherland for allowing me to undertake a PhD within his group and for all his support over the past four years.

Thanks also to my second supervisor Sally Pimlott for all of her guidance on radiochemistry and help with physiochemical testing.

A massive cheers to the technical staff for all their assistance over the past 4 years- David Adam (NMR), Jim Tweedie (Mass Spec), Stuart Mackay and Arlene Sloan (IT) and Ted (Stores).

Thank you to Dr Holger Becker and Maria Clara Liuzzi for performing the biological testing of my compounds.

To everyone in the Loudon lab, past and present- I have never really felt like I fit in anywhere until I met you bunch of weirdos! Getting to spend my days with you guys has honestly made this PhD the best experience of my life.

To my amazing family- Firstly, congratulations for putting up with me for the past 26 years. I cannot thank you enough for everything you have done for me. Particular thanks to my brother Scott O'Rourke (the empty potato bucket) for being my life long partner in crime and the Ross to my Monica. Love you bro!

To Stephanie Hamill, Aidan Reid and Chris Greig- Whether I've needed a cuddle, a tough love speech or just someone to hand me a glass of wine, knowing you guys are always there has truly meant the world to me.

EPSRC and SHIL are also gratefully acknowledged for their funding of this PhD.

Author's Declaration

I declare that, except where explicit reference is made to the contribution of others, this thesis represents the original work of Kerry M. O'Rourke and has not been submitted for any other degree at the University of Glasgow or any other institution. The research was carried out at the University of Glasgow in the Loudon Laboratory under the supervision of Dr Andrew Sutherland between October 2014 to March 2018. Aspects of the work described herein have been published elsewhere as listed below.

S. Webster, K. M. O'Rourke, C. Fletcher, S. L. Pimlott, A. Sutherland and A.-L. Lee, *Chem. Eur. J.*, 2018, **24**, 937.

K. M. O'Rourke, E. S. Johnstone, S. L. Pimlott and A. Sutherland, *Tetrahedron*, 2018, **74**, 4086.

Abbreviations

ADP	Adenosine diphosphate
AED	Anti-epileptic drug
AGP	α_1 -Acid glycoprotein
AIBN	Azobisisobutyronitrile
AMPA	α -Amino-3-hydroxy-5-methyl-4-isoxazolepropionic acid
Ar	Aromatic
ATL	Anterior temporal lobectomy
ATP	Adenosine Triphosphate
BBB	Blood brain barrier
BER	Base excision repair
Boc	<i>tert</i> -Butyloxycarbonyl
br	Broad
BRCA	Breast cancer susceptibility protein
CHCA	α -Cyano-4-hydroxycinnamate
CHI	Chromatographic hydrophobicity index
CI	Chemical ionisation
CNS	Central nervous system
cod	1,5-cyclooctadiene
COSY	Correlation spectroscopy
CT	Computed tomography
d	Doublet
dba	Dibenzylideneacetone
DEPT	Distortionless enhancement by polarisation transfer
DIPEA	<i>N,N'</i> -Diisopropylethylamine

DMAP	4-(Dimethylamino)pyridine
DMC	Dimethyl carbonate
DMF	<i>N,N'</i> -Dimethylformamide
DMSO	Dimethylsulfoxide
DNA	Deoxyribonucleic acid
DSB	Double strand DNA breaks
EDCI	Ethyl 3-(3-dimethylaminopropyl)carbodiimide hydrochloride
EEG	Electroencephalography
EI	Electron impact
equiv.	Equivalent
ESI	Electrospray ionisation
Et	Ethyl
ETLE	Extratemporal lobe epilepsy
g	Grams
GABA	Gamma aminobutyric acid
GBM	Glioblastoma
GBq	Gigabecquerel
h	Hour
HBC	Hydrogen bond count
HBTU	<i>O</i> -(benzotriazol-1-yl)- <i>N,N,N',N'</i> -tetramethyluronium hexafluorophosphate
HPLC	High performance liquid chromatography
HR	Homologous recombination
HSA	Human serum albumin
HSQC	Heteronuclear single quantum coherence
HWE	Horner-Wadsworth-Emmons

Hz	Hertz
IAM	Immobilised artificial membrane
IC ₅₀	Half maximal inhibitory concentration
K ₂₂₂	Kryptofix® 222
K _m	Membrane partition coefficient
lit.	Literature
Log <i>D</i>	Distribution coefficient
Log <i>P</i>	Partition coefficient
M	Molar
m	Multiplet
<i>m</i> -	<i>meta</i>
MBq	Megabecquerel
MCT	Monocarboxylate transporter
Me	Methyl
MeCN	Acetonitrile
MIE	Medically intractable epilepsy
min	Minutes
mL	Millilitres
mmol	Millimoles
mol	Moles
Mp	Melting point
MRI	Magnetic resonance imaging
MW	Molecular weight
NAD	Nicotinamide adenine dinucleotide
NBS	<i>N</i> -bromosuccinimide

NCS	<i>N</i> -chlorosuccinimide
NIS	<i>N</i> -iodosuccinimide
NMP	<i>N</i> -methyl-2-pyrrolidone
NMR	Nuclear magnetic resonance
<i>o</i> -	<i>Ortho</i>
<i>p</i> -	<i>Para</i>
PAR	Poly(ADP-ribose)
PARG	Poly(ADP-ribose) glycohydrolase
PARP	Poly(ADP-ribose) polymerase
PET	Positron emission tomography
Ph	Phenyl
PhMe	Toluene
Pin	Pinacol
P_m	Permeability
PPA	Polyphosphoric acid
PPB	Plasma protein binding
q	Quartet
RCY	Radiochemical yield
rt	Room temperature
s	Singlet
SAH	Selective amygdalohippocampectomies
S_NAr	Nucleophilic aromatic substitution
SPECT	Single photon emission computed tomography
SSB	Single strand DNA breaks
t	Triplet

TBAB	Tetrabutylammonium bromide
TCICA	Trichloroisocyanuric acid
Tf	Triflate
THF	Tetrahydrofuran
TLC	Thin layer chromatography
TLE	Temporal lobe epilepsy
TM	Transmembrane helice
UV	Ultraviolet
μM	Micromolar
μmol	Micromole
μW	Microwave
$^{\circ}\text{C}$	Degrees centigrade

1. Introduction to PET and SPECT imaging

1.1. Molecular imaging

Molecular imaging is a non-invasive technique used to detect the interactions of a specific cellular target *in vivo* using an injected molecular imaging agent.¹ This can provide visualisation of biological processes at the molecular and cellular level and can be used for the diagnosis and characterisation of disease. Molecular imaging can also be used to ascertain a drug's mechanism of action and therefore guide treatment and dosage decisions. The molecular imaging agents (often referred to as molecular probes or tracers) must bind to the biological targets with high affinity and specificity in order to obtain good visualisation. The nuclear imaging techniques, positron emission tomography (PET) and single photon emission computed tomography (SPECT) are the most sensitive techniques and can be used to provide a detailed picture of the *in vivo* target. However, the spatial resolution of these techniques is relatively low and as such, they are often used in conjunction with techniques like computed tomography (CT) or magnetic resonance imaging (MRI), which provide images of a higher resolution (**Figure 1**).²

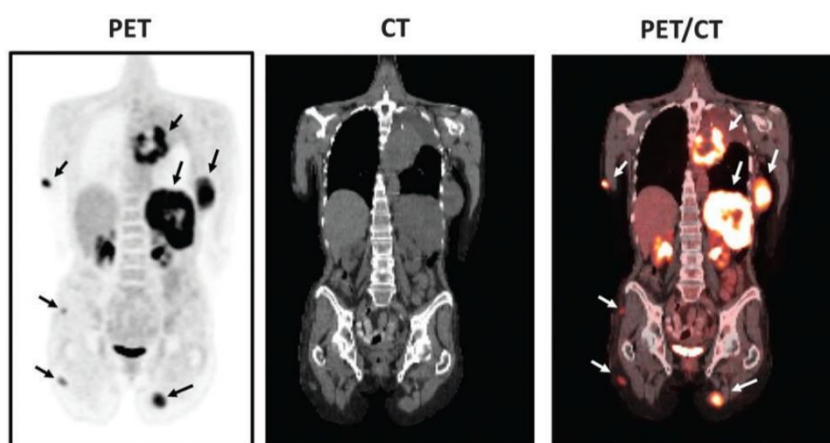


Figure 1: PET-CT images of a cancer using [¹⁸F]fluorodeoxyglucose (FDG). The cancerous tissue (indicated by the arrows) can be clearly seen in the combined image. (From *Science*, 2013, **342**, 429. Reprinted with permission from AAAS).²

1.2. PET imaging

The information gained from a PET scan relies on imaging agents labelled with radionuclides which decay by the emission of a positron.³ The emitted positron annihilates on collision with a neighbouring electron, producing two 511 keV γ -rays which are emitted simultaneously in opposite directions (180° from each other). These γ -rays are detected by

surrounding γ -detectors (**Figure 2**). After emission from the nucleus, the positron travels a certain distance into the tissue before annihilation (this distance is referred to as the positron range). The distance travelled is important because a greater positron range leads to decreased spatial resolution. After several emissions, the information recorded about positron annihilation can be reconstructed into an image, which shows the spatial distribution of radioactivity as a function of time.^{4,5}

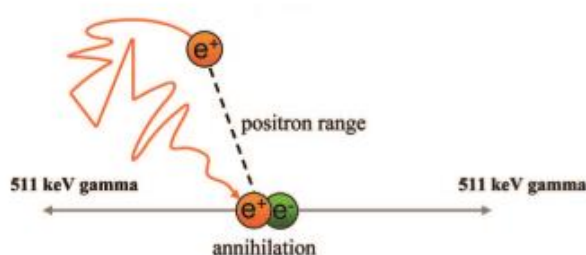


Figure 2: Positron emission from a nucleus and subsequent γ -ray emission to generate a molecular image. (Reprinted with permission from *Chem. Rev.*, 2008, **108**, 1501. Copyright 2008 American Chemical Society).⁵

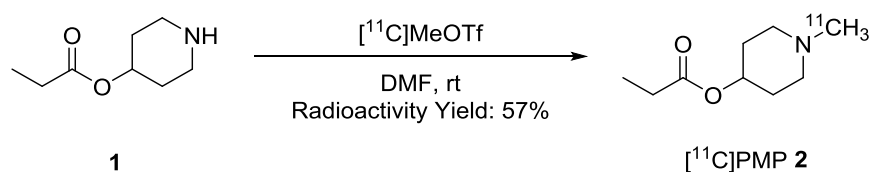
There are several different radionuclides which can be employed for PET imaging (**Table 1**). These isotopes have short half-lives, therefore, the synthesis and purification of molecular imaging agents for PET must be fast and normally an on-site cyclotron is required for isotope production. The most commonly used radioisotopes for small molecule imaging are carbon-11 and fluorine-18. The advantage of using carbon-11 labelling is that this can be used to replace a carbon-12 atom in an organic compound. This should exhibit the same physiochemical properties, other than a negligible isotope effect.⁶ However, fluorine-18 is a more useful nuclide for PET imaging due to its low positron energy and long half-life (when compared to other PET radionuclides).⁷ The low positron energy can lead to images with a higher resolution and the longer half-life allows for a more complex radiosynthesis and longer *in vivo* studies. Fluorine-18 is normally employed as a biosteric replacement for hydrogen and due to their similar size, this only causes a small change in the overall steric hindrance of the compound. The higher electronegativity of fluorine however, does result in a change of electronic and biochemical properties along with a general decrease in lipophilicity. In some cases, it has been reported that replacement of hydrogen with fluorine can have a beneficial effect on the potency of a molecular probe.⁵

Table 1: Radionuclides used for PET imaging.

Radionuclide	Half-life (mins)	Maximum energy (MeV)
^{11}C	20	0.97
^{13}N	10	1.20
^{18}F	110	0.64
^{68}Ga	68	1.92

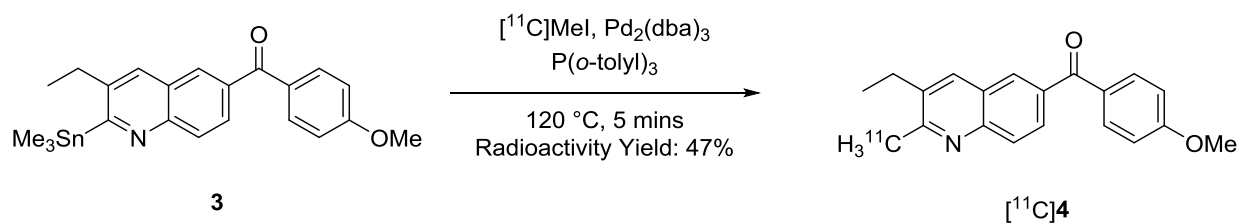
1.2.1. Radiolabelling techniques for the production of PET imaging agents

Carbon-11 can be generated in a cyclotron by the bombardment of nitrogen-14 with protons.⁸ Trace amounts of either oxygen or hydrogen are then added to produce either $[^{11}\text{C}]\text{CO}_2$ or $[^{11}\text{C}]\text{CH}_4$. These compounds are then usually converted into a more reactive species, the most common being $[^{11}\text{C}]\text{methyl iodide}$ or $[^{11}\text{C}]\text{methyl triflate}$. The radiolabel can then be incorporated into an imaging agent by direct methylation of nitrogen, oxygen or thiol groups. For example, $[^{11}\text{C}]\text{N-methylpiperidin-4-yl propionate}$ ($[^{11}\text{C}]\text{PMP}$), which is used to map the activity of acetylcholinesterase in Alzheimer's patients, was synthesised *via* the *N*-methylation of 4-piperidiny propionate with $[^{11}\text{C}]\text{methyl triflate}$ (**Scheme 1**).⁹ This gave $[^{11}\text{C}]\text{PMP}$ in a 57% radioactivity yield (the isolated yield after purification) with a total reaction time of 35 minutes, including purification.



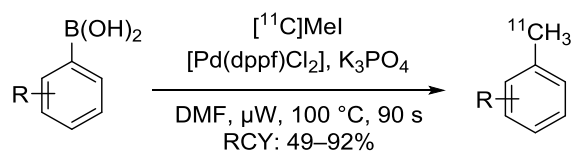
Scheme 1: Synthesis of $[^{11}\text{C}]\text{PMP 2}$ by *N*-methylation with carbon-11 labelled methyl triflate.⁹

In the past decade, palladium mediated methylation has found wider applications in the synthesis of PET imaging agents. PET tracer $[^{11}\text{C}]\text{4}$, used in the imaging of the metabotropic glutamate 1 receptor, was synthesised using a Stille cross-coupling reaction (**Scheme 2**).¹⁰ The highest radioactivity yield for this reaction was obtained when bulky ligand $\text{P}(o\text{-tolyl})_3$ was used. This is due to the large cone angle of the ligand, which relieves steric strain during the transmetallation step.¹¹ Radiolabelling of stanane **3** to give PET tracer $[^{11}\text{C}]\text{4}$ occurred in a 47% radioactivity yield.



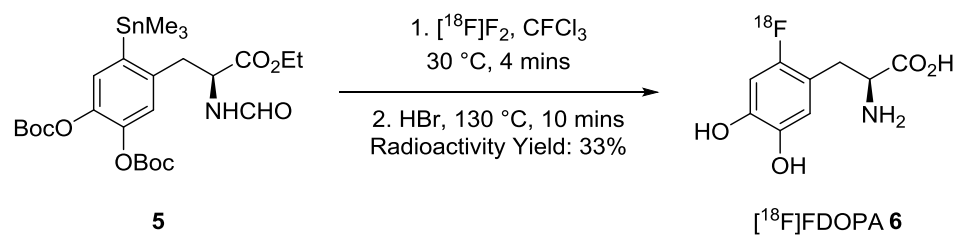
Scheme 2: Synthesis of PET tracer [^{11}C]4 *via* a Stille cross-coupling reaction.¹⁰

Despite these reactions being effective, the use of stannanes is not ideal due to their toxicity, which can be problematic for use *in vivo*. Therefore, an attractive option for palladium-catalysed methylation using carbon-11 is *via* a Suzuki cross coupling reaction. For example, in 2005, Hostetler and co-workers demonstrated that boronic acids could be coupled with [^{11}C]methyl iodide to give a range of radiolabelled products in high radiochemical yields (**Scheme 3**).¹² Under microwave heating, these couplings also have the added advantage of very short reaction times.



Scheme 3: The use of a Suzuki cross-coupling reaction to access carbon-11 labelled aromatic compounds.

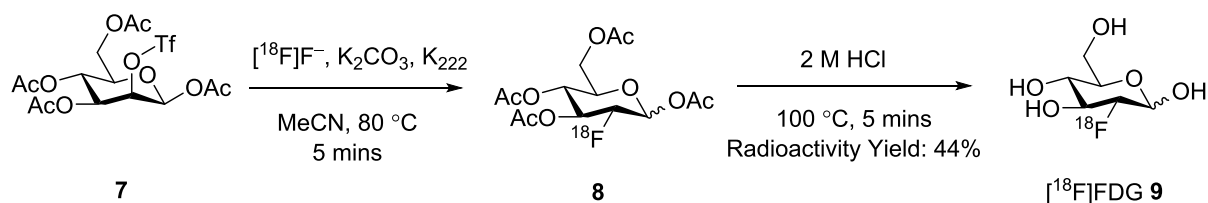
There are several methods available for the incorporation of ^{18}F into a compound, either by electrophilic or nucleophilic radiofluorinations. For electrophilic fluorinations, labelled elemental fluorine ($^{18}\text{F}_2$) is produced in a cyclotron using enriched $^{18}\text{O}_2$ gas.⁷ Due to the high reactivity of elemental fluorine, it is then commonly converted to [^{18}F]acetyl hypofluorite which is a less reactive and more selective reagent. These materials can then participate in direct electrophilic substitution or demetalation reactions to generate the desired fluorine-18 labelled compound.¹³ For example, the synthesis of [^{18}F]FDOPA **6**, which is commonly used to study movement disorders like Parkinson's disease, was achieved by a destannylation reaction using [^{18}F]F₂ as the fluorinating agent (**Scheme 4**).¹⁴ After acidic removal of the protecting groups and HPLC purification, a radioactivity yield of 33% was achieved with a total synthesis time of 40 minutes.



Scheme 4: Synthesis of [^{18}F]FDOPA **6** via a destannylation reaction.

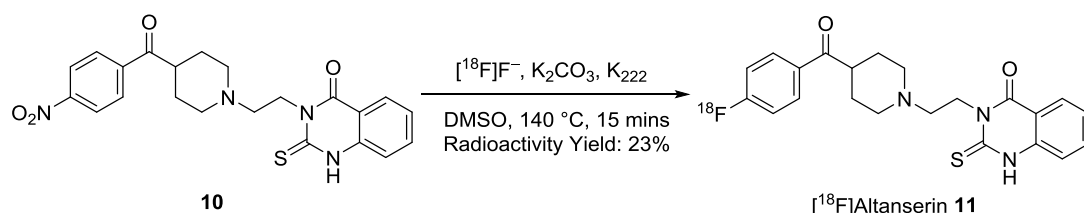
The disadvantage to electrophilic methods of radiofluorination is that only one of the atoms in the [^{18}F]F $_2$ source carries an ^{18}F and therefore the maximum theoretical yield for electrophilic substitution is 50%. Therefore, nucleophilic fluorinations are more commonly used.

Nucleophilic methods employ [^{18}F]fluoride as the fluorinating agent, which can be prepared by irradiation of ^{18}O enriched water.⁷ The nucleophilicity of the fluoride ion normally needs to be increased in order to participate in nucleophilic substitution reactions. The fluoride ion can be activated with cryptands and alkali salts. When activated, the [^{18}F]fluoride can be used in an S $_N2$ reaction. For example, [^{18}F]FDG **9**, which is the most commonly used tracer for imaging cancer, can be obtained through a nucleophilic substitution (**Scheme 5**).¹⁵



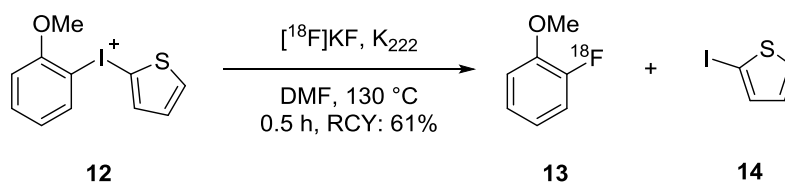
Scheme 5: Synthesis of [^{18}F]FDG **9** by nucleophilic substitution.

Another common method for radiofluorination is through a nucleophilic aromatic substitution reaction (S $_N\text{Ar}$). This requires the aromatic ring to be activated towards S $_N\text{Ar}$, which can be achieved by the inclusion of an electron withdrawing substituent in the *ortho*- or *para*-position, with respect to the leaving group.¹³ [^{18}F]Altanserin **11**, which is used to study 5-HT $_2\text{A}$ neuroreceptors, was synthesised *via* S $_N\text{Ar}$ and was obtained in a 23% radioactivity yield (**Scheme 6**).¹⁶



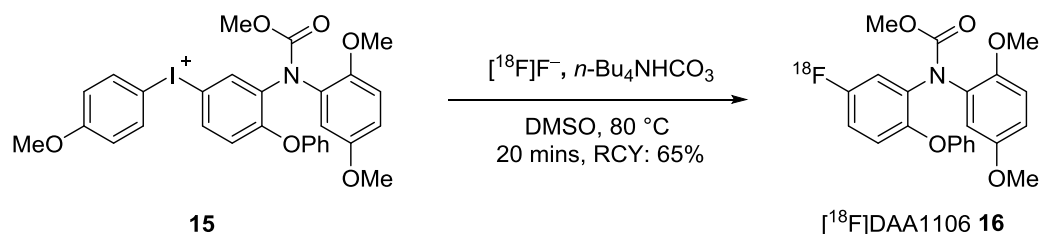
Scheme 6: The synthesis of [^{18}F]altanserin **11** via nucleophilic aromatic substitution.¹⁶

One way to radiofluorinate aromatic rings which are not activated towards nucleophilic substitution is *via* the reaction of diaryliodonium salts with the fluoride ion (**Scheme 7**).^{1,17} This reaction can occur in the presence of electron-donating and electron-withdrawing substituents. The regioselectivity of the fluorination can be controlled electronically and sterically (*via* the *ortho*-effect). Without the presence of an *ortho*-substituent, the fluorination occurs preferentially on the most electron-deficient ring. However, electron-rich rings can be fluorinated in this manner by incorporating a substituent *ortho*- to the labelling site, which will direct attack of the fluorine ion onto that ring.



Scheme 7: Radiofluorination using diaryliodonium salts.

This method has been used in the synthesis of [^{18}F]DAA1106 **16**, a PET tracer used for the imaging of peripheral-type benzodiazepine receptors in the brain (**Scheme 8**).¹⁸ Reaction of diphenyliodonium salt **15** with radiolabelled fluoride and tetrabutylammonium bicarbonate gave the desired PET tracer **16** in a 61% radiochemical yield, with the fluorination occurring preferentially on the more electron-deficient ring.



Scheme 8: Synthesis of [^{18}F]DAA1106 **16** using radiolabelled fluoride and diphenyliodonium salt **15**.¹⁸

1.3. SPECT imaging

SPECT operates in a similar fashion to PET however, the radionuclides used are of lower energy and emit γ -rays directly. A collimator is placed in front of a gamma-camera to detect the γ -rays and evaluate their angle of incidence.¹ This technique is less sensitive and provides a less resolved image than PET, however radiolabelling of SPECT imaging agents is far more practical. Due to the longer half-lives of the commonly used radionuclides, a longer radiosynthesis is possible and unlike the synthesis of many PET tracers, an on-site cyclotron is not required (**Table 2**). The extended half-life of SPECT compounds is also advantageous since the imaging of a target or biological process can take place over a longer period of time.³

Radionuclide technetium-99m is popular for SPECT imaging as it can be formed simply from the decay of its parent nuclide molybdenum-99.¹⁹ However, the production of technetium-99m imaging agents involves chelation to an organic compound, forming a metal complex which can affect its permeability through the blood brain barrier (BBB). This limits the use of technetium-99m in the imaging of neurological processes. Therefore, it is often more practical to use radionuclides such as iodine-123, which can be more easily incorporated into an organic compound.

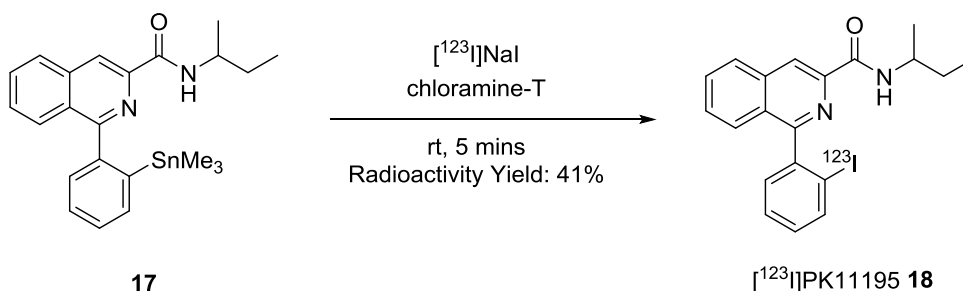
Table 2: Radionuclides used for SPECT imaging.

Radionuclide	Half-life (h)	Photon emission energy (MeV)
^{99m} Tc	6	0.14
¹²³ I	13.2	0.16
¹¹¹ In	67.9	0.17/0.25
⁶⁷ Ga	78.3	0.09/0.19/0.30

1.3.1. Radiolabelling techniques for the production of SPECT imaging agents

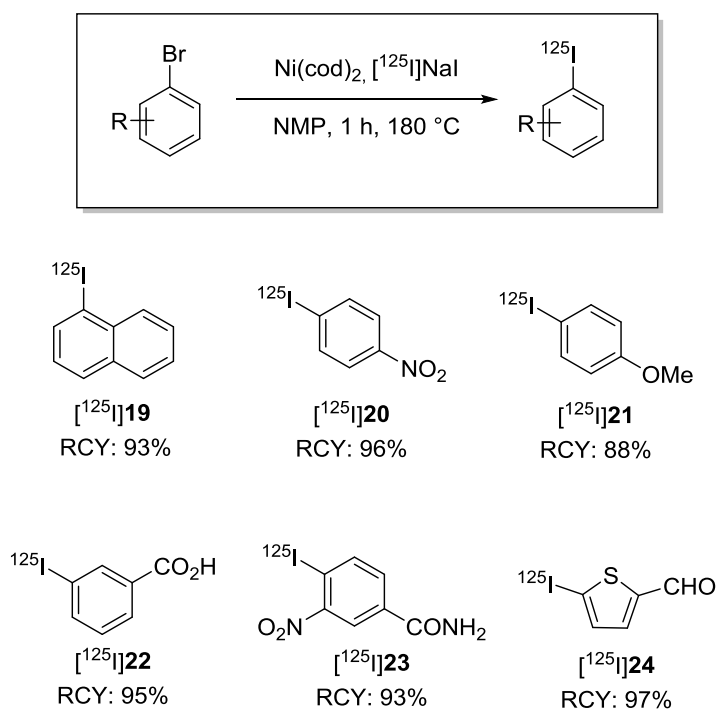
Radioiodine isotopes are usually produced in the form of radiolabelled sodium iodide. This can be oxidised *in situ* to an electrophilic form of iodine using an oxidant such as peracetic acid or chloramine-T, allowing it to facilitate efficient electrophilic reactions. Electrophilic radioiodination can occur directly, however this is limited to aromatic rings that are activated towards electrophilic substitution. Therefore, these reactions occur more commonly *via* a demetalation reaction. In the Sutherland group, a destannylation reaction

was developed and adopted for the synthesis of [^{123}I]PK11195 **18** which can be used to assess neuroinflammation in the brain (**Scheme 9**).²⁰



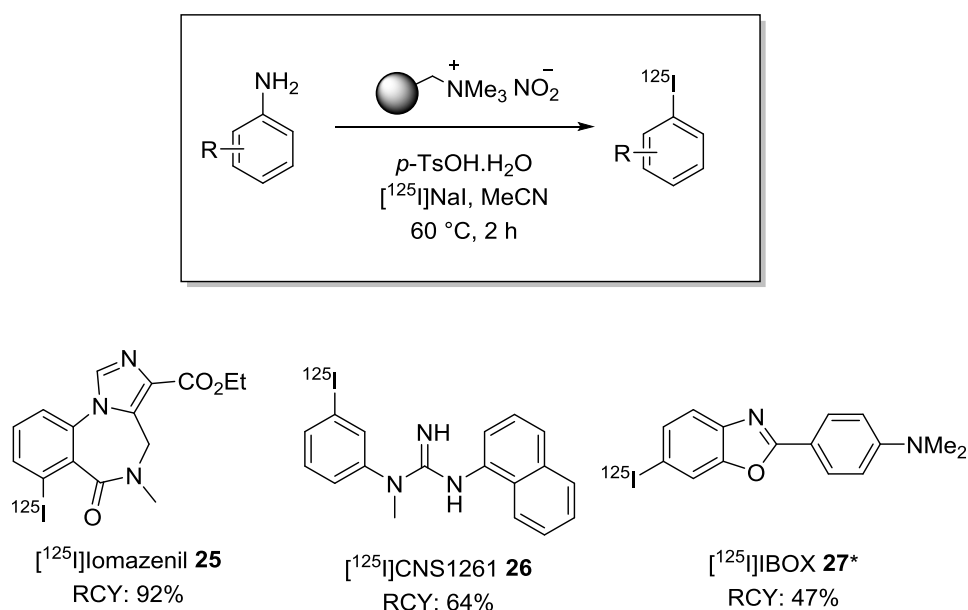
Scheme 9: Synthesis of [^{123}I]PK11195 **18** via iododestannylation.²⁰

Another common method for iodination is using a halogen exchange reaction with aryl bromides or chlorides. In the Sutherland group, a radioiodination halogen exchange method was developed using nickel(0) catalysis. This allowed for the synthesis of iodine-125 labelled aryl rings containing both electron-withdrawing and electron-donating substituents in high radiochemical yields (**Scheme 10**).²¹ The reaction proceeds *via* an oxidative addition of an aryl bromide with a nickel(0) catalyst to give a nickel(II) species. This species then undergoes a halogen exchange reaction with radiolabelled sodium iodide. Finally a reductive elimination occurs to give the desired aryl iodide and regenerate the nickel(0) species.



Scheme 10: Examples of nickel(0)-catalysed halogen exchange for the radioiodination of aryl bromides.²¹

Another approach for the synthesis of aryl iodides is *via* a Sandmeyer type reaction using diazonium salts. The wider applications of this method were initially limited by the inherent instability of various diazonium salts, causing them to be potentially explosive. However, recently it has been shown that thermally stable diazonium salts can be prepared using polymer supported nitrite reagents and mildly acidic conditions.^{22,23} Within the Sutherland group a one-pot tandem diazotisation-radioiodination procedure was developed (**Scheme 11**).²⁴ The reaction occurred *via* diazonium salt formation using a polymer supported nitrite and *p*-toluenesulfonic acid, followed by direct radioiodination using [¹²⁵I]NaI. This method was used to successfully prepare a small library of iodine-125 labelled aromatic rings, containing a variety of functional groups and substitution patterns, in high radiochemical yields. A number of SPECT imaging agents were also prepared in this fashion. For example, [¹²⁵I]iomazenil **25** (a SPECT tracer for central type benzodiazepine receptors),²⁵ [¹²⁵I]CNS1261 **26** (a radioligand of the *N*-methyl-D-aspartate receptor)²⁶ and [¹²⁵I]IBOX **27** (an imaging agent for amyloid plaques)²⁷ were all synthesised using this method.



Scheme 11: Synthesis of SPECT imaging agents using a one-pot diazotisation-radioiodination reaction.²⁴ *Reaction was carried out at 20 °C

1.4. PET and SPECT imaging of neurological disorders

All imaging agents used for the imaging of neurological disorders should follow a number of guidelines in order to be successful. First of all, PET and SPECT imaging agents should

have high affinity and selectivity for the target receptor, with binding affinities in the sub-nanomolar range. However, it has been observed that if the affinities are too high then the uptake of the tracer is no longer dependant on the rate of binding but becomes dependant on the blood flow rate, rendering the imaging agent unsuitable.²⁸ The compounds should also have a relatively high specific activity so that the agents can be injected in small doses. A common source of failure for CNS imaging probes is an inability to permeate the BBB and for this reason the molecular weight of the compound should be low and the number of atoms capable of hydrogen bond formation with water should be kept to a minimum.^{29,30} These imaging agents should also not be a substrate for P-glycoprotein 1 which operates at the BBB and is capable of actively back-transporting hydrophobic drugs out of cells and into the blood. Finally, it is also crucial that these agents are metabolically stable and have low plasma protein binding.

PET and SPECT imaging probes have had a wide applicability in the imaging of neurodegenerative diseases and they have been used to target a variety of receptors. For example, both PET and SPECT imaging agents can target dopamine receptors and are therefore often used in the diagnosis of Parkinson's disease. A common PET imaging agent for the dopamine receptor is [¹⁸F]FDOPA **6**. For SPECT imaging, [¹²³I]FP-CIT **28** is the most widely used tracer for this purpose.^{31,32} Dopamine allows messages to be sent to the parts of the brain which control movement but patients with Parkinson's disease exhibit a loss of dopamine generating neurons. Therefore, by targeting dopamine receptors in the brain the progress of Parkinson's disease can be effectively monitored by PET or SPECT (**Figure 3**).

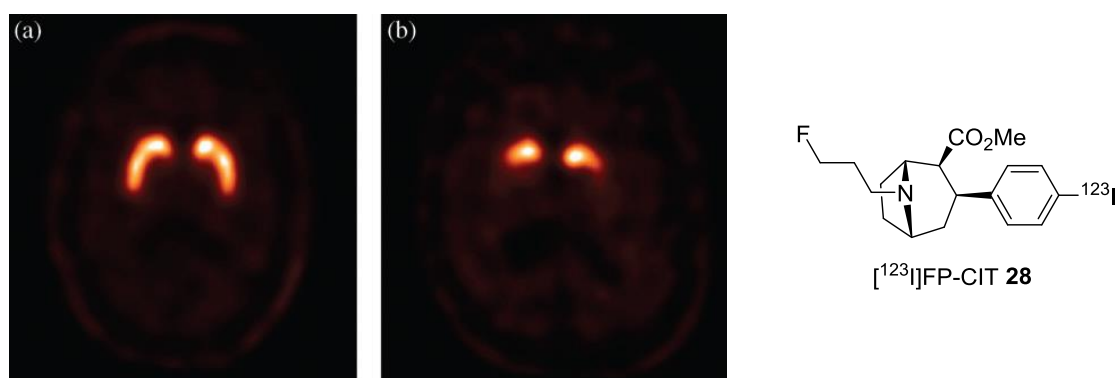


Figure 3: SPECT images using [¹²³I]FP-CIT **28**. (a) Image of a normal brain. (b) Image of a brain with Parkinson's disease, showing a reduction in the binding of **28** to dopamine receptors (*Chem. Soc. Rev.*, 2011, **40**, 149–162. Reproduced by permission of The Royal Society of Chemistry).¹

2. The synthesis of novel PET and SPECT imaging agents for MCT 1 and 2

2.1. Introduction

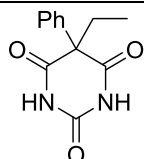
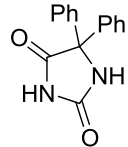
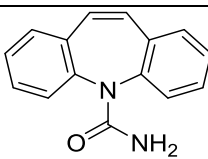
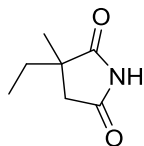
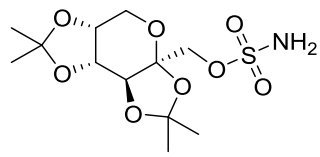
2.1.1. Epilepsy- Current treatments and the need for advanced imaging techniques

Epilepsy is a life shortening brain disorder affecting more than 40 million people worldwide.³³ It is characterised by spontaneous epileptic seizures and is often associated with mental health disorders including anxiety and depression. There are many different types of epileptic seizure and the visible effects can vary between momentary losses of awareness to uncontrollable jerking movements, all of which have a severe impact on the patient's quality of life. These seizures are due to a disturbance in neuronal activity within the cerebral cortex (usually caused by a spontaneous excess of electrical discharges). Epilepsy can be widely defined as generalised epilepsy (otherwise known as idiopathic epilepsy) or focal epilepsy (also referred to as symptomatic epilepsy).³³ In generalised epilepsy, most or all of the brain is affected and the condition is thought to be caused by a genetic mutation. In focal epilepsy, the seizures begin in a localised part of the brain and are normally caused by pathological changes in that region, like a tumour, severe head injury or specific parts of the brain not developing properly.

Treatment of epilepsy is dominated by anti-epileptic drugs (AEDs). Currently, there are no drugs which prevent the progression of the disease before the onset of the first seizure. However, there are a large number of drugs which significantly reduce the amount of seizures experienced by the patient (**Table 3**).³⁴ The overall effect of these drugs is primarily to reduce the amount of excessive electrical activity present in the cerebral cortex and therefore stop the generation of seizures. Different drugs have varying mechanisms of action depending on which receptor or channel in the brain is being targeted. Phenobarbital (**29**) is the oldest AED still in use and like many AED's, it has a broad spectrum of activity for different seizure types. It works by stimulating the production of gamma aminobutyric acid (GABA) which is an inhibitory neurotransmitter used to counter balance neuronal excitation by allowing the movement of chloride ions into neurons.³⁵ A number of AED's like phenytoin (**30**) and carbamazepine (**31**) bind to sodium ion channels with the aim of slowing down or disrupting ion movement in order to decrease neuronal firing.^{36,37} Drugs for treating absence seizures (a non-convulsive generalised seizure that is marked by the transient impairment or loss of consciousness) like ethosuximide (**32**) tend to target T-type calcium channels.³⁸ These channels become blocked when the AED is bound, stopping the release of neurotransmitters and reducing neuronal excitability. Some

AED's work on a combination of targets. For example topiramate (**33**) targets the GABA receptor and inhibits sodium and calcium ion channels. Lastly, topiramate also acts as an α -amino-3-hydroxy-5-methyl-4-isoxazolepropionic acid (AMPA) receptor antagonist.³⁹ These receptors are responsible for glutamate-mediated excitation of neural cells, so antagonistic drugs such as topiramate should counteract seizure onset.

Table 3: Examples of clinically approved AED's

AED	Main Use	AED Target
 Phenobarbital (29)	Broad use for generalised and focal seizures	GABA Receptor
 Phenytoin (30)	Generalised and complex focal seizures	Sodium channel
 Carbamazepine (31)	Focal seizures	Sodium channel
 Ethosuximide (32)	Absence seizures	T-type calcium channel
 Topiramate (33)	Broad use for generalised and focal seizures	GABA receptor Calcium channel/sodium channel/AMPA receptor

Despite the wide range of AED's available, 30% of all patients are unresponsive to these and continue to suffer from regular seizures.³⁴ This type of epilepsy is referred to as

medically intractable epilepsy (MIE) which is defined by persistent seizure activity despite maximal medical treatment. Patients are normally diagnosed with MIE after the failure of two or three different AED's. There are many theories for AED resistance and it is most likely due to a combination of various different factors.^{40,41} A popular theory is the 'drug transporter hypothesis' where the reason for drug resistance is due to inadequate penetration of AED's across the BBB. This is caused by the overexpression of drug efflux transporters, such as P-glycoprotein 1 at epileptogenic zones. A less studied but equally popular theory is the 'drug target hypothesis' where the targeted channels or receptors are structurally or functionally modified making them less sensitive to the drugs targeting them. A third theory is the 'network hypothesis' which proposes that structural brain alterations (for example, hippocampal sclerosis) are involved in resistance to AED's. The type of epilepsy is crucial in choosing which treatment route to follow and in many cases, misdiagnosis results in ineffective medical treatment and pseudo-resistance.

For patients with epilepsy who are diagnosed with MIE, the best option for symptomatic treatment is through resective surgery. In many cases, this results in complete seizure freedom or reduced seizure frequency. In other cases, it can reverse certain drug resistance so that the patient's condition can be kept under control *via* AED's after surgery.⁴² The main aim of these surgeries is to resect the epileptogenic zones while leaving as much of the neo cortex intact as possible. Whether or not an individual is a candidate for resective surgery depends on the location of the epileptogenic zone and the extent to which this region which can be physically removed without causing major side effects.⁴³ The most common type of MIE is temporal lobe epilepsy (TLE) and treatment for this condition involves resection of mesial temporal structures. The two most common surgeries (accounting for 80% of all epileptic resections) performed are anterior temporal lobectomies (ATL) and selective amygdalohippocampectomies (SAH).⁴⁴ ATL involves complete removal of the anterior portion of the temporal lobe and SAH is the removal of the hippocampus and amygdalae. There is little evidence to suggest which method is more effective as both result in seizure freedom in more than 60% of patients. The side effects of temporal lobe resection can include verbal memory impairment and visual perception deficits. The third most common type of resective surgery is for the treatment of focal extratemporal lobe epilepsy (ETLE). With these patients, the epileptogenic foci are located in various regions throughout the cortex, often near eloquent brain structures, which control speech, motor function and senses. Therefore, this type of surgery is significantly more difficult and higher risk than TLE resection. ETLE resective treatment is

significantly less effective than TLE treatment with only 36% of patients becoming completely seizure free. This is due to only partial resection of the epileptogenic zone being possible in many patients due to the close proximity to eloquent brain structures.

Clearly, in performing resective surgery, imaging techniques showing the precise location of the epileptogenic foci are crucial. Common methods for locating the epileptogenic zone and determining the extent of resection include electroencephalography (EEG) and structural approaches like magnetic resonance imaging (MRI). However, 25% of patients being considered for epileptic resection have a normal structural MRI, so there is an extensive need for more advanced imaging methods (**Figure 4**).⁴³ Radiological techniques like PET and SPECT are more sensitive than MRI and could be used to detect in a structural or behavioural manner, abnormal brain tissue in the epileptogenic zone more efficiently.

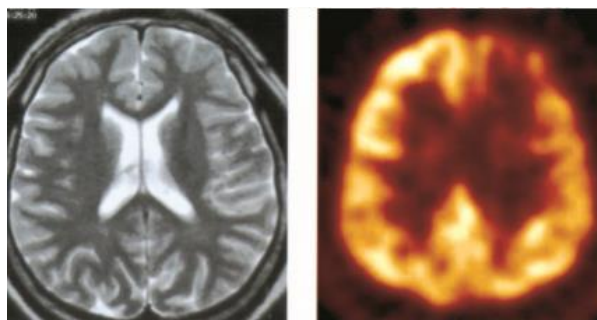


Figure 4: Scans from a patient with frontal lobe epilepsy. Left: MRI scan showing a normal brain image. Right: [¹⁸F]FDG PET scan showing decreased metabolism in left frontal lobe. (This figure was originally published *J. Nucl. Med.*, 2002, **43**, 1167 © SNMMI).⁴⁵

2.1.2. Monocarboxylate transporters 1 and 2 and their role in epilepsy

One way of imaging epilepsy and determining the affected areas of the brain is to target receptors that are disrupted by this disorder with molecular imaging agents. Patients with epilepsy suffer from a severe disruption in energetic and metabolic brain function.⁴⁶ Therefore, the expressions of compounds crucial for brain metabolism are substantially affected by this disorder. Monocarboxylates; lactate, pyruvate, acetoacetate and β -hydroxybutyrate have been found to play a role in the pathophysiology of epilepsy (TLE in particular). These compounds are crucial for regulating the energetics of brain metabolism. Lactate is particularly important since this is the end product of glycolysis and its intracellular build up results in glycolysis inhibition.⁴⁷ Cerebral metabolism of lactate and

other carboxylates depends on the concentrations of these compounds in the blood but also on their ability to permeate the BBB. These compounds are transported across plasma membranes primarily by monocarboxylate transporter 1 (MCT 1) and monocarboxylate transporter 2 (MCT 2) and therefore brain metabolism has a dependence on the abundance of these monocarboxylate transporters.^{46,48} Monocarboxylate transporters are a family of proton-linked transporter proteins which facilitate the transport of monocarboxylates across plasma membranes.⁴⁹ Each family member has 12 transmembrane helices (TM's) with intracellular C- and N-termini and a large cytosolic loop between TM's 6 and 7. MCT 1 is found on astrocytes and in endothelial cells of the blood brain barrier and MCT 2 is found in astrocytes and neurons. However, in epileptogenic zones of patients suffering from TLE, redistribution occurs and MCT 1 is predominantly found on astrocytes, whereas MCT 2 is found on astrocyte plasma membranes.⁵⁰ The reason for this redistribution has not been proven, however, it is hypothesised that due to the increased uptake of glutamate during epileptic seizures, more ATP is needed to remove this from cells. More lactate is generated as the side product from this ATP formation leading to an increase in MCT's for lactate clearance.⁵¹ Clearly, MCT 1 and MCT 2 play a major role in maintaining normal brain function and their distribution in the brain is majorly affected by epilepsy. Therefore, by using radiolabelled imaging agents that bind to MCT receptors, the epileptic regions of the brain could be visualised using PET or SPECT imaging.

2.1.3. MCT 1 and 2 inhibitors

In order to image MCT 1 and 2 and be able to monitor the parts of the brain affected by epilepsy, a radiolabel must be attached to a compound which binds to these receptors with high affinity and selectivity. There have been several compounds prepared which bind to MCT 1 or MCT 2 with the primary aim of being used as anti-cancer drugs. One commonly referenced compound is α -cyano-4-hydroxycinnamate (CHCA) **34** which was found to inhibit MCT 1 and cause hypoxic tumour cell death in mice (**Figure 5**).^{52,53} In 2015, Mereddy and co-workers attempted to create novel MCT 1 inhibitors based on CHCA.⁵⁴ It was found that having a diarylamine or dialkylamine unit in place of the hydroxyl group led to increased potency. It was also observed that the inhibitory activity could be further optimised with the addition of a methoxy unit on the aryl ring. The most potent compound in this series was diarylamine **35**, which was found to be active at low nanomolar concentration and inhibit tumour growth in nude mice xenograft models.

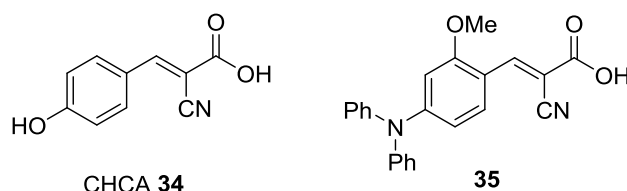
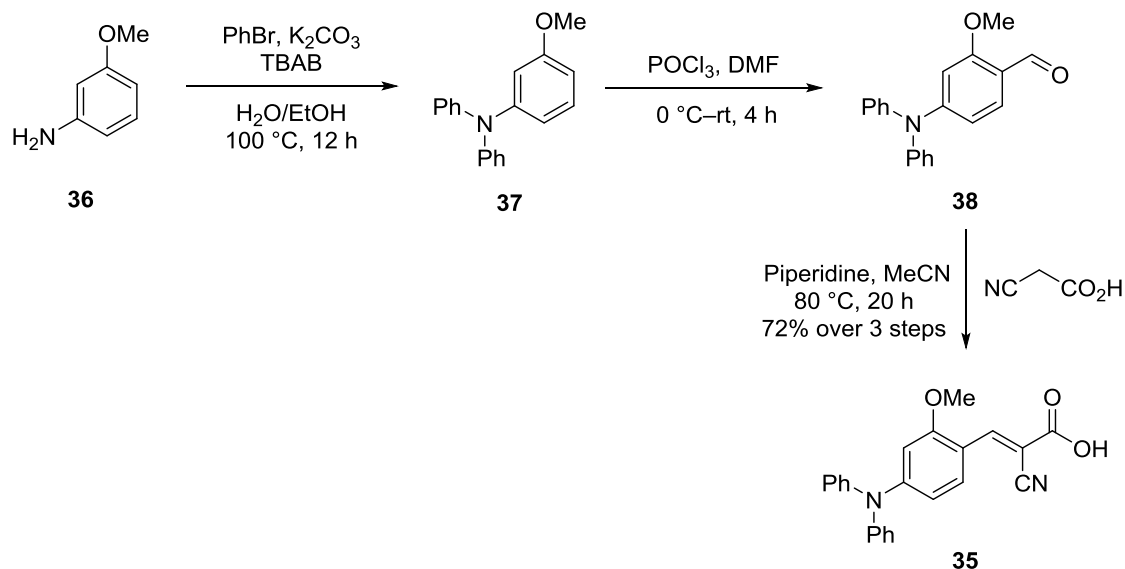


Figure 5: MCT 1 inhibitors that can potentially be used in cancer treatment.

The synthesis of **35** occurred in three steps from *m*-anisidine (**36**), starting with the diarylation of the amino group, using bromobenzene and a catalytic amount of tetrabutylammonium bromide (TBAB). The next step is a Vilsmeier–Haack formylation to give aldehyde **38** followed by condensation with cyanoacetic acid to synthesise cyanocinnamic acid **35** (Scheme 12).



Scheme 12: Synthesis of CHCA derivative **35**, a potent inhibitor of MCT 1.⁵⁴

Despite the high potency, it has been shown that these types of compounds are not selective for MCT's but are in fact several orders of magnitude more potent for the inhibition of the mitochondrial pyruvate carrier.^{55,56} If radiolabelled compounds were to be used as a guide for epileptic resection, it would be crucial for these compounds to be highly specific for the target receptors. Therefore, CHCA **34** and its derivatives would not be of use for this application.

Bannister and co-workers synthesised a series of novel pteridinedione and trione compounds as dual inhibitors of MCT 1 and MCT 2.⁵⁷ **Figure 6** shows the two most potent inhibitors from each series. These compounds were also found to impair Raji lymphoma cell proliferation at submicromolar doses. It was observed that a hydrocarbon side chain

containing a hydroxyl group on either the 5- or 6-position of the scaffold was necessary to ensure high potency. If these compounds were to be used as imaging agents, the labelling site would likely be installed on the aryl ring at position 7. However, the nature of the aryl group and its effect on MCT 1 and 2 inhibition has not yet been investigated. Therefore, further investigation on the structure-activity relationship in this region would be required to ascertain whether a radiolabel could be installed, while maintaining high binding affinities to the target.

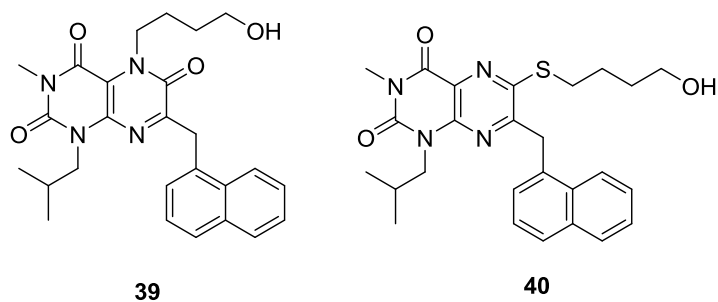


Figure 6: MCT 1 and 2 inhibitors, pteridinetriene **39** and pteridinedione **40**.⁵⁷

The most successful inhibitor of MCT 1 and 2 came from a series of thienopyrimidines synthesised by AstraZeneca.^{58,59} The compound with the best combination of potency and lipophilicity was AR-C155858 which has been advanced into clinical trials for treating various malignancies (**Figure 7**).⁶⁰

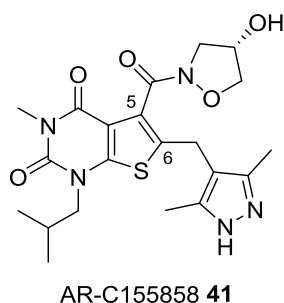


Figure 7: The most potent MCT 1 and 2 inhibitor synthesised by AstraZeneca as part of a thienopyrimidinedione series.

Several analogues of this compound were synthesised with different amides at the 5-position and various aromatic and heteroaromatic side chains at position 6. High binding affinities for MCT 1 and 2 were observed for many of these analogues, showing great potential for diversification. This, along with the highly selective binding, makes thienopyrimidinediones containing a potential labelling site an attractive target for the production of novel PET and SPECT imaging agents for MCT 1 and 2.

2.1.4. Proposed research

Based on the success of AR-C155858 **41** as an inhibitor of MCT 1 and 2, the main aim of this project was to design a variety of AR-C155858 analogues with a potential radiolabelling site. The first aim was the preparation of the thienopyrimidinedione core. The second objective was to create several small libraries of possible imaging agents with potential radiolabelling sites incorporated within the aryl ring which could target MCT 1 and 2 (**Figure 8**).

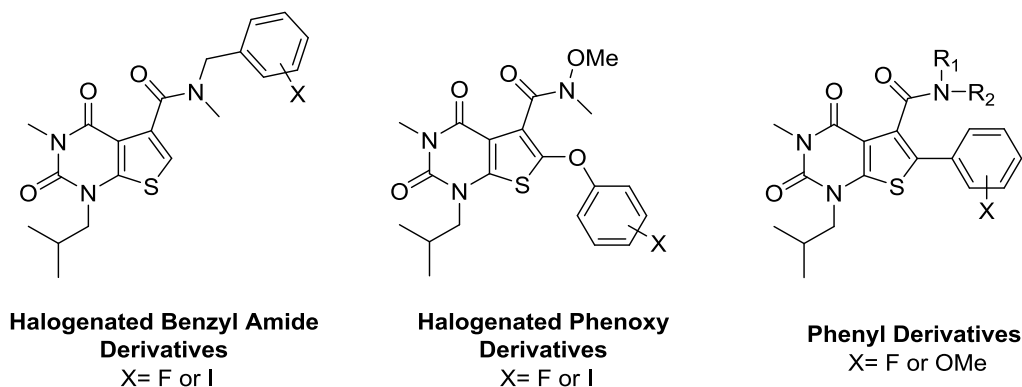


Figure 8: Structures of potential PET or SPECT imaging agents.

AstraZeneca showed that for good binding affinities along with the appropriate lipophilicity, it was necessary to have an amide at the 5-position along with a substituent at the 6-position of the thiophene ring.⁶¹ Although the halogenated benzyl derivatives have no substituent at the 6-position, it was proposed that the benzyl amide may be able to access the same region of the 6-substituent binding pocket. In the halogenated phenoxy derivatives, the aryl group is attached *via* an ether linkage which based on similar AstraZeneca compounds, should lead to high biological activity. In the case of all the potential compounds, it was essential to ensure high rigidity, since it was shown that the compounds could exist as rotamers, complicating their pharmacology.⁶¹ With this in mind, the phenyl system was proposed, with the aryl group directly attached to the thiophene ring. In this final set of compounds, several different amides would also be explored in order to assess which type is most beneficial.

All of these compounds would contain “cold” isotopes of fluorine, iodine or carbon in order to mimic their radiological counterparts. The aim was to prepare and then test these cold compounds for appropriate physiological properties such as lipophilicity, permeability and plasma protein binding. The compounds with the most suitable physiochemical properties would then be tested for their ability to bind to MCT 1 and 2. The compounds

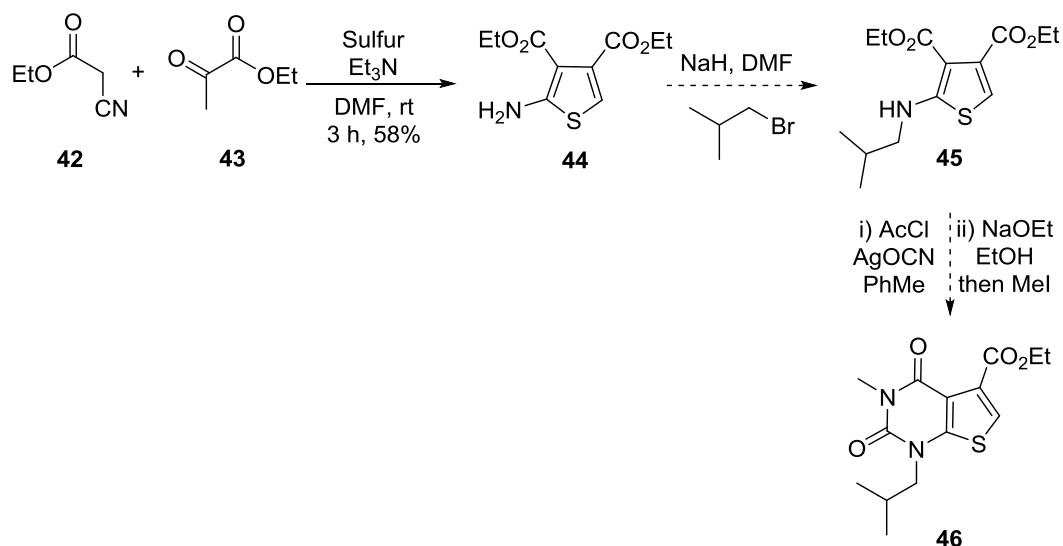
with the highest affinity would then undergo radiolabelling with fluorine-18, carbon-11 or iodine-125 for PET or SPECT imaging, respectively.

In summary, a small library of AR-C155858 analogues would be prepared using synthetic routes which allow for the late stage introduction of diversity. Moieties that can undergo activation and subsequent radiolabelling would then be introduced. Identification of active compounds with the appropriate physicochemical properties would lead to novel PET and SPECT imaging agents for MCT 1 and 2 receptors.

2.2 Results and discussion

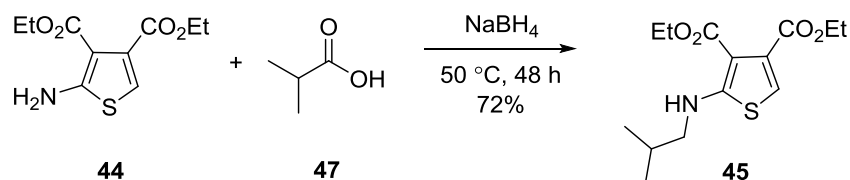
2.2.1 Synthesis and optimisation of the thienopyrimidinedione core

The first aim of the project was to synthesise the core structure before diversification. The original plan for the synthesis of **46** is shown in **Scheme 13**. It was proposed that the synthesis of 2-amino substituted thiophene **44** could be achieved by reaction of ethyl cyanoacetate (**42**) with ethyl pyruvate (**43**) in the presence of sulfur. The amine would then be alkylated with isobutyl bromide using sodium hydride to give **45**. Then, reaction with acetyl chloride in the presence of silver cyanate followed by sodium ethoxide addition and subsequent methylation would complete the synthesis of **46**. For the synthesis of **44**, the reaction mixture was originally stirred for 3 hours using 1 equivalent of triethylamine.⁶² This reaction gave the desired product in a 30% yield. It was found that increasing the timescale of the reaction to 6 hours did not significantly affect the yield. However, it was observed that adding more base did have a beneficial effect, with 5 equivalents of triethylamine being the optimum amount. Using these conditions, the yield was improved to 58%.



Scheme 13: Proposed synthesis of the thienopyrimidinedione core.

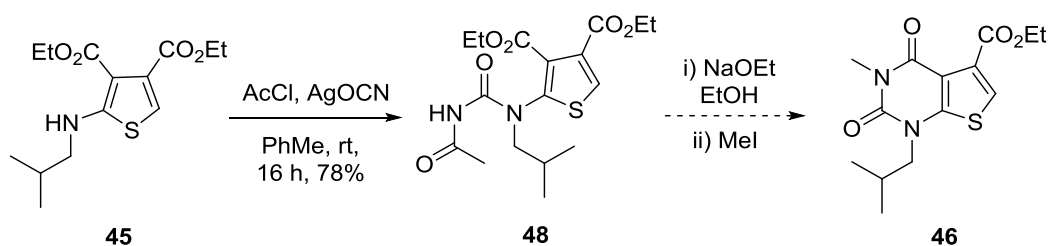
It was proposed that compound **44** could be alkylated using isobutyl bromide and sodium hydride. However, none of the desired product was formed. Therefore, an alternative method towards compound **45** was employed (**Scheme 14**).⁶² This method involved a reductive coupling with isobutyric acid and sodium borohydride. The optimum yield of 72% was achieved by adding the sodium borohydride portionwise over 2 days and heating to 50 °C.



Scheme 14: Alternative route towards compound **45**.

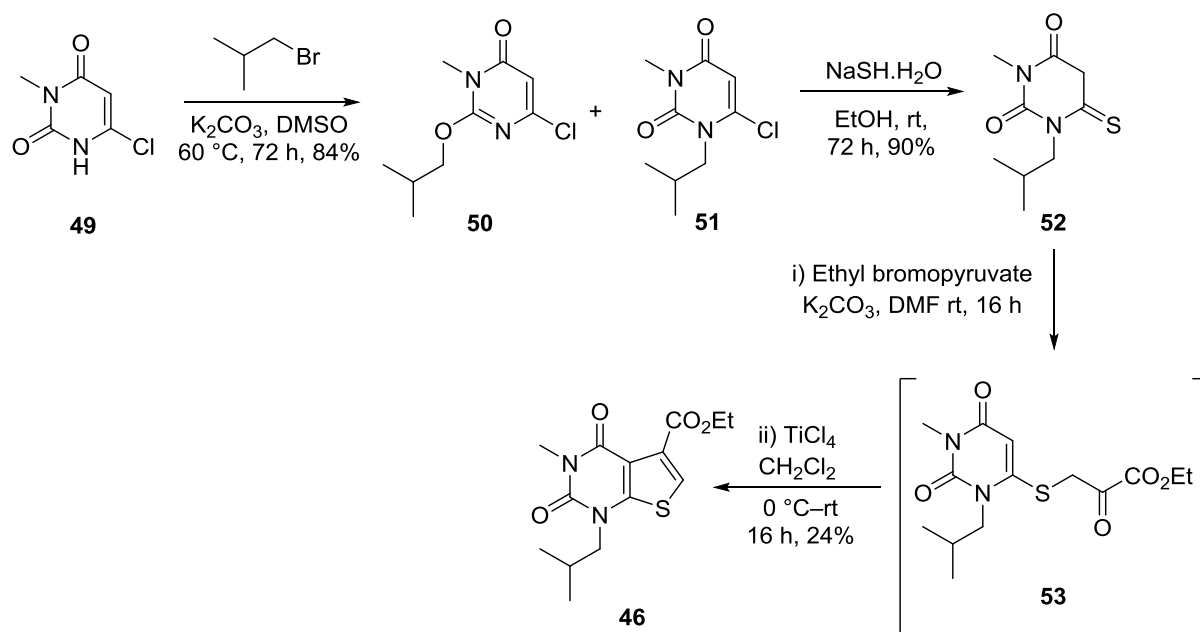
The proposed next steps involved the reaction of acetyl chloride with silver cyanate to form acetyl isocyanate. Compound **45** would then be added to give intermediate **48**. This would be followed by a sodium ethoxide mediated intramolecular cyclisation. Finally, methylation *via* the addition of methyl iodide would give the desired thienopyrimidinedione **46** (**Scheme 15**).⁶² The synthesis of **48** was successful, resulting in a 78% yield after 16 hours. However, the synthesis of **46** by this method was unsuccessful under a variety of conditions. After 3 hours of stirring at room temperature, NMR analysis showed decomposition of **48** and no desired product formation. It was proposed that the sodium ethoxide base was too nucleophilic for this reaction and was likely reacting at more than one position, causing **48** to fragment and decompose. It was proposed that using a

more sterically hindered base such as sodium *tert*-butoxide should solve the problem. However, when this base was used decomposition still occurred and no product was formed.



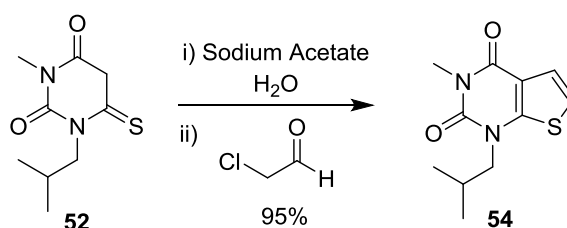
Scheme 15: Attempted route towards compound **46**.

At this point it was decided that a different route towards **46** would be investigated (**Scheme 16**). The first step was the *N*-alkylation of 6-chloro-3-methyluracil (**49**) with isobutyl bromide. After stirring for 2 days at 60 °C a 10:1 mixture (better than reported literature ratio of 5:1) of *N*-alkylated to *O*-alkylated products was obtained (45% crude yield) however, the reaction had not gone to completion.⁵⁷ The temperature of this reaction was then increased to improve the conversion from starting material to product. At 70 °C the crude yield was improved to 55% however, this gave a 5:1 ratio of *N*-alkylated to *O*-alkylated products. Therefore, increasing the temperature yielded less of the desired product and so 60 °C was chosen as the optimum temperature. The reaction time was increased to 3 days and a yield of 84% was obtained. During the substitution reaction to form thioamide **52**, it was found that only the *N*-alkylated product **51** reacted with sodium hydrosulfide. This allowed for the easy separation of thioamide **52** from the *O*-alkylated product **50** during work up. Overall, this gave **52** in a 90% yield. Formation of compound **46** was initially attempted *via* a two-stage process involving *S*-alkylation with ethyl 3-bromopyruvate followed by a titanium tetrachloride mediated cyclisation.⁶¹ Although intermediate **53** was formed cleanly, cyclisation and dehydration with titanium tetrachloride gave only a 24% yield of **46** and a high number of side products. This reaction was also difficult to reproduce, with an average yield of 10% being achieved. As a result of the poor yields, other methods to synthesise **46** were investigated.



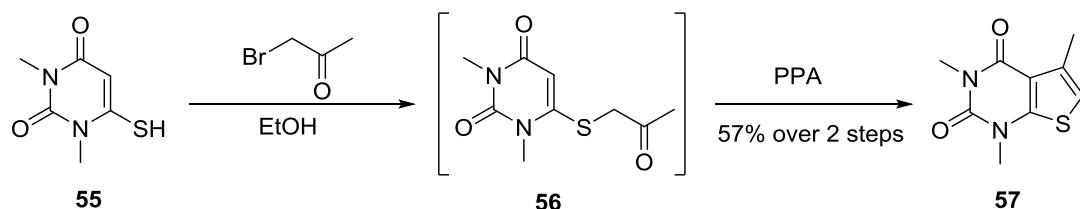
Scheme 16: Alternative route towards compound **46**.

Thienopyrimidinediones have been previously synthesised from the reaction of **52** with α -halocarbonyl compounds. For example AstraZeneca synthesised 3-methyl-1-(2-methylpropyl)thieno[2,3-*d*]pyrimidin-2,4(1*H*,3*H*)-dione (**54**) *via* deprotonation of **52**, followed by nucleophilic substitution and intramolecular cyclisation of chloroacetaldehyde. This gave the desired product in a 95% yield (**Scheme 17**).⁶³



Scheme 17: Cyclisation using chloroacetaldehyde for the synthesis of 3-methyl-1-(2-methylpropyl)thieno[2,3-*d*]pyrimidin-2,4(1*H*,3*H*)-dione (**54**).

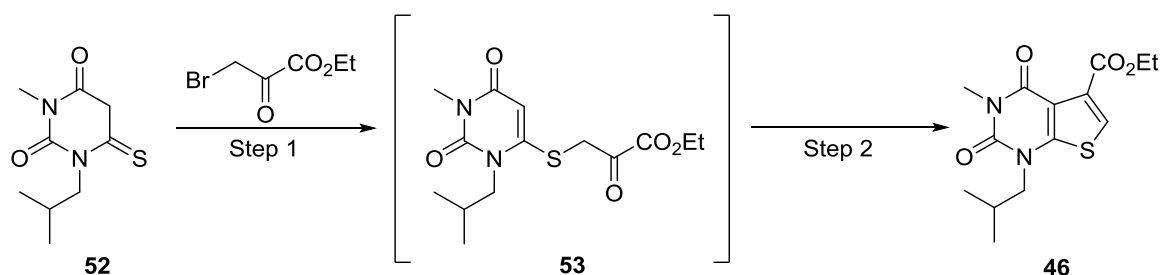
However, application of this method using thioamide **52** and ethyl bromopyruvate gave only a 10% yield of **46** (**Table 4, entry 2**). The next attempted method was based on a similar analogue synthesised by Ogura, Sakaguchi and co-workers (**Scheme 18**).⁶⁴ In this method, uracil **55** was treated with bromoacetone to yield alkylated product **56**. This was isolated, purified and then converted to thienopyrimidine **57** by dehydration with polyphosphoric acid (PPA).



Scheme 18: Acid mediated cyclisation reaction using bromoacetone.

When this method was applied to the reaction of **52** with ethyl 3-bromopyruvate, the alkylation occurred efficiently. However, the product could not be isolated and purified due to significant decomposition. Therefore, **53** was directly converted to **46** via the PPA mediated cyclisation. The cyclisation was initially performed at 100 °C and gave a yield of 35% in 12 hours (**entry 3**). Further optimisation of this step led to a yield of 54% in 3 hours when a temperature of 145 °C was used (**entry 5**). This reaction was found to be reproducible and could be used for the multigram synthesis of **46**.

Table 4: Optimisation of the synthesis of thienopyrimidinedione **46**.



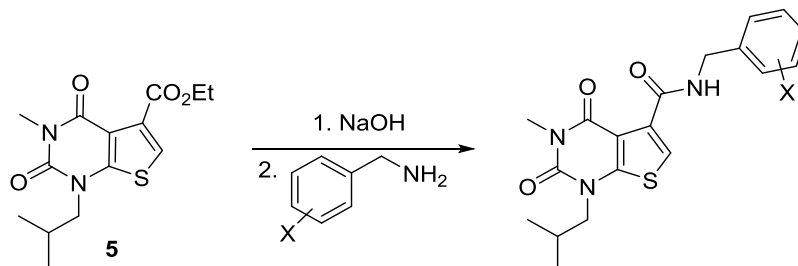
Entry	Step 1	Step 2	Yield of 46 (%)
1	K ₂ CO ₃ , DMF, rt, 16 h	TiCl ₄ , CH ₂ Cl ₂ , 0 °C–rt, 16 h	24%
2	NaOAc, H ₂ O, rt, 5 h	60 °C, 48 h	10%
3	EtOH, rt	PPA, 100 °C, 12 h	35%
4	EtOH, rt	PPA, 130 °C, 6 h	41%
5	EtOH, rt	PPA, 145 °C, 3 h	54%

2.2.2 Synthesis of potential imaging agents

2.2.2.1 Synthesis of benzyl amide derivatives

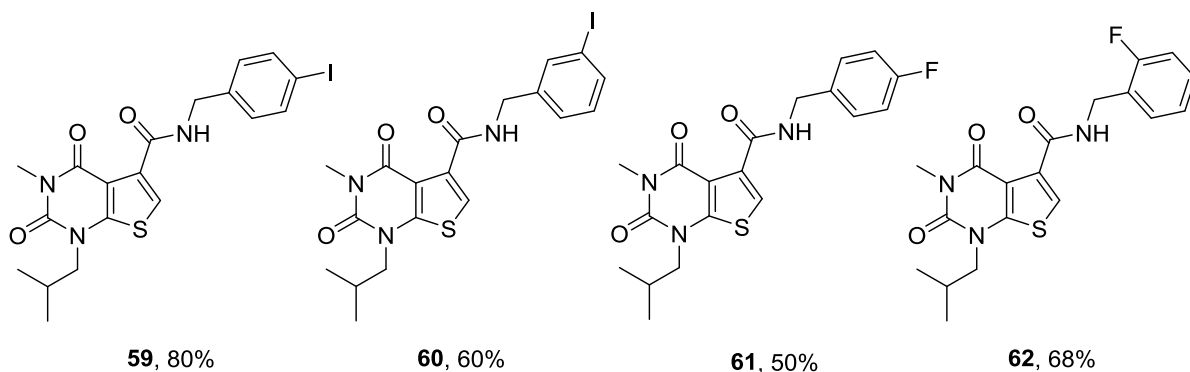
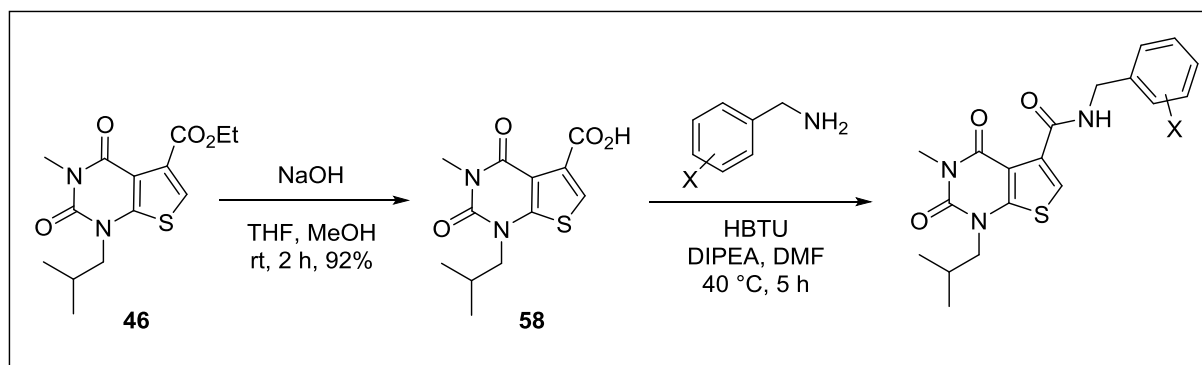
The first set of target compounds incorporated a benzyl amide at the 5-position of the thienopyrimidinedione core. It was proposed that these structures would occupy the same binding pockets as the highly active AstraZeneca compounds which contain an aryl ring at

the 6-position. These compounds were synthesised by the hydrolysis of compound **46** followed by an amide coupling to incorporate a benzylamide at the 5-position (**Scheme 19**). Different benzylamines were used with either fluorine or iodine atoms present on the aryl ring at various positions.



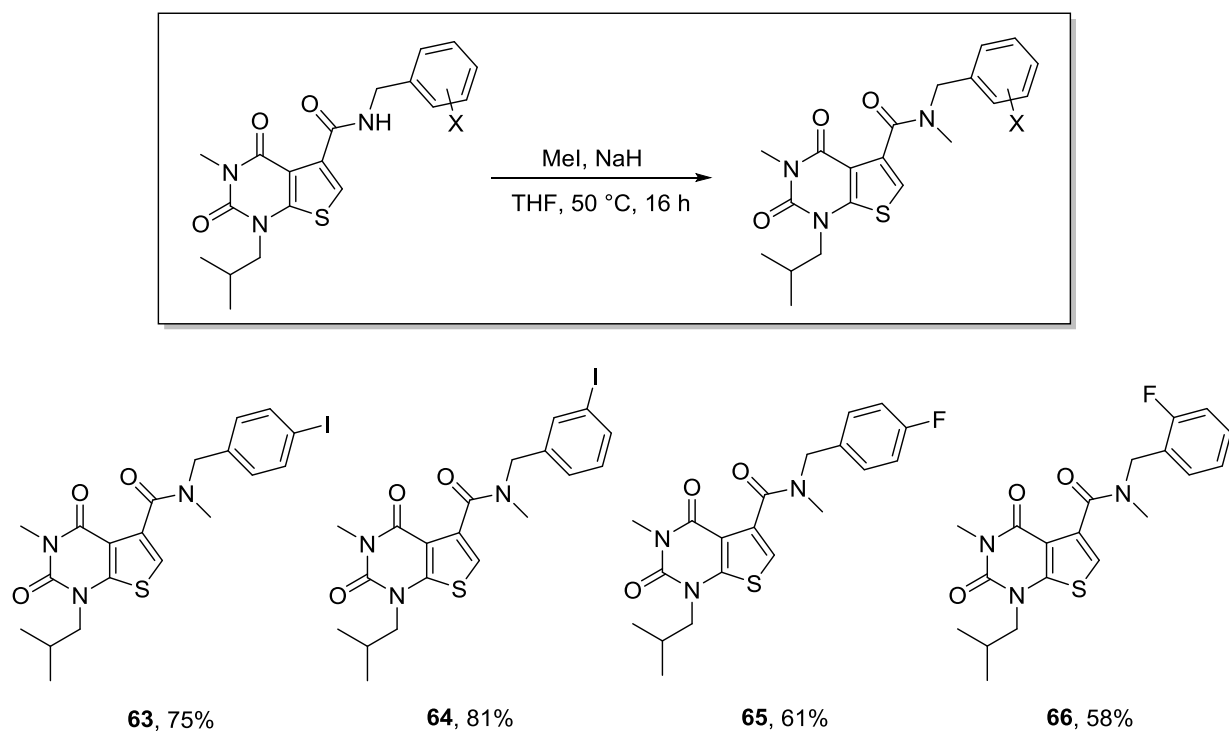
Scheme 19: Route towards the first library of potential imaging agents where X= F or I.

Compound **46** was first hydrolysed with sodium hydroxide and this gave carboxylic acid **58** in a 92% yield (**Scheme 20**). Using 4-iodobenzylamine, several amide coupling methods were attempted in order to acquire the highest yield. The first method used oxalyl chloride and DMF to form the acid chloride from carboxylic acid **58**, followed by direct coupling with 3-iodobenzylamine. However, as this gave a poor yield, it was decided to attempt the amide formation *via* a coupling agent. The best yield was achieved using HBTU and diisopropylethylamine, which gave **59** in an 80% yield. The optimised coupling was then applied using a range of benzylamines and this gave a small library of targets in good yields.



Scheme 20: Synthesis of benzylamides **59–62**.

The final step in the synthesis of the halogenated benzylamide derivatives was methylation of the amide. This reaction was carried out under standard conditions with methyl iodide and sodium hydride, using an optimal temperature of 50 °C (**Scheme 21**). From this series of reactions, four potential imaging agents were prepared with an *N*-methyl, *N*-benzylamide at the 5-position of the thiophene ring.



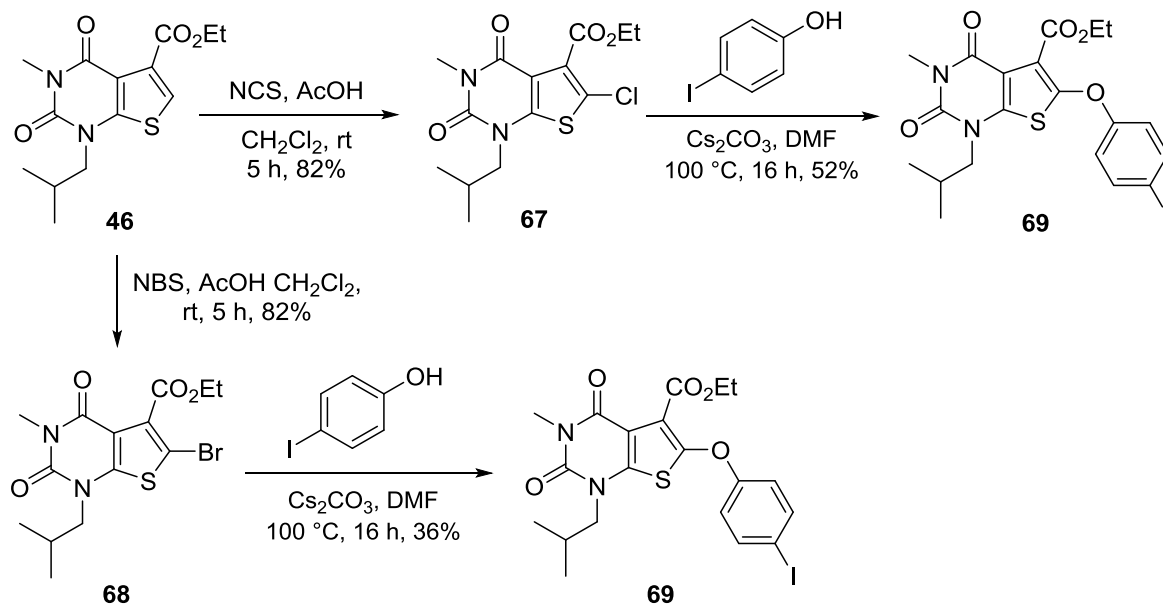
Scheme 21: Final products obtained by a methylation reaction.

2.2.2.2 Synthesis of halogenated phenoxy derivatives

The next set of target compounds contained an aryl group at the 6-position of the thiophene ring *via* an ether linkage. Several of the analogues synthesised by AstraZeneca also contained an ether linkage and many of these compounds bound strongly to MCT 1 or 2.⁶¹ It was therefore proposed that this library should yield highly active compounds. This set of potential imaging agents also incorporated a Weinreb amide at the 5-position. It was previously observed by AstraZeneca that many standard amide derivatives with a thienopyrimidinedione core existed as conformational isomers which complicated their pharmacology and that having a Weinreb amide in the 5-position circumvented this problem by reducing the barriers to rotation around the amide bond.⁶¹

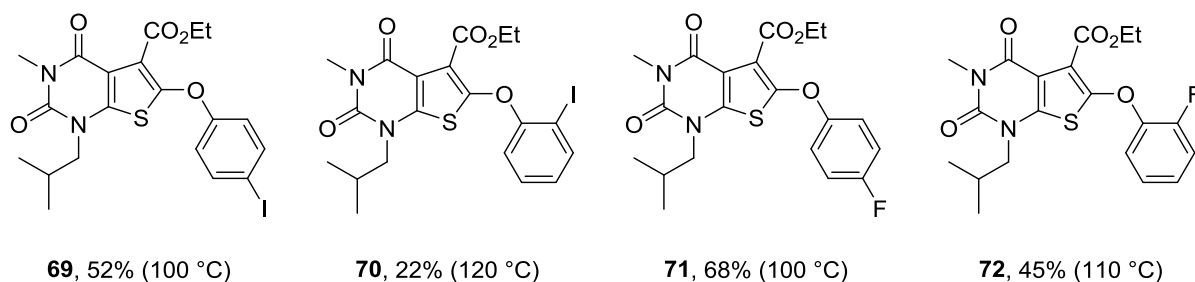
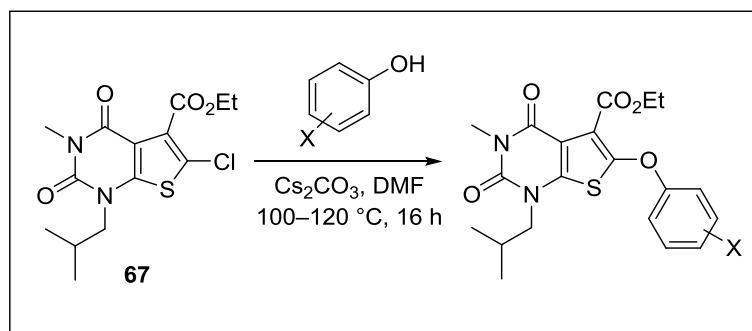
In order to install the aryl group, the first step was the halogenation of the 6-position, followed by a nucleophilic aromatic substitution reaction using fluorinated or iodinated phenols. The halogenation and subsequent substitution was attempted by chlorination and bromination to determine which would result in the highest yields over the two steps (**Scheme 22**).⁶¹ Both the chlorination and bromination of compound **46** were found to give an 82% yield using acetic acid with either *N*-chlorosuccinimide (NCS) or *N*-

bromosuccinimide (NBS). When the substitution reaction was performed using 4-iodophenol, a higher yield was achieved using the chlorinated analogue. Therefore, the synthesis of compound **67** was repeated on a large scale and the material was used to incorporate fluorinated and iodinated aryl units at the 6-position of the thiophene ring.



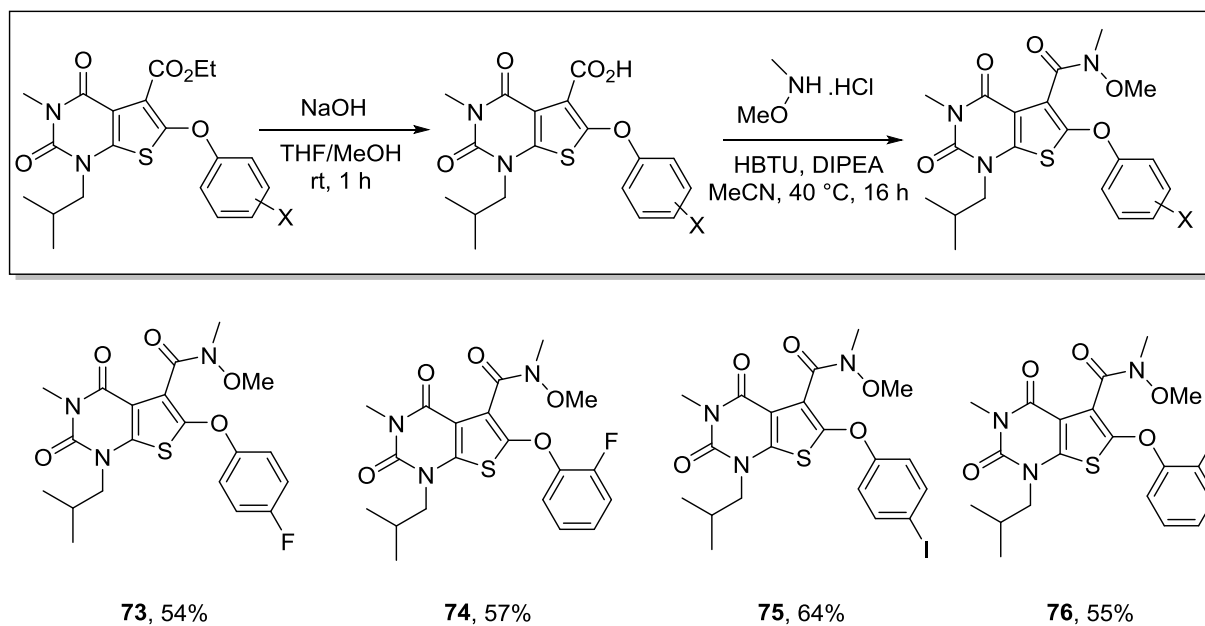
Scheme 22: Synthesis of **69** using halogenation and substitution reactions.

The nucleophilic aromatic substitution reaction worked well for *para*-substituted analogues and the *ortho*-substituted fluoro analogue (**Scheme 23**). When 2-iodophenol was used, the reaction was much slower due to increased steric hindrance. So, for this reaction, a temperature of 120 °C was required to fully react the starting material. Unfortunately, this also caused decomposition of the product and gave only a 22% yield for compound **70**.



Scheme 23: Nucleophilic aromatic substitution products and yields.

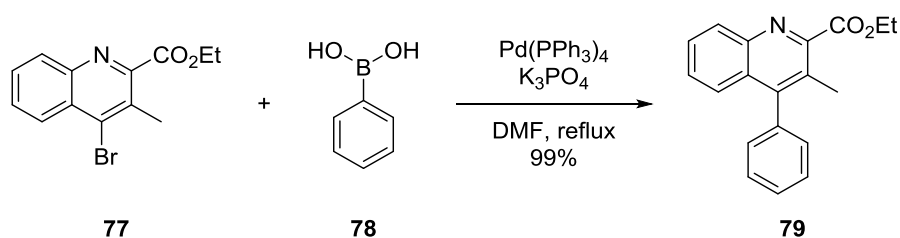
The final two steps in the synthesis of this library were the sodium hydroxide mediated hydrolysis of the ester functionality, followed by Weinreb amide formation (**Scheme 24**). The carboxylic acids formed after the hydrolysis step were found to be unstable even at low temperatures so it was essential that the product was used immediately in the amide coupling step in order to ensure the highest yields possible over the two steps. The amide coupling was performed using HBTU as the coupling partner, which gave the four halogenated phenoxy targets in good yields.



Scheme 24: Hydrolysis and amide coupling steps for products **73–76**.

2.2.2.3 Synthesis of phenyl derivatives

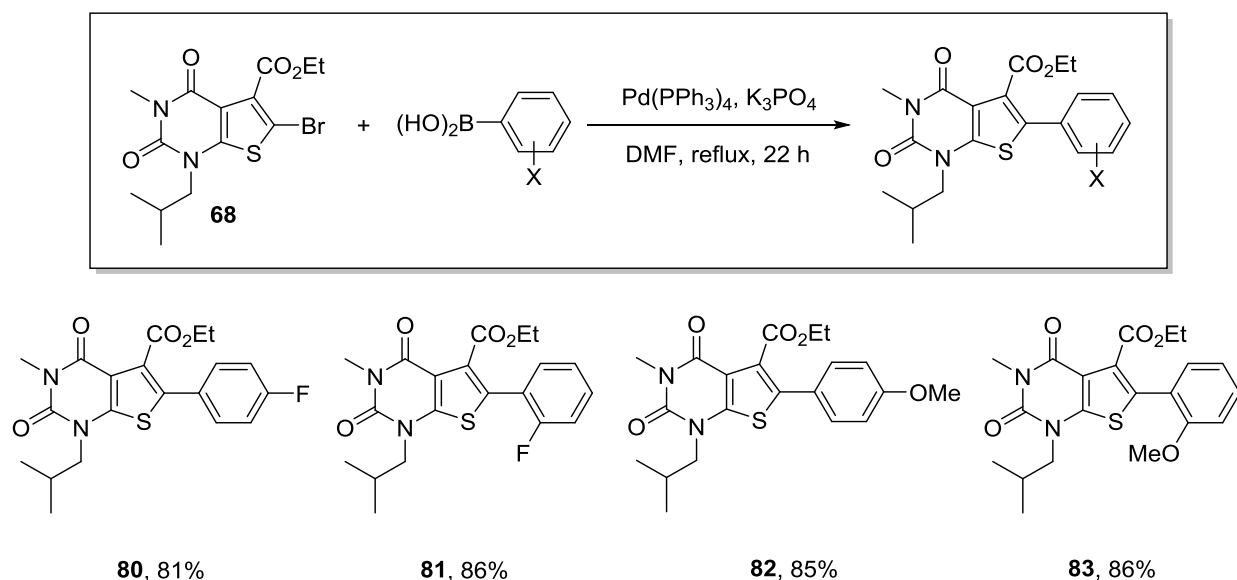
The phenyl library of target compounds were designed with an aryl group at the 6-position of the thiophene ring. Due to the increased rigidity, various amide substituents would be incorporated at the 5-position with a reduced likelihood of rotamers. So as well as the Weinreb amide, it was proposed to incorporate morpholine and diethylamide groups at the 5-position. In order to directly attach an aryl group to the thiophene ring, bromide **68** was used as a precursor for a Suzuki-Miyaura coupling. Conditions for a Suzuki-Miyaura cross-coupling had been optimised within the Sutherland group on a different project. The catalyst of choice was tetrakis(triphenylphosphine)palladium(0), which in combination with potassium phosphate as the base produced quinoline **79** in a 99% yield (**Scheme 25**).⁶⁵



Scheme 25: Literature Suzuki-Miyaura coupling reaction.

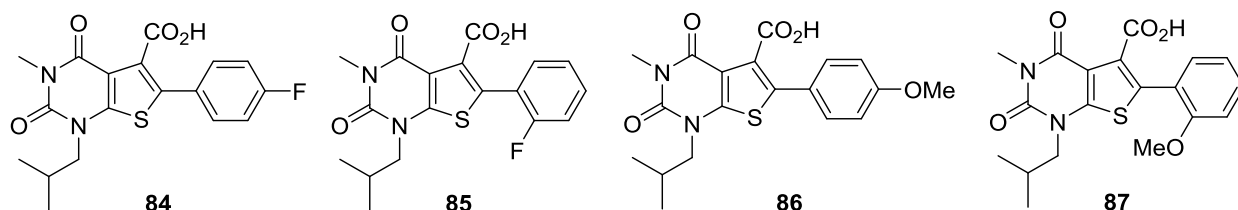
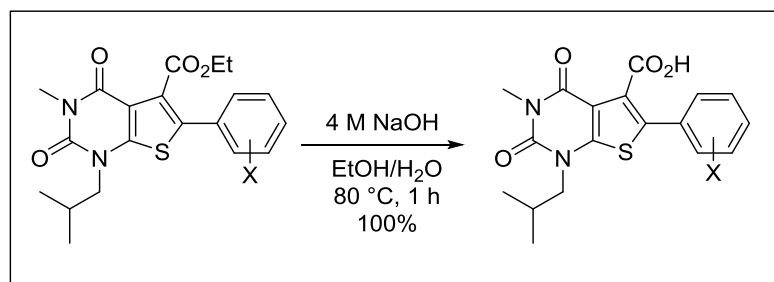
Due to the success of these conditions on a sterically hindered biaryl system, this was the initial procedure applied to the Suzuki-Miyaura coupling of brominated pyrimidinedione **68** with substituted phenylboronic acids. SPECT imaging agents were not prepared in this fashion because of the potential self-reaction of iodinated boronic acids. So, as well as using fluorinated phenylboronic acids, methoxyphenylboronic acids were also employed as mimics for carbon-11 labelled imaging agents.

The literature method shown in **Scheme 25** proved to be successful for this library of compounds and gave four coupled products in high yields (**Scheme 26**). The best yields were obtained when the mixture of reagents in DMF were degassed under argon for one hour prior to the addition of the palladium catalyst.



Scheme 26: Suzuki-Miyaura cross-coupling products and yields.

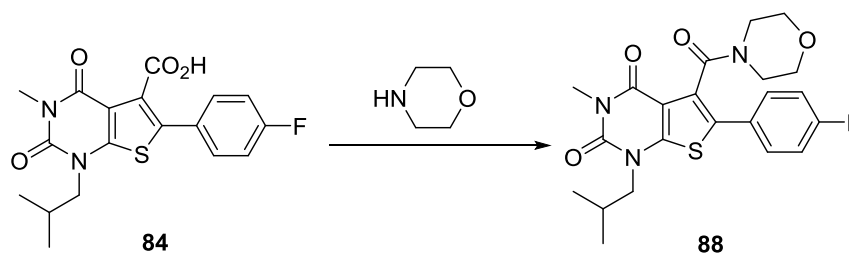
With these compounds synthesised, the next step was to install various amides at the 5-position. In order to do this, the ester was hydrolysed as a precursor for the amide coupling. Using the previous hydrolysis method of sodium hydroxide in methanol and tetrahydrofuran at room temperature (**Scheme 24**) was unsuccessful for this library and only starting material was recovered. It was proposed that this was due to increased steric hindrance and therefore, more forceful conditions were required. With this in mind, the solvent system was changed to a 1:1 mixture of ethanol and water so that the reaction could be heated to higher temperatures. When using this system and heating the reaction to 80 °C for 1 hour, quantitative yields were obtained (**Scheme 27**).



Scheme 27: Hydrolysis reaction to synthesise compounds **84–87**.

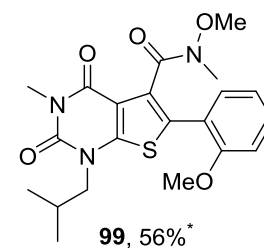
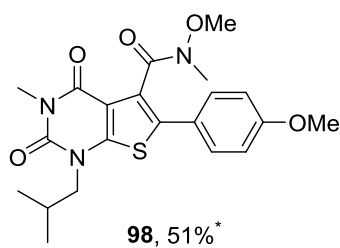
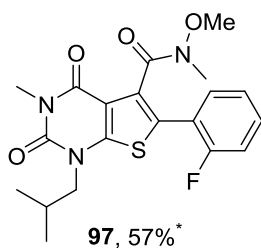
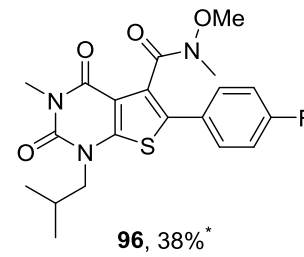
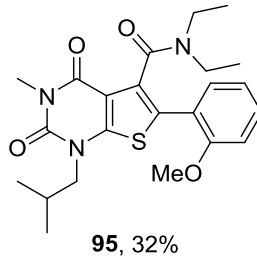
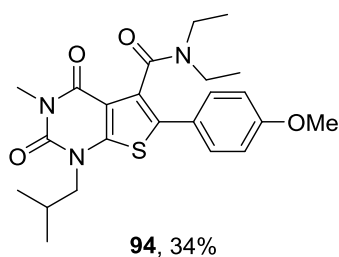
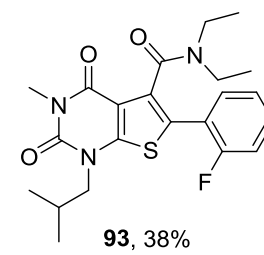
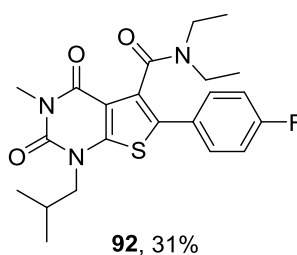
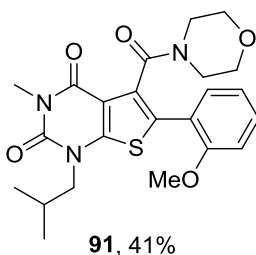
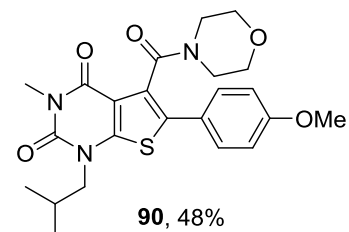
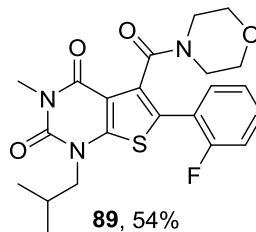
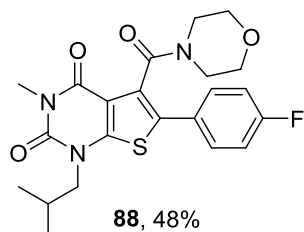
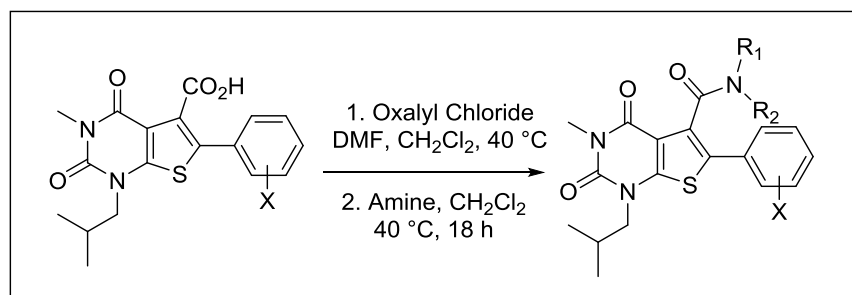
After the hydrolysis was complete, amide coupling conditions were explored, using morpholine and compound **84** for optimisation. The first attempt mimicked the coupling conditions used in the synthesis of the halogenated phenoxy derivatives (**Scheme 24**) however, the yield was only 32% (**Table 5, entry 1**). EDCI was then used as an alternative coupling reagent but this led to even lower yields (**entry 2**). It was thought that due to the enhanced steric hindrance caused by the aryl ring at the 6-position, coupling partners such as HBTU or EDCI might be too bulky to mediate a successful reaction. For this reason, efforts were turned to acid chloride formation. The first attempt at an amide coupling *via* an acid chloride involved carboxylic acid **84** being stirred at 50 °C in thionyl chloride for one hour prior to the addition of the amine. However, this reaction only gave a 21% yield after 48 hours and significant decomposition of the starting material was observed (**entry 3**). This led to the use of oxalyl chloride, a milder reagent for the formation of acid chlorides. This set of conditions led to the best yield of 48% (**entry 4**).

Table 5: Attempted amide coupling conditions.



Entry	Coupling conditions	Solvent	Temperature (°C)	Yield (%)
1	HBTU, DIPEA, morpholine	MeCN	40	32
2	EDCI, DMAP, DIPEA, morpholine	DMF	50	9
3	i) SOCl ₂ ii) Morpholine	1. Neat 2. CH ₂ Cl ₂	1. 50 2. 40	21
4	i) Oxalyl chloride, DMF ii) Morpholine	CH ₂ Cl ₂	1. 0–40 2. 0–40	48

This method was then used to complete the synthesis of the phenyl derivatives, using various amines (**Scheme 28**). For the Weinreb amide series, *N,O*-dimethylhydroxylamine hydrochloride was used as the coupling partner. Therefore, Hünig's base was also used during this coupling reaction. To further explore the structure activity relationship of this series, a cyclic amine, morpholine and an acyclic amine, diethylamine were also used. The reaction worked less well for the diethyl carboxamides. This is likely due to the less rigid and less reactive nature of diethylamine.



Scheme 28: Synthesis of various phenyl derivatives. *Diisopropylethylamine was also used in the amidation step.

2.2.3 Synthesis of a known inhibitor of MCT 1

With the series of target thienopyrimidinediones in hand, the next steps were to evaluate the physiochemical properties of each compound and test the most suitable compounds for biological activity against MCT 1 and 2. As a control for the various stages of assessment, a known high affinity MCT 1 agent was also prepared (**Figure 8**).⁶¹

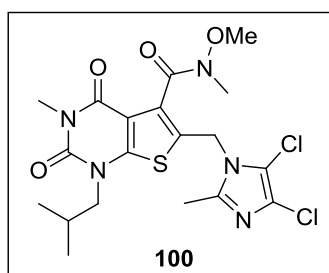
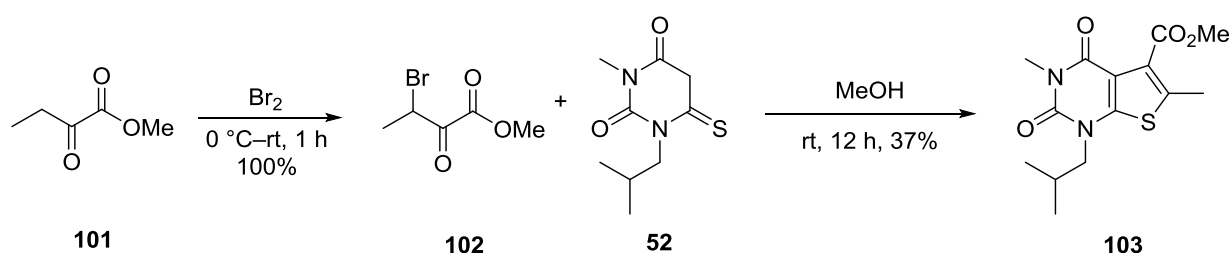


Figure 9: Standard MCT 1 inhibitor chosen as a control during biological testing.

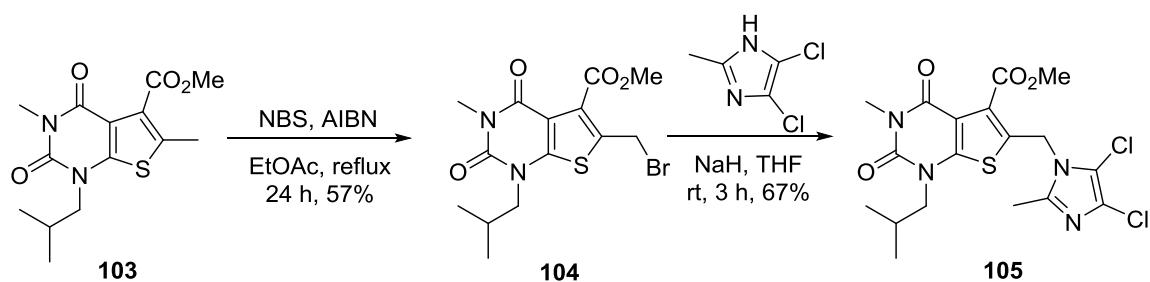
The core structure of compound **100** was synthesised by the reaction of mercaptopyrimidinedione **52** with methyl 3-bromo-2-oxobutanoate (**102**) (**Scheme 29**). The methyl 3-bromo-2-oxobutanoate (**102**) was prepared by the α -halogenation of methyl 2-oxobutanoate (**101**). This reaction was complete in 1 hour, giving a quantitative yield of the desired product.⁶⁶ Compound **102** was then used in the *S*-alkylation of compound **52**, followed by a subsequent cyclisation and dehydration sequence. It was found that for this substrate, an additional dehydrating agent was not required for the formation of thienopyrimidinedione **103**.



Scheme 29: Bromination of methyl 2-oxobutanoate (**101**) followed by alkylation and cyclisation to give thienopyrimidinedione **103**.

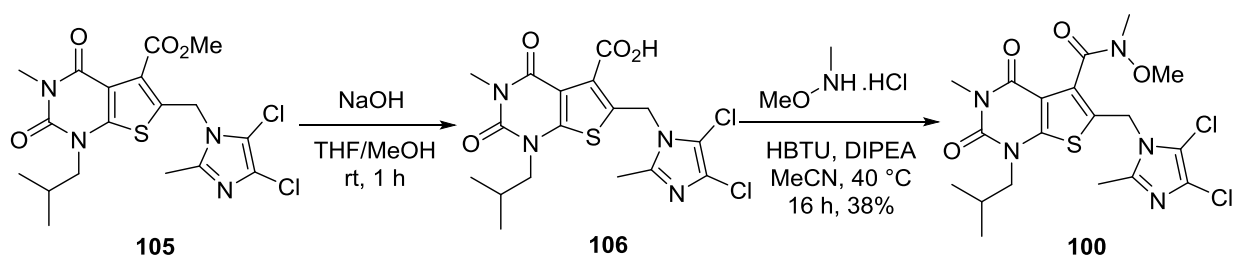
The next step in the synthesis was to incorporate the aryl side chain at the 5-position of the thiophene ring. This was achieved by bromination of the methyl group *via* an AIBN initiated radical reaction with NBS. This gave brominated analogue **104** in a 57% yield.

Substitution with 4,5-dichloro-2-methylimidazole in the presence of sodium hydride incorporated the desired heteroaromatic substituent in a 67% yield (**Scheme 30**).



Scheme 30: AIBN initiated radical bromination followed by a substitution reaction to give compound **105**.

The final step was the formation of a Weinreb amide unit at the 6-position. This was carried out by hydrolysis of the ester, followed by an amide coupling using HBTU to give the desired product in 38% yield over the two steps (**Scheme 31**).



Scheme 31: Final steps towards the synthesis of compound **100**.

2.2.4 Assessment of physicochemical properties

Some of the key physicochemical properties of all the synthesised compounds were assessed to provide an insight into the potential bioavailability of these scaffolds. The properties evaluated were the partition coefficient ($\text{Log}P$), permeability (P_m), membrane partition coefficient (K_m) and percentage plasma protein binding (%PPB). These values were quantified using established HPLC methodology.⁶⁷

The biological targets for these compounds lie within the central nervous system which means that they must be able to penetrate the BBB. $\text{Log}P$ acts as a descriptor of lipophilic character as it expresses the affinity of the compound for a lipophilic octanol phase relative to an aqueous water phase. This is defined according to the equation shown below.

$$\text{Log}P = \text{Log} \left(\frac{[\text{Compound}]_{\text{octanol}}}{[\text{Compound}]_{\text{water}}} \right)$$

Some lipophilic character is required in order for a compound to cross the BBB *via* passive diffusion. However, compounds with too high LogP values are more likely to undergo rapid metabolic clearance and be involved in off-target binding.^{68,69} It was found that this value could be determined using HPLC methodology with a C₁₈ column (see page 136). This method offers several advantages over the classic “shake flask” method.⁷⁰ Since this process is automated, it allows for the rapid testing of a large number of compounds and it is also highly reproducible.

Penetration of the BBB is greatly affected by solute-membrane interactions and therefore the membrane partition coefficient (K_m) must be examined. K_m represents all possible interactions between a solute and the membrane and is frequently a rate-limiting step in drug absorption. This can be measured using immobilised artificial membrane (IAM) chromatography where cell membrane phospholipid molecules are covalently bonded to silica particles and used to mimic the membrane-lipid environment of cells.^{71,72} Permeation of a drug through the membrane by passive diffusion is directly proportional to K_m according to the equation shown below where MW refers to molecular weight.

$$P_m = \frac{K_m}{MW}$$

The percentage plasma protein binding (%PPB) refers to the degree to which a drug molecule will attach itself to proteins in the blood. The two most abundant plasma proteins are α_1 -acid glycoprotein (AGP) and human serum albumin (HSA). This parameter can have a large effect on the efficiency of a radiotracer, since only the unbound portion of the compound is free to penetrate the BBB. High %PPB also contributes to a higher degree of nuclear image noise, originating from a build-up of protein bound compound in the blood vasculature. This leads to images of a much poorer quality and accuracy. The %PPB can also be determined by HPLC methodology, using a column coated in HSA.⁷²

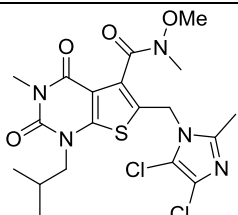
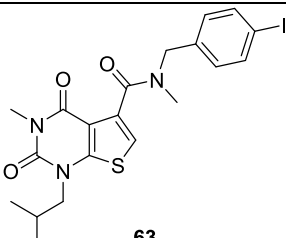
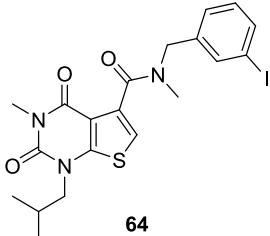
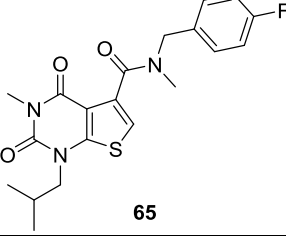
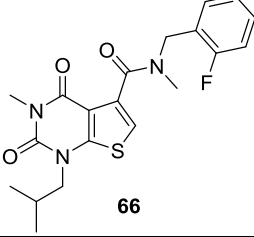
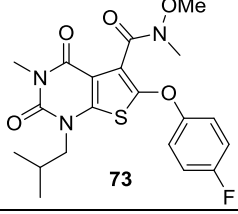
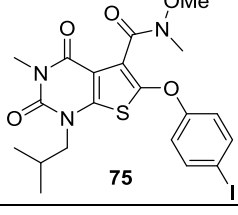
Previous work by Taveres *et al.* established the ideal values for these parameters based on the HPLC testing of ten molecules which had previously been used as radiotracers. The limits of these values are shown below (**Table 6**).⁶⁷

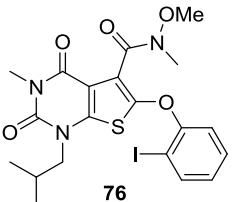
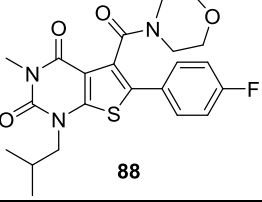
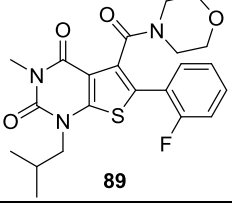
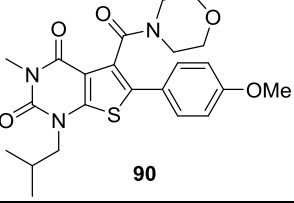
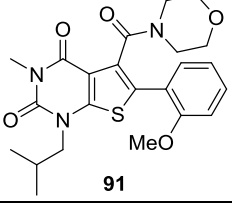
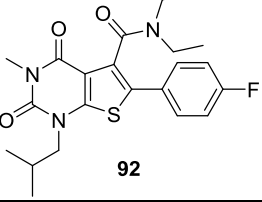
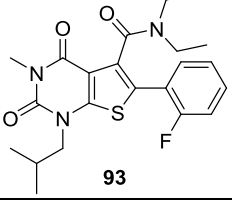
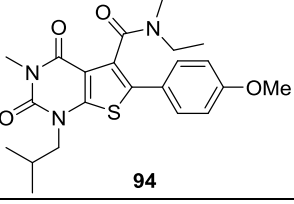
Table 6: Ideal limits on the physicochemical properties of a potential imaging agent.

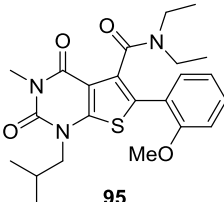
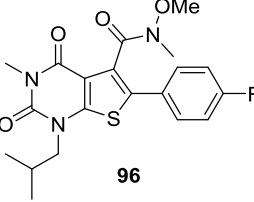
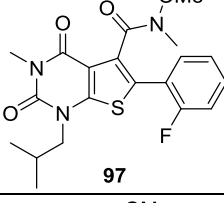
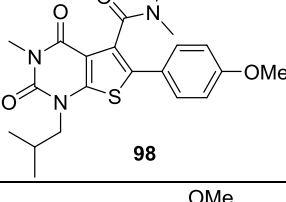
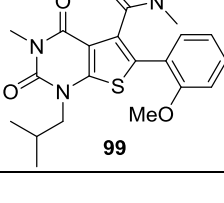
Physicochemical Property	Ideal Measurement
$\text{Log}P$	< 4.0
P_m	< 0.5
K_m	< 250
%PPB	$< 95\%$

All the compounds prepared in this project were assessed using these methods (**Table 7**). The results which lie out with the desired parameters are shown in red. For the majority of these potential imaging agents, excellent physicochemical properties are shown, with all of the values falling well within the ideal limits. The $\text{Log}P$ values were low, but as expected the iodinated compounds showed higher values than observed for the fluorinated counterparts. In the case of the C-6 phenyl derivatives, an increase in $\text{Log}P$ was observed for the diethyl carboxamide analogues. However, the $\text{Log}P$ values for these compounds were only marginally higher than the desired upper limit which is why some of these were chosen for further testing (see compound **95**). In the case of several iodinated compounds, the %PPB is slightly higher than the ideal limit yet in the case of **63**, where every other parameter is good, this was still deemed acceptable. Based on this preliminary assessment, a number of these compounds were selected for biological testing.

Table 7: Physiochemical properties of synthesised compounds

Structure	MW	LogP	P_m	K_m	%PPB	Selected for biological testing?
 <p>100</p>	488.38	2.68	0.07	34.17	84.9	Yes
 <p>63</p>	511.38	3.67	0.45	228.74	96.3	Yes
 <p>64</p>	511.38	4.18	0.39	199.26	96.6	No
 <p>65</p>	403.47	3.78	0.18	74.57	88.9	Yes
 <p>66</p>	403.47	3.28	0.17	68.17	87.8	No
 <p>73</p>	435.47	3.84	0.21	92.93	91.1	Yes
 <p>75</p>	543.38	4.11	0.57	310.25	98.9	No

 <p>76</p>	543.38	4.01	0.40	216.53	95.9	No
 <p>88</p>	445.51	3.02	0.12	248.28	87.8	Yes
 <p>89</p>	445.51	2.97	0.17	77.39	93.2	Yes
 <p>90</p>	457.55	2.94	0.18	82.00	90.5	Yes
 <p>91</p>	457.55	2.87	0.16	75.01	92.4	Yes
 <p>92</p>	431.53	3.67	0.44	189.16	95.8	Yes
 <p>93</p>	431.53	3.63	0.42	181.54	96.4	No
 <p>94</p>	443.56	3.69	0.25	111.51	90.5	No

 <p>95</p>	443.56	4.22	0.33	147.24	93.4	Yes
 <p>96</p>	419.47	3.38	0.23	96.05	87.8	Yes
 <p>97</p>	419.47	3.32	0.17	69.68	88.2	No
 <p>98</p>	431.51	3.52	0.20	88.19	88.4	Yes
 <p>99</p>	431.51	3.53	0.18	76.75	86.3	Yes

2.2.5 Biological evaluation

A selection of compounds then underwent preliminary testing in an activation assay performed by Dr Holger Becker at the Institute of Physiological Chemistry, University of Veterinary Medicine in Hannover, Germany. In this assay, the compounds were tested as lactate uptake inhibitors of monocarboxylates 1, 2, and 4 in *Xenopus* oocytes (**Figure 10**). Along with the selected compounds and the known inhibitor **100**, a blank control experiment was carried out with no inhibitor included. Neither of the tested benzyl amide derivatives (**63** and **65**) showed any inhibitory effect against any of the monocarboxylate transporters. This suggests that having a substituent at the 6-position of the core structure is vital. None of the C-6 phenyl derivatives showed any reduction in lactate uptake against MCT 1 however, morpholine carboxamide **89** did exhibit substantial activity against MCT 2 at a 1 μ M concentration. Several other morpholine carboxamides also showed a small reduction in lactate uptake in MCT 2 and a considerable amount against MCT 4 (see **88**

and **91**). This indicates that a morpholine amide is more suitable for activity against MCT 2 and MCT 4 than a Weinreb amide or a diethylamide. The only compound which showed any significant decrease in lactate uptake against MCT 1 was **73**, which implies that the shape of the compound caused by the ether linkage at the 6-position of the thiophene ring is important.

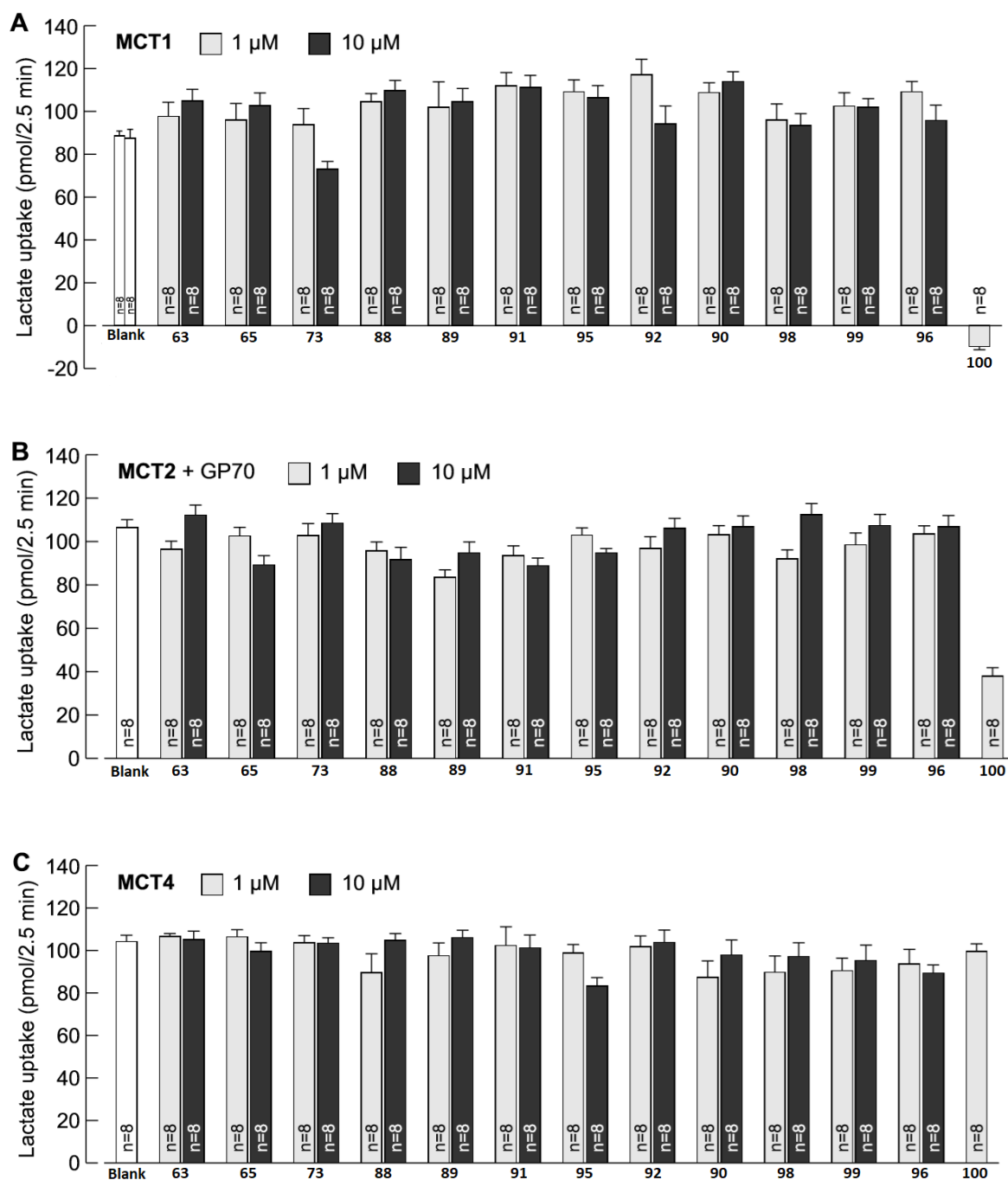


Figure 10: Graphs showing the amount of lactate uptake by MCT 1 (A), MCT 2 (B) and MCT 4 (C) at both 1 μM and 10 μM of injected compound.

Although most of these compounds are not extremely active, this study has demonstrated the structure activity relationship within these scaffolds. The next stage of biological evaluation will subject these compounds to a competitive binding assay since the most important aspect of a potential imaging agent is strong binding to the biological target.

2.2.6 Second generation compounds

Based on the results from physicochemical testing and the activation assay, a second series of compounds was proposed which would bind more strongly to MCT 1 and 2 (**Figure 11**). With 4-fluorophenoxy derivative, **73** being the most active compound against MCT 1, it was proposed that the shape of these compounds caused by the ether linkage, allowed access to a binding pocket which was unable to be reached when aryl groups were directly attached to the thiophene core. Therefore, the new scaffolds would either contain an ether or a methylene linkage to the aryl substituent at the 6-position.

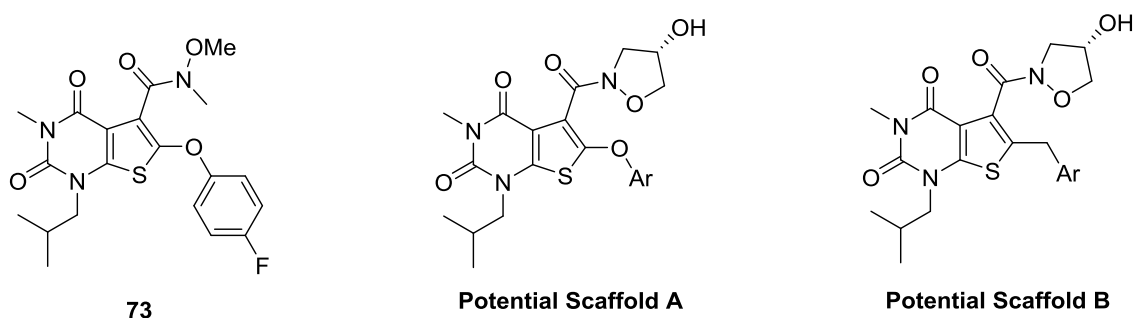
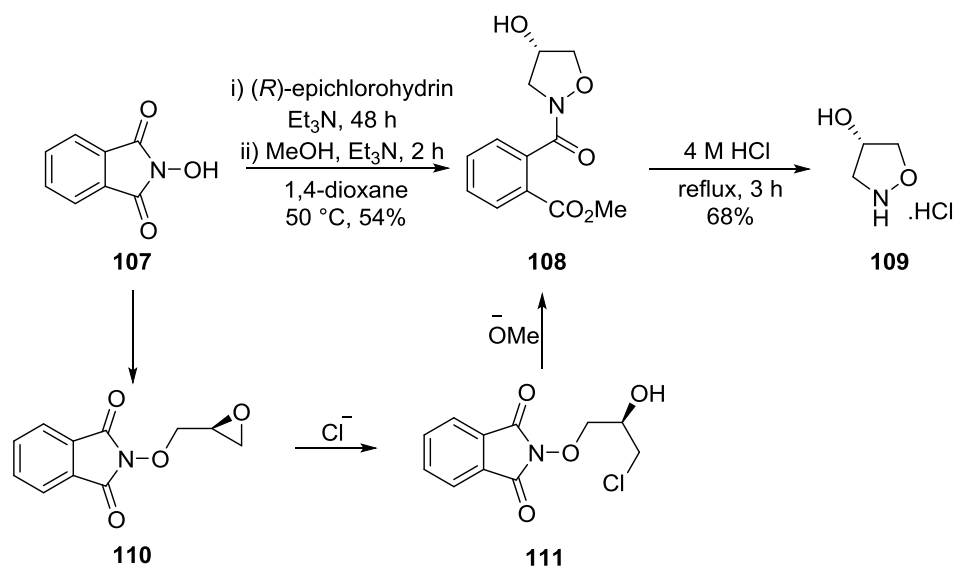


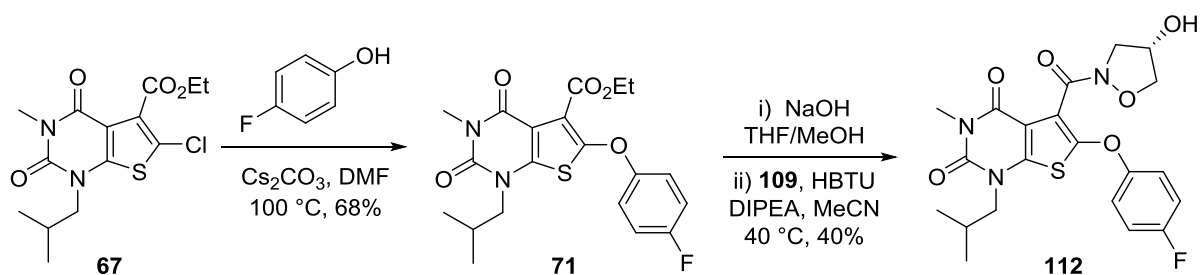
Figure 11: Potential scaffolds for a new series of potential imaging agents.

Furthermore, these new compounds would be prepared with a (4*S*)-hydroxyisoxazolidine component at the 5-position. In studies conducted by AstraZeneca, this amide was found to yield extremely active compounds. (4*S*)-Hydroxyisoxazolidine was synthesised as the hydrochloride salt in two steps from *N*-hydroxyphthalimide (**Scheme 32**).⁷³ Firstly, *N*-hydroxyphthalimide was alkylated with epichlorohydrin, followed by chloride anion opening of the oxirane ring. Intermediate **111** then undergoes nucleophilic attack at the carbonyl of the phthalimide by methoxide. The next step is an intramolecular *N*-alkylation, giving compound **108** in a 54% yield. Acidic hydrolysis using 4 M hydrochloric acid was then carried out to furnish desired compound **109** in a 68% yield.



Scheme 32: The two-step synthesis of (4*S*)-hydroxyisoxazolidine hydrochloride.

The first new compound contained the 4-fluorophenoxy component, installed *via* a substitution reaction between **67** and 4-fluorophenol (**Scheme 33**). Compound **71** then underwent base mediated hydrolysis, followed by an amide coupling with **109** to give compound **112** in a 40% yield over the two steps.

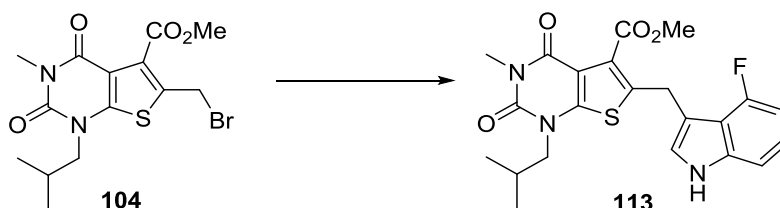


Scheme 33: Route towards compound **112**.

In order to examine the effects of a methylene unit at the 6-position, 4-fluoroindole was chosen as a side chain. The presence of a heteroatom could lead to favourable hydrogen bonding interactions within the binding site. Compound **104** was employed for the alkylation with 4-fluoroindole (**Table 8**). Several conditions were examined to generate the alkylated compound **113**. During the synthesis of compound **105**, sodium hydride was used to facilitate the alkylation (**Scheme 30**). However, in this case no product was formed under these conditions (**entry 1**). It was thought that this was due to sodium hydride being a hard base, therefore other methods were investigated. In a second attempt, 4-fluoroindole was treated with *n*-butyllithium and zinc chloride (used in a transmetallation reaction to

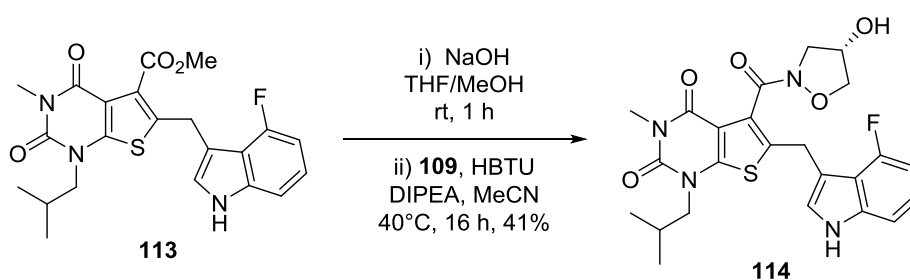
furnish a softer nucleophile). Compound **104** was then added along with a catalytic amount of sodium iodide (used to improve the leaving group ability of **104**). Although a reaction was observed in this method, the yield was poor and difficult to reproduce (**entry 2**). A final attempt used sodium hydrogen carbonate as a base for the alkylation (**entry 3**). This gave adduct **113** in a modest 30% yield.

Table 8: Methods for the synthesis of compound **113**.



Entry	Reagents	Yield (%)
1	NaH, THF, rt, 24 h,	No Reaction
2	i) <i>n</i> -BuLi, ZnCl ₂ , THF, 0°C–rt, 3 h ii) NaI, toluene, rt, 72 h	15
3	NaHCO ₃ , CHCl ₃ , H ₂ O, rt, 72 h	30

Compound **113** was then hydrolysed with sodium hydroxide and the resulting carboxylic acid was used to install the (4*S*)-hydroxyisoxazolidine moiety at the 5-position *via* an HBTU mediated coupling. This gave novel compound **114** in a 41% yield (**Scheme 34**).

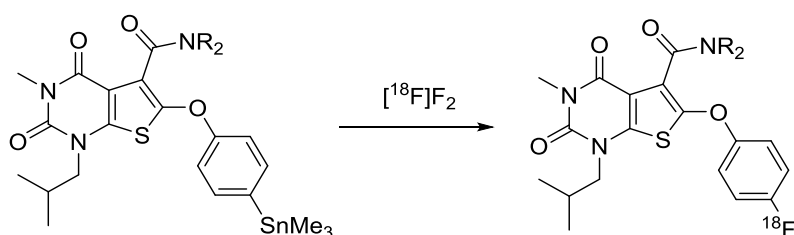


Scheme 34: The two-step synthesis of **114** by ester hydrolysis and HBTU mediated amide coupling.

2.3 Conclusions and future work

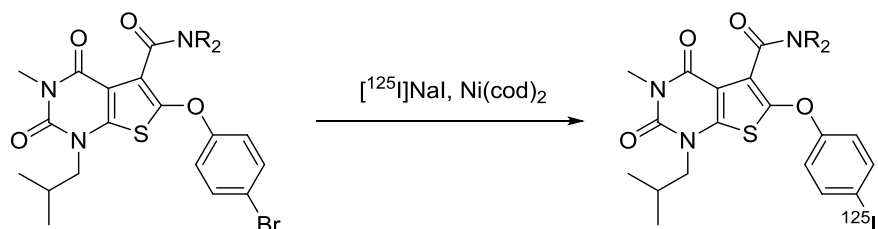
Several series of AR-C155858 **41** analogues have been synthesised with aryl groups in various positions which have the ability to be radiolabelled. The physicochemical properties were assessed, showing that the majority of these compounds will demonstrate good bioavailability. A select group of these compounds were tested for the inhibitory effect on lactate uptake against MCT 1, 2 and 4. These results led to the synthesis of a further series of compounds, which based on the structure-activity relationship observed, should bind more strongly to MCT 1 and 2.

The next stage for these compounds is to undergo a displacement binding assay to assess whether or not they have high affinity for MCT 1 and 2. The best candidates will be radiolabelled for PET or SPECT imaging. For PET imaging, the most likely method will be *via* a fluorodestannylation reaction, using an electrophilic fluorine source (**Scheme 35**).



Scheme 35: An example of electrophilic radiofluorination using a fluorodestannylation reaction.

For SPECT imaging, the iodine-125 unit would most likely be installed *via* a nickel catalysed halogen exchange reaction (**Scheme 36**).²¹ Once the lead candidates have been successfully radiolabelled, the development of these compounds for the imaging of MCT in mouse models would then begin.



Scheme 36: An example of a nickel catalysed halogen exchange reaction for radioiodination.

3. The synthesis of novel PET imaging agents based on PARP-1 inhibitors

3.1 Introduction

3.1.1 PARP-1 and its function in DNA repair

The poly(ADP-ribose) polymerase (PARP) family consists of 17 different proteins. Within this family, PARP 1–4 and tankyrases 1 and 2 have the ability to perform post-translational modifications *via* poly ADP-ribosylation.⁷⁴ PARP-1, which accounts for more than 90% of ADP-ribosylation, consists of 3 domains. The DNA binding domain consists of two zinc fingers which are used in the binding of PARP-1 to single strand DNA breaks (SSB's). The automodification domain includes glutamate and lysine residues which serve as acceptors of ADP-ribose and allow the enzyme to poly ADP-ribosylate itself. Finally, the catalytic domain is used to transfer ADP-ribose moieties from nicotinamide adenine dinucleotide (NAD⁺) to protein acceptors, forming ADP-ribose polymers.⁷⁵ PARP-1 activity is stimulated by various types of DNA damage. Using the two zinc fingers, PARP-1 binds to the damaged DNA and ADP-ribosylation occurs, rapidly consuming NAD⁺. Due to the large size and charge density of the poly(ADP-ribose) (PAR) formed, the functions of modified proteins such as histones and DNA protein kinases are altered. This causes the DNA to unwind and for the damaged DNA to become exposed. The presence of PAR recruits various DNA repair proteins, which fix DNA *via* base excision repair (BER). Poly(ADP-ribose) glycohydrolase (PARG) is also recruited and is used to break down the ADP-ribose polymers so the site is more accessible for the DNA repair enzymes (**Figure 12**).

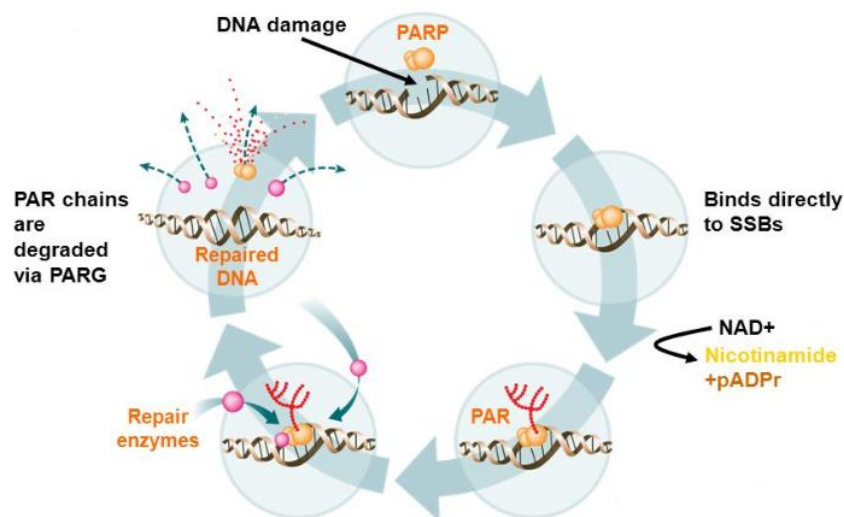


Figure 12: The role of PARP-1 in the repair of damaged DNA. Reprinted with permission from *Journal of Oncology*, 2010, Article ID 151750.⁷⁶

3.1.2 PARP-1 inhibitors in cancer treatment

PARP-1 inhibitors can be used in the treatment of cancer *via* two different approaches. The first is the combination of PARP-1 inhibitors with DNA-damaging chemotherapy. When a chemotherapeutic agent is used in the destruction of cancer cells, PARP-1 can be used to repair these cells, leading to drug resistance and continued tumour growth. However, inhibition of PARP-1 would hinder cancer cell DNA repair and ultimately lead to cell death.^{77,78} The second type of therapeutic action is to target cells which are predisposed to die when PARP activity is lost. For example, PARP-1 inhibitors are particularly effective in tumours which are deficient in breast cancer susceptibility protein 1 (BRCA-1) and 2 (BRCA-2). BRCA-1 and 2 are used in the repair of double strand DNA breaks through homologous recombination (HR). However, in BRCA-1 and 2 deficient tumours, this process cannot occur and therefore, cancer cells rely on the presence of PARP enzymes to repair DNA by base excision. Therefore, PARP-1 inhibition in these types of tumours lead to genomic instability and cell death. This process is referred to as synthetic lethality (**Figure 13**).⁷⁹

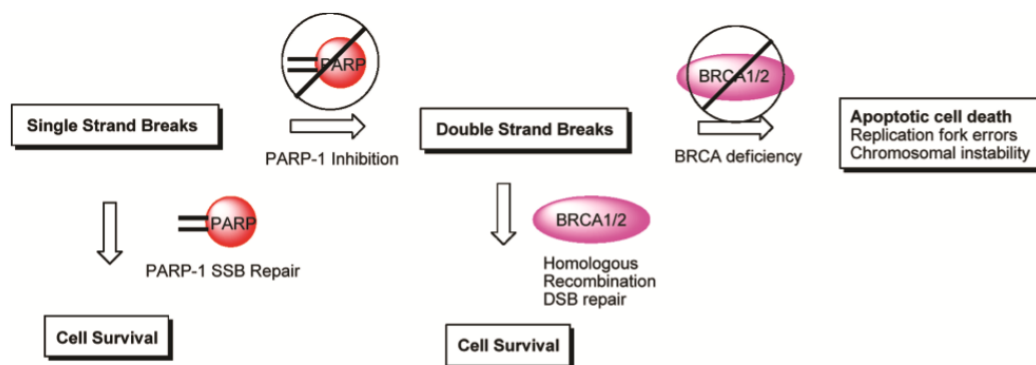


Figure 13: Synthetic lethality caused by PARP inhibition in BRCA-1 and 2 deficient tumours. (Reprinted with permission from *J. Med. Chem.*, 2010, **53**, 4561. Copyright 2010 American Chemical Society).⁷⁷

There have been many PARP-1 inhibitors synthesised for this purpose, one of the most successful being olaparib **115** (**Figure 14**) which has recently been licensed as a drug for advanced BRCA deficient ovarian cancer.⁸⁰

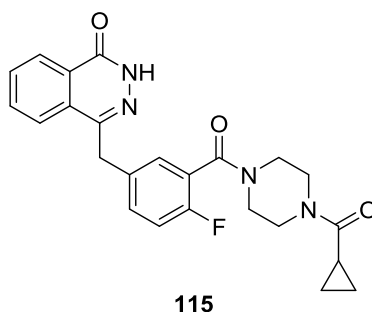


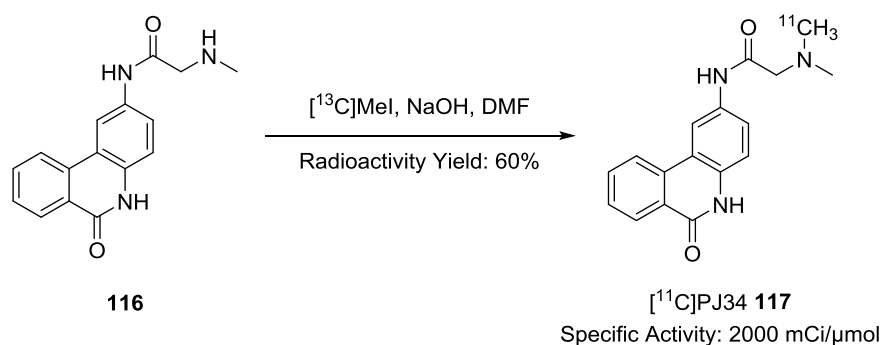
Figure 14: Olaparib- A potent PARP-1 inhibitor used in the treatment of BRCA deficient ovarian cancer.

3.1.3 Imaging agents targeting PARP-1

The non-invasive imaging of PARP-1 using a radiolabelled PARP inhibitor could have many clinical advantages. It could guide dosing decisions by assessing the extent of uptake and retention of the PARP-inhibitor in different tissues, and therefore the duration of the inhibition effect. This approach could be particularly important in cases where PARP inhibitors are used in combination with DNA damaging chemotherapy drugs since bone marrow toxicity has previously been observed as a result of these combinations.^{81,82} Imaging of PARP-1 can also be used to diagnose and monitor various tumours. For example, glioblastomas (GBM) are known to overexpress PARP-1, therefore, this type of

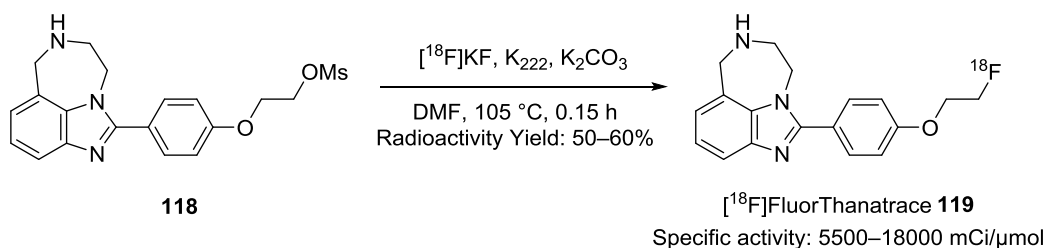
cancer could be monitored *via* PET imaging assuming the tracers were able to penetrate the BBB.⁸³

One of the first PARP-1 imaging agents was the phenathridinone PJ34 **117** which was used initially to assess the PARP-1 activity in tissues undergoing necrosis.⁸⁴ It was able to bind to PARP-1 with high affinity and was found to accumulate in tissues where PARP-1 is hyperactivated. The radiolabelling was carried out by a methylation using carbon-11 labelled methyl iodide and sodium hydroxide, giving the desired product in a good radioactivity yield and high specific activity (**Scheme 37**).



Scheme 37: Synthesis of $[^{11}\text{C}]\text{PJ34 117}$ *via* radioactive methylation using carbon-11 labelled methyl iodide.

One of the most successful recent PARP-1 imaging agents is $[^{18}\text{F}]\text{FluorThanatrace 119}$ developed by Zou *et al.*⁸⁴ This tracer has been found to bind to PARP-1 with high affinity and also has proven to be metabolically stable. PET studies also showed an increased uptake of **119** in tumour cells. Pre-treatment with olaparib **115** was found to block the uptake of **119**, proving that this binds to PARP-1 with high specificity *in vivo*. The radiolabelling of **118** was carried out *via* a substitution of the mesylate group using $[^{18}\text{F}]\text{potassium fluoride}$ to give **119** in a high radioactivity yield (**Scheme 38**).



Scheme 38: Radiosynthesis of $[^{18}\text{F}]\text{FluorThanatrace 119}$.

3.1.4 Previous work and proposed research

Within the Sutherland group various analogues of olaparib **115** have been previously synthesised. Three lead compounds for the PET and SPECT imaging of PARP-1 were identified (**Figure 15**).

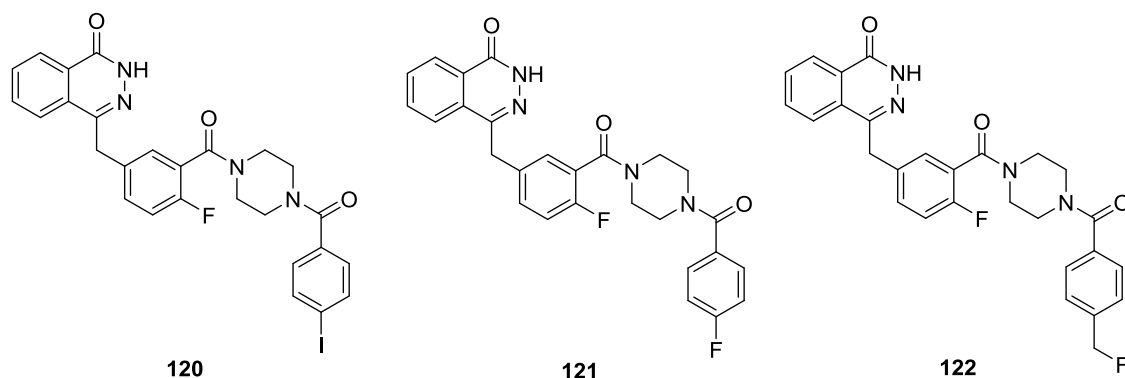
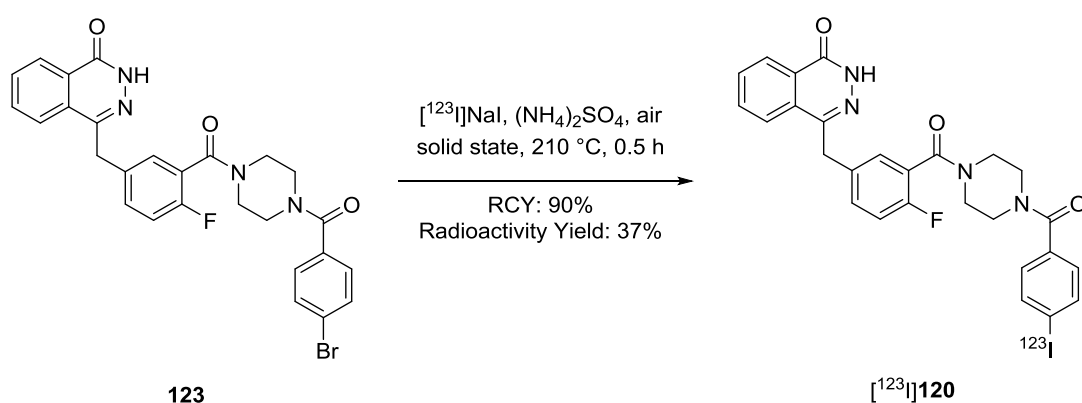


Figure 15: Initial lead PARP-1 inhibitors to be used as PET or SPECT imaging agents.

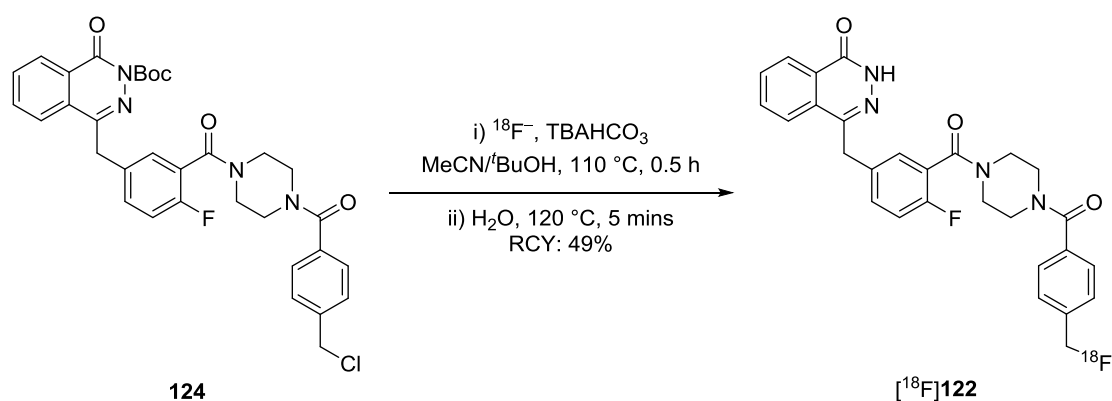
Compound [¹²³I]**120** was synthesised from corresponding bromide **123** using a solid state halogen exchange reaction to give the desired product in high radioactivity yield (**Scheme 39**).⁸⁵ This compound was found to be a potent inhibitor of PARP-1 in two human glioblastoma cell lines and was also highly stable in mouse plasma. It was further evaluated *via ex vivo* biodistribution studies where tumour tissue retention and specific binding to PARP-1 was observed. However, the intrinsic clearance was significantly greater than for olaparib **115**, suggesting a more rapid *in vivo* metabolism.



Scheme 39: Solid state halogen exchange reaction used to synthesis [¹²³I]**120**.

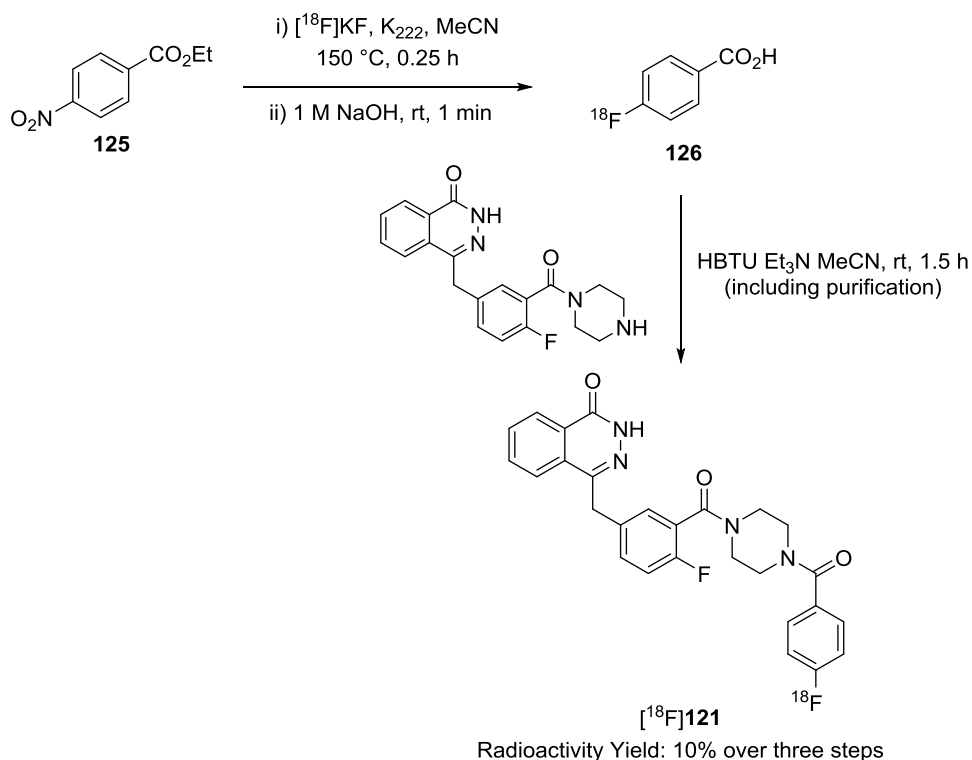
The radiosynthesis of [¹⁸F]**121** was examined to generate a potential PET imaging agent. However, under various conditions the radiochemical yields were very poor. Therefore, compound **122** was synthesised as an alternative PET tracer since the formation of an

alkyl-fluorine bond would be less challenging than aryl C-F bond formation. [^{18}F]**122** was synthesised by nucleophilic substitution of the chlorine analogue **124** (Scheme 40).⁸⁶ The phthalazinone-NH had to first be protected with a Boc group, as it was found that self oligomerisation occurred through nucleophilic substitution between the phthalazinone core and the chlorine bearing carbon. After fluorination and subsequent Boc deprotection, a radiochemical yield of 49% was achieved. Unfortunately, this compound underwent partial *in vivo* metabolic defluorination in mouse studies, causing free radiofluoride to bind to the bone. This limits the use of [^{18}F]**122** as a PET imaging agent due to the potential signal noise radiating from the skull as a consequence of [^{18}F]fluoride uptake.



Scheme 40: Radiofluorination *via* nucleophilic substitution of **124** and successive Boc deprotection.

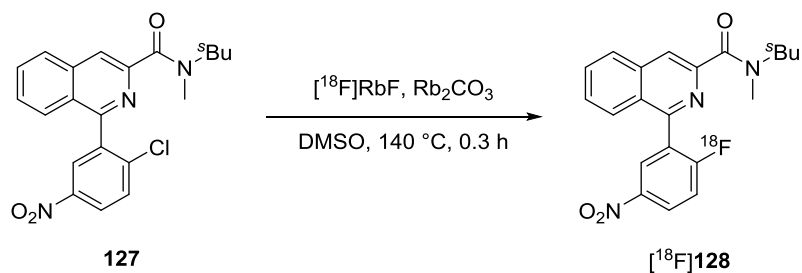
In 2015, Reiner and co-workers synthesised [^{18}F]**121** and were able to show that this compound can be used to non-invasively image PARP-1 expression of gliomas in mouse models *via* PET imaging.⁸⁷ This compound also does not appear to undergo the metabolic defluorination associated with [^{18}F]**122**. However, the radiosynthesis of [^{18}F]**121** requires early incorporation of radiofluorine into a benzoic ester derivative, which then must be hydrolysed and coupled with a phthalazine-1-one (Scheme 41). Due to the early incorporation of the radiolabel and the relatively short half-life of fluorine-18, a radiochemical yield of only 10% was achieved.



Scheme 41: Route towards $[^{18}\text{F}]\mathbf{121}$ developed by Reiner and co-workers.

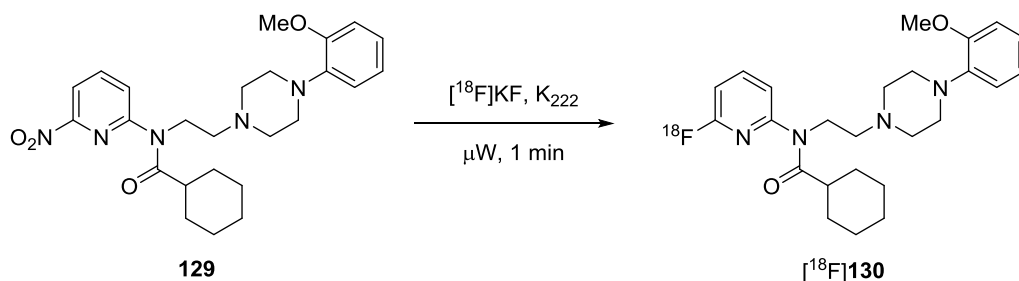
Clearly having the fluorine-18 moiety installed onto an aromatic system could lead to a more promising PET imaging agent for PARP-1 than one with an alkyl-fluorine moiety present. However, installing the radiolabel should ideally be the last step for an efficient and high yielding synthesis. So based on these observations, this research project focused on the synthesis of novel PET imaging agents for PARP-1 with benzamide units activated towards facile radiofluorination.

In 2016, Gouverner and co-workers published a review which quantified the features required on an aromatic ring to facilitate nucleophilic aromatic substitution reactions with radiofluorine.¹³ It is well known that having electron-withdrawing groups present can activate a ring towards $\text{S}_{\text{N}}\text{Ar}$ reactions. It was found that in particular, having a nitro group present at either the *ortho*- or *para*- position to the leaving group resulted in the most successful reactions. **Scheme 42** shows an example of a *para*-nitro group being used to facilitate the radiolabelling of $[^{18}\text{F}]\text{PK14105}$ **128**, which is used in PET studies of peripheral type benzodiazepine binding site receptors.⁸⁸



Scheme 42: The radiosynthesis of [^{18}F]PK14105 **128**.

The π -deficient ring of pyridine containing compounds can also promote easy radiofluorination. **Scheme 43** shows radiofluorination *via* an $\text{S}_{\text{N}}\text{Ar}$ reaction on a pyridine ring to give a [6-pyridinyl- ^{18}F]-labelled derivative of WAY-100635 **130**, a potential PET imaging agent for brain 5-HT $_{1\text{A}}$ receptors.⁸⁸



Scheme 43: Radiofluorination facilitated by the presence of a π -deficient pyridine ring.

Therefore, it was proposed that the new potential imaging agents synthesised would either contain appropriately placed electron withdrawing groups on the aromatic ring to be labelled or a π -deficient pyridine ring with a potential labelling site (**Figure 16**).

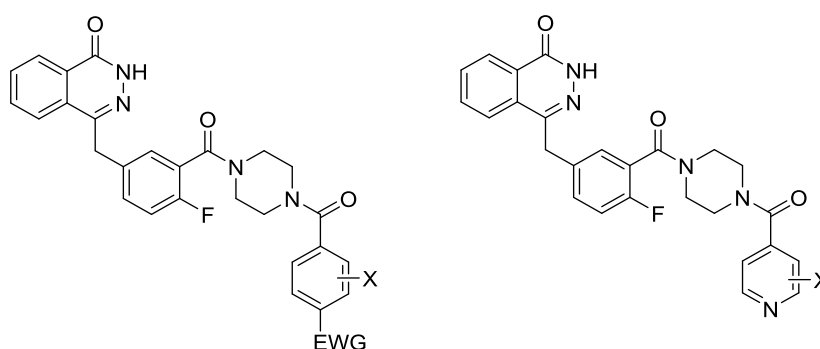


Figure 16: Proposed novel PET imaging agents (X= Fluorine-18).

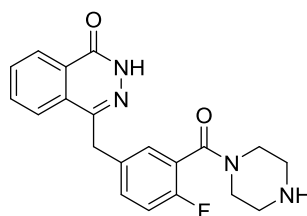
The new compounds were synthesised as the “cold” fluorine-19 analogues to act as a mimic for the radioactive counterparts during physiochemical and biological testing.

Analogues which contain appropriate leaving groups were also prepared in order to explore potential radiofluorination methods.

3.2 Results and discussion

3.2.1 Synthesis of the olaparib core structure

The first project aim was to synthesis the olaparib core structure **131** (**Figure 17**). It has previously been demonstrated that provided this core structure is present, groups of various size and electronic properties can be installed at the 4-position of the piperazine ring without significantly affecting the affinity of the compounds for the PARP-1 binding site, or their inhibition activities against the enzyme.⁸⁹



131

Figure 17: Olaparib core structure.

Several key interactions have been identified between PARP inhibitors and the PARP-1 binding site (**Figure 18**). It was found that non-polar π - π stacking occurs between the aromatic region of the phthalazinone core and tyrosine-907. The amide portion of the phthalazinone is able to hydrogen bond to a serine residue and also to a glycine residue *via* a bidentate interaction. Finally, the *meta*-benzyl positioned carbonyl acts as a hydrogen bond acceptor and is able to interact with methionine-890.^{90,91}

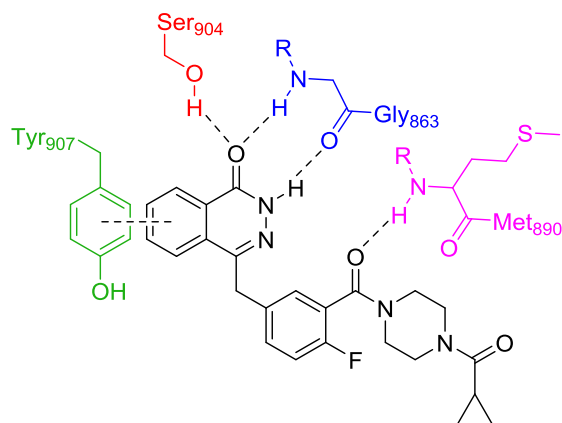
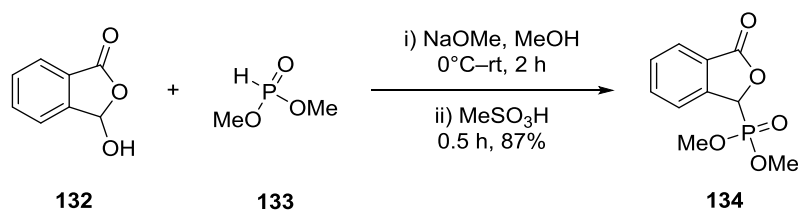


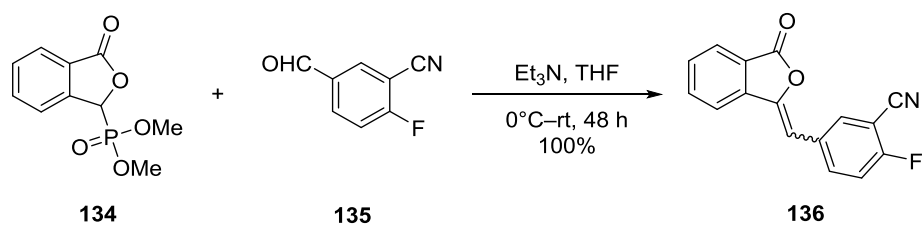
Figure 18: An image showing olaparib **115** and the key interactions with the PARP-1 binding site.

The synthesis of this core structure was initially reported by Menear *et al.* and further optimised by Adele Blair, a previous member of the Sutherland group.⁹² The first step of this sequence is the phosphorylation of carboxybenzaldehyde **132**. This was achieved by coupling with dimethylphosphite (**133**) in the presence of sodium methoxide to give phosphonate ester **134** in an 87% yield (**Scheme 44**).



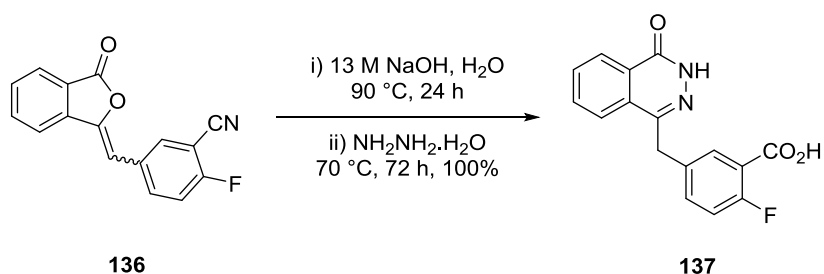
Scheme 44: Phosphorylation of carboxybenzaldehyde **132**.

The next stage involves a Horner-Wadsworth-Emmons (HWE) reaction with 2-fluoro-5-formylbenzonitrile (**135**) and phosphonate ester **134**, which gave **136** in a quantitative yield (**Scheme 45**). Due to the *E*-selective nature of the HWE reaction, a 75:25 mixture of the *E* and *Z* isomers was obtained (as observed by ¹H NMR spectroscopy). These isomers were not separated because both react in the next step.



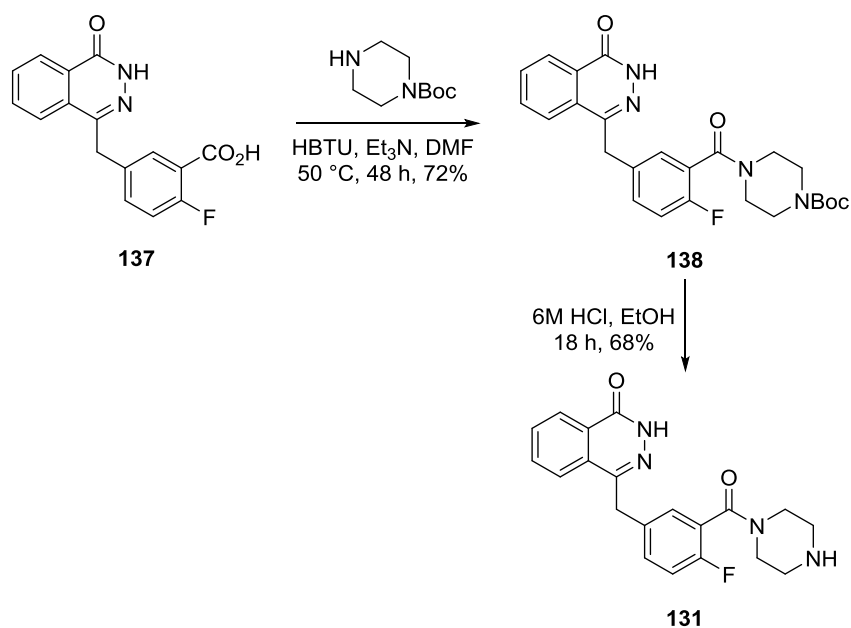
Scheme 45: Horner-Wadsworth-Emmons reaction to generate alkene **136**.

The phthalazinone moiety was prepared *via* a one-pot, two-step reaction which occurred in a quantitative yield over the two steps. The first step involved hydrolysis with 13 M sodium hydroxide, followed by reaction with hydrazine monohydrate to give phthalazinone **137** (Scheme 46).



Scheme 46: Synthesis of phthalazinone **137** by a one-pot, two-step reaction.

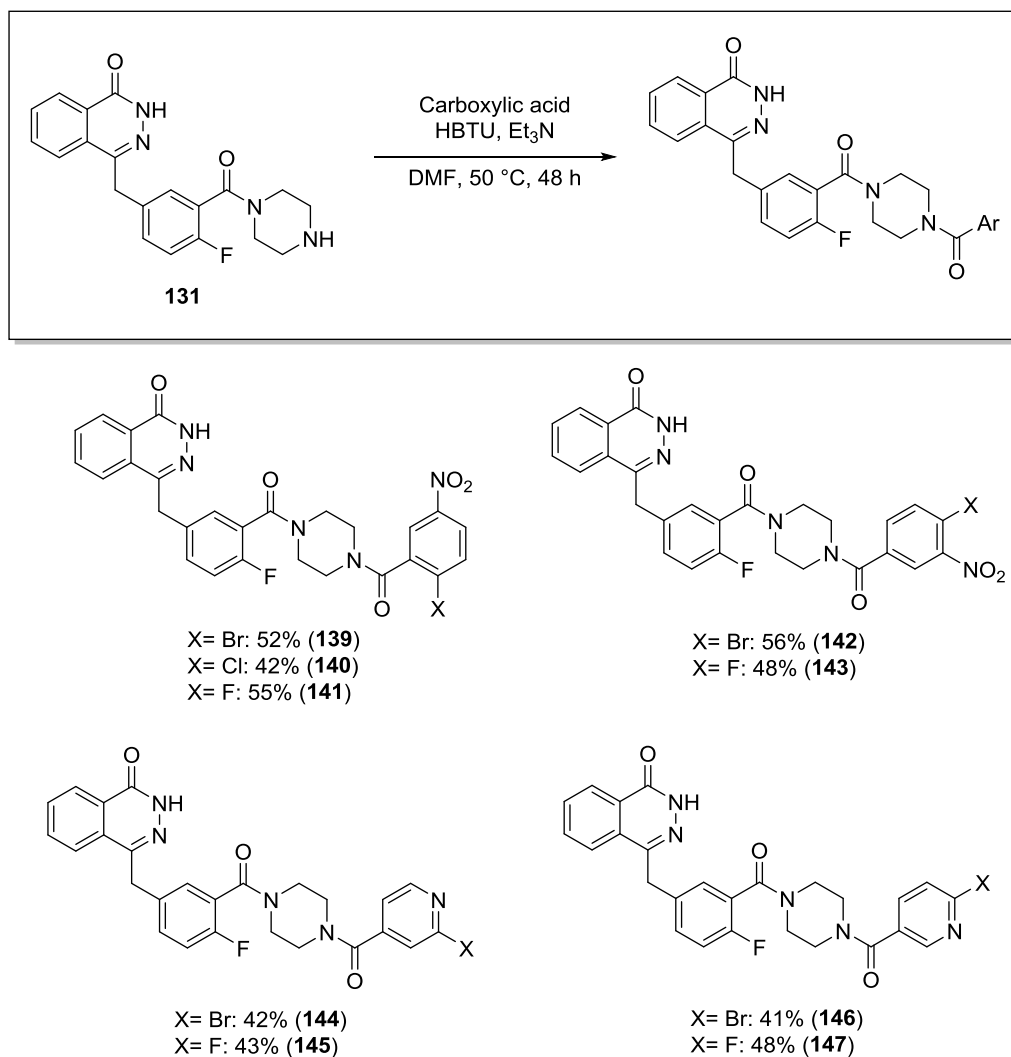
The piperazine ring was installed by coupling carboxylic acid **137** with a Boc-protected piperazine unit. This was achieved using HBTU as the coupling reagent and gave amide **138** in a 72% yield. The final step was Boc-deprotection of the piperazine unit which gave the olaparib core **131** in a 68% yield (Scheme 47).



Scheme 47: Synthesis of the olaparib core structure *via* an amide coupling and hydrolysis.

3.2.2 Synthesis of potential PARP-1 imaging agents

With the olaparib core synthesised, the next stage was to install an electron-deficient benzamide group onto the 4-position of the piperazine ring. This was achieved by an amide coupling using various carboxylic acids and HBTU as the coupling agent (**Scheme 48**). Compounds **139–143** contain a nitro group in either the *ortho*- or *para*- position (with respect to the labelling site) as this aromatic system has previously been shown to aid nucleophilic aromatic substitution-type fluorination. Compounds **144–147** contain a pyridine ring with the labelling site *ortho*- to the nitrogen. These compound are also promising in terms of facile fluorination due to the π -deficient ring system. Each type of compound was prepared with a fluorine in the labelling site, mimicking the radioactive counterpart. Each scaffold was also synthesised with either a bromine or a chlorine in the labelling position to be used as a leaving group when examining radiofluorination methods. All of these novel olaparib analogues were synthesised in moderate to good yields.



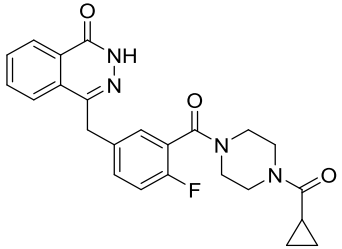
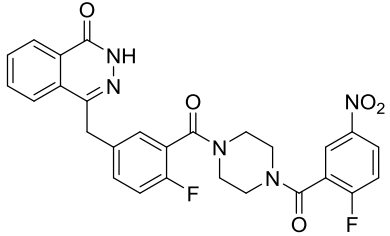
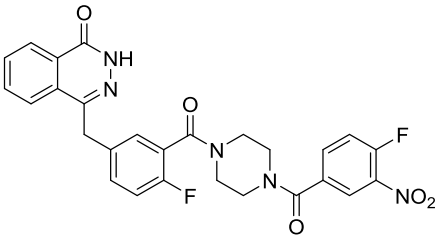
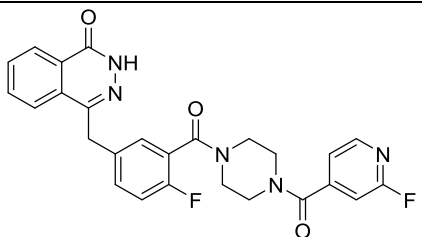
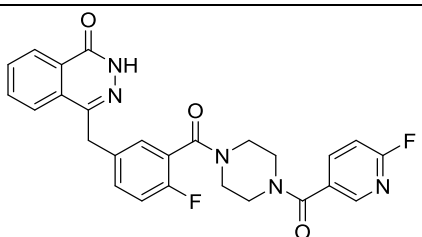
Scheme 48: Synthesis of novel PARP-1 inhibitors by an HBTU mediated amide coupling.

3.2.3 Physicochemical testing and biological evaluation of potential PARP-1 imaging agents

To determine whether these compounds would be appropriate imaging agents, their physicochemical properties were determined by HPLC methodology (see **Section 2.2.4**).⁶⁷ Based on all of the properties examined, all four scaffolds have significant potential as PARP-1 imaging agents (**Table 9**). The Log*P* and %PPB values are higher than reported for olaparib itself, however the given values still lie well below the upper limits for a suitable imaging agent (**Section 2.2.4, Table 6**). The membrane partition coefficient and permeability exhibited by these compounds is also extremely promising. Maria Clara Liuzzi of the Sutherland group recently tested these scaffolds for the ability to bind to and inhibit PARP-1. This was done *via* a PARP cellular immunofluorescence assay, performed

in G7 stem cell lines. The IC₅₀ value for olaparib **115** was also obtained using this method to act as a standard. The inhibitory properties of compound **143** could not be assessed because the compound itself showed some fluorescent properties which interfered with the immunofluorescence assay. The tested compounds were all shown to be effective PARP-1 inhibitors, with compounds **141** and **147** being even more potent than olaparib **115**.

Table 9: Physicochemical properties and IC₅₀ values of potential PARP-1 imaging agents.

Structure	MW	LogP	P _m	K _m	%PPB	IC ₅₀
 <p style="text-align: center;">115</p>	434.47	1.95	N/A	N/A	75.9	1.17
 <p style="text-align: center;">141</p>	533.49	2.66	0.07	33.51	89.7	0.93
 <p style="text-align: center;">143</p>	533.49	2.69	0.12	63.66	90.8	N/A
 <p style="text-align: center;">145</p>	489.48	2.18	0.03	13.92	84.2	1.23
 <p style="text-align: center;">147</p>	489.48	2.16	0.03	13.62	83.6	0.38

3.2.4 Synthesis of a novel olaparib based scaffold

As mentioned in section 3.2.1, it has been extensively demonstrated that capping groups of various size and shape can be installed onto the 4-position of the piperazine ring, without affecting compound potency, assuming the phthalazinone core is present. In 2010, Reiner *et al.* demonstrated that even very large functional groups, with long hydrocarbon chains could be installed without a detrimental effect on PARP-1 binding affinity or its inhibition (e.g. **Figure 19**).⁹³ This can be rationalised by the presence of a large hydrophobic pocket in the PARP-1 binding site.

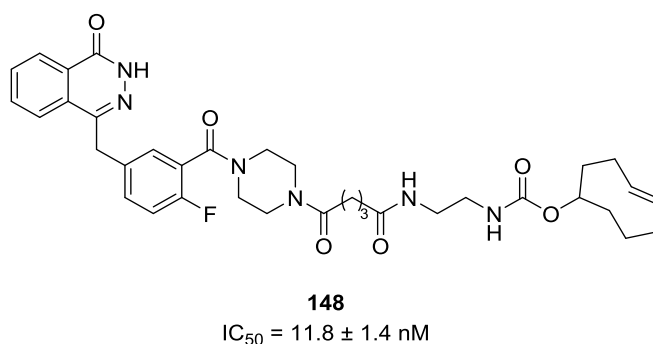
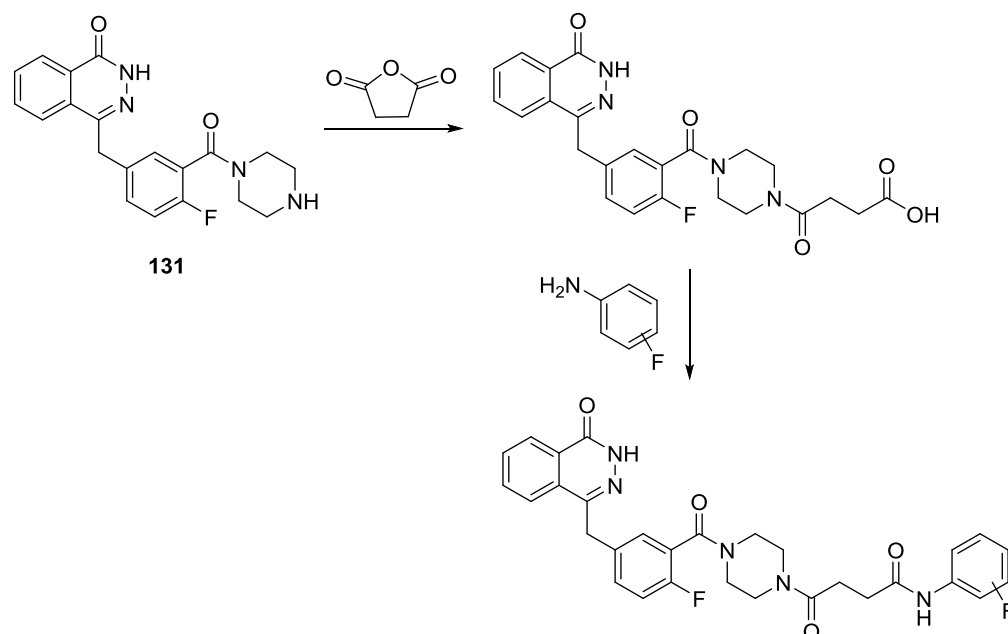


Figure 19: PARP-1 inhibitor with large capping group at the 4-NH-piperazine moiety.

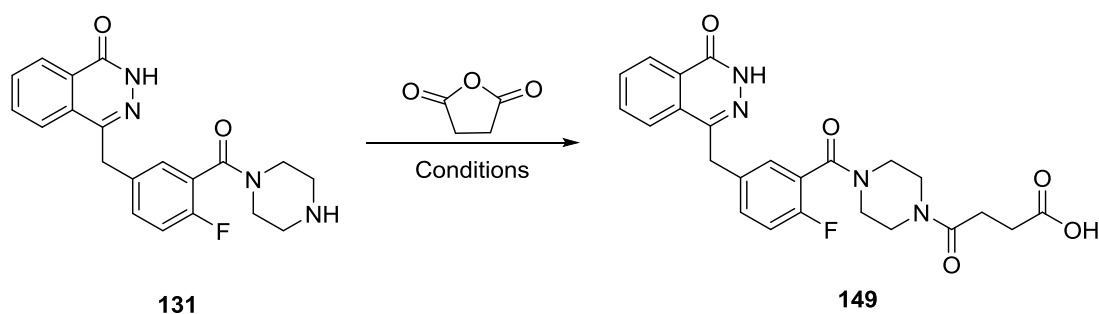
Based on the success of these structures, it was proposed that potential novel imaging agents could be synthesised using a similar scaffold. It was suggested that a reaction between the piperazine moiety of phthalazinone **131** and succinic anhydride could occur to acetylate the amine and incorporate a pendent carboxylic acid group. Several fluorinated anilines would then be used in an amide coupling reaction to generate new potential imaging agents and further explore the structure activity relationship within the PARP-1 binding site (**Scheme 49**).



Scheme 49: Proposed route to alternative imaging agents with a succinic acid linker.

The acetylation was initially attempted by heating under reflux in dichloromethane (**Table 10, entry 1**). However, when no conversion was observed it was thought that a base may be required to initiate the reaction. Triethylamine was used in a second attempt (**entry 2**). Unfortunately, after 48 hours only starting material was present. The next attempt investigated the use of 4-dimethylaminopyridine as a catalyst (**entry 3**). This reaction was very slow and after 72 hours only a 20% conversion was achieved. Addition of a base did not seem to increase the rate of the reaction (**entry 4**). Therefore, the solvent was changed to DMF so that higher temperatures could be used (**entry 5**). This led to complete decomposition. Therefore, acetonitrile and a temperature of 80 °C was chosen as an alternative (**entry 6**). Under these optimised conditions, the desired carboxylic acid product was synthesised in an 82% yield.

Table 10: Optimisation of the acetylation reaction between olaparib core **131** and succinic anhydride.



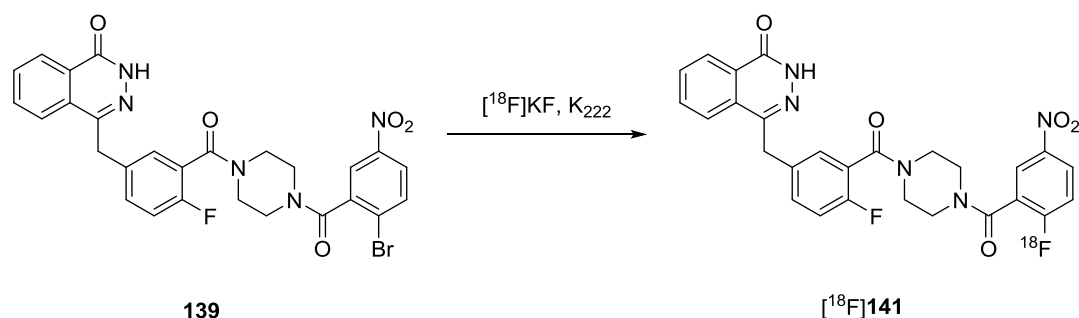
Entry	Solvent	Temperature (°C)	Additive	Time (h)	Result
1	CH ₂ Cl ₂	40	None	48	No reaction
2	CH ₂ Cl ₂	40	Et ₃ N	48	No reaction
3	CH ₂ Cl ₂	40	DMAP	72	20% conversion
4	CH ₂ Cl ₂	40	Et ₃ N, DMAP	48	No reaction
5	DMF	120	Et ₃ N, DMAP	12	Decomposition
6	MeCN	80	DMAP	24	82% yield

With the successful synthesis of the hydrocarbon linker, the next step will be to incorporate various aromatic amines with the potential for radiofluorination. These compounds will then be tested to ascertain whether they have the appropriate physicochemical properties and whether they are capable of specifically binding to the PARP-1 enzyme.

3.3 Conclusions and future work

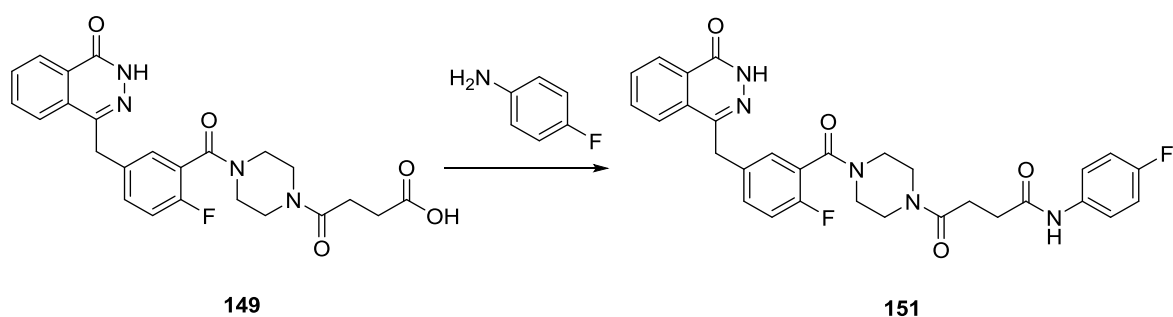
A small library of novel potential imaging agents for PARP-1 have been synthesised. These compounds all exhibit excellent physicochemical properties and due to the electron deficient ring systems, have great potential for facile radiofluorination. These compounds were also tested *via* a PARP cellular immunofluorescence assay to determine whether they bind to PARP-1. Compounds **141** and **147** were found to be potent inhibitors of PARP-1 in G7 stem cell lines. The next stage is to find a suitable method for the radiofluorination of these compounds. To do this, a “cold” fluorination reaction will first be optimised using the brominated or chlorinated analogues. This method will then be adapted for the radiochemical version. A likely successful method would be a nucleophilic aromatic

substitution reaction using labelled potassium fluoride and K_{222} , used to complex the potassium and increase the nucleophilicity of the fluorine anion (**Scheme 50**).



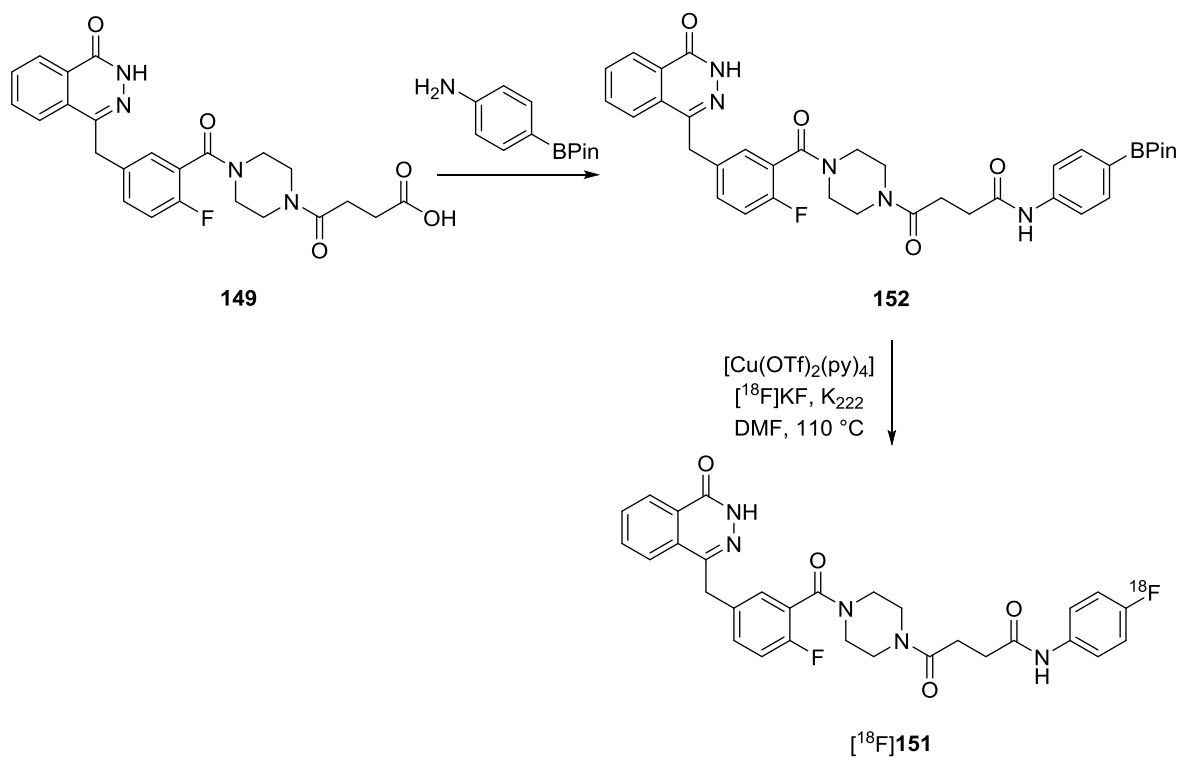
Scheme 50: Radiofluorination of compound **139** via nucleophilic aromatic substitution.

A new scaffold based on Reiner's work has also been synthesised to further explore the structure activity relationships within the PARP-1 binding site. The carboxylic acid moiety of compound **149** will next undergo amide couplings with several fluorinated anilines (**Scheme 51**).



Scheme 51: Example of a potential PARP PET imaging agent formed by an amide coupling with carboxylic acid **149**.

These new compounds will also be tested for binding affinity to PARP-1 and for appropriate physicochemical properties. One of the ways to potentially radiolabel this class of compound is via a copper catalysed fluoro-deboronation using conditions developed by Gouverneur *et al.*⁹⁴ The Gouverneur group has shown this reaction to be successful for a wide range of substrates, many of which would not be amenable to nucleophilic aromatic substitution. This method would first require the synthesis of a boronate ester derivative via an amide coupling with carboxylic acid **149** (**Scheme 52**).



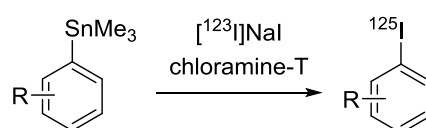
Scheme 52: Potential radiofluorination using a copper catalysed fluoro-deboronation procedure.

4. Gold catalysed radioiododeboronation

4.1 Introduction

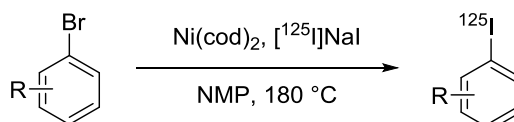
4.1.1 Modern radioiodination methods

Due to the increasing need for novel SPECT imaging agents, many efforts have focused on the development of the efficient radioiodination of aromatic rings. A common method is iododestannylation, discussed in section 1.3.1 (**Scheme 53**).²⁰ Although this method tends to be high yielding, the organotin species is unstable and highly toxic, so there are many safety concerns as well as restrictions in distribution and storage.



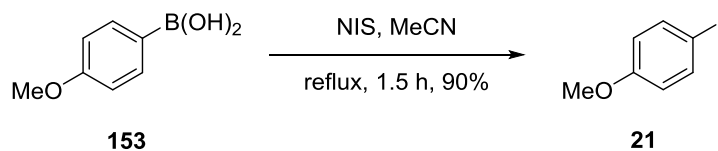
Scheme 53: Radioiodination using a destannylation reaction.²⁰

Another method developed within the Sutherland group involves a nickel-catalysed halogen exchange reaction, discussed in section 1.3.1 (**Scheme 54**).²¹ This method was successful for the radioiodination of aromatic rings containing both electron-donating and electron-withdrawing substituents and could also be used to generate SPECT imaging agents. A disadvantage of this method is the high temperature of 180 °C, which could make it unsuitable for the synthesis of less stable substrates.



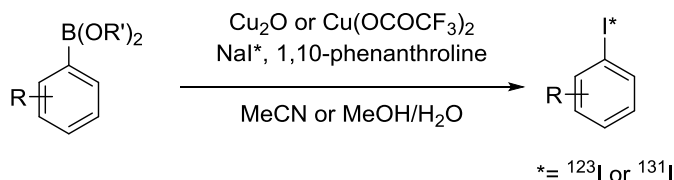
Scheme 54: Nickel-catalysed radioiodination *via* a halogen exchange.²¹

Another common method for iodination is *via* the *ipso*-substitution of aryl boronic acids using *N*-iodosuccinimide (NIS). The reaction was initially developed by Olah and co-workers and high yields were obtained for electron-rich substrates (**Scheme 55**).⁹⁵ However, poor yields were observed for aryl boronic acids containing electron-withdrawing groups, even when long reaction times were employed. Therefore, this method has not been widely adopted in radiosynthesis.



Scheme 55: Iodination *via* an *ipso*-substitution of aryl boronic acids.⁹⁵

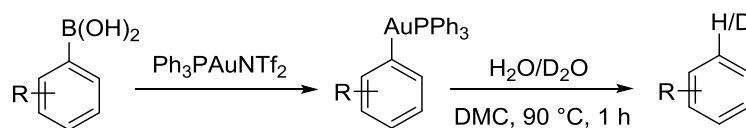
Many variations of this work have been developed with the aim of improving the substrate scope and finding an effective method for the synthesis of SPECT imaging agents. Most recently, there have been various examples of copper-catalysed iododeboronations. For example, in 2016 the groups of Gouverneur and Zhang described a method for the copper-catalysed radioiodination of aryl boronic acids and esters (**Scheme 56**).⁹⁶ The reaction could be performed at room temperature, using a copper catalyst and 1,10-phenanthroline as the ligand. This method is tolerant of electron-rich and electron-poor substrates and can be used to generate SPECT imaging agents in high radiochemical yields. Despite the improved substrate scope, this method does have its limitations. There is still a need to develop a faster radioiodination procedure for arenes, which utilises green solvents and is operationally simple.



Scheme 56: Copper-catalysed radioiododeboronation of boronic acids and esters.⁹⁶

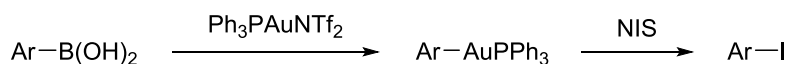
4.1.2 Previous work and proposed research

In 2015, the Lee group developed a gold-catalysed protodeboronation procedure (**Scheme 57**).⁹⁷ This reaction was found to proceed *via* transmetalation of the gold(I) catalyst with an aryl boronic acid to give an organogold intermediate.⁹⁸ The reaction was tolerant of a wide range of functional groups and was able to be extended to deuterodeboronations.



Scheme 57: Gold catalysed protodeboronation and deuterodeboronation.⁹⁷

Based on the success of this procedure, a method for radioiodination was developed using the same gold(I) phosphine catalyst (Gagosz's catalyst) and the environmentally friendly solvent dimethyl carbonate.^{99,100} It was proposed that if the organogold intermediate was to react with NIS, it could provide easy access to the corresponding aryl iodide (**Scheme 58**).¹⁰¹



Scheme 58: Proposed synthesis of aryl iodides by a gold-catalysed iododeboronation.

This reaction was found to be successful for a wide range of substrates, including electron-deficient ring systems. The iododeboronation can be performed in the presence of air and water, simplifying the practicalities of the reaction procedure. Moreover, for the majority of substrates, these iodinations occurred within 5 minutes when heated to 90 °C.¹⁰¹

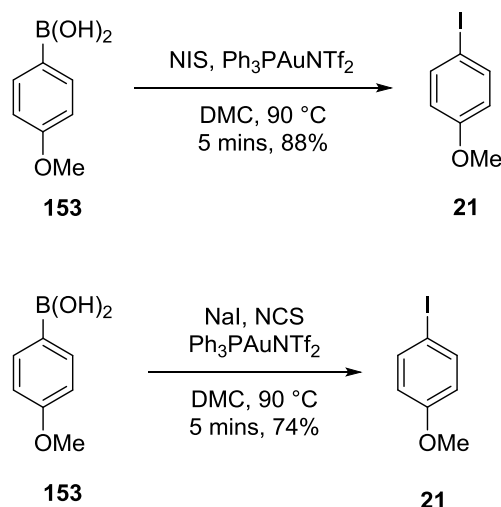
Due to the reaction being practically simple and very fast, it was proposed that the synthesis of SPECT imaging agents *via* this method would be very effective. Therefore, this project focused on the further development of this reaction for radioiodinations. Initially, the aim of the project was to optimise the transformation and explore the scope of the reaction for the rapid and efficient radioiodination of aryl boronic acids. The second aim was to apply this optimised method for the production of SPECT imaging agents.

4.2 Results and discussion

4.2.1 The development of a gold-catalysed radioiododeboronation procedure and the synthesis of radiolabelled aryl iodides

To adapt this procedure for radioiodination, NIS had to be formed *in situ* from NCS and a source of radioactive iodide, [¹²⁵I]NaI. Therefore, the first step was to compare the iododeboronation procedure developed by the Lee group with an iodination using *in situ* formation of NIS (**Scheme 59**). When using 4-methoxybenzeneboronic acid (**153**) and NIS, the reaction was complete within 5 minutes giving an 88% yield of iodinated product **21**. To form NIS *in situ*, sodium iodide and NCS were stirred together at room temperature for 10 minutes before the addition of boronic acid **153** and the gold(I) phosphine catalyst. Under these conditions, 4-iodoanisole (**21**) was synthesised in a 74% yield, with a total

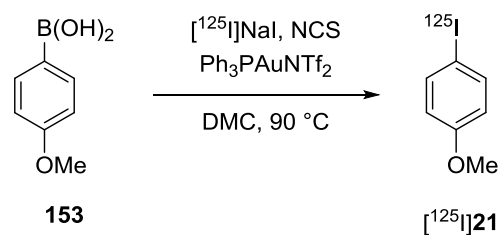
reaction time of 15 minutes. Both reactions gave comparable yields and the products could be easily purified using silica gel chromatography.



Scheme 59: Iododeboronation directly and *via* the *in situ* formation of NIS.

Since the “cold” iododeboronation reaction was comparable with the literature procedure, the next step was to attempt this using [¹²⁵I]NaI (4–6 MBq solution in water) as the limiting reagent. Using 50 mol% of the catalyst and the standard reaction time of 5 minutes, a 63% radiochemical yield of [¹²⁵I]21 was achieved (**Table 11, entry 1**). Extending the reaction time to 20 minutes was found to be optimal (**entry 3**) and gave a quantitative radiochemical yield. To understand the role of the gold catalyst, a control reaction with no catalyst present was carried out (**entry 4**). It was observed that the rate of reaction was significantly reduced without gold catalysis and only a 47% radiochemical yield was achieved in 20 minutes. Therefore, the catalyst is vital in ensuring a high yield within the desired reaction time. Under the optimised conditions, the radiochemical reaction occurred cleanly, with no other radioactive by-products observed by radio-HPLC (**Figure 20**).

Table 11: Optimisation of the radioiododeboronation procedure using 4-methoxybenzeneboronic acid (**153**).



Entry	Time (mins)	Ph ₃ PAuNTf ₂ (mol%)	RCY (%)
1	5	50	63
2	15	50	96
3	20	50	100
4	20	0	47

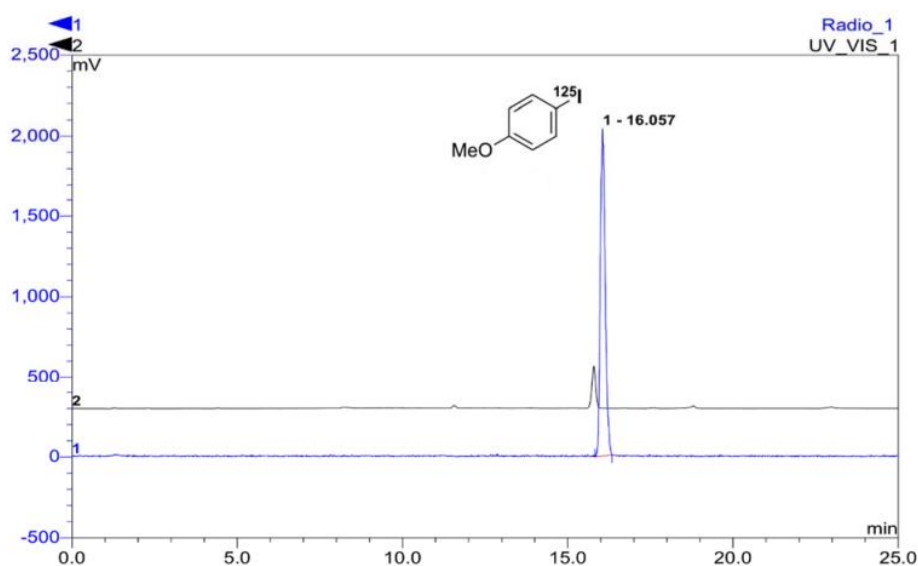
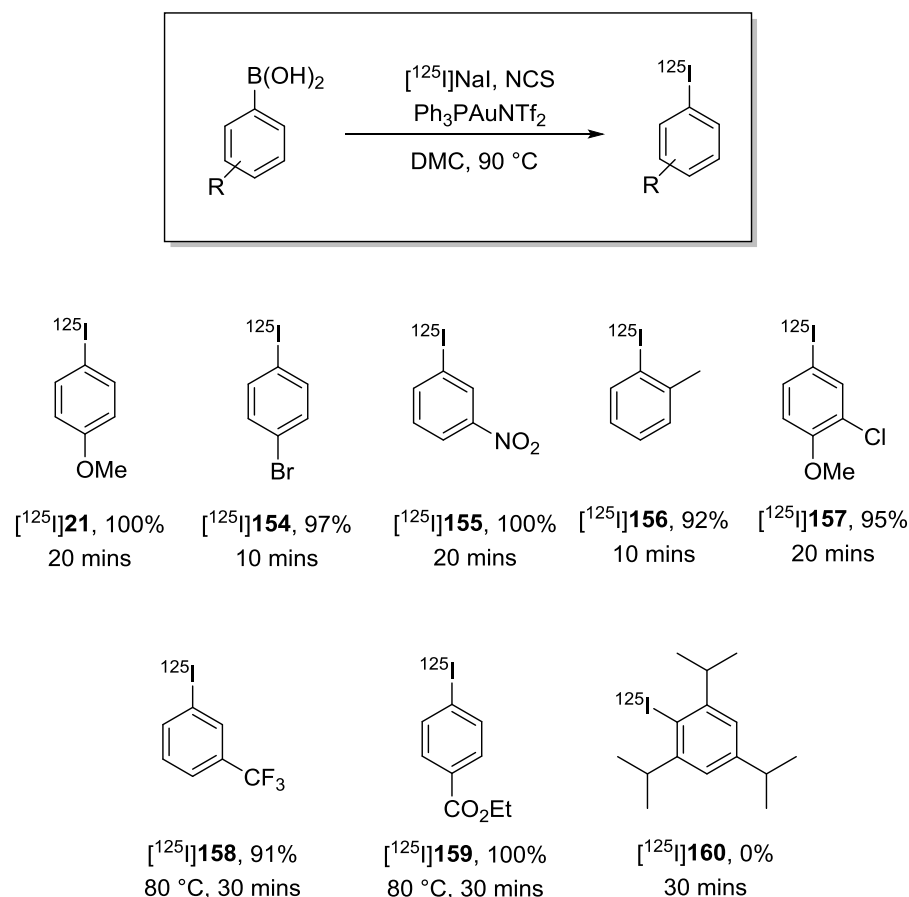


Figure 20: Chromatogram obtained by analytical radio-HPLC (blue) of the reaction mixture from the radioiodination of boronic acid **153**. An overlay of the UV/Vis HPLC trace (black) of unlabelled product **21** is also shown.

The scope of the gold mediated radioiodination was then examined using a variety of aryl boronic acids (**Scheme 60**).¹⁰¹ Under these conditions, electron-rich and electron-deficient boronic acids with a variety of substitution patterns were found to be suitable for the iodination procedure, giving the iodine-125 labelled products in excellent radiochemical yields. Initially the reactions of the trifluoromethyl **158** and the ethyl ester **159** analogues under the optimised conditions, gave several radiolabelled by-products. By reducing the

temperature to 80 °C and using a longer reaction time of 30 minutes, a much cleaner transformation occurred and high radiochemical yields of the desired labelled products were achieved. Due to significant steric hindrance, 2,4,6-triisopropylphenylboronic acid showed no reaction under these conditions. Even after 30 minutes at 90 °C, only unreacted iodide was observed by radio-HPLC.

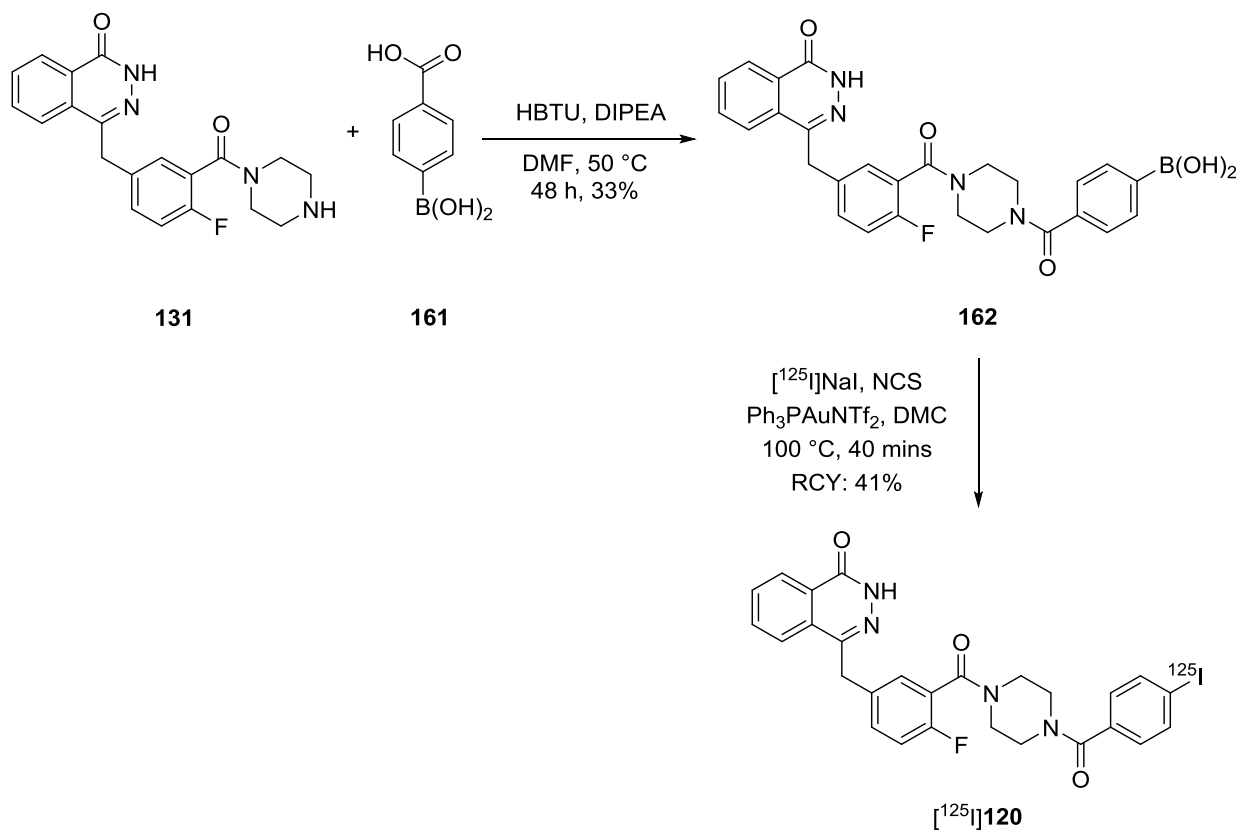


Scheme 60: Substrate scope of the gold(I)-catalysed radioiododeboronation procedure showing radiochemical yields.

4.2.2 Synthesis of SPECT imaging agents

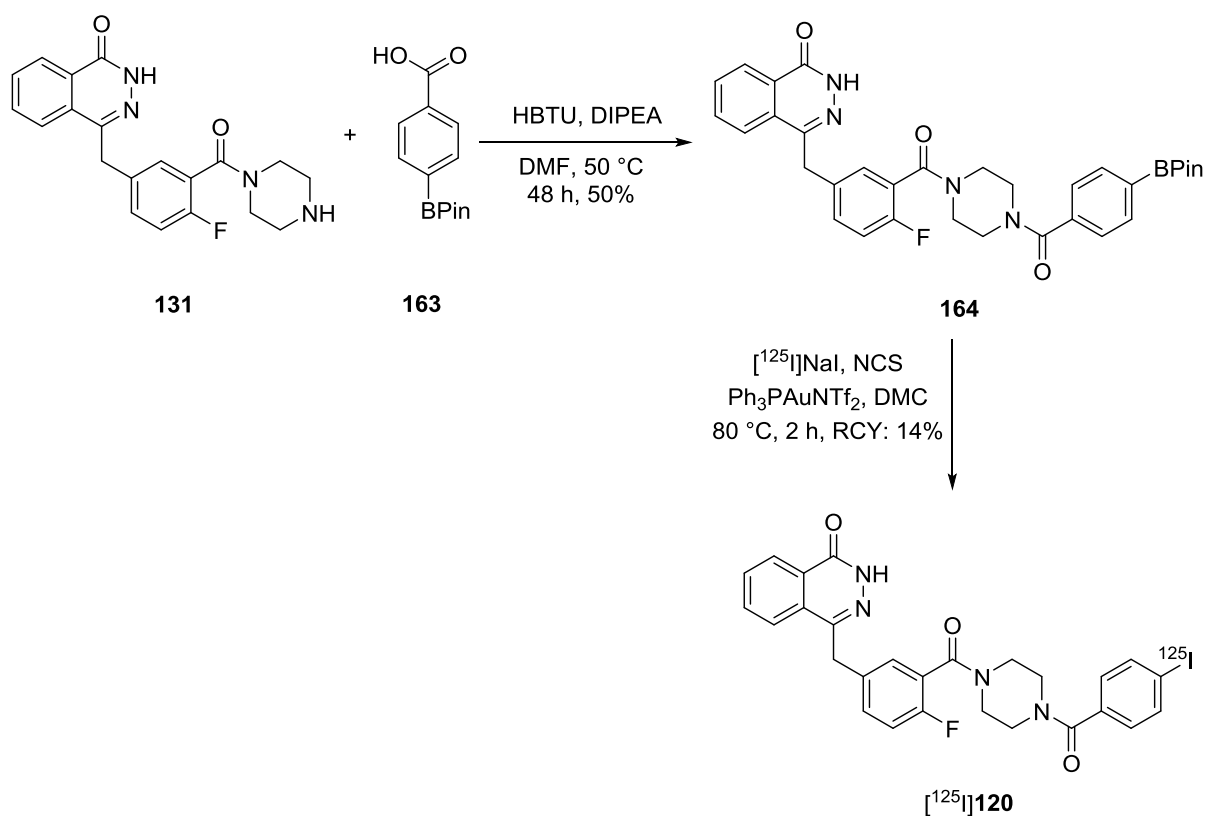
Having developed an effective radiosynthesis of simple aromatic iodides, the next step was to investigate the use of gold-catalysed radioiododeboronation to prepare [¹²⁵I]-labelled SPECT imaging agents. The first target was phthalazinone **120**, a SPECT imaging agent for PARP-1. In order to investigate the iododeboronation process, the boronic acid precursor **162** was synthesised (**Scheme 61**). This was achieved by an HBTU mediated amide coupling of phthalazinone **131** (synthesis shown in section 3.2.1) with 4-carboxyphenylboronic acid (**161**). Boronic acid **162** was then subject to the radioiododeboronation procedure. However, under the standard conditions of 90 °C for 20

minutes, the reaction was very slow and a large amount of unreacted iodide remained. When the temperature was increased to 100 °C and the reaction time increased to 40 minutes, all of the iodide was consumed and a radiochemical yield of 41% was achieved. Due to the complex structure of this substrate, several radioactive side products were also observed by radio-HPLC.



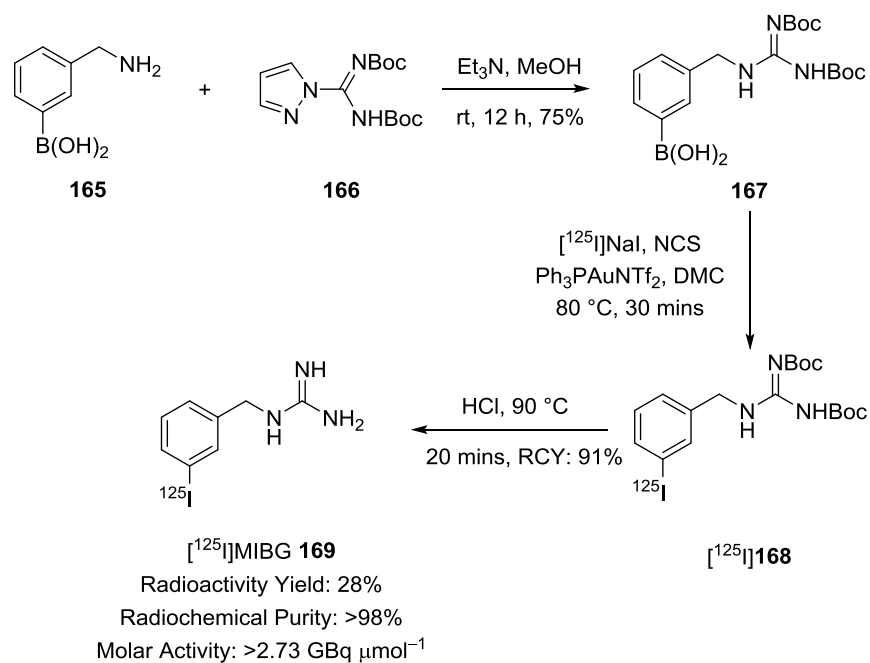
Scheme 61: Synthesis of PARP-1 SPECT imaging agent $[^{125}\text{I}]\mathbf{120}$ using the gold(I)-catalysed radioiodination procedure.

It was proposed that a cleaner reaction may occur if the radioiodination took place *via* the boronic acid pinacol ester precursor **164**. This was synthesised in the same way as the boronic acid, giving the olaparib-derived pinacol ester in a 50% yield (**Scheme 62**). Unfortunately, the gold-catalysed radioiodination reaction to furnish the desired SPECT imaging agent $[^{125}\text{I}]\mathbf{120}$ was not improved. Due to the less reactive nature of the pinacol ester, the highest radiochemical yield was 14% after heating at 80 °C for 2 hours.



Scheme 62: Synthesis of SPECT imaging agent [^{125}I]**120** *via* radioiododeboronation of the boronic acid pinacol ester precursor **164**.

The next imaging agent synthesised was [^{125}I]MIBG **169** (**Scheme 63**). As the iodine-123 form, MIBG is a commercially available radiopharmaceutical that is used for the SPECT imaging of human norepinephrine transporter-expressing cancers.¹⁰² The boronic acid precursor **167** was synthesised by the coupling of 3-(aminomethyl)benzeneboronic acid (**165**) with Boc-protected carboxamidine **166** to give the desired product in a 75% yield. The gold catalysed radioiodination was found to be most effective at a temperature of 80 °C, giving Boc-protected [^{125}I]MIBG **168** in a quantitative radiochemical yield after 30 minutes. The reaction mixture was then treated with hydrochloric acid and heated to 90 °C to remove the protecting groups giving [^{125}I]MIBG **169** in a 91% radiochemical yield over the two steps. Due to the success of this reaction, [^{125}I]MIBG **169** was then resynthesised *via* this method and purified by HPLC. The radioiodinated product was isolated in a 28% radioactivity yield with a radiochemical purity >98% and a molar activity >2.73 GBq μmol^{-1} . Identification of the product was confirmed using analytical HPLC by co-elution with a sample of unlabelled MIBG (**Figure 21**).



Scheme 63: Radiosynthesis of [¹²⁵I]MIBG **169** using the gold(I)-catalysed iododeboronation process.

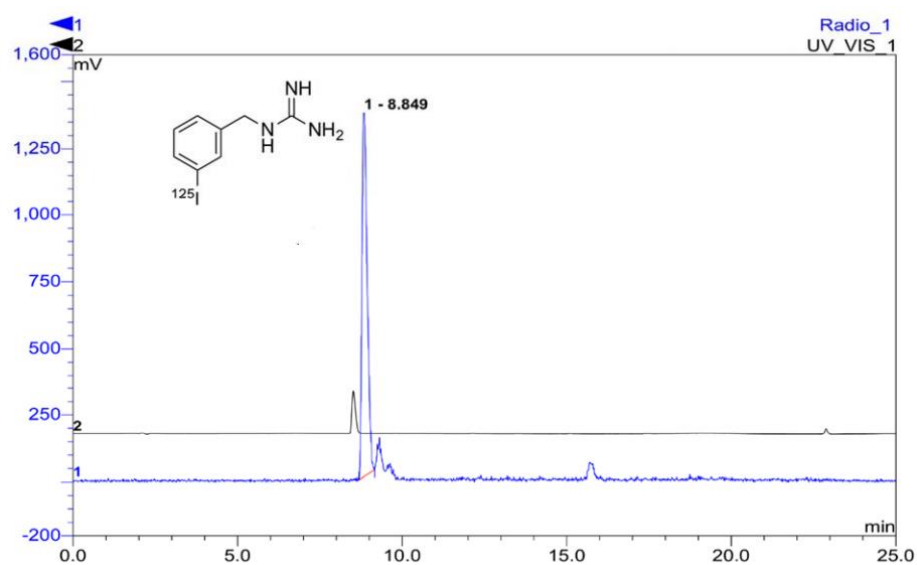


Figure 21: Chromatogram obtained by analytical radio-HPLC (blue) of the reaction mixture from the radioiodination of boronic acid **167**. An overlay of the UV/Vis HPLC trace (black) of unlabelled product **169** is also shown.

4.3 Conclusions and future work

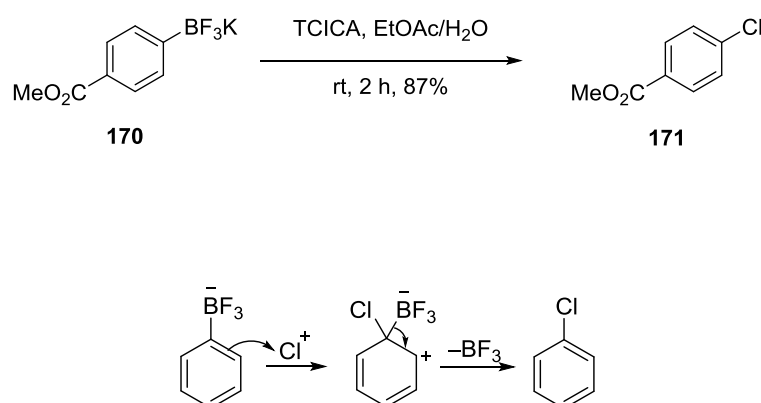
A novel gold(I)-catalysed *ipso*-radioiododeboronation procedure has been developed. This method was found to be fast, air and water stable and uses an environmentally friendly solvent. A small library of substrates with a variety of electronic and steric properties as well as two SPECT imaging agents were radioiodinated in excellent radiochemical yields. The general method was then further validated by the efficient synthesis and isolation of [¹²⁵I]MIBG **169** in a radioactivity yield which compares favourably with previous approaches. This demonstrates the potential of this methodology for widespread use in generating radioiodine-labelled imaging agents. The next step is to investigate the extension of this methodology for the preparation of existing and novel SPECT imaging agents.

5. Base catalysed radioiododeboronation for the development of SPECT tracers

5.1 Introduction

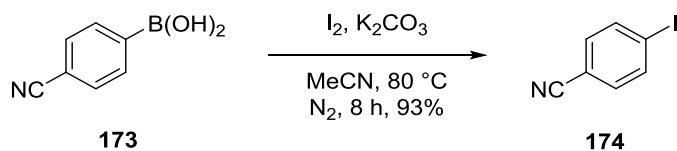
5.1.1 Transition metal-free halodeboronations

With the majority of efficient iododeboronation reactions relying on transition metal catalysis, the development of a metal free radioiodination is highly desirable. As well as this being more cost effective, eliminating the use of a metal catalyst can significantly simplify the purification procedures for the synthesis of SPECT imaging agents. There are already examples in the literature of halodeboronations occurring in high yields without the use of a metal catalyst. For example, in 2011, Molander and co-workers developed a metal-free chlorodeboronation of organotrifluoroborates using trichloroisocyanuric acid (TCICA) as the chlorinating agent.¹⁰³ Using aryl potassium trifluoroborate **170**, the chlorination occurred in an 87% yield in 2 hours. It was proposed that this reaction proceeded *via* an *ipso*-substitution pathway (**Scheme 64**).



Scheme 64: Example of a chlorodeboronation reaction using TCICA as the chlorinating agent and a proposed *ipso*-substitution mechanism.¹⁰³

In 2014, Fu and co-workers developed a base promoted iodination of aryl boronic acids using iodine and potassium carbonate (**Scheme 65**).¹⁰⁴ The reaction gave high yields for a wide variety of substrates using a temperature of 80 °C (example shows boronic acid **172** undergoing an iododeboronation in a 93% yield). However, to obtain high yields, it was necessary to perform these reactions under a nitrogen atmosphere.

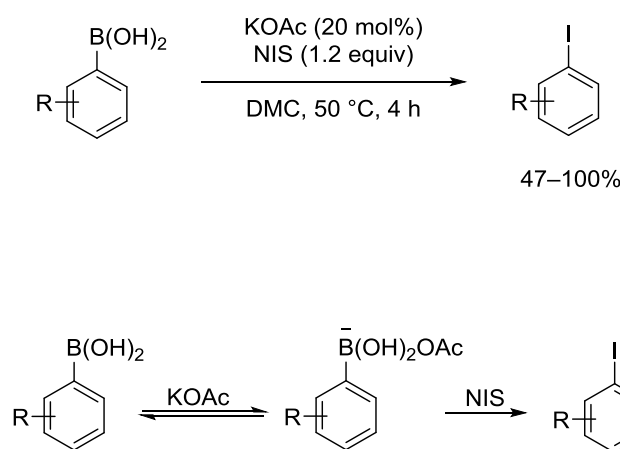


Scheme 65: Metal-free iododeboronation promoted by the use of potassium carbonate.¹⁰⁴

Although it has been shown that aryl boronic acid derivatives can be iodinated without the use of metal catalysis, there have not been many attempts to extend this methodology to include radioiodinations. Therefore, the development of a cost and time effective radioiododeboronation method without the use of a metal catalyst is highly desirable.

5.1.2 Previous work and proposed research

Recently, the Watson group developed a novel base-catalysed iododeboronation procedure using potassium acetate and NIS. A range of aryl iodides with different electronic properties were synthesised in moderate to high yields using only 20 mol% of potassium acetate and a temperature of 50 °C (**Scheme 66**). It was found that this reaction occurred by an *ipso*-substitution pathway *via* a boronate intermediate.



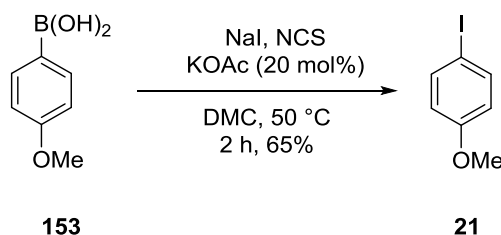
Scheme 66: Potassium acetate mediated iododeboronation and proposed *ipso*-substitution mechanism *via* a boronate intermediate.

This method is operationally simple and can be performed in the presence of air and water. For these reasons, along with the low cost of the potassium acetate catalyst, it is an attractive option for radioiodination and the metal-free synthesis of SPECT imaging agents. Therefore, the aim of this research was to develop a radioiododeboronation method using NIS and a potassium acetate catalyst. Firstly, a small library of simple radioiodinated aryl compounds were synthesised, followed by the production of SPECT imaging agents.

5.2 Results and discussion

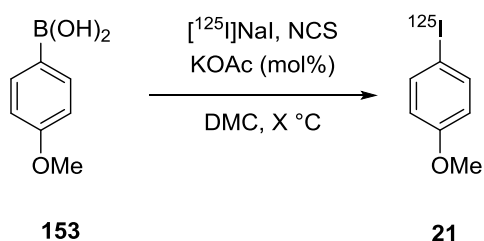
5.2.1 Development of a radioiododeboronation procedure

To ascertain whether this method was suitable for radiosynthesis, a “cold” reaction was performed using 4-methoxybenzeneboronic acid (**153**). The NIS was formed *in situ* and after heating to 50 °C for 2 hours a yield of 65% was achieved (**Scheme 67**).



Scheme 67: Potassium acetate catalysed iododeboronation of 4-methoxybenzeneboronic acid (**153**).

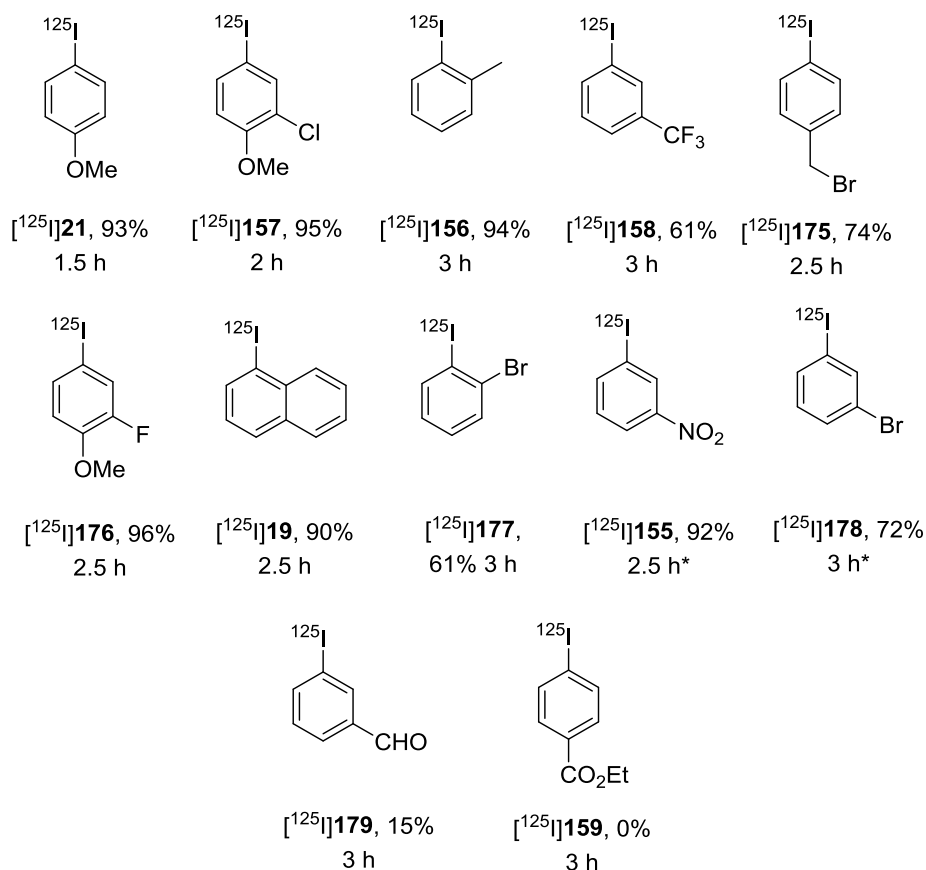
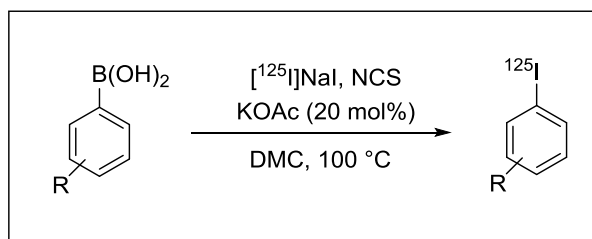
The iododeboronation was then performed using [¹²⁵I]NaI (4–6 MBq solution in water) as the limiting reagent. Under the standard conditions of 20 mol% potassium acetate loading and heating to 50 °C, the radiochemical yield was only 30% after 3 hours (**Table 12, entry 1**). Increasing the amount of potassium acetate to 30 mol% improved the yield to 45% (**entry 2**). Using 50 mol% did not improve the product yield as it was found that increasing the amount of potassium acetate led to the formation of more radioactive impurities (**entry 3**). The next attempt was to increase the temperature of the reaction and lower the amount of potassium acetate. It was thought that this would increase the rate of the reaction as well as minimising radioactive impurities. When a temperature of 70 °C was used along with 10 mol% of potassium acetate, the radiochemical yield was increased to 74% (**entry 4**). This was a clean reaction and no radioactive impurities were observed by radio-HPLC, however, a large amount of unreacted iodide was present. To improve the conversion, the amount of potassium acetate was then increased to 20 mol% and under these conditions a product yield of 98% was achieved in 3 hours (**entry 5**). As time is an important factor in radiosynthesis, the temperature was then increased further to achieve shorter reaction times (**entries 6–8**). It was found that the optimal reaction conditions were a temperature of 100 °C and 20 mol% of potassium acetate (**entry 8**). Using the optimised conditions a radiochemical yield of 93% was obtained after 1.5 hours.

Table 12: Optimisation of the base catalysed radioiododeboronation procedure.

Entry	Temperature (°C)	KOAc (mol%)	Time (h)	RCY (%)
1	50	20	3	30
2	50	30	3	45
3	50	50	3	45
4	70	10	3	74
5	70	20	3	98
6	80	20	2	73
7	90	20	2	93
8	100	20	1.5	93

5.2.2 Radiosynthesis of labelled aryl iodides

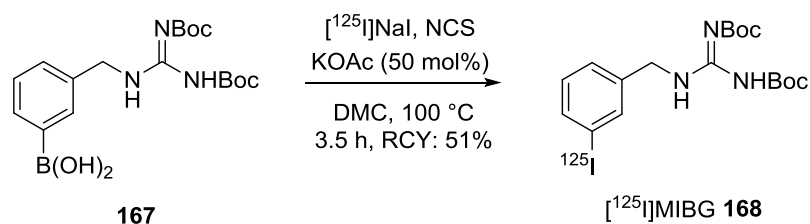
Under the optimised conditions a range of aryl boronic acids were radioiodinated (**Scheme 68**). The substrate scope includes electronically diverse aryl rings with substituents in various substitution patterns. In some cases, the reaction time was increased to 3 hours in order to achieve a high radiochemical yield. In the iodination of 2-bromobenzeneboronic acid, the yield after 3 hours was only 61%, likely due to the increased steric hindrance arising from the *ortho*-substituent. The lower radiochemical yield observed for the iodination of 3-trifluoromethylbenzeneboronic acid can be attributed to the fact that many radioactive impurities were observed by radio-HPLC. When this reaction was attempted at a lower temperature, the yield was not improved since the rate of reaction was significantly decreased. In the synthesis of the 3-nitro derivative [^{125}I]**155** and the 3-bromo derivative [^{125}I]**178**, acetonitrile had to be added as a co-solvent in order to improve the solubility of the boronic acids. No radioiodination was observed when using ethoxycarbonylbenzeneboronic acid despite performing the reaction at a variety of temperatures and catalyst loadings. Likewise, the best radiochemical yield observed when using 3-formylphenylboronic acid was only 15%.



Scheme 68: Substrate scope of the potassium acetate-catalysed radioiododeboronation procedure showing radiochemical yields. *Acetonitrile was added as a co-solvent.

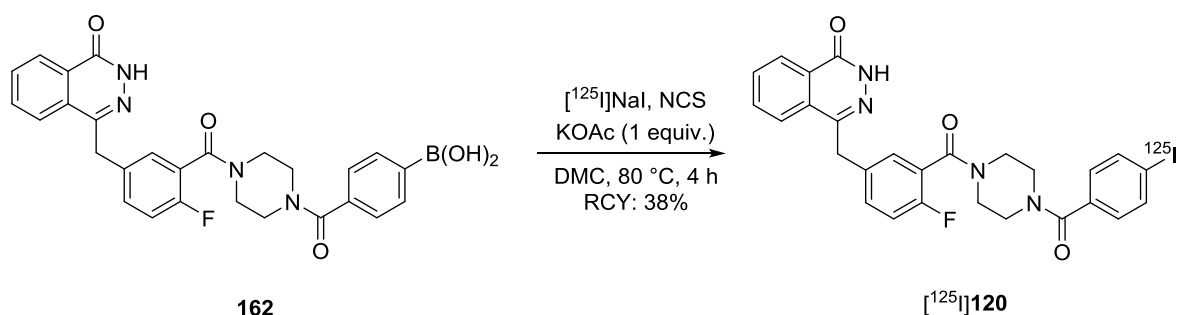
5.2.3 Synthesis of SPECT imaging agents

With the successful radiosynthesis of a range of aryl iodides using the potassium acetate catalysed iododeboronation, the utility of this procedure was then demonstrated with the preparation of iodine-125 labelled SPECT imaging agents. The first imaging agent synthesised was Boc-protected [¹²⁵I]MIBG **168** (**Scheme 69**). The boronic acid precursor **167** was synthesised as previously shown in **Scheme 63**. Under the standard conditions of 100 °C with 20 mol% of potassium acetate, only unreacted iodide was observed by radio-HPLC. Therefore, the amount of potassium acetate was increased to 50 mol% and a radiochemical yield of 51% was obtained.



Scheme 69: The synthesis of Boc-protected MIBG **168** *via* the potassium acetate-catalysed radiiododeboronation of boronic acid **167**.

The next SPECT imaging agent investigated was phthalazinone [¹²⁵I]**120** for the imaging of PARP-1 (**Scheme 70**). The boronic acid precursor **162** was synthesised according to the method shown in **Scheme 61**. The radioiodination of boronic acid **162** was very slow and even when the amount of potassium acetate was increased to 50 mol% there was no conversion to product after 4 hours. Therefore, in order to increase the reaction rate, one equivalent of potassium acetate was used. At 100 °C, although the iodide was completely consumed, no product was observed due to decomposition. Therefore, the best radiochemical yield of 38% was observed when the reaction temperature was decreased to 80 °C.



Scheme 70: Synthesis of PARP-1 imaging agent [¹²⁵I]**120** *via* the radioiodination of boronic acid **162**.

Current work is ongoing to improve the radiochemical yields of both [¹²⁵I]MIBG **168** and PARP-1 imaging agent [¹²⁵I]**120** by this method, with the focus on decreasing the amount of radiochemical impurities formed.

5.3 Conclusions and future work

A novel and transition metal-free *ipso*-radioiododeboronation procedure has been developed. This method is operationally simple and requires only a catalytic amount of potassium acetate. A small library of substrates with a variety of electronic and steric properties were synthesised in high radiochemical yields. Preliminary work on the synthesis of two SPECT imaging agents was also investigated.

Current and future work will focus on extending the substrate scope of this reaction to include different functional groups and aromatic heteroatoms. The more efficient synthesis of both [^{125}I]MIBG **168** and PARP-1 imaging agent [^{125}I]**120** will be explored along with the production of other SPECT imaging agents. For example, work is on-going to synthesis SPECT imaging agents [^{125}I]CNS1261 **26** and [^{125}I]IBOX **27** (Figure 22).^{27,26}

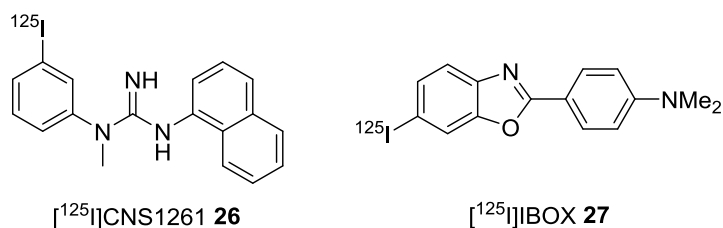


Figure 22: SPECT imaging agents which could potentially be radiolabelled using the potassium acetate-catalysed iododeboronation procedure.

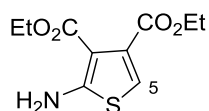
6. Experimental

6.1 General experimental

All reactions were performed under an atmosphere of air unless otherwise stated. All reagents and starting materials were obtained from commercial sources unless otherwise stated. Brine refers to a saturated solution of sodium chloride. All dry solvents were purified using a PureSolv 500 MD solvent purification system. Flash column chromatography was carried out using Merck Feduran Si 60 (40–63 μm). Macherey-Nagel aluminium-backed plates pre-coated with silica gel 60 were used for thin layer chromatography and were visualised under a UV lamp. ^1H NMR and ^{13}C NMR spectra were recorded on a Bruker DPX 400 spectrometer or Bruker DPX 500 spectrometer with chemical shift values in ppm relative to trimethylsilane or residual chloroform as standard. J values are reported in Hz. The assignment of ^1H NMR spectra are based on COSY and HSQC experiments and ^{13}C NMR spectra are based on DEPT experiments. Infrared spectra were recorded using a Shimadzu FTIR-84005 spectrometer directly as either a solid or liquid and mass spectra were obtained using a JEOL JMS-700 spectrometer or a Bruker MicroTOFq high resolution mass spectrometer. Melting points were determined on a Gallenkamp melting point apparatus. Optical rotations were determined as solutions irradiating with the sodium D line ($\lambda = 589 \text{ nm}$) using a polarimeter. $[\alpha]_{\text{D}}$ values are given in units $10^{-1} \text{ deg cm}^2 \text{ g}^{-1}$.

6.2 MCT 1 and 2 experimental

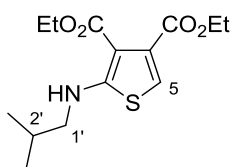
Diethyl 2-amino-thiophene-3,4-dicarboxylate (**44**)⁶²



To a stirred solution of ethyl pyruvate (**43**) (0.339 g, 2.92 mmol), ethyl cyanoacetate (**42**) (0.300 g, 2.65 mmol) and sulfur (0.084 g, 2.65 mmol) in *N,N'*-dimethylformamide (10 mL) was added triethylamine (1.85 mL, 13.5 mmol) dropwise. The reaction mixture was heated to 50 °C and stirred for 6 h. The mixture was diluted with water (30 mL) and an aqueous solution of 5% lithium chloride (20 mL). The product was extracted with diethyl ether (3 \times 30 mL). The combined organic layers were washed with brine (30 mL), dried (MgSO_4), filtered and concentrated *in vacuo*. The resulting material was filtered through a large pad

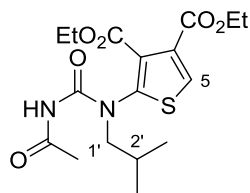
of silica, eluting with 100% diethyl ether to give diethyl 2-amino-thiophene-3,4-dicarboxylate (**44**) as an orange solid (0.373 g, 58%). Spectroscopic data were consistent with the literature.⁶² Mp 115–117 °C; δ_{H} (400 MHz, CDCl_3) 1.30 (3H, t, J 7.2 Hz, OCH_2CH_3), 1.35 (3H, t, J 7.2 Hz, OCH_2CH_3), 4.25 (2H, q, J 7.2 Hz, OCH_2CH_3), 4.28 (2H, q, J 7.2 Hz, OCH_2CH_3), 5.95 (2H, br s, NH_2), 6.59 (1H, s, 5-H); δ_{C} (101 MHz, CDCl_3) 14.2 (CH_3), 14.3 (CH_3), 60.2 (CH_2), 61.2 (CH_2), 105.0 (C), 111.1 (CH), 132.9 (C), 162.9 (C), 164.6 (C), 165.1 (C); m/z (EI) 243 (M^+ , 100%).

Diethyl 2-isobutyl-amino-thiophene-3,4-dicarboxylate (**45**)⁶²



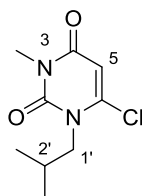
To a stirred suspension of diethyl 2-amino-thiophene-3,4-dicarboxylate (**44**) (0.800 g, 3.29 mmol) in isobutyric acid (**47**) (4.80 mL, 52.6 mmol) was added sodium borohydride (0.498 g, 13.2 mmol) portionwise. The mixture was stirred at room temperature for 16 h. Further sodium borohydride (0.248 g, 6.58 mmol) was added portionwise and the mixture heated to 50 °C and stirred for 5 h. The reaction mixture was diluted with water (50 mL), neutralised with sodium bicarbonate (1.00 g) and the product extracted with diethyl ether (3 × 40 mL). The combined organic layers were dried (MgSO_4), filtered and concentrated *in vacuo*. Purification by flash column chromatography eluting with 30% diethyl ether in hexane gave diethyl 2-isobutyl-amino-thiophene-3,4-dicarboxylate (**45**) as a yellow oil (0.702 g, 72%). Spectroscopic data were consistent with the literature.⁶² δ_{H} (400 MHz, CDCl_3) 0.99 (6H, d, J 6.7 Hz, $\text{CH}(\text{CH}_3)_2$), 1.29 (3H, t, J 7.2 Hz, OCH_2CH_3), 1.34 (3H, t, J 7.2 Hz, OCH_2CH_3), 1.92–2.03 (1H, m, 2'-H), 3.04 (2H, d, J 7.6 Hz, 1'-H₂), 4.24 (2H, q, J 7.2 Hz, OCH_2CH_3), 4.30 (2H, q, J 7.2 Hz, OCH_2CH_3), 6.49 (1H, s, 5-H), 7.70 (1H, br s, NH); δ_{C} (101 MHz, CDCl_3) 14.2 (CH_3), 14.3 (CH_3), 20.1 (2 × CH_3), 28.4 (CH), 55.4 (CH_2), 59.9 (CH_2), 61.2 (CH_2), 101.5 (C) 108.8 (CH), 133.5 (C), 165.1 (C), 165.6 (C), 166.4 (C); m/z (ESI) 322 (MNa^+ , 100%).

Ethyl 2-[(acetylamino)carbonyl-2'-methylpropyl]amino-thiophene-3,4-dicarboxylate (48)⁶²



Acetyl chloride (0.063 mL, 0.89 mmol) was added dropwise to a stirred suspension of silver cyanate (0.132 g, 0.890 mmol) in anhydrous toluene (10 mL). The mixture was stirred under an argon atmosphere at room temperature for 1 h. Diethyl 2-isobutyl-amino-thiophene-3,4-dicarboxylate (**45**) (0.107 g, 0.360 mmol) was then added as a solution in anhydrous toluene (10 mL) and the mixture stirred at room temperature for 16 h. The mixture was then diluted with diethyl ether (10 mL) and filtered. The filtrate was washed with an aqueous saturated solution of sodium bicarbonate (10 mL) and the product extracted with diethyl ether (2 × 10 mL). The organic layers were combined, dried (MgSO₄), filtered and concentrated *in vacuo* to give ethyl 2-[(acetylamino)carbonyl-2'-methylpropyl]amino-thiophene-3,4-dicarboxylate (**48**) as a colourless oil (0.108 g, 78%). Spectroscopic data were consistent with the literature.⁶² δ_{H} (400 MHz, CDCl₃) 0.91 (6H, d, *J* 6.7 Hz, CH(CH₃)₂), 1.34 (3H, t, *J* 7.2 Hz, OCH₂CH₃), 1.35 (3H, t, *J* 7.2 Hz, OCH₂CH₃), 1.82–1.93 (1H, m, 2'-H), 2.42 (3H, s, COCH₃), 3.49 (2H, d, *J* 7.2 Hz, 1'-H₂), 4.33 (2H, q, *J* 7.2 Hz, OCH₂CH₃), 4.34 (2H, q, *J* 7.2 Hz, OCH₂CH₃), 7.70 (1H, s, 5-H), 8.00 (1H, s, NH); δ_{C} (101 MHz, CDCl₃) 13.9 (CH₃), 14.1 (CH₃), 19.9 (2 × CH₃), 24.5 (CH), 27.0 (CH₃), 58.5 (CH₂), 61.1 (CH₂), 62.4 (CH₂), 131.4 (C), 132.1 (CH), 133.1 (C), 143.2 (C), 152.3 (C), 161.1 (C), 163.3 (C), 172.5 (C); *m/z* (ESI) 407 (MNa⁺, 100%).

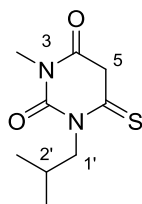
6-Chloro-1-isobutyl-3-methyl-2,4-(1H,3H)-pyrimidinedione (51)⁵⁷



Isobutyl bromide (8.90 mL, 82.2 mmol) was added to a solution of 6-chloro-3-methyluracil (**49**) (12.0 g, 74.7 mmol) and potassium carbonate (12.4 g, 89.7 mmol) in dimethyl sulfoxide (120 mL). The mixture was heated to 60 °C and stirred for 72 h. The mixture was then cooled to room temperature and diluted with water (40 mL) and brine (40 mL). The product was then extracted with diethyl ether (3 × 40 mL). The organic layers were

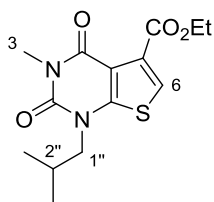
combined, dried (MgSO₄), filtered and concentrated *in vacuo* to provide a 10:1 mixture of the *N*- and *O*-alkylated products **50** and **51** (13.7 g, 84%) as an orange oil. This mixture was used directly in the next step without further purification. The following characterisation data refers to the major product 6-chloro-1-isobutyl-3-methyl-2,4-(1*H*,3*H*)-pyrimidinedione (**51**). Spectroscopic data were consistent with the literature.⁵⁷ δ_{H} (400 MHz, CDCl₃) 0.96 (6H, d, *J* 6.8 Hz, CH(CH₃)₂), 2.11–2.22 (1H, m, 2'-H), 3.34 (3H, s, 3-CH₃), 3.90 (2H, d, *J* 7.6 Hz, 1'-H₂), 5.92 (1H, s, 5-H); δ_{C} (101 MHz, CDCl₃) 19.7 (2 × CH₃), 28.1 (CH₃), 28.3 (CH), 53.5 (CH₂), 101.9 (CH), 146.0 (C), 151.2 (C), 160.9 (C); *m/z* (CI) 217 (MH⁺, 95%), 183 (17), 69 (10).

1-isobutyl-6-mercapto-3-methyl-2,4-(1*H*,3*H*)-pyrimidinedione (52**)⁶¹**



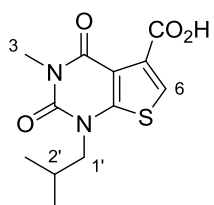
Sodium hydrosulfide monohydrate (1.28 g, 22.7 mmol) was added to a stirred solution of 6-chloro-1-isobutyl-3-methyl-2,4-(1*H*,3*H*)-pyrimidinedione (**51**) (4.10 g, 18.9 mmol) in ethanol (60 mL). The mixture was stirred at room temperature for 24 h before further sodium hydrosulfide monohydrate (1.28 g, 22.7 mmol) was added and stirring continued at room temperature for a further 16 h under an atmosphere of argon. The solution was concentrated *in vacuo* and the resulting oil diluted with water (30 mL) and washed with ethyl acetate (30 mL). The aqueous layer was acidified with an aqueous solution of 1 M hydrochloric acid and extracted with ethyl acetate (3 × 30 mL). The combined organic layers were dried (MgSO₄), filtered and concentrated *in vacuo* to give 1-isobutyl-6-mercapto-3-methyl-2,4-(1*H*,3*H*)-pyrimidinedione (**52**) as a pale yellow solid (3.69 g, 90%). Spectroscopic data were consistent with the literature.⁶¹ Mp 111–113 °C; δ_{H} (400 MHz, CDCl₃) 0.92 (6H, d, *J* 6.8 Hz, CH(CH₃)₂), 2.24–2.31 (1H, m, 2'-H), 3.29 (3H, s, 3-CH₃), 4.14 (2H, s, 5-H₂), 4.27 (2H, d, *J* 7.4 Hz, 1'-H₂); δ_{C} (101 MHz, CDCl₃) 20.1 (2 × CH₃), 26.6 (CH₃), 28.6 (CH), 49.2 (CH₂), 54.5 (CH₂), 150.3 (C), 164.8 (C), 197.2 (C); *m/z* (ESI) 237 (MNa⁺, 60%), 159 (20), 307 (5), 449 (2).

Ethyl 1-isobutyl-3-methyl-2,4-dioxo-1,2,3,4-tetrahydrothieno[2,3-*d*]pyrimidine-5-carboxylate (46)⁶¹



Ethyl bromopyruvate (1.70 mL, 13.3 mmol) was added to a solution of 1-isobutyl-6-mercapto-3-methyl-2,4-(1*H*,3*H*)-pyrimidinedione (**52**) (1.90 g, 8.87 mmol) in ethanol (40 mL) and stirred at room temperature for 0.75 h. The reaction mixture was concentrated *in vacuo* to give a red oil. A mixture of the crude intermediate and polyphosphoric acid (10.0 g) was heated to 145 °C for 3 h and then cooled to room temperature. A saturated aqueous solution of sodium carbonate (15 mL) was added and the mixture extracted with ethyl acetate (3 × 25 mL). The combined organic layers were dried (MgSO₄), filtered and concentrated *in vacuo*. Purification by flash column chromatography eluting with 20% ethyl acetate in petroleum ether gave ethyl 1-isobutyl-3-methyl-2,4-dioxo-1,2,3,4-tetrahydrothieno[2,3-*d*]pyrimidine-5-carboxylate (**46**) as a dark pink solid (1.41 g, 54%). Mp 62–66 °C. Spectroscopic data were consistent with the literature.⁶¹ δ_{H} (400 MHz, CDCl₃) 1.00 (6H, d, *J* 6.9 Hz, CH(CH₃)₂), 1.40 (3H, t, *J* 7.4 Hz, OCH₂CH₃), 2.26–2.38 (1H, m, 2'-H), 3.42 (3H, s, 3-CH₃), 3.81 (2H, d, *J* 7.6 Hz, 1'-H₂), 4.41 (2H, q, *J* 7.4 Hz, OCH₂CH₃), 7.29 (1H, s, 6-H); δ_{C} (101 MHz, CDCl₃) 14.2 (CH₃), 20.0 (2 × CH₃), 27.0 (CH), 28.5 (CH₃), 56.2 (CH₂), 61.9 (CH₂), 112.6 (C), 119.4 (CH), 132.3 (C), 150.8 (C), 154.2 (C), 157.0 (C), 162.9 (C); *m/z* (ESI) 333 (MNa⁺, 100%).

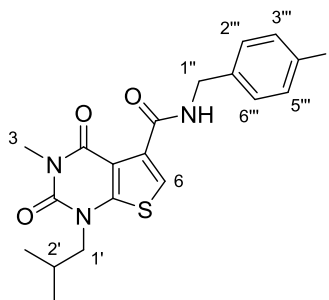
1-Isobutyl-3-methyl-2,4-dioxo-1,2,3,4-tetrahydrothieno[2,3-*d*]pyrimidine-5-carboxylic acid (58)⁶¹



To a stirred solution of ethyl 1-isobutyl-3-methyl-2,4-dioxo-1,2,3,4-tetrahydrothieno[2,3-*d*]pyrimidine-5-carboxylate (**46**) (0.060 g, 0.19 mmol) in tetrahydrofuran (1 mL) and methanol (0.5 mL) was added an aqueous solution of 10% sodium hydroxide (0.3 mL). The mixture was stirred for 2 h at room temperature. The mixture was then diluted with

water (5 mL) and washed with diethyl ether (5 mL). The aqueous layer was acidified with an aqueous solution of 1 M hydrochloric acid and the product extracted with ethyl acetate (3 × 5 mL). The organic layers were dried (MgSO₄), filtered and concentrated *in vacuo* to give 1-isobutyl-3-methyl-2,4-dioxo-1,2,3,4-tetrahydrothieno[2,3-*d*]pyrimidine-5-carboxylic acid (**58**) as a brown oil (0.049 g, 92%). Spectroscopic data were consistent with the literature.⁶¹ δ_{H} (400 MHz, CDCl₃) 1.00 (6H, d, *J* 6.8 Hz, CH(CH₃)₂), 2.29–2.37 (1H, m, 2'-H), 3.50 (3H, s, 3-CH₃), 3.87 (2H, d, *J* 7.6 Hz, 1'-H₂), 8.03 (1H, s, 6-H), 15.00 (1H, br s, OH); δ_{C} (101 MHz, CDCl₃) 20.1 (2 × CH₃), 26.9 (CH₃), 29.3 (CH), 56.6 (CH₂), 109.8 (C), 127.6 (CH), 131.3 (C), 149.6 (C), 156.3 (C), 160.9 (C), 162.0 (C); *m/z* (EI) 282 (M⁺, 100%), 182 (75), 125 (32), 51 (21).

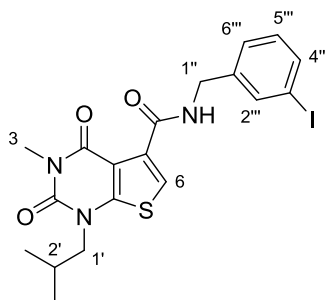
***N*-(4''-Iodobenzyl)-1-isobutyl-3-methyl-2,4-dioxo-1,2,3,4-tetrahydrothieno[2,3-*d*]pyrimidine-5-carboxamide (**59**)**



1-Isobutyl-3-methyl-2,4-dioxo-1,2,3,4-tetrahydrothieno[2,3-*d*]pyrimidine-5-carboxylic acid (**58**) (0.043 g, 0.15 mmol) was dissolved in *N,N'*-dimethylformamide (10 mL) and then *O*-(benzotriazol-1-yl)-*N,N,N',N'*-tetramethyluronium hexafluorophosphate (0.085 g, 0.23 mmol), *N,N'*-diisopropylethylamine (0.052 mL, 0.30 mmol) and 4-iodobenzylamine (0.11 g, 0.45 mmol) were added and the mixture stirred for 5 h at 40 °C. The mixture was diluted with water (10 mL) and a saturated aqueous sodium bicarbonate solution (10 mL). The product was extracted with ethyl acetate (3 × 10 mL). The organic layers were combined and washed with an aqueous solution of 5% lithium chloride (30 mL) and brine (30 mL). The organic layer was dried (MgSO₄), filtered and concentrated *in vacuo* to give the crude product. Purification by flash column chromatography eluting with 40% ethyl acetate in petroleum ether gave *N*-(4''-iodobenzyl)-1-isobutyl-3-methyl-2,4-dioxo-1,2,3,4-tetrahydrothieno[2,3-*d*]pyrimidine-5-carboxamide (**59**) as a yellow solid (0.060 g, 80%). Mp 178–180 °C; ν_{max} (neat)/cm⁻¹ 3032 (NH), 2955 (CH), 1697 (CO), 1627 (CO), 1589 (C=C), 1473, 1296, 1003, 733; δ_{H} (400 MHz, CDCl₃) 1.01 (6H, d, *J* 6.7 Hz, CH(CH₃)₂), 2.31–2.37 (1H, m, 2'-H), 3.46 (3H, s, 3-CH₃), 3.87 (2H, d, *J* 7.6 Hz, 1'-H₂), 4.59 (2H, d, *J* 5.6 Hz, 1''-H₂), 7.14 (2H, d, *J* 8.4 Hz, 2'''-H and 6'''-H), 7.65 (2H, d, *J* 8.4

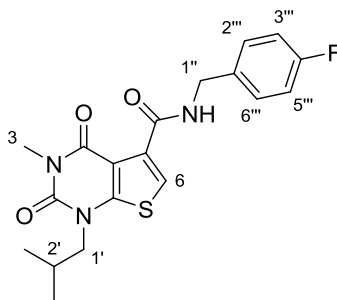
Hz, 3'''-H and 5'''-H), 8.02 (1H, s, 6-H), 11.19 (1H, br s, NH); δ_C (101 MHz, CDCl₃) 20.0 (2 × CH₃), 26.9 (CH₃), 29.1 (CH), 43.3 (CH₂), 56.2 (CH₂), 92.5 (C), 110.4 (C), 124.0 (CH), 129.7 (2 × CH), 134.7 (C), 137.6 (2 × CH), 138.4 (C), 149.9 (C), 156.4 (C), 160.5 (C), 160.7 (C); m/z (ESI) 520.0151 (MNa⁺. C₁₉H₂₀IN₃NaO₃S requires 520.0162).

***N*-(3'''-Iodobenzyl)-1-isobutyl-3-methyl-2,4-dioxo-1,2,3,4-tetrahydrothieno[2,3-*d*]pyrimidine-5-carboxamide (60)**



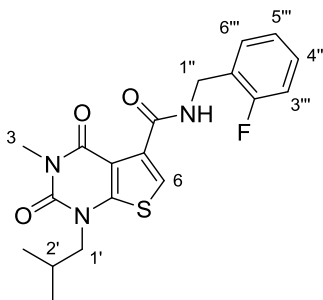
The reaction was carried out according to the previously described procedure for *N*-(4'''-iodobenzyl)-1-isobutyl-3-methyl-2,4-dioxo-1,2,3,4-tetrahydrothieno[2,3-*d*]pyrimidine-5-carboxamide (**59**) using 1-isobutyl-3-methyl-2,4-dioxo-1,2,3,4-tetrahydrothieno[2,3-*d*]pyrimidine-5-carboxylic acid (**58**) (0.047 g, 0.17 mmol) and 3-iodobenzylamine (0.067 mL, 0.50 mmol) and gave *N*-(3'''-iodobenzyl)-1-isobutyl-3-methyl-2,4-dioxo-1,2,3,4-tetrahydrothieno[2,3-*d*]pyrimidine-5-carboxamide (**60**) as a yellow solid (0.050 g, 60%). Mp 150–153 °C; ν_{\max} (neat)/cm⁻¹ 3781 (NH), 2962 (CH), 1705 (CO), 1635 (CO), 1581 (C=C), 1497, 1296, 725; δ_H (400 MHz, CDCl₃) 1.01 (6H, d, *J* 6.7 Hz, CH(CH₃)₂), 2.31–2.37 (1H, m, 2'-H), 3.47 (3H, s, 3-CH₃), 3.87 (2H, d, *J* 7.7 Hz, 1'-H₂), 4.60 (2H, d, *J* 5.6 Hz, 1''-H₂), 7.06 (1H, t, *J* 7.7 Hz, 5'''-H), 7.36 (1H, d, *J* 7.7 Hz, 6'''-H), 7.59 (1H, d, *J* 7.7 Hz, 4'''-H), 7.73 (1H, s, 2'''-H), 8.03 (1H, s, 6-H), 11.20 (1H, br s, NH); δ_C (101 MHz, CDCl₃) 20.0 (2 × CH₃), 26.9 (CH₃), 29.1 (CH), 43.0 (CH₂), 56.3 (CH₂), 94.5 (C), 110.4 (C), 124.4 (CH), 126.9 (CH), 130.3 (CH), 134.7 (C), 136.2 (CH), 136.5 (CH), 141.1 (C), 149.9 (C), 156.4 (C), 160.5 (C), 160.7 (C); m/z (ESI) 520.0153 (MNa⁺. C₁₉H₂₀IN₃NaO₃S requires 520.0162).

***N*-(4'''-Fluorobenzyl)-1-isobutyl-3-methyl-2,4-dioxo-1,2,3,4-tetrahydrothieno[2,3-*d*]pyrimidine-5-carboxamide (61)**



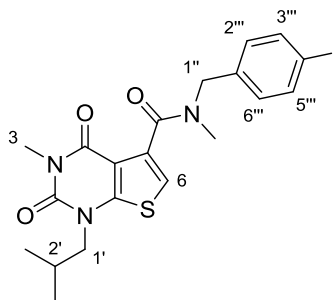
The reaction was carried out according to the previously described procedure for *N*-(4'''-iodobenzyl)-1-isobutyl-3-methyl-2,4-dioxo-1,2,3,4-tetrahydrothieno[2,3-*d*]pyrimidine-5-carboxamide (**59**) using 1-isobutyl-3-methyl-2,4-dioxo-1,2,3,4-tetrahydrothieno[2,3-*d*]pyrimidine-5-carboxylic acid (**58**) (0.052 g, 0.18 mmol) and 4-fluorobenzylamine (0.069 mL, 0.55 mmol) and gave *N*-(4'''-fluorobenzyl)-1-isobutyl-3-methyl-2,4-dioxo-1,2,3,4-tetrahydrothieno[2,3-*d*]pyrimidine-5-carboxamide (**61**) as a yellow solid (0.035 g, 50%). Mp 158–161 °C; ν_{\max} (neat)/ cm^{-1} 3245 (NH), 2361 (CH), 1697 (CO), 1636 (CO), 1582 (C=C), 1466, 1219, 1042, 818, 725; δ_{H} (400 MHz, CDCl_3) 1.00 (6H, d, J 6.7 Hz, $\text{CH}(\text{CH}_3)_2$), 2.30–2.37 (1H, m, 2'-H), 3.45 (3H, s, 3- CH_3), 3.87 (2H, d, J 7.6 Hz, 1'- H_2), 4.62 (2H, d, J 5.6 Hz, 1''- H_2), 7.01 (2H, t, J 8.8 Hz, 3'''-H and 5'''-H), 7.36 (2H, dd, J 8.7, 5.4 Hz, 2'''-H and 6'''-H), 8.03 (1H, s, 6-H), 11.12 (1H, br s, NH); δ_{C} (101 MHz, CDCl_3) 20.0 (2 \times CH_3), 26.9 (CH_3), 29.1 (CH), 43.1 (CH_2), 56.2 (CH_2), 110.4 (C), 115.4 (d, $^2J_{\text{CF}}$ 21.2 Hz, 2 \times CH), 124.3 (CH), 129.4 (d, $^3J_{\text{CF}}$ 8.0 Hz, 2 \times CH), 134.8 (d, $^4J_{\text{CF}}$ 3.0 Hz, C), 134.8 (C), 149.9 (C), 156.4 (C), 160.4 (C), 160.6 (C), 163.2 (d, $^1J_{\text{CF}}$ 247.9 Hz, C); m/z (ESI) 412.1082 (MNa^+ . $\text{C}_{19}\text{H}_{20}\text{FN}_3\text{NaO}_3\text{S}$ requires 412.1102).

***N*-(2''''-Fluorobenzyl)-1-isobutyl-3-methyl-2,4-dioxo-1,2,3,4-tetrahydrothieno[2,3-*d*]pyrimidine-5-carboxamide (62)**



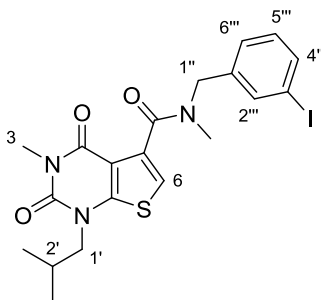
The reaction was carried out according to the previously described procedure for *N*-(4''''-iodobenzyl)-1-isobutyl-3-methyl-2,4-dioxo-1,2,3,4-tetrahydrothieno[2,3-*d*]pyrimidine-5-carboxamide (**59**) using 1-isobutyl-3-methyl-2,4-dioxo-1,2,3,4-tetrahydrothieno[2,3-*d*]pyrimidine-5-carboxylic acid (**58**) (0.066 g, 0.23 mmol) and 2-fluorobenzylamine (0.080 mL, 0.70 mmol) and gave *N*-(2''''-fluorobenzyl)-1-isobutyl-3-methyl-2,4-dioxo-1,2,3,4-tetrahydrothieno[2,3-*d*]pyrimidine-5-carboxamide (**62**) as an orange oil (0.061 g, 68%). ν_{\max} (neat)/ cm^{-1} 3241 (NH), 2963 (CH), 1705 (CO), 1636 (CO), 1574 (C=C), 1496, 1296, 756; δ_{H} (400 MHz, CDCl_3) 1.00 (6H, d, J 6.7 Hz, $\text{CH}(\text{CH}_3)_2$), 2.27–2.38 (1H, m, 2'-H), 3.46 (3H, s, 3- CH_3), 3.86 (2H, d, J 7.6 Hz, 1'- H_2), 4.71 (2H, d, J 5.7 Hz, 1''- H_2), 7.02–7.07 (1H, m, 6''''-H), 7.10 (1H, td, J 7.5, 1.1 Hz, 5''''-H), 7.21–7.27 (1H, m, 3''''-H), 7.44 (1H, td, J 7.5, 1.6 Hz, 4''''-H), 8.03 (1H, s, 6-H), 11.19 (1H, br s, NH); δ_{C} (101 MHz, CDCl_3) 20.0 (2 \times CH_3), 26.9 (CH_3), 29.1 (CH), 37.5 (CH_2), 56.2 (CH_2), 110.4 (C), 115.3 (d, $^2J_{\text{CF}}$ 21.2 Hz, CH), 124.1 (d, $^4J_{\text{CF}}$ 3.4 Hz, CH), 124.3 (CH), 125.5 (d, $^2J_{\text{CF}}$ 14.7 Hz, C), 128.9 (d, $^3J_{\text{CF}}$ 8.0 Hz, CH), 129.9 (d, $^3J_{\text{CF}}$ 4.5 Hz, CH), 134.7 (C), 149.9 (C), 156.3 (C), 160.4 (C), 160.7 (C), 162.1 (d, $^1J_{\text{CF}}$ 246.1 Hz, C); m/z (ESI) 412.1083 (MNa^+ . $\text{C}_{19}\text{H}_{20}\text{FN}_3\text{NaO}_3\text{S}$ requires 412.1102).

***N*-(4''''-Iodobenzyl)-1-isobutyl-3-methyl-*N*-methyl-2,4-dioxo-1,2,3,4-tetrahydrothieno[2,3-*d*]pyrimidine-5-carboxamide (63)**



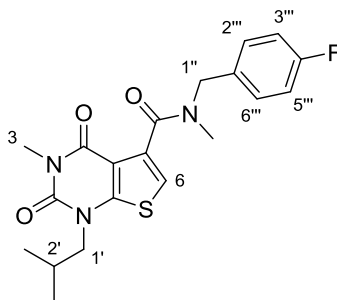
N-(4''''-Iodobenzyl)-1-isobutyl-3-methyl-2,4-dioxo-1,2,3,4-tetrahydrothieno[2,3-*d*]pyrimidine-5-carboxamide (**59**) (0.030 g, 0.060 mmol) and sodium hydride (0.0060 g, 0.15 mmol) were stirred in dry tetrahydrofuran (5 mL) for 1 h at room temperature. Methyl iodide (0.031 mL, 0.48 mmol) was added and the mixture heated to 50 °C and stirred for 16 h. The reaction mixture was quenched with water (10 mL), acidified with an aqueous solution of 1 M hydrochloric acid and the product extracted with ethyl acetate (3 × 10 mL). The combined organic layers were dried (MgSO₄), filtered and concentrated *in vacuo*. Purification by flash column chromatography eluting on a gradient from 50–100% ethyl acetate in petroleum ether gave *N*-(4''''-iodobenzyl)-1-isobutyl-3-methyl-*N*-methyl-2,4-dioxo-1,2,3,4-tetrahydrothieno[2,3-*d*]pyrimidine-5-carboxamide (**63**) as a viscous yellow oil (0.023 g, 75%). The compound exists as a 5:1 mixture of rotamers. Data for the major rotamer: ν_{\max} (neat)/cm⁻¹ 2960 (CH), 1705 (CO), 1645 (CO), 1492, 1467, 1006, 728; δ_{H} (400 MHz, CDCl₃) 1.01 (6H, d, *J* 6.7 Hz, CH(CH₃)₂), 2.27–2.37 (1H, m, 2'-H), 2.78 (3H, s, NCH₃), 3.41 (3H, s, 3-CH₃), 3.81 (2H, d, *J* 7.6 Hz, 1'-H₂), 4.73 (2H, s, 1''-H₂), 6.91 (1H, s, 6-H), 7.21 (2H, d, *J* 8.4 Hz, 2'''-H and 6'''-H), 7.66 (2H, d, *J* 8.4 Hz, 3'''-H and 5'''-H); δ_{C} (101 MHz, CDCl₃) 20.1 (2 × CH₃), 27.0 (CH₃), 28.3 (CH), 35.8 (CH₃), 50.2 (CH₂), 56.4 (CH₂), 93.0 (C), 113.5 (C), 129.0 (2 × CH), 130.3 (CH), 134.3 (C), 136.3 (C), 137.7 (2 × CH), 150.9 (C), 154.0 (C), 157.7 (C), 165.9 (C); *m/z* (ESI) 534.0323 (MNa⁺. C₂₀H₂₂IN₃NaO₃S requires 534.0319).

***N*-(3''''-Iodobenzyl)-1-isobutyl-3-methyl-*N*-methyl-2,4-dioxo-tetrahydrothieno[2,3-*d*]pyrimidine-5-carboxamide (64)**



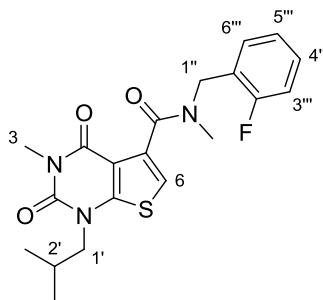
The reaction was carried out according to the previously described procedure for *N*-(4''''-iodobenzyl)-1-isobutyl-3-methyl-*N*-methyl-2,4-dioxo-1,2,3,4-tetrahydrothieno[2,3-*d*]pyrimidine-5-carboxamide (**63**) using *N*-(3''''-iodobenzylamine)-1-isobutyl-3-methyl-2,4-dioxo-5-(3-iodo-benzylaminocarbonyl)-1,2,3,4-tetrahydrothieno[2,3-*d*]pyrimidine (**60**) (0.033 g, 0.070 mmol) and gave *N*-(3''''-iodobenzyl)-1-isobutyl-3-methyl-*N*-methyl-2,4-dioxo-tetrahydrothieno[2,3-*d*]pyrimidine-5-carboxamide (**64**) as a viscous yellow oil (0.029 g, 81%). The compound exists as a 5:1 mixture of rotamers. Data for the major rotamer: ν_{\max} (neat)/ cm^{-1} 2960 (CH), 1705 (CO), 1662 (CO), 1510 (C=C), 1468, 1453, 1064, 775; δ_{H} (400 MHz, CDCl_3) 1.01 (6H, d, J 6.7 Hz, $\text{CH}(\text{CH}_3)_2$), 2.26–2.39 (1H, m, 2'-H), 2.78 (3H, s, NCH_3), 3.43 (3H, s, 3- CH_3), 3.78 (2H, d, J 7.8 Hz, 1'- H_2), 4.78 (2H, s, 1''- H_2), 6.90 (1H, s, 6-H), 7.12 (1H, t, J 7.7 Hz, 5''''-H), 7.44 (1H, d, J 7.7 Hz, 6''''-H), 7.64 (1H, d, J 7.7 Hz, 4''''-H), 7.82 (1H, s, 2''''-H); δ_{C} (101 MHz, CDCl_3) 20.1 ($2 \times \text{CH}_3$), 27.0 (CH_3), 28.3 (CH), 35.8 (CH_3), 49.9 (CH_2), 56.4 (CH_2), 94.6 (C), 112.7 (C), 113.5 (CH), 126.3 (CH), 127.5 (CH), 130.4 (CH), 134.7 (C), 136.1 (CH), 139.0 (C), 150.8 (C), 153.9 (C), 157.5 (C), 167.7 (C); m/z (ESI) 534.0307 (MNa^+ . $\text{C}_{20}\text{H}_{22}\text{IN}_3\text{NaO}_3\text{S}$ requires 534.0319).

***N*-(4'''-Fluorobenzyl)-1-isobutyl-3-methyl-*N*-methyl-2,4-dioxo-tetrahydrothieno[2,3-*d*]pyrimidine-5-carboxamide (65)**



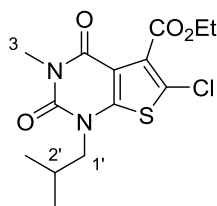
The reaction was carried out according to the previously described procedure for *N*-(4'''-iodobenzyl)-1-isobutyl-3-methyl-*N*-methyl-2,4-dioxo-1,2,3,4-tetrahydrothieno[2,3-*d*]pyrimidine-5-carboxamide (**63**) using *N*-(4'''-fluorobenzyl)-1-isobutyl-3-methyl-2,4-dioxo-1,2,3,4-tetrahydrothieno[2,3-*d*]pyrimidine-5-carboxamide (**61**) (0.035 g, 0.090 mmol) and gave *N*-(4'''-fluorobenzyl)-1-isobutyl-3-methyl-*N*-methyl-2,4-dioxo-tetrahydrothieno[2,3-*d*]pyrimidine-5-carboxamide (**65**) as a viscous yellow oil (0.022 g, 61%). The compound exists as a 5:1 mixture of rotamers. Data for the major rotamer: ν_{\max} (neat)/ cm^{-1} 2960 (CH), 1706 (CO), 1644 (CO), 1510 (C=C), 1493, 1221, 725; δ_{H} (400 MHz, CDCl_3) 1.01 (6H, d, J 6.7 Hz, $\text{CH}(\text{CH}_3)_2$), 2.27–2.37 (1H, m, 2'-H), 2.77 (3H, s, NCH_3), 3.42 (3H, s, 3- CH_3), 3.74–3.89 (2H, m, 1'- H_2), 4.78 (2H, s, 1''- H_2), 6.88 (1H, s, 6-H), 7.06 (2H, t, J 8.7 Hz, 3'''-H and 5'''-H), 7.44 (2H, dd, J 8.6, 5.4 Hz, 2'''-H and 6'''-H); δ_{C} (101 MHz, CDCl_3) 20.0 ($2 \times \text{CH}_3$), 27.0 (CH_3), 28.3 (CH), 35.6 (CH_3), 49.9 (CH_2), 56.4 (CH_2), 112.8 (C), 113.4 (d, $^4J_{\text{CF}}$ 3.1 Hz, C), 115.4 (d, $^2J_{\text{CF}}$ 21.4 Hz, $2 \times \text{CH}$), 115.9 (CH), 130.1 (d, $^3J_{\text{CF}}$ 8.0 Hz, $2 \times \text{CH}$), 132.4 (C), 150.8 (C), 153.9 (C), 157.6 (C), 163.5 (d, $^1J_{\text{CF}}$ 247.1 Hz, C), 165.7 (C); m/z (ESI) 426.1242 (MNa^+ . $\text{C}_{20}\text{H}_{22}\text{FN}_3\text{NaO}_3\text{S}$ requires 426.1258).

***N*-(2''''-fluorobenzyl)-1-isobutyl-3-methyl-*N*-methyl-2,4-dioxo-tetrahydrothieno[2,3-*d*]pyrimidine-5-carboxamide (66)**



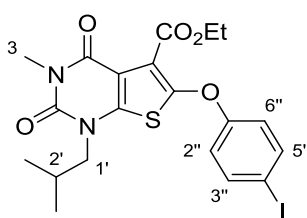
The reaction was carried out according to the previously described procedure for *N*-(4''''-iodobenzyl)-1-isobutyl-3-methyl-*N*-methyl-2,4-dioxo-1,2,3,4-tetrahydrothieno[2,3-*d*]pyrimidine-5-carboxamide (**63**) using *N*-(2''''-fluorobenzyl)-1-isobutyl-3-methyl-2,4-dioxo-1,2,3,4-tetrahydrothieno[2,3-*d*]pyrimidine-5-carboxamide (**62**) (0.034 g, 0.09 mmol) and gave *N*-(2''''-fluorobenzyl)-1-isobutyl-3-methyl-*N*-methyl-2,4-dioxo-tetrahydrothieno[2,3-*d*]pyrimidine-5-carboxamide (**66**) as a yellow oil (0.021 g, 58%). The compound exists as a 5:1 mixture of rotamers. Data for the major rotamer: ν_{\max} (neat)/ cm^{-1} 2961 (CH), 1705 (CO), 1661 (CO), 1510 (C=C), 1491, 1399, 760; δ_{H} (400 MHz, CDCl_3) 1.01 (6H, d, J 6.7 Hz, $\text{CH}(\text{CH}_3)_2$), 2.28–2.37 (1H, m, 2'-H), 2.77 (3H, s, NCH_3), 3.42 (3H, s, 3- CH_3), 3.74–3.86 (2H, m, 1'- H_2), 4.38–4.57 (2H, m, 1''- H_2), 6.88 (1H, s, 6-H), 7.00–7.10 (1H, m, J , 6''''-H), 7.14 (1H, td, J 7.5, 1.6 Hz, 5''''-H), 7.23–7.29 (1H, m, 3''''-H), 7.65 (1H, td, J 7.5, 1.6 Hz, 4''''-H); δ_{C} (101 MHz, CDCl_3) 20.1 ($2 \times \text{CH}_3$), 27.0 (CH_3), 28.3 (CH), 32.8 (CH_3), 44.0 (CH_2), 56.4 (CH_2), 112.8 (C), 115.6 (d, $^2J_{\text{CF}}$ 22.1 Hz, CH), 123.6 (CH), 124.5 (d, $^4J_{\text{CF}}$ 3.4 Hz, CH), 129.1 (d, $^2J_{\text{CF}}$ 15.4 Hz, C), 129.6 (d, $^3J_{\text{CF}}$ 8.0 Hz, CH), 130.8 (d, $^3J_{\text{CF}}$ 4.0 Hz, CH), 134.8 (C), 150.9 (C), 153.9 (C), 157.6 (C), 162.1 (d, $^1J_{\text{CF}}$ 248.9 Hz, C), 165.8 (C); m/z (EI) 403.1366 (M^+ . $\text{C}_{20}\text{H}_{22}\text{FN}_3\text{O}_3\text{S}$ requires 403.1369).

Ethyl 6-chloro-1-isobutyl-3-methyl-2,4-dioxo-1,2,3,4-tetrahydrothieno[2,3-*d*]pyrimidine-5-carboxylate (67)⁶¹



N-Chlorosuccinimide (0.031 g, 0.23 mmol) was added to a stirred solution of ethyl 1-isobutyl-3-methyl-2,4-dioxo-1,2,3,4-tetrahydrothieno[2,3-*d*]pyrimidine-5-carboxylate (**46**) (0.060 g, 0.19 mmol) in dichloromethane (0.5 mL) and acetic acid (0.5 mL). The mixture was stirred at room temperature for 5 h. The reaction mixture was azeotroped under vacuum in the presence of toluene (3 × 2 mL). Purification by flash column chromatography eluting with 20% ethyl acetate in petroleum ether gave ethyl 6-chloro-1-isobutyl-3-methyl-2,4-dioxo-1,2,3,4-tetrahydrothieno[2,3-*d*]pyrimidine-5-carboxylate (**67**) as a white solid (0.054 g, 82%). Mp 81–83 °C. Spectroscopic data were consistent with the literature.⁶¹ δ_{H} (400 MHz, CDCl₃) 0.99 (6H, d, *J* 6.7 Hz, CH(CH₃)₂), 1.42 (3H, t, *J* 7.2 Hz, OCH₂CH₃), 2.24–2.32 (1H, m, 2'-H), 3.39 (3H, s, 3-CH₃), 3.72 (2H, d, *J* 7.6 Hz, 1'-H₂), 4.47 (2H, q, *J* 7.2 Hz, OCH₂CH₃); δ_{C} (101 MHz, CDCl₃) 14.1 (CH₃), 20.0 (2 × CH₃), 27.1 (CH₃), 28.4 (CH), 56.5 (CH₂), 62.5 (CH₂), 112.0 (C), 121.0 (C), 129.4 (C), 150.5 (C), 150.8 (C), 156.6 (C), 162.0 (C); *m/z* (ESI) 367 (MNa⁺ 100%).

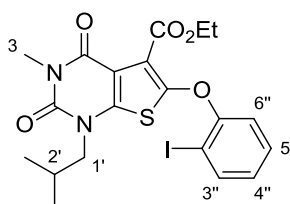
Ethyl 6-(4''-iodophenoxy)-1-isobutyl-3-methyl-2,4-dioxo-1,2,3,4-tetrahydrothieno[2,3-*d*]pyrimidine-5-carboxylate (69)



Ethyl 6-chloro-1-isobutyl-3-methyl-2,4-dioxo-1,2,3,4-tetrahydrothieno[2,3-*d*]pyrimidine-5-carboxylate (**67**) (0.107 g, 0.310 mmol) was dissolved in dry *N,N*-dimethylformamide (5 mL). Caesium carbonate (0.302 g, 0.930 mmol) and 4-iodophenol (0.103 g, 0.470 mmol) were added and the reaction stirred at 100 °C for 16 h. The reaction mixture was then diluted with water (10 mL) and the product extracted with ethyl acetate (3 × 10 mL). The organic layers were washed with an aqueous solution of 5% lithium chloride (10 mL) and brine (10 mL). The combined organic layers were dried (MgSO₄), filtered and concentrated

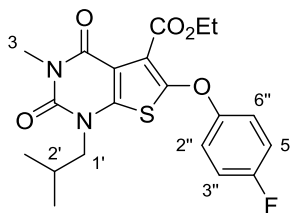
in vacuo. Purification by flash column chromatography eluting with 30% diethyl ether in petroleum ether gave ethyl 6-(4''-iodophenoxy)-1-isobutyl-3-methyl-2,4-dioxo-1,2,3,4-tetrahydrothieno[2,3-*d*]pyrimidine-5-carboxylate (**69**) as a colourless oil (0.0850 g, 52%). ν_{\max} (neat)/ cm^{-1} 2963 (CH), 1736 (CO), 1667 (CO), 1551 (C=C), 1481, 1173, 1011, 826; δ_{H} (400 MHz, CDCl_3) 0.97 (6H, d, J 6.7 Hz, $\text{CH}(\text{CH}_3)_2$), 1.25 (3H, t, J 7.1 Hz, OCH_2CH_3), 2.02–2.29 (1H, m, 2'-H), 3.41 (3H, s, 3- CH_3), 3.71 (2H, d, J 7.7 Hz, 1'- H_2), 4.32 (2H, q, J 7.1 Hz, OCH_2CH_3), 6.89 (2H, d, J 8.8 Hz, 2''-H and 6''-H), 7.65 (2H, d, J 8.8 Hz, 3''-H and 5''-H); δ_{C} (101 MHz, CDCl_3) 14.0 (CH_3), 20.0 ($2 \times \text{CH}_3$), 27.1 (CH_3), 28.3 (CH), 56.3 (CH_2), 62.2 (CH_2), 87.8 (C), 109.5 (C), 119.1 ($2 \times \text{CH}$), 119.3 (C), 138.8 ($2 \times \text{CH}$), 146.6 (C), 149.2 (C), 150.8 (C), 157.1 (C), 158.2 (C), 161.8 (C); m/z (ESI) 551.0094 (MNa^+ . $\text{C}_{20}\text{H}_{21}\text{IN}_2\text{NaO}_5\text{S}$ requires 551.0108).

Ethyl 6-(2''-iodophenoxy)-1-isobutyl-3-methyl-2,4-dioxo-1,2,3,4-tetrahydrothieno[2,3-*d*]pyrimidine-5-carboxylate (70)



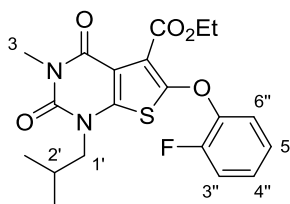
The reaction was carried out according to the previously described procedure for 6-(4''-iodophenoxy)-1-isobutyl-3-methyl-2,4-dioxo-1,2,3,4-tetrahydrothieno[2,3-*d*]pyrimidine-5-carboxylate (**69**) using ethyl 6-chloro-1-isobutyl-3-methyl-2,4-dioxo-1,2,3,4-tetrahydrothieno[2,3-*d*]pyrimidine-5-carboxylate (**67**) (0.119 g, 0.350 mmol) and 2-iodophenol (0.117 g, 0.530 mmol). The mixture was heated at 120 °C. This gave ethyl 6-(2''-iodophenoxy)-1-isobutyl-3-methyl-2,4-dioxo-1,2,3,4-tetrahydrothieno[2,3-*d*]pyrimidine-5-carboxylate (**70**) as a colourless oil (0.040 g, 22%). ν_{\max} (neat)/ cm^{-1} 2926 (CH), 1708 (CO), 1661 (CO), 1547 (C=C), 1464, 1292, 756; δ_{H} (400 MHz, CDCl_3) 0.97 (6H, d, J 6.7 Hz, $\text{CH}(\text{CH}_3)_2$), 1.26 (3H, t, J 7.2 Hz, OCH_2CH_3), 2.21–2.29 (1H, m, 2'-H), 3.41 (3H, s, 3- CH_3), 3.70 (2H, d, J 7.5 Hz, 1'- H_2), 4.33 (2H, q, J 7.2 Hz, OCH_2CH_3), 6.93 (1H, td, J 7.9, 1.3 Hz, 5''-H), 7.12 (1H, dd, J 7.9, 1.3 Hz, 6''-H), 7.33 (1H, td, J 7.9, 1.3 Hz, 4''-H), 7.83 (1H, dd, J 7.9, 1.3 Hz, 3''-H); δ_{C} (101 MHz, CDCl_3) 14.0 (CH_3), 20.0 ($2 \times \text{CH}_3$), 27.1 (CH_3), 28.3 (CH), 56.3 (CH_2), 62.2 (CH_2), 85.9 (C), 109.5 (C), 117.3 (CH), 118.8 (C), 126.5 (CH), 129.9 (CH), 140.0 (CH), 146.5 (C), 150.0 (C), 150.8 (C), 157.2 (C), 157.5 (C), 161.7 (C); m/z (ESI) 551.0090 (MNa^+ . $\text{C}_{20}\text{H}_{21}\text{IN}_2\text{NaO}_5\text{S}$ requires 551.0108).

Ethyl 6-(4''-fluorophenoxy)-1-isobutyl-3-methyl-2,4-dioxo-1,2,3,4-tetrahydrothieno[2,3-*d*]pyrimidine-5-carboxylate (71)



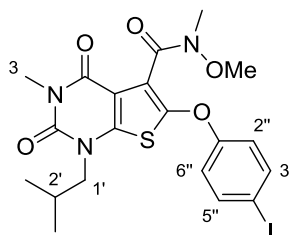
The reaction was carried out according to the previously described procedure for 6-(4''-iodophenoxy)-1-isobutyl-3-methyl-2,4-dioxo-1,2,3,4-tetrahydrothieno[2,3-*d*]pyrimidine-5-carboxylate (**69**) using ethyl 6-chloro-1-isobutyl-3-methyl-2,4-dioxo-1,2,3,4-tetrahydrothieno[2,3-*d*]pyrimidine-5-carboxylate (**67**) (0.12 g, 0.33 mmol) and 4-fluorophenol (0.056 mL, 0.50 mmol). This gave ethyl 6-(4''-fluorophenoxy)-1-isobutyl-3-methyl-2,4-dioxo-1,2,3,4-tetrahydrothieno[2,3-*d*]pyrimidine-5-carboxylate as a colourless oil (**71**) (0.094 g, 68%). ν_{\max} (neat)/ cm^{-1} 2963 (CH), 1705 (CO), 1667 (CO), 1551 (C=C), 1497, 1180, 841; δ_{H} (400 MHz, CDCl_3) 0.96 (6H, d, J 6.7 Hz, $\text{CH}(\text{CH}_3)_2$), 1.28 (3H, t, J 7.1 Hz, OCH_2CH_3), 2.20–2.30 (1H, m, 2'-H), 3.41 (3H, s, 3- CH_3), 3.70 (2H, d, J 7.7 Hz, 1'- H_2), 4.35 (2H, q, J 7.1 Hz, OCH_2CH_3), 7.02–7.07 (2H, m, 3''-H and 5''-H), 7.11 (2H, dd, J 9.3, 4.4 Hz, 2''-H and 6''-H); δ_{C} (101 MHz, CDCl_3) 14.0 (CH_3), 20.0 ($2 \times \text{CH}_3$), 27.1 (CH_3), 28.3 (CH), 56.3 (CH_2), 62.2 (CH_2), 109.5 (C), 116.6 (d, $^2J_{\text{CF}}$ 22.3 Hz, $2 \times \text{CH}$), 118.3 (C), 118.4 (d, $^3J_{\text{CF}}$ 8.3 Hz, $2 \times \text{CH}$), 146.3 (C), 150.6 (C), 150.8 (C), 154.1 (d, $^4J_{\text{CF}}$ 3.2 Hz, C), 157.2 (C), 160.5 (d, $^1J_{\text{CF}}$ 249.8 Hz, C), 162.0 (C); m/z (ESI) 443.1029 (MNa^+ . $\text{C}_{20}\text{H}_{21}\text{FN}_2\text{NaO}_5\text{S}$ requires 443.1047).

Ethyl 6-(2''-fluorophenoxy)-1-isopropyl-3-methyl-2,4-dioxo-1,2,3,4-tetrahydrothieno[2,3-*d*]pyrimidine-5-carboxylate (72)



The reaction was carried out according to the previously described procedure for 6-(4''-iodophenoxy)-1-isobutyl-3-methyl-2,4-dioxo-1,2,3,4-tetrahydrothieno[2,3-*d*]pyrimidine-5-carboxylate (**69**) using ethyl 6-chloro-1-isobutyl-3-methyl-2,4-dioxo-1,2,3,4-tetrahydrothieno[2,3-*d*]pyrimidine-5-carboxylate (**67**) (0.11 g, 0.31 mmol) and 2-fluorophenol (0.042 mL, 0.46 mmol). The mixture was heated at 110 °C. This gave ethyl 6-(2''-fluorophenoxy)-1-isobutyl-3-methyl-2,4-dioxo-1,2,3,4-tetrahydrothieno[2,3-*d*]pyrimidine-5-carboxylate (**72**) as a colourless oil (0.059 g, 45%). ν_{\max} (neat)/ cm^{-1} 2960 (CH), 1708 (CO), 1661 (CO), 1549 (C=C), 1468, 1387, 1291, 1086; δ_{H} (400 MHz, CDCl_3) 0.96 (6H, d, J 6.7 Hz, $\text{CH}(\text{CH}_3)_2$), 1.28 (3H, t, J 7.1 Hz, OCH_2CH_3), 2.21–2.29 (1H, m, 2'-H), 3.41 (3H, s, 3- CH_3), 3.70 (2H, d, J 7.6 Hz, 1'- H_2), 4.33 (2H, q, J 7.1 Hz, OCH_2CH_3), 7.11 (1H, td, J 7.9, 1.9 Hz, 5''-H), 7.14–7.19 (2H, m, 3''-H and 6''-H), 7.20 (1H, td, J 7.9, 2.0 Hz, 4''-H); δ_{C} (101 MHz, CDCl_3) 14.0 (CH_3), 20.0 ($2 \times \text{CH}_3$), 27.1 (CH_3), 28.3 (CH), 56.4 (CH_2), 62.2 (CH_2), 109.5 (C), 117.2 (d, $^2J_{\text{CF}}$ 18.7 Hz, CH), 118.9 (C) 119.5 (CH), 124.8 (d, $^3J_{\text{CF}}$ 3.8 Hz, CH), 125.9 (d, $^3J_{\text{CF}}$ 7.9 Hz, CH), 145.5 (d, $^2J_{\text{CF}}$ 11.5 Hz, C), 146.2 (C), 150.4 (C), 150.8 (C), 153.7 (d, $^1J_{\text{CF}}$ 248.7 Hz, C), 157.2 (C), 161.8 (C); m/z (ESI) 443.1037 (MNa^+ . $\text{C}_{20}\text{H}_{21}\text{FN}_2\text{NaO}_5\text{S}$ requires 443.1047).

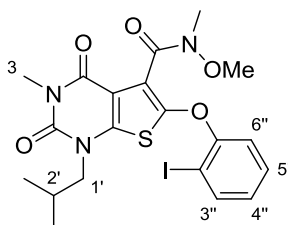
6-(4''-Iodophenoxy)-1-isobutyl-3-methyl-2,4-dioxo-1,2,3,4-tetrahydrothieno[2,3-d]pyrimidine-5-(*N*-methoxy-*N*-methyl)carboxamide (75)



Ethyl 6-(4''-iodophenoxy)-1-isobutyl-3-methyl-2,4-dioxo-1,2,3,4-tetrahydrothieno[2,3-d]pyrimidine-5-carboxylate (**69**) (0.087 g, 0.16 mmol) was dissolved in tetrahydrofuran (0.50 mL) and methanol (0.25 mL). An aqueous solution of 10% sodium hydroxide (0.15 mL) was added and the mixture stirred for 1 h. The reaction mixture was diluted with water (5 mL) and washed with diethyl ether (5 mL). The aqueous layer was acidified with an aqueous solution of 1 M hydrochloric acid (5 mL) and extracted with ethyl acetate (3 × 5 mL). The organic layers were combined, dried (MgSO₄), filtered and concentrated *in vacuo*. The resulting material was dissolved in acetonitrile (10 mL) then *O*-(benzotriazol-1-yl)-*N,N,N',N'*-tetramethyluronium hexafluorophosphate (0.084 g, 0.23 mmol), *N,N'*-diisopropylethylamine (0.052 mL 0.30 mmol) and *N,O*-dimethylhydroxylamine (0.043 g, 0.45 mmol) were added and the mixture stirred at 40 °C for 16 h. The mixture was diluted with water (10 mL) and washed with a saturated aqueous solution of sodium bicarbonate (10 mL). The mixture was extracted with ethyl acetate (3 × 10 mL). The organic layers were combined and washed with an aqueous solution of 5% lithium chloride (30 mL) and brine (30 mL). The organic layer was dried (MgSO₄), filtered and concentrated *in vacuo* to give the crude product. Purification by flash column chromatography eluting with 40% ethyl acetate in petroleum ether gave ethyl 6-(4''-iodophenoxy)-1-isobutyl-3-methyl-2,4-dioxo-1,2,3,4-tetrahydrothieno[2,3-d]pyrimidine-5-(*N*-methoxy-*N*-methyl)carboxamide (**75**) as a yellow oil (0.053 g, 64%). ν_{\max} (neat)/cm⁻¹ 2960 (CH), 1707 (CO), 1663 (CO), 1549 (C=C), 1477, 1223, 1007, 769; The compound exists as a 5:1 mixture of rotamers. Data for the major rotamer: δ_{H} (400 MHz, CDCl₃) 0.97 (6H, d, *J* 6.7 Hz, CH(CH₃)₂), 2.21–2.30 (1H, m, 2'-H), 3.37 (3H, s, NCH₃), 3.40 (3H, s, 3-CH₃), 3.60 (1H, dd, *J* 14.3, 7.8 Hz, 1'-HH), 3.62 (3H, s, OCH₃), 3.81 (1H, dd, *J* 14.3, 7.8 Hz, 1'-HH), 6.94 (2H, d, *J* 8.9 Hz, 2''-H and 6''-H), 7.64 (2H, d, *J* 8.9 Hz, 3''-H and 5''-H); δ_{C} (101 MHz, CDCl₃) 20.0 (CH₃), 20.1 (CH₃), 27.1 (CH₃), 28.3 (CH), 32.8 (CH₃), 56.4 (CH₂), 61.8 (CH₃), 88.0 (C), 109.8 (C), 119.5 (2 × CH), 120.6 (C), 138.8 (2 × CH), 145.9 (C), 146.6 (C), 150.9 (C),

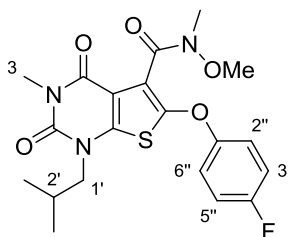
157.5 (C), 158.1(C), 163.1 (C); m/z (ESI) 566.0201 (MNa^+ . $C_{20}H_{22}IN_3NaO_5S$ requires 566.0217).

6-(2''-Iodophenoxy)-1-isobutyl-3-methyl-2,4-dioxo-1,2,3,4-tetrahydrothieno[2,3-*d*]pyrimidine-5-(*N*-methoxy-*N*-methyl)carboxamide (76)



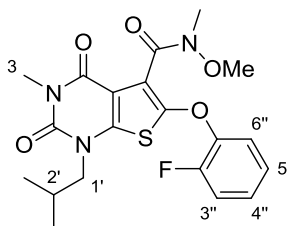
The reaction was carried out according to the previously described procedure for 6-(4''-iodophenoxy)-1-isobutyl-3-methyl-2,4-dioxo-1,2,3,4-tetrahydrothieno[2,3-*d*]pyrimidine-5-(*N*-methoxy-*N*-methyl)carboxamide (**75**) using ethyl 6-(2''-iodophenoxy)-1-isobutyl-3-methyl-2,4-dioxo-1,2,3,4-tetrahydrothieno[2,3-*d*]pyrimidine-5-carboxylate (**70**) (0.038 g, 0.070 mmol). This gave 6-(2''-iodophenoxy)-1-isobutyl-3-methyl-2,4-dioxo-1,2,3,4-tetrahydrothieno[2,3-*d*]pyrimidine-5-(*N*-methoxy-*N*-methyl)carboxamide (**76**) as a yellow oil (0.021 g, 55%). ν_{\max} (neat)/ cm^{-1} 2926 (CH), 1707 (CO), 1663 (CO), 1545 (C=C), 1464, 1223, 1105, 769; The compound exists as a 6:1 mixture of rotamers. Data for the major rotamer: δ_H (400 MHz, $CDCl_3$) 0.97 (6H, d, J 6.7 Hz, $CH(CH_3)_2$), 2.23–2.29 (1H, m, 2'-H), 3.39 (3H, s, NCH_3), 3.40 (3H, s, 3- CH_3), 3.64 (1H, dd, J 14.3, 7.9 Hz, 1'- HH), 3.72 (3H, s, OCH_3), 3.77 (1H, dd, 14.3, 7.9 Hz, 1'- HH), 6.91 (1H, td, J 7.7, 1.3 Hz, 5''-H), 7.24 (1H, dd, J 7.7, 1.3 Hz, 6''-H), 7.33 (1H, td, J 7.7, 1.3 Hz, 4''-H), 7.81 (1H, dd, J 7.7, 1.3 Hz, 3''-H); δ_C (101 MHz, $CDCl_3$) 20.0 (2 \times CH_3), 27.1 (CH_3), 28.3 (CH), 32.9 (CH_3), 56.4 (CH_2), 62.1 (CH_3), 85.8 (C), 109.9 (C), 117.8 (CH), 120.4 (C), 126.5 (CH), 130.1 (CH), 139.7 (CH), 146.1 (C), 146.6 (C), 151.0 (C), 152.3 (C), 157.6 (C), 163.3 (C); m/z (ESI) 566.0202 (MNa^+ . $C_{20}H_{22}IN_3NaO_5S$ requires 566.0217).

6-(4''-Fluorophenoxy)-1-isobutyl-3-methyl-2,4-dioxo-1,2,3,4-tetrahydrothieno[2,3-*d*]pyrimidine-5-(*N*-methoxy-*N*-methyl)carboxamide (73)



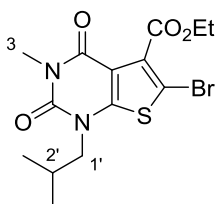
The reaction was carried out according to the previously described procedure for 6-(4''-iodophenoxy)-1-isobutyl-3-methyl-2,4-dioxo-1,2,3,4-tetrahydrothieno[2,3-*d*]pyrimidine-5-(*N*-methoxy-*N*-methyl)carboxamide (**75**) using ethyl 6-(4''-fluorophenoxy)-1-isobutyl-3-methyl-2,4-dioxo-1,2,3,4-tetrahydrothieno[2,3-*d*]pyrimidine-5-carboxylate (**71**) (0.097 g, 0.23 mmol). This gave 6-(4''-fluorophenoxy)-1-isobutyl-3-methyl-2,4-dioxo-1,2,3,4-tetrahydrothieno[2,3-*d*]pyrimidine-5-(*N*-methoxy-*N*-methyl)carboxamide (**73**) as a yellow oil (0.042 g, 54%). ν_{\max} (neat)/ cm^{-1} 2929 (CH), 1706 (CO), 1656 (CO), 1549 (C=C), 1494, 1389, 1179, 1107, 729; The compound exists as a 6:1 mixture of rotamers. Data for the major rotamer: δ_{H} (400 MHz, CDCl_3) 0.97 (6H, d, J 6.7 Hz, $\text{CH}(\text{CH}_3)_2$), 2.22–2.28 (1H, m, 2'-H), 3.38 (3H, s, NCH_3), 3.40 (3H, s, 3- CH_3), 3.60 (1H, dd, J 14.0, 7.9 Hz, 1'- HH), 3.64 (3H, s, OCH_3), 3.79 (1H, dd, J 14.0, 7.9 Hz, 1'- HH), 7.04 (2H, t, J 8.9 Hz, 3''-H and 5''-H), 7.16 (2H, dd, J 8.9, 4.3 Hz, 2''-H and 6''-H); δ_{C} (101 MHz, CDCl_3) 20.0 (CH_3), 20.1 (CH_3), 27.1 (CH_3), 28.3 (CH), 32.8 (CH_3), 56.3 (CH_2), 61.8 (CH_3), 109.8 (C), 116.5 (d, $^2J_{\text{CF}}$ 23.5 Hz, 2 \times CH), 119.1 (d, $^3J_{\text{CF}}$ 8.6 Hz, 2 \times CH), 119.6 (C), 146.3 (C), 147.3 (C), 151.0 (C), 154.2 (d, $^4J_{\text{CF}}$ 2.8 Hz, C), 157.6 (C), 160.5 (d, $^1J_{\text{CF}}$ 247.3 Hz, C), 163.3 (C); m/z (ESI) 458.1135 (MNa^+ . $\text{C}_{20}\text{H}_{22}\text{FN}_3\text{NaO}_5\text{S}$ requires 458.1156).

6-(2''-Fluorophenoxy)-1-isopropyl-3-methyl-2,4-dioxo-1,2,3,4-tetrahydrothieno[2,3-*d*]pyrimidine-5-(*N*-methoxy-*N*-methyl)carboxamide (74)



The reaction was carried out according to the previously described procedure for 6-(4''-iodophenoxy)-1-isobutyl-3-methyl-2,4-dioxo-1,2,3,4-tetrahydrothieno[2,3-*d*]pyrimidine-5-(*N*-methoxy-*N*-methyl)carboxamide (**75**) using ethyl 6-(2''-fluorophenoxy)-1-isobutyl-3-methyl-2,4-dioxo-1,2,3,4-tetrahydrothieno[2,3-*d*]pyrimidine-5-carboxylate (**72**) (0.056 g, 0.13 mmol). This gave 6-(2''-fluorophenoxy)-1-isobutyl-3-methyl-2,4-dioxo-1,2,3,4-tetrahydrothieno[2,3-*d*]pyrimidine-5-(*N*-methoxy-*N*-methyl)carboxamide (**74**) as a yellow oil (0.030 g, 57%). ν_{\max} (neat)/ cm^{-1} 2927 (CH), 1708 (CO), 1664 (CO), 1549 (C=C), 1498, 1257, 1110, 769; δ_{H} (400 MHz, CDCl_3) 0.96 (6H, d, J 6.7 Hz, $\text{CH}(\text{CH}_3)_2$), 2.22–2.29 (1H, m, 2'-H), 3.40 (3H, s, NCH_3), 3.40 (3H, s, 3- CH_3), 3.62 (1H, dd, J 14.3, 7.7 Hz, 1'- HH), 3.66 (3H, s, OCH_3), 3.79 (1H, dd, J 14.3, 7.7 Hz, 1'- HH), 7.10–7.19 (3H, m, 3''-H, 5''-H and 6''-H), 7.31 (1H, td, J 8.2, 2.1 Hz, 4''-H); δ_{C} (101 MHz, CDCl_3) 20.0 (CH_3), 20.1 (CH_3), 27.1 (CH_3), 28.3 (CH), 32.8 (CH_3), 56.3 (CH_2), 61.9 (CH_3), 109.9 (C), 117.1 (d, $^2J_{\text{CF}}$ 18.3 Hz, CH), 119.4 (C) 120.2 (CH), 124.9 (d, $^3J_{\text{CF}}$ 4.2 Hz, CH), 126.0 (d, $^3J_{\text{CF}}$ 7.5 Hz, CH), 145.5 (d, $^2J_{\text{CF}}$ 11.5 Hz, C), 146.1 (C), 147.1 (C), 151.0 (C), 153.7 (d, $^3J_{\text{CF}}$ 246.5 Hz, C), 157.6 (C), 163.2 (C); m/z (ESI) 458.1136 (MNa^+ . $\text{C}_{20}\text{H}_{22}\text{FN}_3\text{NaO}_5\text{S}$ requires 458.1156).

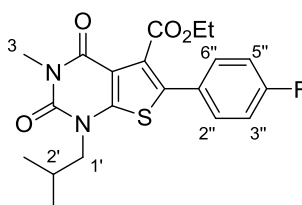
Ethyl 6-bromo-1-isobutyl-3-methyl-2,4-dioxo-1,2,3,4-tetrahydrothieno[2,3-*d*]pyrimidine-5-carboxylate (68)



N-Bromosuccinimide (0.598 g, 3.36 mmol) was added to a stirred solution of ethyl 1-isobutyl-3-methyl-2,4-dioxo-1,2,3,4-tetrahydrothieno[2,3-*d*]pyrimidine-5-carboxylate (**46**) (0.870 g, 2.80 mmol) in dichloromethane (15 mL) and acetic acid (15 mL) and stirred at room temperature for 5 h. The reaction mixture was azeotroped under vacuum in the presence of toluene (3 × 30 mL). Purification by flash column chromatography eluting

with 20% ethyl acetate in petroleum ether gave ethyl 6-bromo-1-isobutyl-3-methyl-2,4-dioxo-1,2,3,4-tetrahydrothieno[2,3-*d*]pyrimidine-5-carboxylate (**68**) as a white solid (0.911 g, 84%). Mp 110–114 °C; ν_{\max} (neat)/ cm^{-1} 2961 (CH), 1736 (CO), 1707 (CO), 1661 (CO), 1481, 1283, 1238; δ_{H} (400 MHz, CDCl_3) 0.99 (6H, d, J 6.7 Hz, $\text{CH}(\text{CH}_3)_2$), 1.42 (3H, t, J 7.1 Hz, OCH_2CH_3), 2.24–2.33 (1H, m, 2'-H), 3.40 (3H, s, 3- CH_3), 3.72 (2H, d, J 7.8 Hz, 1'- H_2), 4.48 (2H, q, J 7.1 Hz, OCH_2CH_3); δ_{C} (101 MHz, CDCl_3) 14.1 (CH_3), 20.0 ($2 \times \text{CH}_3$), 27.0 (CH), 28.4 (CH_3), 56.5 (CH_2), 62.6 (CH_2), 103.5 (C), 113.1 (C), 132.5 (C), 150.5 (C), 153.2 (C), 156.4 (C), 162.7 (C); m/z (ESI) 410.9972 (MNa^+ , $\text{C}_{14}\text{H}_{17}^{79}\text{BrN}_2\text{NaO}_4\text{S}$ requires 410.9985).

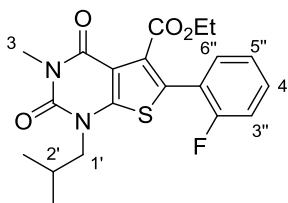
Ethyl 6-(4''-fluorophenyl)-1-isobutyl-3-methyl-2,4-dioxo-1,2,3,4-tetrahydrothieno[2,3-*d*]pyrimidine-5-carboxylate (80**)**



Potassium phosphate (0.18 g, 0.78 mmol) was suspended in a solution of 6-bromo-1-isobutyl-3-methyl-2,4-dioxo-1,2,3,4-tetrahydrothieno[2,3-*d*]pyrimidine-5-carboxylate (**68**) (0.15 g, 0.39 mmol) and 4-fluorophenylboronic acid (0.070 g, 0.50 mmol) in *N,N'*-dimethylformamide (10 mL) and degassed for 1 h. Tetrakis(triphenylphosphine)palladium(0) (0.045 g, 0.039 mmol) was added and the reaction heated under reflux for 22 h. The reaction mixture was cooled to room temperature, extracted with ethyl acetate (30 mL) and washed with an aqueous solution of 5% lithium chloride (4×25 mL) and brine (2×20 mL). The organic layers were combined, dried (MgSO_4), filtered and concentrated *in vacuo*. Purification by flash column chromatography eluting with 20% ethyl acetate in petroleum ether gave ethyl 6-(4''-fluorophenyl)-1-isobutyl-3-methyl-2,4-dioxo-1,2,3,4-tetrahydrothieno[2,3-*d*]pyrimidine-5-carboxylate (**80**) as a white solid (0.13 g, 81%). Mp 143–145 °C; ν_{\max} (neat)/ cm^{-1} 2963 (CH), 1732 (CO), 1707 (CO), 1663 (CO), 1537, 1483, 1294, 1206; δ_{H} (400 MHz, CDCl_3) 1.02 (6H, d, J 7.0 Hz, $\text{CH}(\text{CH}_3)_2$), 1.30 (3H, t, J 7.3 Hz, OCH_2CH_3), 2.30–2.40 (1H, m, 2'-H), 3.42 (3H, s, 3- CH_3), 3.81 (2H, d, J 7.7 Hz, 1'- CH_2), 4.38 (2H, q, J 7.3 Hz, OCH_2CH_3), 7.01–7.13 (2H, m, 2''-H and 6''-H), 7.46–7.51 (2H, m, 3''-H and 5''-H); δ_{C} (101 MHz, CDCl_3) 14.0 (CH_3), 20.0 ($2 \times \text{CH}_3$), 27.1 (CH_3), 28.3 (CH), 56.4 (CH_2), 62.3 (CH_2), 114.0 (C), 116.2 (d, $^2J_{\text{CF}}$ 22.3 Hz, $2 \times \text{CH}$), 127.2 (d, $^4J_{\text{CF}}$ 3.8 Hz, C), 128.1 (C), 129.0 (C), 130.2

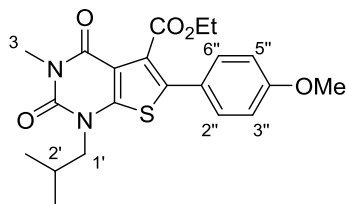
(d, $^3J_{\text{CF}}$ 9.8 Hz, $2 \times \text{CH}$), 150.7 (C), 152.3 (C), 157.5 (C), 162.8 (d, $^1J_{\text{CF}}$ 250.7 Hz, C), 167.7 (C); m/z (ESI) 427.1093 (MNa^+ . $\text{C}_{20}\text{H}_{21}\text{FN}_2\text{NaO}_4\text{S}$ requires 427.1098).

Ethyl 6-(2''-fluorophenyl)-1-isobutyl-3-methyl-2,4-dioxo-1,2,3,4-tetrahydrothieno[2,3-*d*]pyrimidine-5-carboxylate (81)



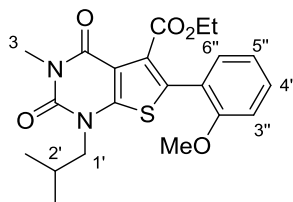
The reaction was carried out according to the previously described procedure for ethyl 6-(4''-fluorophenyl)-1-isobutyl-3-methyl-2,4-dioxo-1,2,3,4-tetrahydrothieno[2,3-*d*]pyrimidine-5-carboxylate (**80**) using 6-bromo-1-isobutyl-3-methyl-2,4-dioxo-1,2,3,4-tetrahydrothieno[2,3-*d*]pyrimidine-5-carboxylate (**68**) (0.20 g, 0.51 mmol) and 2-fluorophenylboronic acid (0.11 g, 0.67 mmol). This gave ethyl 6-(2''-fluorophenyl)-1-isobutyl-3-methyl-2,4-dioxo-1,2,3,4-tetrahydrothieno[2,3-*d*]pyrimidine-5-carboxylate (**81**) as a light pink solid (0.18 g, 86%). Mp 94–98 °C; ν_{max} (neat)/ cm^{-1} 2963 (CH), 1732 (CO), 1707 (CO), 1661 (CO), 1487, 1223, 1018, 758; δ_{H} (400 MHz, CDCl_3) 1.01 (6H, d, J 7.3 Hz, $\text{CH}(\text{CH}_3)_2$), 1.26 (3H, t, J 7.1 Hz, OCH_2CH_3), 2.30–2.40 (1H, m, 2'-H), 3.42 (3H, s, 3- CH_3), 3.82 (2H, d, J 7.5 Hz, 1'- CH_2), 4.35 (2H, q, J 7.1 Hz, OCH_2CH_3), 7.13–7.18 (1H, m, 3''-H), 7.20 (1H, td, J 7.8, 1.2 Hz, 5''-H), 7.36–7.42 (1H, m, 6''-H), 7.51 (1H, td, J 7.8, 1.6 Hz, 4''-H); δ_{C} (101 MHz, CDCl_3) 14.0 (CH_3), 20.1 ($2 \times \text{CH}_3$), 27.0 (CH_3), 28.3 (CH), 56.3 (CH_2), 62.1 (CH_2), 113.4 (C), 116.1 (d, $^2J_{\text{CF}}$ 21.7 Hz, CH), 118.9 (d, $^2J_{\text{CF}}$ 15.1 Hz, C), 124.5 (d, $^4J_{\text{CF}}$ 3.9 Hz, CH), 126.2 (C), 129.7 (C), 131.1 (d, $^3J_{\text{CF}}$ 8.0 Hz, CH), 131.1 (d, $^3J_{\text{CF}}$ 9.8 Hz, CH), 150.7 (C), 153.4 (C), 157.4 (C), 159.5 (d, $^1J_{\text{CF}}$ 251.9 Hz, C), 164.1 (C); m/z (ESI) 427.1087 (MNa^+ . $\text{C}_{20}\text{H}_{21}\text{FN}_2\text{NaO}_4\text{S}$ requires 427.1098).

Ethyl 1-isobutyl-6-(4''-methoxyphenyl)-3-methyl-2,4-dioxo-1,2,3,4-tetrahydrothieno[2,3-*d*]pyrimidine-5-carboxylate (82)



The reaction was carried out according to the previously described procedure for ethyl 6-(4''-fluorophenyl)-1-isobutyl-3-methyl-2,4-dioxo-1,2,3,4-tetrahydrothieno[2,3-*d*]pyrimidine-5-carboxylate (**80**) using 6-bromo-1-isobutyl-3-methyl-2,4-dioxo-1,2,3,4-tetrahydrothieno[2,3-*d*]pyrimidine-5-carboxylate (**68**) (0.20 g, 0.51 mmol) and 4-methoxyphenylboronic acid (0.10 g, 0.67 mmol). This gave ethyl 1-isobutyl-6-(4''-methoxyphenyl)-3-methyl-2,4-dioxo-1,2,3,4-tetrahydrothieno[2,3-*d*]pyrimidine-5-carboxylate (**82**) as a white solid (0.18 g, 85%). Mp 129–131 °C; ν_{\max} (neat)/ cm^{-1} 2961 (CH), 1730 (CO), 1705 (CO), 1659 (CO), 1537, 1483, 1294, 1252, 1204, 1020, 831, 729; δ_{H} (400 MHz, CDCl_3) 1.01 (6H, d, J 6.7 Hz, $\text{CH}(\text{CH}_3)_2$), 1.31 (3H, t, J 7.3 Hz, OCH_2CH_3), 2.30–2.40 (1H, m, 2''-H), 3.41 (3H, s, 3- CH_3), 3.80 (2H, d, J 7.7 Hz, 1'- CH_2), 3.84 (3H, s, 4''- OCH_3), 4.39 (2H, q, J 7.3 Hz, OCH_2CH_3), 6.92 (2H, d, J 8.8 Hz, 3''-H and 5''-H), 7.43 (2H, d, J 8.8 Hz, 2''-H and 6''-H); δ_{C} (101 MHz, CDCl_3) 14.0 (CH_3), 20.0 ($2 \times \text{CH}_3$), 27.1 (CH_3), 28.3 (CH), 55.4 (CH_3), 56.3 (CH_2), 62.2 (CH_2), 114.0 (C), 114.4 ($2 \times \text{CH}$), 123.5 (C), 126.2 (C), 129.5 ($2 \times \text{CH}$), 132.9 (C), 150.8 (C), 151.8 (C), 157.6 (C), 160.3 (C), 165.0 (C); m/z (ESI) 439.1283 (MNa^+ . $\text{C}_{21}\text{H}_{24}\text{N}_2\text{NaO}_5\text{S}$ requires 439.1298).

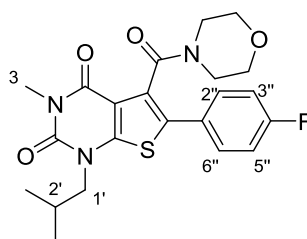
Ethyl 1-isobutyl-6-(2''-methoxyphenyl)-3-methyl-2,4-dioxo-1,2,3,4-tetrahydrothieno[2,3-*d*]pyrimidine-5-carboxylate (83)



The reaction was carried out according to the previously described procedure for ethyl 6-(4''-fluorophenyl)-1-isobutyl-3-methyl-2,4-dioxo-1,2,3,4-tetrahydrothieno[2,3-*d*]pyrimidine-5-carboxylate (**80**) using 6-bromo-1-isobutyl-3-methyl-2,4-dioxo-1,2,3,4-tetrahydrothieno[2,3-*d*]pyrimidine-5-carboxylate (**68**) (0.20 g, 0.51 mmol) and 2-methoxyphenylboronic acid (0.10 g, 0.67 mmol). This gave ethyl 1-isobutyl-6-(2''-

methoxyphenyl)-3-methyl-2,4-dioxo-1,2,3,4-tetrahydrothieno[2,3-*d*]pyrimidine-5-carboxylate (**83**) as a yellow solid (0.18 g, 86%). Mp 119–123 °C; ν_{\max} (neat)/ cm^{-1} 2963 (CH), 1730 (CO), 1705 (CO), 1659 (CO), 1489, 1479, 1244, 1200, 1020, 729; δ_{H} (500 MHz, CDCl_3) 1.01 (6H, d, J 6.3 Hz, $\text{CH}(\text{CH}_3)_2$), 1.23 (3H, t, J 7.3 Hz, OCH_2CH_3), 2.31–2.41 (1H, m, 2'-H), 3.42 (3H, s, 3- CH_3), 3.81 (2H, d, J 7.8 Hz, 1'- CH_2), 3.84 (3H, s, 2''- OCH_3), 4.32 (2H, q, J 7.3 Hz, OCH_2CH_3), 6.95 (1H, br d, J 7.9 Hz, 3''-H), 6.98 (1H, td, J 7.9, 1.4 Hz, 5''-H), 7.36 (1H, td, J 7.9, 1.4 Hz, 4''-H), 7.43 (1H, dd, J 7.9, 1.4 Hz, 6''-H); δ_{C} (101 MHz, CDCl_3) 13.9 (CH_3), 20.0 ($2 \times \text{CH}_3$), 27.0 (CH_3), 28.4 (CH), 55.5 (CH_3), 56.1 (CH_2), 61.8 (CH_2), 111.2 (CH), 113.0 (C), 119.9 (C), 120.8 (CH), 128.7 (C), 129.8 (C), 130.6 (CH), 130.9 (CH), 150.9 (C), 153.2 (C), 156.4 (C), 157.5 (C), 164.6 (C); m/z (ESI) 439.1281 (MNa^+ . $\text{C}_{21}\text{H}_{24}\text{N}_2\text{NaO}_5\text{S}$ requires 439.1298).

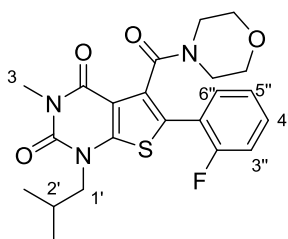
6-(4''-Fluorophenyl)-1-isobutyl-3-methyl-2,4-dioxo-1,2,3,4-tetrahydrothieno[2,3-*d*]pyrimidine-5-*N*-morpholinecarboxamide (88**)**



Ethyl 6-(4''-fluorophenyl)-1-isobutyl-3-methyl-2,4-dioxo-1,2,3,4-tetrahydrothieno[2,3-*d*]pyrimidine-5-carboxylate (**80**) (0.18 g, 0.44 mmol) was dissolved in ethanol (4 mL) and water (4 mL) prior to the addition of 4 M sodium hydroxide (1.5 mL, 2.0 mmol) and stirred at 80 °C for 1 h. The reaction mixture was diluted with water (10 mL) and washed with diethyl ether (2×10 mL). The aqueous layer was acidified with an aqueous solution of 1 M hydrochloric acid and extracted with ethyl acetate (3×10 mL). The combined organic layers were dried (MgSO_4), filtered and concentrated *in vacuo*. The resulting yellow solid was dissolved in dichloromethane (5 mL) and *N,N'*-dimethylformamide (2 drops) and cooled to 0 °C prior to the addition of oxalyl chloride (0.045 mL, 0.53 mmol). The reaction mixture was warmed to 40 °C and stirred for 3 h. After being cooled to room temperature, the reaction mixture was concentrated *in vacuo* to yield the acid chloride, which was used without further purification. The crude acid chloride was dissolved in dichloromethane (5 mL) and cooled to 0 °C. Morpholine (0.19 mL, 2.2 mmol) was added dropwise to the stirring acid chloride solution. The reaction mixture was stirred at 40 °C for 18 h under argon. The reaction mixture was cooled to room temperature, diluted in water (10 mL) and extracted with dichloromethane (3×10 mL). The organic layers were combined, dried

(MgSO₄), filtered and concentrated *in vacuo*. Purification by flash column chromatography eluting with 60% ethyl acetate in petroleum ether gave 6-(4''-fluorophenyl)-1-isobutyl-3-methyl-2,4-dioxo-1,2,3,4-tetrahydrothieno[2,3-*d*]pyrimidine-5-*N*-morpholinecarboxamide (**88**) (0.094 g, 48%) as a colourless oil. ν_{\max} (neat)/cm⁻¹ 2970 (CH), 1740 (CO), 1724 (CO), 1366, 1229, 1217; δ_{H} (400 MHz, CDCl₃) 1.03 (6H, d, *J* 5.6 Hz, CH(CH₃)₂), 2.31–2.40 (1H, m, 2'-H), 3.05 (1H, ddd, *J* 8.5, 5.8, 2.4 Hz, NCHH), 3.10 (1H, ddd, *J* 10.6, 4.6, 2.4 Hz, NCHH), 3.26 (1H, ddd, *J* 10.6, 5.8, 2.4 Hz, NCHH), 3.41 (3H, s, 3-CH₃), 3.47–3.57 (2H, m, NCHH and OCHH), 3.68 (1H, dd, *J* 11.4, 6.0 Hz, 1'-HH), 3.74–3.86 (3H, m, OCHH and OCH₂), 3.97 (1H, dd, *J* 11.4, 6.4 Hz, 1'-HH), 7.10–7.14 (2H, m, 2''-H and 6''-H), 7.51–7.54 (2H, m, 3''-H and 5''-H); δ_{C} (101 MHz, CDCl₃) 20.0 (CH₃), 20.1 (CH₃), 27.1 (CH₃), 28.3 (CH), 42.3 (CH₂), 47.0 (CH₂), 56.5 (CH₂), 66.2 (CH₂), 66.3 (CH₂), 113.9 (C), 116.4 (d, ²*J*_{CF} 22.3 Hz, 2 × CH), 127.4 (d, ⁴*J*_{CF} 3.8 Hz, C), 128.9 (C), 129.1 (C), 129.8 (d, ³*J*_{CF} 8.2 Hz, 2 × CH), 150.7 (C), 152.9 (C), 157.7 (C), 163.1 (d, ¹*J*_{CF} 250.7 Hz, C), 164.0 (C); *m/z* (ESI) 468.1350 (MNa⁺. C₂₂H₂₄FN₃NaO₄S requires 468.1364).

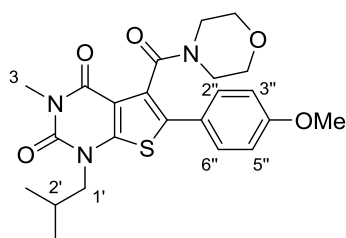
6-(2''-Fluorophenyl)-1-isobutyl-3-methyl-2,4-dioxo-1,2,3,4-tetrahydrothieno[2,3-*d*]pyrimidine-5-*N*-morpholinecarboxamide (89**)**



The reaction was carried out according to the previously described procedure for 6-(4''-fluorophenyl)-1-isobutyl-3-methyl-2,4-dioxo-1,2,3,4-tetrahydrothieno[2,3-*d*]pyrimidine-5-*N*-morpholinecarboxamide (**88**) using ethyl 6-(2''-fluorophenyl)-1-isobutyl-3-methyl-2,4-dioxo-1,2,3,4-tetrahydrothieno[2,3-*d*]pyrimidine-5-carboxylate (**81**) (0.178 g, 0.440 mmol) and morpholine (0.193 mL, 2.21 mmol). This gave 6-(2''-fluorophenyl)-1-isobutyl-3-methyl-2,4-dioxo-1,2,3,4-tetrahydrothieno[2,3-*d*]pyrimidine-5-*N*-morpholinecarboxamide (**89**) as a colourless oil (0.105 g, 54%). ν_{\max} (neat)/cm⁻¹ 2961 (CH), 1707 (CO), 1663 (CO), 1489, 1113, 1001, 762; δ_{H} (400 MHz, CDCl₃) 1.02 (3H, d, *J* 5.6 Hz, CH(CH₃)), 1.02 (3H, d, *J* 5.2 Hz, CH(CH₃)), 2.30–2.40 (1H, m, 2'-H), 3.04 (1H, ddd, *J* 8.8, 6.0, 2.4 Hz, NCHH), 3.16 (1H, ddd, *J* 10.6, 4.4, 2.4 Hz, NCHH), 3.29 (1H, ddd, *J* 10.6, 6.0, 2.4 Hz, NCHH), 3.42 (3H, s, 3-CH₃), 3.43–3.47 (1H, m, OCHH), 3.56 (1H, ddd, *J* 8.8, 4.4, 2.4 Hz, NCHH), 3.65–3.74 (2H, m, OCHH and 1'-HH), 3.77–3.84 (2H, m, OCH₂), 3.97 (1H, dd, *J* 11.2, 6.4 Hz, 1'-HH), 7.15–7.20 (1H, m, 6''-H), 7.22 (1H, td, *J* 7.7, 1.3 Hz, 4''-H), 7.38–7.42 (1H, m,

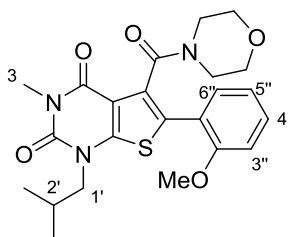
3''-H), 7.65 (1H, td, J 7.7, 1.3 Hz, 5''-H); δ_C (101 MHz, CDCl₃) 20.0 (CH₃), 20.1 (CH₃), 27.1 (CH₃), 28.3 (CH), 42.2 (CH₂), 47.0 (CH₂), 56.4 (CH₂), 66.2 (CH₂), 66.3 (CH₂), 113.1 (C), 116.0 (d, $^2J_{CF}$ 22.7 Hz, CH), 118.7 (d, $^2J_{CF}$ 14.5 Hz, C), 123.2 (C), 124.9 (d, $^4J_{CF}$ 3.8 Hz, CH), 131.2 (d, $^3J_{CF}$ 8.3 Hz, CH), 131.5 (C), 131.5 (d, $^3J_{CF}$ 9.3 Hz, CH), 150.8 (C), 154.2 (C), 157.6 (C), 159.4 (d, $^1J_{CF}$ 252.8 Hz, C), 163.6 (C); m/z (EI) 445.1490 (M⁺. C₂₂H₂₄FN₃O₄S requires 445.1472).

1-Isobutyl-6-(4''-methoxyphenyl)-3-methyl-2,4-dioxo-1,2,3,4-tetrahydrothieno[2,3-*d*]pyrimidine-5-*N*-morpholinecarboxamide (90)



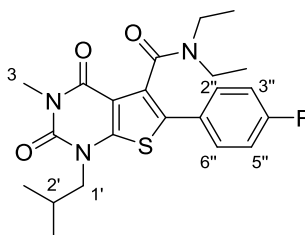
The reaction was carried out according to the previously described procedure for 6-(4''-fluorophenyl)-1-isobutyl-3-methyl-2,4-dioxo-1,2,3,4-tetrahydrothieno[2,3-*d*]pyrimidine-5-*N*-morpholinecarboxamide (**88**) using ethyl 6-(4''-methoxyphenyl)-1-isobutyl-3-methyl-2,4-dioxo-1,2,3,4-tetrahydrothieno[2,3-*d*]pyrimidine-5-carboxylate (**82**) (0.20 g, 0.48 mmol) and morpholine (0.21 mL, 2.4 mmol). This gave 1-isobutyl-6-(4''-methoxyphenyl)-3-methyl-2,4-dioxo-1,2,3,4-tetrahydrothieno[2,3-*d*]pyrimidine-5-*N*-morpholinecarboxamide (**90**) (0.11 g, 48%) as a colourless oil. ν_{\max} (neat)/cm⁻¹ 2961 (CH), 1738 (CO), 1703 (CO), 1659 (CO), 1535 (C=C), 1485, 1252, 1113, 729; δ_H (400 MHz, CDCl₃) 1.02 (6H, d, J 6.8 Hz, CH(CH₃)₂), 2.29–2.41 (1H, m, 2'-H), 3.00 (1H, ddd, J 10.8, 7.2, 2.8 Hz, NCHH), 3.12 (1H, ddd, J 13.2, 5.2, 2.8 Hz, NCHH), 3.26 (1H, ddd, J 13.2, 7.6, 3.2 Hz, NCHH), 3.40 (3H, s, 3-CH₃), 3.47–3.54 (2H, m, NCHH and OCHH), 3.67 (1H, dd, J 14.2, 7.6 Hz, 1'-HH), 3.72–3.90 (6H, m, OCHH, OCH₂ and 4''-OCH₃), 3.94 (1H, dd, J 14.2, 7.6 Hz, 1'-HH), 6.93 (2H, d, J 8.8 Hz, 3''-H and 5''-H), 7.46 (2H, d, J 8.8 Hz, 2''-H and 6''-H); δ_C (101 MHz, CDCl₃) 20.0 (CH₃), 20.1 (CH₃), 27.1 (CH₃), 28.3 (CH), 42.2 (CH₂), 47.0 (CH₂), 55.4 (CH₃), 56.4 (CH₂), 66.2 (CH₂), 66.3 (CH₂), 113.9 (C), 114.6 (2 × CH), 123.6 (C), 127.6 (C), 129.2 (2 × CH), 130.5 (C), 150.7 (C), 152.4 (C), 157.6 (C), 160.3 (C), 164.3 (C); m/z (ESI) 480.1546 (MNa⁺. C₂₃H₂₇N₃NaO₅S requires 480.1564).

1-Isobutyl-6-(2''-methoxyphenyl)-3-methyl-2,4-dioxo-1,2,3,4-tetrahydrothieno[2,3-*d*]pyrimidine-5-*N*-morpholinecarboxamide (91)



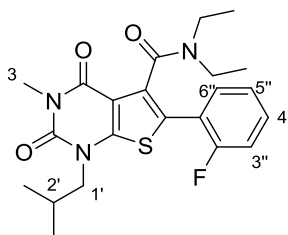
The reaction was carried out according to the previously described procedure for 6-(4''-fluorophenyl)-1-isobutyl-3-methyl-2,4-dioxo-1,2,3,4-tetrahydrothieno[2,3-*d*]pyrimidine-5-*N*-morpholinecarboxamide (**88**) using ethyl 1-isobutyl-6-(2''-methoxyphenyl)-3-methyl-2,4-dioxo-1,2,3,4-tetrahydrothieno[2,3-*d*]pyrimidine-5-carboxylate (**83**) (0.18 g, 0.44 mmol) and morpholine (0.19 mL, 2.2 mmol). This gave 1-isobutyl-6-(2''-methoxyphenyl)-3-methyl-2,4-dioxo-1,2,3,4-tetrahydrothieno[2,3-*d*]pyrimidine-5-*N*-morpholinecarboxamide (**91**) (0.082 g, 41%) as a colourless oil. ν_{\max} (neat)/ cm^{-1} 2961 (CH), 1705 (CO), 1661 (CO), 1532 (C=C), 1489, 1256, 1113, 731; δ_{H} (400 MHz, CDCl_3) 1.02 (3H, d, J 6.7 Hz, $\text{CH}(\text{CH}_3)_2$), 2.28–2.42 (1H, m, 2'-H), 2.84 (1H, ddd, J 10.4, 7.6, 2.8 Hz, NCHH), 3.15 (1H, ddd, J 13.2, 5.2, 3.2 Hz, NCHH), 3.26 (1H, ddd, J 13.2, 6.4, 2.8 Hz, NCHH), 3.36 (1H, ddd, J 10.4, 7.6, 2.8 Hz, NCHH), 3.40 (3H, s, 3- CH_3), 3.48 (1H, ddd, J 11.4, 7.6, 2.8 Hz, OCHH), 3.59–3.67 (2H, m, OCHH and 1'-HH), 3.76 (1H, ddd, J 11.4, 6.4, 3.2 Hz, OCHH), 3.81–3.87 (4H, m, OCHH and 2''- OCH_3), 4.01 (1H, dd, J 14.0, 8.0 Hz, 1'-HH), 6.97 (1H, br d, J 7.9 Hz, 3''-H), 7.01 (1H, td, J 7.9, 1.4 Hz, 5''-H), 7.38 (1H, td, J 7.9, 1.4 Hz, 4''-H), 7.58 (1H, dd, J 7.9, 1.4 Hz, 6''-H); δ_{C} (101 MHz, CDCl_3) 20.0 (CH_3), 20.2 (CH_3), 27.1 (CH_3), 28.2 (CH), 42.2 (CH_2), 47.0 (CH_2), 55.6 (CH_3), 56.1 (CH_2), 66.3 (CH_2), 66.3 (CH_2), 111.0 (CH), 112.7 (C), 119.7 (C), 121.3 (CH), 126.7 (C), 130.1 (C), 130.8 (CH), 131.4 (CH), 150.9 (C), 154.1 (C), 156.2 (C), 157.7 (C), 164.1 (C); m/z (ESI) 480.1544 (MNa^+ . $\text{C}_{23}\text{H}_{27}\text{N}_3\text{NaO}_5\text{S}$ requires 480.1564).

6-(4''-Fluorophenyl)-1-isobutyl-3-methyl-2,4-dioxo-1,2,3,4-tetrahydrothieno[2,3-*d*]pyrimidine-5-*N*-diethylcarboxamide (92)



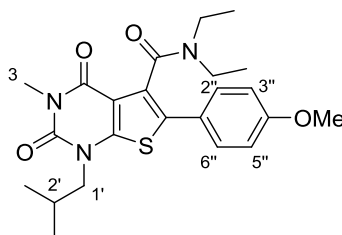
The reaction was carried out according to the previously described procedure for 6-(4''-fluorophenyl)-1-isobutyl-3-methyl-2,4-dioxo-1,2,3,4-tetrahydrothieno[2,3-*d*]pyrimidine-5-*N*-morpholinecarboxamide (**88**) using ethyl 6-(4''-fluorophenyl)-1-isobutyl-3-methyl-2,4-dioxo-1,2,3,4-tetrahydrothieno[2,3-*d*]pyrimidine-5-carboxylate (**80**) (0.12 g, 0.30 mmol) and diethylamine (0.16 mL, 1.5 mmol). This gave 6-(4''-fluorophenyl)-1-isobutyl-3-methyl-2,4-dioxo-1,2,3,4-tetrahydrothieno[2,3-*d*]pyrimidine-5-*N*-diethylcarboxamide (**92**) (0.040 g, 31%) as a colourless oil. ν_{\max} (neat)/ cm^{-1} 2963 (CH), 1707 (CO), 1665 (CO), 1636 (CO), 1533 (C=C), 1487, 1294, 1238, 841; δ_{H} (400 MHz, CDCl_3) 0.80 (3H, t, J 7.2 Hz, NCH_2CH_3), 1.02 (3H, d, J 6.4 Hz, $\text{CH}(\text{CH}_3)$), 1.03 (3H, d, J 6.8 Hz, $\text{CH}(\text{CH}_3)$), 1.21 (3H, t, J 7.2 Hz, NCH_2CH_3), 2.30–2.41 (1H, m, 2'-H), 3.03–3.14 (2H, m, NCH_2CH_3), 3.40 (3H, s, 3- CH_3), 3.43–3.52 (1H, m, NCHHCH_3), 3.60–3.71 (2H, m, NCHHCH_3 and 1'- HH), 3.96 (1H, dd, J 14.0, 7.6 Hz, 1'- HH), 7.06–7.10 (2H, m, 2''-H and 6''-H), 7.54–7.58 (2H, m, 3''-H and 5''-H); δ_{C} (101 MHz, CDCl_3) 12.2 (CH_3), 13.5 (CH_3), 20.0 (CH_3), 20.1 (CH_3), 27.1 (CH_3), 28.3 (CH), 39.2 (CH_2), 43.0 (CH_2), 56.4 (CH_2), 114.0 (C), 116.1 (d, $^2J_{\text{CF}}$ 21.6 Hz, 2 \times CH), 127.8 (d, $^4J_{\text{CF}}$ 3.8 Hz, C), 128.4 (C), 129.8 (d, $^3J_{\text{CF}}$ 9.8 Hz, 2 \times CH), 130.3 (C), 150.8 (C), 152.7 (C), 157.6 (C), 162.8 (d, $^1J_{\text{CF}}$ 250.7 Hz, C), 164.7 (C); m/z (ESI) 454.1560 (MNa^+ . $\text{C}_{22}\text{H}_{26}\text{FN}_3\text{NaO}_3\text{S}$ requires 454.1571).

6-(2''-Fluorophenyl)-1-isobutyl-3-methyl-2,4-dioxo-1,2,3,4-tetrahydrothieno[2,3-*d*]pyrimidine-5-*N*-diethylcarboxamide (93)



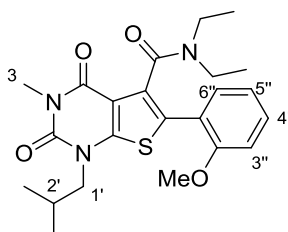
The reaction was carried out according to the previously described procedure for 6-(4''-fluorophenyl)-1-isobutyl-3-methyl-2,4-dioxo-1,2,3,4-tetrahydrothieno[2,3-*d*]pyrimidine-5-*N*-morpholinecarboxamide (**88**) using ethyl 6-(2''-fluorophenyl)-1-isobutyl-3-methyl-2,4-dioxo-1,2,3,4-tetrahydrothieno[2,3-*d*]pyrimidine-5-carboxylate (**81**) (0.178 g, 0.440 mmol) and diethylamine (0.228 mL, 2.20 mmol). This gave 6-(2''-fluorophenyl)-1-isobutyl-3-methyl-2,4-dioxo-1,2,3,4-tetrahydrothieno[2,3-*d*]pyrimidine-5-*N*-diethylcarboxamide (**93**) (0.0710 g, 38%) as a colourless oil. ν_{\max} (neat)/ cm^{-1} 2961 (CH), 1707 (CO), 1663 (CO), 1643 (CO), 1533 (C=C), 1485, 1227, 1113, 839; δ_{H} (400 MHz, CDCl_3) 0.82 (3H, t, J 7.2 Hz, NCH_2CH_3), 1.02 (3H, d, J 6.8 Hz, $\text{CH}(\text{CH}_3)$), 1.03 (3H, d, J 6.4 Hz, $\text{CH}(\text{CH}_3)$), 1.14 (3H, t, J 7.2 Hz, NCH_2CH_3), 2.32–2.40 (1H, m, 2'-H), 3.03–3.17 (2H, m, NCH_2CH_3), 3.34–3.43 (4H, m, 3- CH_3 and NCHHCH_3), 3.59–3.70 (2H, m, NCHHCH_3 and 1'- HH), 4.00 (1H, dd, J 14.0, 8.0 Hz, 1'- HH), 7.11–7.20 (2H, m, 4''-H and 6''-H), 7.33–7.39 (1H, m, 3''-H), 7.75 (1H, td, J 7.6, 1.6 Hz, 5''-H); δ_{C} (101 MHz, CDCl_3) 12.2 (CH_3), 13.4 (CH_3), 20.0 (CH_3), 20.2 (CH_3), 27.0 (CH_3), 28.3 (CH), 39.0 (CH_2), 43.0 (CH_2), 56.3 (CH_2), 113.1 (C), 115.7 (d, $^2J_{\text{CF}}$ 21.7 Hz, CH), 119.1 (d, $^2J_{\text{CF}}$ 15.1 Hz, C), 122.3 (C), 124.7 (d, $^4J_{\text{CF}}$ 3.9 Hz, CH), 130.7 (d, $^3J_{\text{CF}}$ 8.4 Hz, CH), 131.7 (d, $^3J_{\text{CF}}$ 9.8 Hz, CH), 132.7 (C), 150.9 (C), 154.1 (C), 157.6 (C), 158.9 (d, $^1J_{\text{CF}}$ 251.9 Hz, C), 164.5 (C); m/z (ESI) 454.1558 (MNa^+ . $\text{C}_{22}\text{H}_{26}\text{FN}_3\text{NaO}_3\text{S}$ requires 454.1571).

1-Isobutyl-6-(4''-methoxyphenyl)-3-methyl-2,4-dioxo-1,2,3,4-tetrahydrothieno[2,3-*d*]pyrimidine-5-*N*-diethylcarboxamide (94)



The reaction was carried out according to the previously described procedure for 6-(2''-fluorophenyl)-1-isobutyl-3-methyl-2,4-dioxo-1,2,3,4-tetrahydrothieno[2,3-*d*]pyrimidine-5-(*N*-methoxy-*N*-methyl)carboxamide (**88**) using ethyl 1-isobutyl-6-(4''-methoxyphenyl)-3-methyl-2,4-dioxo-1,2,3,4-tetrahydrothieno[2,3-*d*]pyrimidine-5-carboxylate (**82**) (0.083 g, 0.20 mmol). This gave 1-isobutyl-6-(4''-methoxyphenyl)-3-methyl-2,4-dioxo-1,2,3,4-tetrahydrothieno[2,3-*d*]pyrimidine-5-*N*-diethylcarboxamide (**94**) (0.026 g, 34%) as a green oil. ν_{\max} (neat)/ cm^{-1} 2963 (CH), 1778 (CO), 1705 (CO), 1665 (CO), 1439, 1294, 1254, 1182; δ_{H} (400 MHz, CDCl_3) 0.81 (3H, t, J 7.2 Hz, NCH_2CH_3), 1.01 (3H, d, J 6.8 Hz, $\text{CH}(\text{CH}_3)$), 1.02 (3H, d, J 6.8 Hz, $\text{CH}(\text{CH}_3)$), 1.20 (3H, t, J 7.2 Hz, NCH_2CH_3), 2.32–2.39 (1H, m, 2'-H), 3.02–3.14 (2H, m, NCH_2CH_3), 3.40 (3H, s, 3- CH_3), 3.48 (1H, dt, J 13.6, 7.2 Hz, NCHHCH_3), 3.61–3.70 (2H, m, NCHHCH_3 and 1'- HH), 3.82 (3H, s, 4''- OCH_3), 3.96 (1H, dd, J 14.0, 8.0 Hz, 1'- HH), 6.89 (2H, d, J 8.9 Hz, 3''-H and 5''-H), 7.49 (2H, d, J 8.9 Hz, 2''-H and 6''-H); δ_{C} (101 MHz, CDCl_3) 12.3 (CH_3), 13.5 (CH_3), 20.1 (CH_3), 20.2 (CH_3), 27.1 (CH_3), 28.3 (CH), 39.2 (CH_2), 43.0 (CH_2), 55.3 (CH_3), 56.3 (CH_2), 114.0 (C), 114.4 (2 \times CH), 124.1 (C), 129.0 (C), 129.2 (2 \times CH), 129.7 (C), 150.9 (C), 152.3 (C), 157.6 (C), 160.0 (C), 165.0 (C); m/z (ESI) 466.1764 (MNa^+). $\text{C}_{23}\text{H}_{29}\text{N}_3\text{NaO}_4\text{S}$ requires 466.1771).

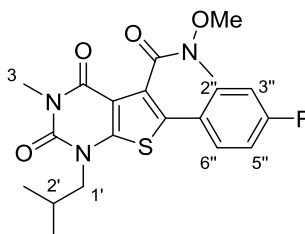
1-Isobutyl-6-(2''-methoxyphenyl)-3-methyl-2,4-dioxo-1,2,3,4-tetrahydrothieno[2,3-*d*]pyrimidine-5-*N*-diethylcarboxamide (95)



The reaction was carried out according to the previously described procedure for 6-(4''-fluorophenyl)-1-isobutyl-3-methyl-2,4-dioxo-1,2,3,4-tetrahydrothieno[2,3-*d*]pyrimidine-5-*N*-morpholinecarboxamide (**88**) using ethyl 1-isobutyl-6-(2''-methoxyphenyl)-3-methyl-

2,4-dioxo-1,2,3,4-tetrahydrothieno[2,3-*d*]pyrimidine-5-carboxylate (**83**) (0.182 g, 0.440 mmol) and diethylamine (0.227 mL, 2.20 mmol). This gave 1-isobutyl-6-(2''-methoxyphenyl)-3-methyl-2,4-dioxo-1,2,3,4-tetrahydrothieno[2,3-*d*]pyrimidine-5-*N*-diethylcarboxamide (**95**) as a colourless oil (0.0680 g, 32%). ν_{\max} (neat)/ cm^{-1} 2963 (CH), 1705 (CO), 1661 (CO), 1634 (CO), 1487, 1251, 1020, 750; δ_{H} (400 MHz, CDCl_3) 0.78 (3H, t, J 7.2 Hz, NCH_2CH_3), 1.01 (3H, d, J 6.8 Hz, $\text{CH}(\text{CH}_3)$), 1.02 (3H, d, J 6.8 Hz, $\text{CH}(\text{CH}_3)$), 1.11 (3H, t, J 7.2 Hz, NCH_2CH_3), 2.30–2.41 (1H, m, 2'-H), 3.00–3.19 (2H, m, NCH_2CH_3), 3.31–3.43 (4H, m, 3- CH_3 and NCHHCH_3), 3.59–3.68 (2H, m, NCHHCH_3 and 1'- HH), 3.88 (3H, s, 2''- OCH_3), 4.03 (1H, dd, J 14.0, 8.0 Hz, 1'- HH), 6.92–6.99 (2H, m, 3''-H and 5''-H), 7.33 (1H, td, J 7.8, 1.6 Hz, 4''-H), 7.68 (1H, dd, J 7.8, 1.6 Hz, 6''-H); δ_{C} (101 MHz, CDCl_3) 12.2 (CH_3), 13.4 (CH_3), 20.0 (CH_3), 20.2 (CH_3), 27.1 (CH_3), 28.2 (CH), 39.0 (CH_2), 42.9 (CH_3), 55.6 (CH_2), 56.1 (CH_2), 110.8 (CH), 112.7 (C), 120.1 (C), 121.1 (CH), 125.7 (C), 130.3 (CH), 131.5 (CH and C), 151.0 (C), 154.0 (C), 156.0 (C), 157.7 (C), 165.0 (C); m/z (EI) 443.1867 (M^+ . $\text{C}_{23}\text{H}_{29}\text{N}_3\text{O}_4\text{S}$ requires 443.1879), 371 (28%), 344 (8), 315 (19), 230 (9), 155 (7), 117 (9), 105 (12), 84 (82), 72 (100).

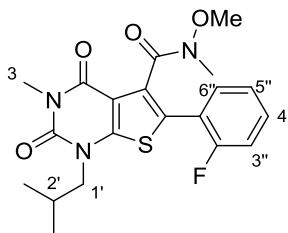
6-(4''-Fluorophenyl)-1-isobutyl-3-methyl-2,4-dioxo-1,2,3,4-tetrahydrothieno[2,3-*d*]pyrimidine-5-(*N*-methoxy-*N*-methyl)carboxamide (96**)**



The reaction was carried out according to the previously described procedure for 6-(4''-fluorophenyl)-1-isobutyl-3-methyl-2,4-dioxo-1,2,3,4-tetrahydrothieno[2,3-*d*]pyrimidine-5-*N*-morpholinecarboxamide (**88**) using ethyl 6-(4''-fluorophenyl)-1-isobutyl-3-methyl-2,4-dioxo-1,2,3,4-tetrahydrothieno[2,3-*d*]pyrimidine-5-carboxylate (**80**) (0.080 g, 0.20 mmol) and a combination of *N,O*-dimethylhydroxylamine hydrochloride (0.064 g, 0.66 mmol) and *N,N'*-diisopropylethylamine (0.23 mL, 1.3 mmol). This gave 6-(4''-fluorophenyl)-1-isobutyl-3-methyl-2,4-dioxo-1,2,3,4-tetrahydrothieno[2,3-*d*]pyrimidine-5-(*N*-methoxy-*N*-methyl)carboxamide (**96**) as a viscous yellow oil (0.040 g, 38%). ν_{\max} (neat)/ cm^{-1} 2959 (CH), 1707 (CO), 1662 (CO), 1535, 1486, 1390, 991, 773; The compound exists as a 3:1 mixture of rotamers. Data for the major rotamer: δ_{H} (400 MHz, CDCl_3) 1.02 (6H, d, J 6.8 Hz, $\text{CH}(\text{CH}_3)_2$), 2.31–2.42 (1H, m, 2'-H), 3.35 (3H, s, NCH_3), 3.36 (3H, s, OCH_3), 3.41 (3H, s, 3- CH_3), 3.68 (1H, dd, J 14.1, 7.7 Hz, 1'- HH), 3.95 (1H, dd, J 14.1, 7.7 Hz, 1'- HH),

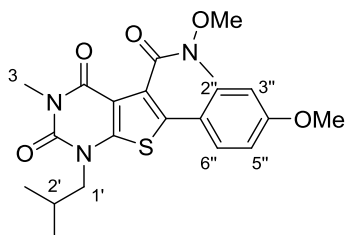
7.10 (2H, t, J 8.8 Hz, 2''-H and 6''-H), 7.57 (2H, dd, J 8.8, 5.2 Hz, 3''-H and 5''-H); δ_C (101 MHz, CDCl₃) 20.0 (CH₃), 20.1 (CH₃), 27.1 (CH₃), 28.3 (CH), 33.1 (CH₃), 56.5 (CH₂), 61.5 (CH₃), 114.4 (C), 116.3 (d, $^2J_{CF}$ 22.2 Hz, 2 \times CH), 127.7 (d, $^4J_{CF}$ 3.1 Hz, C), 128.7 (C), 129.2 (C), 129.8 (d, $^3J_{CF}$ 8.4 Hz, 2 \times CH), 150.8 (C), 152.1 (C), 157.8 (C), 162.9 (d, $^1J_{CF}$ 248.9 Hz, C), 166.4 (C); m/z (ESI) 442.1191 (MNa⁺. C₂₀H₂₂FN₃NaO₄S requires 442.1207).

6-(2''-Fluorophenyl)-1-isobutyl-3-methyl-2,4-dioxo-1,2,3,4-tetrahydrothieno[2,3-*d*]pyrimidine-5-(*N*-methoxy-*N*-methyl)carboxamide (97)



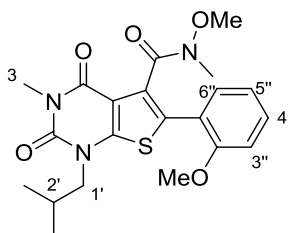
The reaction was carried out according to the previously described procedure for 6-(4''-fluorophenyl)-1-isobutyl-3-methyl-2,4-dioxo-1,2,3,4-tetrahydrothieno[2,3-*d*]pyrimidine-5-*N*-morpholinecarboxamide (**88**) using ethyl 6-(2''-fluorophenyl)-1-isobutyl-3-methyl-2,4-dioxo-1,2,3,4-tetrahydrothieno[2,3-*d*]pyrimidine-5-carboxylate (**81**) (0.070 g, 0.17 mmol) and a combination of *N,O*-dimethylhydroxylamine hydrochloride (0.017 g, 0.18 mmol) and *N,N'*-diisopropylethylamine (0.080 mL, 0.48 mmol). This gave 6-(2''-fluorophenyl)-1-isobutyl-3-methyl-2,4-dioxo-1,2,3,4-tetrahydrothieno[2,3-*d*]pyrimidine-5-(*N*-methoxy-*N*-methyl)carboxamide (**97**) as a viscous yellow oil (0.038 g, 57%). ν_{\max} (neat)/cm⁻¹ 2970 (CH), 1740 (CO), 1728 (CO), 1663 (CO), 1533 (C=C), 1366, 1217, 1119, 991; The compound exists as a 3:1 mixture of rotamers. Data for the major rotamer: δ_H (400 MHz, CDCl₃) 1.02 (6H, d, J 6.7 Hz, CH(CH₃)₂), 2.31–2.41 (1H, m, 2'-H), 3.32 (3H, s, NCH₃), 3.37 (3H, s, OCH₃), 3.42 (3H, s, 3-CH₃), 3.68 (1H, dd, J 14.1, 7.5 Hz, 1'-HH), 3.97 (1H, dd, J 14.1, 7.5 Hz, 1'-HH), 7.13–7.22 (2H, m, 4''-H and 6''-H), 7.33–7.41 (1H, m, 3''-H), 7.72 (1H, td, J 8.0, 1.6 Hz, 5''-H); δ_C (101 MHz, CDCl₃) 20.0 (CH₃), 20.1 (CH₃), 27.0 (CH₃), 28.3 (CH), 33.1 (CH₃), 56.3 (CH₂), 61.4 (CH₃), 113.5 (C), 115.9 (d, $^2J_{CF}$ 21.8 Hz, CH), 119.2 (d, $^2J_{CF}$ 14.0 Hz, C), 123.2 (C), 124.8 (d, $^3J_{CF}$ 3.5 Hz, CH), 130.8 (d, $^3J_{CF}$ 9.0 Hz, CH), 131.1 (C), 131.5 (d, $^2J_{CF}$ 2.8 Hz, CH), 150.7 (C), 153.4 (C), 157.7 (C), 159.3 (d, $^1J_{CF}$ 250.4 Hz, C), 166.1 (C); m/z (ESI) 442.1191 (MNa⁺. C₂₀H₂₂FN₃NaO₄S requires 442.1207).

1-Isobutyl-6-(4''-methoxyphenyl)-3-methyl-2,4-dioxo-1,2,3,4-tetrahydrothieno[2,3-*d*]pyrimidine-5-(*N*-methoxy-*N*-methyl)carboxamide (98)



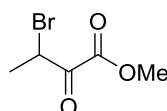
The reaction was carried out according to the previously described procedure for 6-(4''-fluorophenyl)-1-isobutyl-3-methyl-2,4-dioxo-1,2,3,4-tetrahydrothieno[2,3-*d*]pyrimidine-5-*N*-morpholinecarboxamide (**88**) using ethyl 1-isobutyl-6-(4''-methoxyphenyl)-3-methyl-2,4-dioxo-1,2,3,4-tetrahydrothieno[2,3-*d*]pyrimidine-5-carboxylate (**82**) (0.296 g, 0.710 mmol) and a combination of *N,O*-dimethylhydroxylamine hydrochloride (0.227 g, 2.32 mmol) and *N,N'*-diisopropylethylamine (0.930 mL, 4.64 mmol). This gave 1-isobutyl-6-(4''-methoxyphenyl)-3-methyl-2,4-dioxo-1,2,3,4-tetrahydrothieno[2,3-*d*]pyrimidine-5-(*N*-methoxy-*N*-methyl)carboxamide (**98**) as a viscous yellow oil (0.102 g, 51%). ν_{\max} (neat)/ cm^{-1} 2961 (CH), 1705 (CO), 1657 (CO), 1537, 1485, 1254, 1180, 733; The compound exists as a 3:1 mixture of rotamers. Data for the major rotamer: δ_{H} (400 MHz, CDCl_3) 1.02 (3H, d, J 6.0 Hz, $\text{CH}(\text{CH}_3)_2$), 2.29–2.42 (1H, m, 2'-H), 3.35 (3H, s, NCH_3), 3.37 (3H, s, OCH_3), 3.41 (3H, s, 3- CH_3), 3.68 (1H, dd, J 14.1, 7.5 Hz, 1'- HH), 3.83 (3H, s, 4''- OCH_3), 3.95 (1H, dd, J 14.1, 7.5 Hz, 1'- HH), 6.92 (2H, d, J 8.8 Hz, 3''-H and 5''-H), 7.52 (2H, d, J 8.8 Hz, 2''-H and 6''-H); δ_{C} (101 MHz, CDCl_3) 20.0 (CH_3), 20.1 (CH_3), 27.1 (CH_3), 28.3 (CH), 33.2 (CH_3), 55.4 (CH_3), 56.4 (CH_2), 61.5 (CH_3), 114.4 (C), 114.6 (2 \times CH), 124.0 (C), 127.5 (C), 129.2 (2 \times CH), 130.5 (C), 150.8 (C), 151.7 (C), 157.9 (C), 160.0 (C), 166.8 (C); m/z (ESI) 454.1393 (MNa^+ . $\text{C}_{21}\text{H}_{25}\text{N}_3\text{NaO}_5\text{S}$ requires 454.1407)

1-Isobutyl-6-(2''-methoxyphenyl)-3-methyl-2,4-dioxo-1,2,3,4-tetrahydrothieno[2,3-*d*]pyrimidine-5-(*N*-methoxy-*N*-methyl)carboxamide (99)



The reaction was carried out according to the previously described procedure for 6-(4''-fluorophenyl)-1-isobutyl-3-methyl-2,4-dioxo-1,2,3,4-tetrahydrothieno[2,3-*d*]pyrimidine-5-*N*-morpholinecarboxamide (**88**) using ethyl 1-isobutyl-6-(2''-methoxyphenyl)-3-methyl-2,4-dioxo-1,2,3,4-tetrahydrothieno[2,3-*d*]pyrimidine-5-carboxylate (**83**) (0.119 g, 0.29 mmol) and a combination of *N,O*-dimethylhydroxylamine hydrochloride (0.0933 g, 0.960 mmol) and *N,N'*-diisopropylethylamine (0.334 mL, 1.92 mmol). This gave 1-isobutyl-6-(2''-methoxyphenyl)-3-methyl-2,4-dioxo-1,2,3,4-tetrahydrothieno[2,3-*d*]pyrimidine-5-(*N*-methoxy-*N*-methyl)carboxamide (**99**) (0.070 g, 56%). ν_{\max} (neat)/ cm^{-1} 2961 (CH), 1703 (CO), 1657 (CO), 1533 (C=C), 1489, 1252, 1123, 991, 729; The compound exists as a 3:1 mixture of rotamers. Data for the major rotamer: δ_{H} (400 MHz, CDCl_3) 1.01 (6H, d, J 6.8 Hz, $\text{CH}(\text{CH}_3)_2$), 2.29–2.41 (1H, m, 2'-H), 3.31 (3H, s, NCH_3), 3.34 (3H, s, OCH_3), 3.41 (3H, s, 3- CH_3), 3.64 (1H, dd, J 14.1, 7.7 Hz, 1'- HH), 3.87 (3H, s, 2''- OCH_3), 4.00 (1H, dd, J 14.1, 7.7 Hz, 1'- HH), 6.95 (1H, d, J 7.8 Hz, 3''-H), 7.00 (1H, t, J 7.8 Hz, 5''-H), 7.34 (1H, td, J 7.8, 1.6 Hz, 4''-H), 7.66 (1H, dd, J 7.8, 1.6 Hz, 6''-H); δ_{C} (101 MHz, CDCl_3), 20.0 (CH_3), 20.2 (CH_3), 27.1 (CH_3), 28.2 (CH), 33.1 (CH_3), 55.6 (CH_2), 56.1 (CH_3), 61.3 (CH_3), 111.1 (CH), 113.0 (C), 120.3 (C), 121.2 (CH), 128.1 (C), 129.9 (C), 130.3 (CH), 131.2 (CH), 151.0 (C), 153.3 (C), 156.1 (C), 157.8 (C), 166.8 (C); m/z (ESI) 454.1389 (MNa^+ , $\text{C}_{21}\text{H}_{25}\text{N}_3\text{NaO}_5\text{S}$ requires 454.1407).

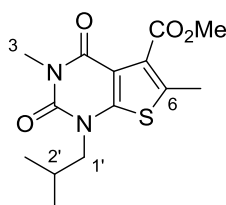
Methyl 3-bromo-2-oxobutanoate (102)⁶⁶



Bromine solution (0.500 mL, 9.50 mmol) was added dropwise to neat methyl 2-oxobutanoate (**101**) (1.10 mL, 9.50 mmol) at 0 °C. The mixture was warmed to room temperature and stirred for 1 h. An aqueous saturated solution of sodium bicarbonate (20 mL) was added and the mixture was extracted with ethyl acetate (3 × 20 mL). The organic

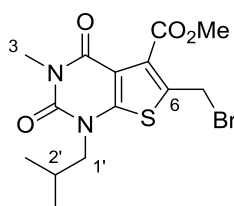
layers were combined and washed with an aqueous solution of 1 M sodium thiosulfate (30 mL) and brine (30 mL). The organic layer was dried (MgSO₄), filtered and concentrated *in vacuo* to give methyl 3-bromo-2-oxobutanoate (**102**) as a colourless liquid (1.85 g, 100%). Spectroscopic data were consistent with the literature.⁶⁶ δ_{H} (400 MHz, CDCl₃) 1.82 (3H, d, *J* 6.7 Hz, CHCH₃), 3.93 (3H, s, OCH₃), 5.17 (1H, q, *J* 6.7 Hz, CHCH₃); δ_{C} (101 MHz, CDCl₃) 18.4 (CH₃), 42.3 (CH), 53.4 (CH₃), 161.0 (C), 185.7 (C).

Methyl 3,6-dimethyl-1-isobutyl-2,4-dioxo-1,2,3,4-tetrahydrothieno[2,3-*d*]pyrimidine-5-carboxylate (103**)**⁶¹



Methyl-3-bromo-2-oxobutanoate (**102**) (0.650 g, 3.36 mmol) was added to a solution of 1-isobutyl-6-mercapto-3-methyl-2,4-(1*H*,3*H*)-pyrimidinedione (**52**) (0.600 g, 2.80 mmol) in methanol (20 mL) and stirred at room temperature for 12 h. The reaction mixture was concentrated *in vacuo* to give the crude product. Purification by flash column chromatography eluting with 20% ethyl acetate in petroleum ether gave methyl 3,6-dimethyl-1-isobutyl-2,4-dioxo-1,2,3,4-tetrahydrothieno[2,3-*d*]pyrimidine-5-carboxylate (**103**) as viscous yellow oil (0.322 g, 37%). Spectroscopic data were consistent with the literature.⁶¹ δ_{H} (400 MHz, CDCl₃) 0.98 (6H, d, *J* 6.6 Hz, CH(CH₃)₂), 2.26–2.32 (1H, m, 2'-H), 2.45 (3H, s, 6-CH₃), 3.39 (3H, s, 3-CH₃), 3.75 (2H, d, *J* 7.6 Hz, 1-H₂), 3.96 (3H, s, OCH₃); δ_{C} (101 MHz, CDCl₃) 13.4 (CH₃), 20.0 (2 × CH₃), 27.1 (CH₃), 28.3 (CH), 52.5 (CH₃), 56.3 (CH₂), 113.0 (C), 127.6 (C), 131.7 (C), 150.8 (C), 151.4 (C), 157.2 (C), 164.7 (C); *m/z* (ESI) 333 (MNa⁺, 100%).

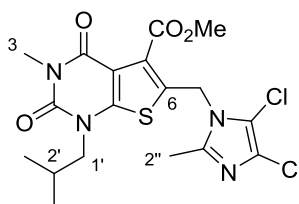
Methyl 6-(bromomethyl)-1-isobutyl-3-methyl-2,4-dioxo-1,2,3,4-tetrahydrothieno[2,3-*d*]pyrimidine-5-carboxylate (104**)**⁶¹



Methyl 3,6-dimethyl-1-isobutyl-2,4-dioxo-1,2,3,4-tetrahydrothieno[2,3-*d*]pyrimidine-5-carboxylate (**103**) (1.20 g, 3.87 mmol), *N*-bromosuccinimide (0.760 g, 4.25 mmol) and

azobisisobutyronitrile (0.0450 g, 0.270 mmol) were dissolved in ethyl acetate (70 mL) and stirred under reflux for 24 h. The solution was cooled to room temperature and washed with an aqueous solution of 0.5 M sodium hydroxide (35 mL). The organic layer was washed with brine, dried (MgSO₄), filtered and concentrated *in vacuo*. Purification by flash column chromatography eluting with 80% ethyl acetate in petroleum ether gave methyl 6-(bromomethyl)-1-isobutyl-3-methyl-2,4-dioxo-1,2,3,4-tetrahydrothieno[2,3-*d*]pyrimidine-5-carboxylate (**104**) as a colourless oil (0.865 g, 57%). Spectroscopic data were consistent with the literature.⁶¹ δ_{H} (400 MHz, CDCl₃) 1.00 (6H, d, *J* 6.7 Hz, CH(CH₃)₂), 2.26–2.36 (1H, m, 2'-H), 3.39 (3H, s, 3-CH₃), 3.78 (2H, d *J* 7.7 Hz, 1'-H₂), 4.00 (3H, s, OCH₃), 4.67 (2H, s, 6-CH₂); δ_{C} (101 MHz, CDCl₃) 20.0 (2 × CH₃), 23.2 (CH₂), 27.0 (CH₃), 28.4 (CH), 53.1 (CH₃), 56.5 (CH₂), 112.7 (C), 130.0 (C), 132.2 (C), 150.1 (C), 153.3 (C), 157.0 (C), 163.6 (C); *m/z* (ESI) 411 (MNa⁺, 100%).

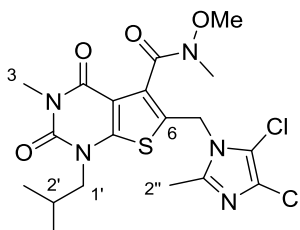
Methyl 6-[(4,5-dichloro-2-methyl-1*H*-imidazol-1-yl)methyl]-1-isobutyl-3-methyl-2,4-dioxo-1,2,3,4-tetrahydrothieno[2,3-*d*]pyrimidine-5-carboxylate (105**)⁶¹**



4,5-Dichloro-2-methylimidazole (0.0370 g, 0.240 mmol) in a solution of tetrahydrofuran (2 mL) was added dropwise to a suspension of sodium hydride (0.0100 g, 0.240 mmol) in tetrahydrofuran (2 mL) and stirred for 0.25 h. Methyl 6-(bromomethyl)-1-isobutyl-3-methyl-2,4-dioxo-1,2,3,4-tetrahydrothieno[2,3-*d*]pyrimidine-5-carboxylate (**104**) (0.087 g, 0.22 mmol) was then added dropwise as a solution in tetrahydrofuran (2 mL) and the mixture stirred under argon at room temperature for 3 h. The resulting mixture was diluted with water (10 mL) and extracted with ethyl acetate (3 × 10 mL). The organic layers were combined, dried (MgSO₄), filtered and concentrated *in vacuo*. Purification by flash column chromatography eluting with 50 % ethyl acetate in petroleum ether gave methyl 6-[(4,5-dichloro-2-methyl-1*H*-imidazol-1-yl)methyl]-1-isobutyl-3-methyl-2,4-dioxo-1,2,3,4-tetrahydrothieno[2,3-*d*]pyrimidine-5-carboxylate (**105**) as a white solid (0.0680 g, 67%). Mp 175–178 °C; Spectroscopic data were consistent with the literature.⁶¹ δ_{H} (400 MHz, CDCl₃) 0.97 (6H, d, *J* 6.7 Hz, CH(CH₃)₂), 2.19–2.30 (1H, m, 2'-H), 2.38 (3H, s, 2''-CH₃), 3.40 (3H, s, 3-CH₃), 3.73 (2H, d, *J* 7.8 Hz, 1'-H₂), 4.00 (3H, s, OCH₃), 5.26 (2H, s, 6-CH₂); δ_{C} (101 MHz, CDCl₃) 13.9 (CH₃), 19.9 (2 × CH₃), 27.0 (CH₃), 28.5 (CH), 41.6 (CH₂), 53.2

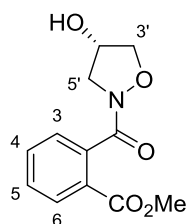
(CH₃), 56.5 (CH₂), 111.8 (C), 112.7 (C), 125.3 (C), 129.1 (C), 129.9 (C), 143.3 (C), 150.5 (C), 153.1 (C), 157.0 (C), 163.7 (C); *m/z* (ESI) 481 (MNa⁺, 100%)

6-[(4,5-Dichloro-2-methyl-1*H*-imidazol-1-yl)methyl]-1-isobutyl-3-methyl-2,4-dioxo-1,2,3,4-tetrahydrothieno-[2,3-*d*]pyrimidine-5(-*N*-methoxy-*N*-methyl)-carboxamide (100)⁶¹



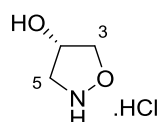
The reaction was carried out according to the previously described procedure for 6-(4''-iodophenoxy)-1-isobutyl-3-methyl-2,4-dioxo-1,2,3,4-tetrahydrothieno[2,3-*d*]pyrimidine-5(-*N*-methoxy-*N*-methyl)carboxamide (**75**) using methyl 6-[(4,5-dichloro-2-methyl-1*H*-imidazol-1-yl)methyl]-1-isobutyl-3-methyl-2,4-dioxo-1,2,3,4-tetrahydrothieno[2,3-*d*]pyrimidine-5-carboxylate (**105**) (0.030 g, 0.07 mmol). This gave 6-[(4,5-dichloro-2-methyl-1*H*-imidazol-1-yl)methyl]-1-isobutyl-3-methyl-2,4-dioxo-1,2,3,4-tetrahydrothieno[2,3-*d*]pyrimidine-5(-*N*-methoxy-*N*-methyl)-carboxamide (**100**) as a yellow oil (0.013 g, 38%). Spectroscopic data were consistent with the literature.⁶¹ The compound exists as a 3:1 mixture of rotamers. Data for the major rotamer: δ_{H} (400 MHz, CDCl₃) 0.96 (3H, d, *J* 6.7 Hz, CHCH₃), 0.97 (3H, d, *J* 6.7 Hz, CHCH₃), 2.21–2.29 (1H, m, 2'-H), 2.39 (3H, s, 2''-H), 3.38 (3H, s, NCH₃), 3.42 (3H, s, 3-CH₃), 3.48 (3H, s, OCH₃), 3.62 (1H, dd, *J* 14.1, 7.8 Hz, 1'-HH), 3.82 (1H, dd, *J* 14.1, 7.8 Hz, 1'-HH), 5.11 (1H, d, *J* 16.8 Hz, 6-CHH), 5.20 (1H, d, *J* 16.8 Hz, 6-CHH); δ_{C} (101 MHz, CDCl₃) 19.9 (CH₃), 20.1 (CH₃), 27.0 (CH₃), 28.4 (CH), 30.9 (CH₃), 32.8 (CH₃), 41.6 (CH₂), 56.2 (CH₂), 61.6 (CH₃), 112.0 (C), 113.2 (C), 124.8 (C), 125.5 (C), 131.3 (C), 143.7 (C), 150.6 (C), 152.7 (C), 157.4 (C), 164.2 (C); *m/z* (ESI) 510 (MNa⁺, 100%).

Methyl (4'S)-2-(4'-hydroxyisoxazolidine-2-carbonyl)benzoate (**108**)⁷³



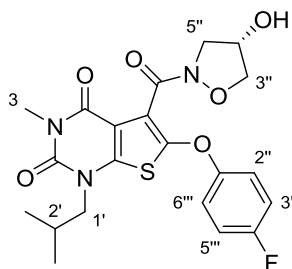
Triethylamine (0.050 mL, 0.35 mmol) was added to a solution of *N*-hydroxyphthalimide (**107**) (0.47 g, 2.88 mmol) and (4*R*)-epichlorohydrin (0.40 mL, 4.32 mmol) in anhydrous 1,4-dioxane (15 mL) and the mixture was stirred under argon at 50 °C for 48 h. Triethylamine (0.80 mL, 2.88 mmol) and methanol (15 mL) were added to the mixture and stirring continued at 50 °C for a further 2 h. The mixture was concentrated *in vacuo* to give the crude product. Purification by flash column chromatography eluting with 60% ethyl acetate in petroleum ether gave methyl (4*S*)-2-(4'-hydroxyisoxazolidine-2-carbonyl)benzoate (**108**) as a yellow oil (0.39 g, 54%). $[\alpha]_{\text{D}}^{24}$ -31.1 (*c* 1.0, CHCl₃); Spectroscopic data was consistent with the literature.⁷³ δ_{H} (400 MHz, CDCl₃) 3.84–3.91 (4H, m, OCH₃ and 5'-*HH*), 3.98 (2H, d, *J* 8.7 Hz, 3'-H₂), 4.13–4.21 (1H, m, 5'-*HH*), 4.73–4.81 (1H, m, 4'-H), 7.45 (1H, d, *J* 7.5 Hz, 3-H), 7.48 (1H, t, *J* 7.5 Hz, 4-H), 7.61 (1H, t, *J* 7.5 Hz, 5-H), 7.99 (1H, d, *J* 7.5 Hz, 6-H); δ_{C} (101 MHz, CDCl₃) 52.8 (CH₃), 53.6 (CH₂), 73.1 (CH), 77.1 (CH₂), 127.0 (C), 128.0 (CH), 129.3 (CH), 129.9 (CH), 132.9 (CH), 137.5 (C), 167.0 (C), 170.9 (C); *m/z* (ESI) 274 (MNa⁺. 100%).

(4*S*)-Hydroxyisoxazolidine hydrochloride (**109**)⁷³



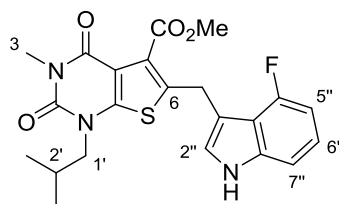
A solution of methyl (4'*S*)-2-(4'-hydroxyisoxazolidine-2-carbonyl)benzoate (**108**) (0.400 g, 1.59 mmol) in 4 M hydrochloric acid (10 mL) was heated under reflux for 3 h. The resulting mixture was filtered and the filtrate concentrated *in vacuo*. The residue was recrystallised from propan-2-ol to give (4*S*)-hydroxyisoxazolidine hydrochloride (**109**) as a pink solid (0.140 g, 68%). Mp 152–155 °C; $[\alpha]_{\text{D}}^{24}$ + 13.8 (*c* 1.0, MeOH); Spectroscopic data was consistent with the literature.⁷³ δ_{H} (400 MHz, DMSO-*d*₆) 3.37 (1H, d, *J* 11.4 Hz, 5-*HH*), 3.49 (1H, dd, *J* 11.4, 4.6 Hz, 5-*HH*), 4.04 (1H, dd, *J* 8.6, 3.5 Hz, 3-*HH*), 4.09 (1H, d, *J* 8.6 Hz, 3-*HH*), 4.79–4.81 (1H, m, 4-H), 5.83 (1H, br s, OH), 12.39 (2H, br s, NH₂); δ_{C} (101 MHz, DMSO-*d*₆) 54.0 (CH₂), 71.9 (CH), 78.0 (CH₂); *m/z* (CI) 90 (MH⁺. 100%), 79 (10), 113 (5).

(4''S)-6-(4'''-fluorophenoxy)-1-isobutyl-3-methyl-2,4-dioxo-1,2,3,4-tetrahydrothieno[2,3-d]pyrimidine-5-(4''-hydroxyisoxazolidine)-carboxamide (112)



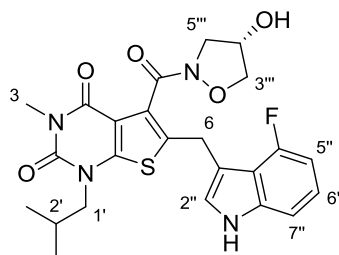
The reaction was carried out according to the previously described procedure for ethyl 6-(4''-iodophenoxy)-1-isobutyl-3-methyl-2,4-dioxo-1,2,3,4-tetrahydrothieno[2,3-d]pyrimidine-5-(*N*-methoxy-*N*-methyl)carboxamide (**75**) using ethyl 6-(4''-fluorophenoxy)-1-isobutyl-3-methyl-2,4-dioxo-1,2,3,4-tetrahydrothieno[2,3-d]pyrimidine-5-carboxylate (**71**) (0.13 g, 0.34 mmol) and (4*S*)-hydroxyisoxazolidine hydrochloride (**109**) (0.051 g, 0.41 mmol). This gave (4''*S*)-6-(4'''-fluorophenoxy)-1-isobutyl-3-methyl-2,4-dioxo-1,2,3,4-tetrahydrothieno[2,3-d]pyrimidine-5-(4''-hydroxyisoxazolidine)-carboxamide (**112**) as an orange oil (0.062 g, 40%). ν_{\max} (neat)/ cm^{-1} 3435 (OH), 2961 (CH), 1705 (CO), 1655 (CO), 1551 (C=C), 1466, 1180, 747; $[\alpha]_{\text{D}}^{24}$ -12.4 (*c* 1.0, CHCl_3); δ_{H} (400 MHz, CDCl_3) 0.97 (6H, d, *J* 6.7 Hz, $\text{CH}(\text{CH}_3)_2$), 2.23–2.29 (1H, m, 2'-H), 3.40 (3H, s, 3- CH_3), 3.50 (1H, dd, *J* 12.0, 4.3 Hz, 5''-HH), 3.63 (1H, dd, *J* 14.2, 7.6 Hz, 1'-HH), 3.80 (1H, dd, *J* 14.2, 7.6 Hz, 1'-HH), 4.04 (1H, d, *J* 8.8 Hz, 3''-HH), 4.10 (1H, dd, *J* 8.8, 4.0 Hz, 3''-HH), 4.52 (1H, d, *J* 12.0 Hz, 5''-HH), 4.68–4.71 (1H, m, 4''-H), 4.91 (1H, d, *J* 12.0 Hz, OH), 7.03 (2H, t, *J* 8.8 Hz, 3'''-H and 5'''-H), 7.17 (2H, dd, *J* 8.8, 4.2 Hz, 2'''-H and 6'''-H); δ_{C} (101 MHz, CDCl_3) 20.0 (CH_3), 20.1 (CH_3), 27.1 (CH_3), 28.6 (CH), 54.0 (CH_2), 56.6 (CH_2), 73.1 (CH), 77.4 (CH_2), 109.0 (C), 116.5 (d, $^2J_{\text{CF}}$ 23.0 Hz, 2 × CH), 119.0 (C), 119.1 (d, $^3J_{\text{CF}}$ 9.5 Hz, 2 × CH), 147.1 (C), 148.6 (C), 150.5 (C), 154.2 (d, $^4J_{\text{CF}}$ 2.8 Hz, C), 158.5 (C), 160.8 (d, $^1J_{\text{CF}}$ 244.3 Hz, C), 161.9 (C); *m/z* (ESI) 486.1109 (MNa^+ . $\text{C}_{21}\text{H}_{22}\text{FN}_3\text{NaO}_6\text{S}$ requires 486.1106).

Methyl 6-[(4''-fluoro-1*H*-indol-3'-yl)methyl]-1-isobutyl-3-methyl-2,4-dioxo-1,2,3,4-tetrahydrothieno[2,3-*d*]pyrimidine-5-carboxylate (113)



Methyl 6-(bromomethyl)-1-isobutyl-3-methyl-2,4-dioxo-1,2,3,4-tetrahydrothieno[2,3-*d*]pyrimidine-5-carboxylate (**104**) (0.10 g, 0.26 mmol) and 4-fluoroindole (0.053 g, 0.39 mmol) were dissolved in chloroform (2 mL) and water (2 mL). Sodium bicarbonate (0.066 g, 0.78 mmol) was added and the reaction mixture stirred for 72 h at room temperature. The solution was diluted with water (10 mL) and extracted with dichloromethane (3×10 mL). The organic layers were combined, dried (MgSO_4), filtered and concentrated *in vacuo*. Purification by flash column chromatography eluting with 50% ethyl acetate in petroleum ether gave methyl 6-[(4''-fluoro-1*H*-indol-3'-yl)methyl]-1-isobutyl-3-methyl-2,4-dioxo-1,2,3,4-tetrahydrothieno[2,3-*d*]pyrimidine-5-carboxylate (**113**) as a viscous yellow oil (0.035 g, 30%). ν_{max} (neat)/ cm^{-1} 3204 (NH), 2962 (CH), 1707 (CO), 1663 (CO), 1486, 1282, 1141, 1016; δ_{H} (400 MHz, CDCl_3) 0.91 (6H, d, J 6.7 Hz, $\text{CH}(\text{CH}_3)_2$), 2.18–2.25 (1H, m, 2'-H), 3.38 (3H, s, 3- CH_3), 3.67 (2H, d, J 7.7 Hz, 1'- H_2), 3.94 (3H, s, OCH_3), 4.38 (2H, s, 6- CH_2), 6.76 (1H, dd, J 11.0, 7.4 Hz, 5''-H), 7.05 (1H, d, J 1.8 Hz, 2''-H), 7.08–7.15 (2H, m, 6''-H and 7''-H), 8.34 (1H, br s, NH); δ_{C} (101 MHz, CDCl_3) 19.9 ($2 \times \text{CH}_3$), 25.1 (CH_2), 26.9 (CH_3), 28.3 (CH), 52.8 (CH_3), 56.2 (CH_2), 105.1 (d, $^2J_{\text{CF}}$ 19.2 Hz, CH), 107.5 (d, $^4J_{\text{CF}}$ 3.7 Hz, CH), 111.7 (d, $^3J_{\text{CF}}$ 3.3 Hz, C), 112.8 (C), 115.6 (d, $^2J_{\text{CF}}$ 19.8 Hz, C), 123.0 (d, $^3J_{\text{CF}}$ 7.5 Hz, CH), 123.3 (d, $^4J_{\text{CF}}$ 1.1 Hz, CH), 126.5 (C), 138.0 (C), 139.0 (d, $^3J_{\text{CF}}$ 10.7 Hz, C), 150.8 (C), 151.9 (C), 157.5 (C), 158.3 (d, $^1J_{\text{CF}}$ 249.0 Hz, C), 164.9 (C); m/z (ESI) 466.1202 (MNa^+ . $\text{C}_{22}\text{H}_{22}\text{FN}_3\text{NaO}_4\text{S}$ requires 466.1207).

(4''''S)-6-[(4''-fluoro-1*H*-indol-3''-yl)methyl]-5-(4''''-hydroxyisoxazolidine-2-carbonyl)-1-isobutyl-3-methylthieno[2,3-*d*]pyrimidine-2,4(1*H*,3*H*)-dione (114)



The reaction was carried out according to the previously described procedure for ethyl 6-(4-iodophenoxy)-1-isobutyl-3-methyl-2,4-dioxo-1,2,3,4-tetrahydrothieno[2,3-*d*]pyrimidine-5-(*N*-methoxy-*N*-methyl)carboxamide (**75**) using methyl 6-((4''-fluoro-1*H*-indol-3''-yl)methyl)-1-isobutyl-3-methyl-2,4-dioxo-1,2,3,4-tetrahydrothieno[2,3-*d*]pyrimidine-5-carboxylate (**113**) (0.041 g, 0.090 mmol) and (4*S*)-isoxazolidin-4-ol hydrochloride (**109**) (0.010 g, 0.080 mmol). This gave (4*S*)-6-((4''-fluoro-1*H*-indol-3''-yl)methyl)-5-(4''''-hydroxyisoxazolidine-2-carbonyl)-1-isobutyl-3-methylthieno[2,3-*d*]pyrimidine-2,4(1*H*,3*H*)-dione (**114**) as an orange oil (0.016 g, 41%). ν_{\max} (neat)/ cm^{-1} 3203 (NH/OH), 2924 (CH), 1635 (CO), 1431, 1267, 1005, 731; $[\alpha]_{\text{D}}^{24}$ -40.4 (*c* 1.0, CHCl_3); δ_{H} (400 MHz, CDCl_3) 0.92 (6H, d, *J* 6.7 Hz, $\text{CH}(\text{CH}_3)_2$), 2.20–2.28 (1H, m, 2''-H), 3.37 (3H, s, 3- CH_3), 3.52 (1H, dd, *J* 12.1, 4.5 Hz, 5''''-*HH*), 3.60 (1H, dd, *J* 14.1, 7.8 Hz, 1''-*HH*), 3.78 (1H, dd, *J* 14.1, 7.8 Hz, 1''-*HH*), 4.00–4.02 (2H, m, 3''''- H_2), 4.36 (2H, s, 6- CH_2), 4.58 (1H, d, *J* 12.1 Hz, 5''''-*HH*), 4.70 (1H, m, 4''''-H), 5.07 (1H, d, *J* 12.1 Hz, OH), 6.76 (1H, dd, *J* 10.8, 7.7 Hz, 5''-H), 7.05–7.14 (3H, m, 2''-H, 6''-H and 7''-H), 8.45 (1H, br s, NH); δ_{C} (101 MHz, CDCl_3) 20.0 (CH_3), 20.1 (CH_3), 24.9 (CH_2), 26.9 (CH_3), 28.5 (CH), 54.0 (CH_2), 56.3 (CH_2), 73.1 (CH), 76.7 (CH_2), 104.8 (d, $^2J_{\text{CF}}$ 19.2 Hz, CH), 107.4 (d, $^4J_{\text{CF}}$ 3.8 Hz, CH), 111.5 (d, $^3J_{\text{CF}}$ 3.3 Hz, C), 112.2 (C), 115.7 (d, $^2J_{\text{CF}}$ 20.0 Hz, C), 122.8 (d, $^3J_{\text{CF}}$ 7.6 Hz, CH), 123.8 (CH), 127.6 (C), 135.7 (C), 138.8 (d, $^3J_{\text{CF}}$ 11.6 Hz, C), 150.5 (C), 152.5 (C), 158.3 (d, $^1J_{\text{CF}}$ 248.9 Hz, C), 158.6 (C), 164.2 (C); *m/z* (ESI) 523.1411 (MNa^+ , $\text{C}_{24}\text{H}_{25}\text{FN}_4\text{NaO}_5\text{S}$ requires 523.1422).

6.3 HPLC methods for physicochemical analysis⁶⁷

All physicochemical analyses were performed using a Dionex Ultimate 3000 series, and data acquisition and processing performed using Chromeleon 6.8 Chromatography software. Standard and test compounds were dissolved in 1:1 organic/aqueous phases, and prepared to a concentration of 0.5 mg/mL. The HPLC system was set to 25 °C, and UV detection achieved using a diode array detector (190–800 nm). Analysis was performed using 5 µL sample injections.

C18 chromatography for determination of lipophilicity ($\text{Log}P$)⁶⁷

$\text{Log}P$ values were determined using a Phenomenex Luna 5 micron C18 100 A (50 + 3 mm) column. The retention time for each compound of interest was measured using filtered acetonitrile and 0.01 mM phosphate buffered saline as the mobile phase at pH 7.4, pH 4.0 and pH 10.0, and pH was adjusted by the addition of concentrated hydrochloric acid or 0.05 M sodium hydroxide solution, respectively. The mobile phase flow rate was set at 1.0 mL/min. The CHI value for all compounds of interest was determined by measuring the retention time of each compound under the following mobile phase conditions: 0–10.5 min, 0–100% acetonitrile; 10.5–11.5 min, 100% acetonitrile; 11.5–12.0 min, 100–0% acetonitrile; 12.0–15.0 min, 0% acetonitrile. System calibration was achieved using the following compounds and plotting their mean CHI values against the measured retention time under all three pH conditions: theophylline (CHI = 15.76), phenyltetrazole (CHI = 20.18), benzimidazole (CHI = 30.71), colchicine (CHI = 41.37), acetophenone (CHI = 64.90), indole (CHI = 69.15), butyrophenone (CHI = 88.49) and valerophenone (CHI = 97.67). Using the calibration curves obtained and the following equations from a validated study, the $\text{Log}P$ of the compounds were calculated using Excel 2016 Software.

$$\text{CHI Log}D = 0.054 \text{ CHI} - 1.467$$

Where CHI Log D is the CHI value projected to the logarithmic scale

$$\text{Log}P = 0.047\text{CHIN} + 0.36\text{HBC} - 1.10$$

Where CHIN is the gradient chromatographic hydrophobicity index of the nonionised compound and HBC is hydrogen bond donor count.

Immobilised Artificial Membrane (IAM) chromatography for determination of membrane permeability (P_m) and membrane partition coefficient (K_m)⁶⁷

P_m and K_m values were determined using previously developed methodology on a Registech IAM.PC.DD2 (15 cm × 4.6 mm) column. Acetonitrile and 0.01 mM phosphate buffered saline at pH 7.4 was used as the mobile phase, with a flow rate of 1.0 mL/min. The retention time of each compound was measured under an isocratic mobile phase with the percentage acetonitrile ranging from 30–70%. The retention time of citric acid, as an unretained compound, under an isocratic mobile phase of 100% phosphate buffered saline was used for system corrections. The following equations were used to calculate P_m and K_m of the compounds of interest using Excel 2016 Software.

$$k_{IAM} = \frac{(t_r - t_0)}{t_0}$$

Where k_{IAM} = solute capacity factor on the column, t_r = compound retention time and t_0 = unretained compound retention time.

$$k_{IAM} = \left(\frac{V_s}{V_m} \right) \times K_m$$

Where V_s = volume of the IAM interphase created by the immobilised phospholipids, V_m = total volume of the solvent within the IAM column and K_m = membrane partition coefficient.

$$V_m = \frac{W_{PhC}}{\rho_{PhC}} + \frac{W_{C10}}{\rho_{C10}} + \frac{W_{C3}}{\rho_{C3}}$$

Where the specific weight of PhC (ρ_{PhC}) = 1.01779 g/mL and C_{10}/C_3 ($\rho_{C10/C3}$) = 0.86 g/mL; W_{PhC} = 133 mg, W_{C10} = 12.73 mg and W_{C3} = 2.28 mg.

$$V_m = f_r \times t_0$$

Where f_r = flow rate.

$$P_m = \frac{K_m}{MW}$$

Where P_m = permeability and MW = molecular weight.

Human Serum Albumin (HSA) chromatography for determination of percentage of plasma protein binding (%PPB)⁶⁷

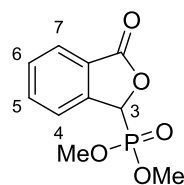
%PPB values were determined using previously developed methodology on a ChromTech HSA 5 μm (3.0 \times 50 mm) column. Isopropanol and 0.01 mM phosphate buffered saline at pH 7.4 was used as the mobile phase, with a flow rate of 1.8 mL/min. The retention time of each compound was measured under the following mobile phase conditions: 0–3 min, 0–30% isopropanol; 3–10 min, 30% isopropanol; 10.5–11.0 min, 30–0% isopropanol; 11.0–15.0 min, 0% isopropanol. System calibration was achieved using the following compounds and plotting %PPB values against their mean retention times: warfarin (%PPB = 98.0), nizatidine (%PPB = 35.0), bromazepam (%PPB = 60.0), carbamazepine (%PPB = 75.0), nicardipine (%PPB = 95.0), ketoprofen (%PPB = 98.7), indomethacin (%PPB = 99.0) and diclofenac (%PPB = 99.8). For each standard compound, the literature %PPB value was converted to its corresponding Log k value, which when plotted against t_r on the HSA column, afforded a line equation from which the Log $_k$ value of the unknown compounds could be extracted. The Log $_k$ values of the unknown compounds could then be converted to %PPB. Log $_k$ and subsequent %PPB calculations for the compounds of interest were performed using Excel 2016 Software.

$$\text{Log}_k = \text{Log} \left[\frac{\%PPB}{101 - \%PPB} \right]$$

$$\%PPB = \left[\frac{(101 - 10^{\text{Log}_k})}{(1 + 10^{\text{Log}_k})} \right]$$

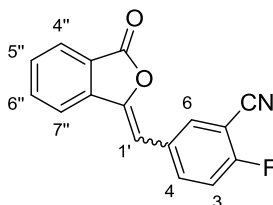
6.4 PARP-1 experimental

(±)-3-Dimethoxyphosphoryl-3H-2-benzofuran-1-one (**134**)⁷⁸



A solution of sodium methoxide (1.73 g, 32.0 mmol) in methanol (30 mL) was cooled to 0 °C, and to this was added dimethyl phosphite (**133**) (2.70 mL, 30.0 mmol) dropwise. 2-Carboxybenzaldehyde (**132**) (3.00 g, 20.0 mmol) was then added in portions to the reaction mixture, which was gradually warmed to ambient temperature and stirred for 2 h. Methanesulfonic acid (2.30 mL, 36.0 mmol) was added dropwise to the reaction mixture and a white suspension formed. The mixture was concentrated *in vacuo* and resuspended in water (30 mL). The crude product was extracted with dichloromethane (3 × 30 mL). The organic layers were combined, dried (MgSO₄), filtered and concentrated *in vacuo*. Purification by trituration with diethyl ether gave (±)-3-dimethoxyphosphoryl-3H-2-benzofuran-1-one (**134**) as a white solid (4.20 g, 87%). Mp 90–93 °C (lit.⁷⁸ 90–91 °C); δ_H (400 MHz, CD₃OD) 3.72 (3H, d, *J* 11.2 Hz, OCH₃), 3.91 (3H, d, *J* 11.2 Hz, OCH₃), 6.10 (1H, d, *J* 10.8 Hz, 3-H), 7.64–7.70 (1H, m, 5-H), 7.73–7.77 (1H, m, 4-H), 7.83 (1H, t, *J* 7.6 Hz, 6-H), 7.94 (1H, dd, *J* 7.6, 0.8 Hz, 7-H); δ_C (101 MHz, CD₃OD) 53.7 (CH₃, d, ²*J*_{C-O-P} 7.1 Hz), 54.1(d, ²*J*_{C-O-P} 6.7 Hz, CH₃), 75.3 (d, ¹*J*_{CP} 166.1 Hz, CH), 123.5 (CH), 125.1 (d, ²*J*_{CP} 4.2 Hz, C), 125.6 (CH), 130.0 (CH), 134.7 (CH), 144.0 (d, ³*J*_{CP} 4.0 Hz, C), 170.1 (C); *m/z* (CI) 243.0423 (MH⁺. C₁₀H₁₂O₅P requires 243.0422), 242 (33%), 213 (8), 133 (87), 105 (6).

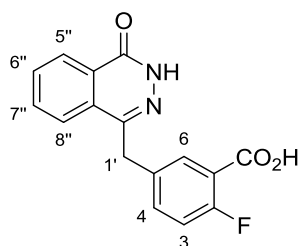
2-Fluoro-5-[(*Z/E*)-(3''-oxo-2''-benzofuran-1''-ylidene)methyl]benzonitrile (**136**)⁷⁸



A solution of (±)-3-dimethoxyphosphoryl-3H-2-benzofuran-1-one (**134**) (5.30 g, 21.9 mmol) and 2-fluoro-5-formylbenzonitrile (**135**) (3.00 g, 19.9 mmol) in tetrahydrofuran (60 mL) was cooled to 0 °C, and to this was added triethylamine (3.10 mL, 21.9 mmol) dropwise. The resultant solution was allowed to warm to ambient temperature and

vigorously stirred for 24 h. The resultant suspension was concentrated *in vacuo* and water (40 mL) was added to the residue. The product was collected by vacuum filtration and washed with water (2 × 50 mL), hexane (2 × 50 mL) and diethyl ether (2 × 50 mL) before drying under high vacuum to give 2-fluoro-5-[(*Z/E*)-(3''-oxo-2''-benzofuran-1''-ylidene)methyl]benzonitrile (**136**) as a white solid (5.27 g, 100%). NMR spectra showed a 75:25 mixture of *E* and *Z* isomers, of which only the signals for the major isomer are recorded. The product was carried forward without prior separation of the isomers. Mp 163–165 °C (lit.⁷⁸ 164–167 °C); δ_{H} (500 MHz, DMSO-*d*₆) 6.96 (1H, s, 1'-H), 7.63 (1H, t, *J* 9.1 Hz, ArH), 7.70–7.74 (1H, m, ArH), 7.90–7.94 (1H, m, ArH), 7.99 (1H, dt, *J* 8.0, 1.0 Hz, ArH), 8.08 (1H, dt, *J* 8.0, 1.0 Hz, ArH), 8.15–8.21 (2H, m, 2 × ArH); δ_{C} (126 MHz, DMSO-*d*₆) 100.9 (d, ²*J*_{CF} 16.2 Hz, C), 103.4 (CH), 113.7 (C), 117.3 (d, ²*J*_{CF} 20.1 Hz, CH), 120.9 (CH), 122.6 (C), 125.3 (CH), 130.9 (CH), 131.0 (d, ⁴*J*_{CF} 3.8 Hz, C), 134.2 (CH), 135.3 (CH), 136.7 (d, ³*J*_{CF} 9.0 Hz, CH), 139.6 (C), 145.4 (C), 161.5 (d, ¹*J*_{CF} 258.3 Hz, C), 165.9 (C); *m/z* (EI) 265.0543 (M⁺. C₁₆H₈FNO₂ requires 265.0539), 237 (15%), 208 (93), 182 (12), 133 (24), 104 (28), 84 (41).

2-Fluoro-5-[(4''-oxo-3''*H*-phthalazin-1''-yl)methyl]benzoic acid (**137**)⁷⁸

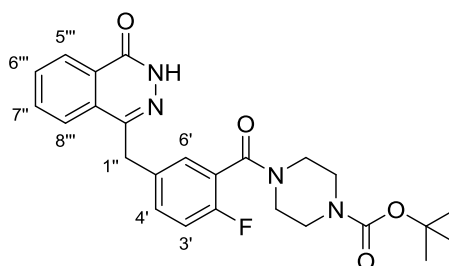


To a suspension of 2-fluoro-5-[(*Z/E*)-(3''-oxo-2''-benzofuran-1''-ylidene)methyl]benzonitrile (**136**) (3.50 g, 13.2 mmol) in water (130 mL) was added a 13 M sodium hydroxide solution (20 mL), and the resultant mixture stirred vigorously at 90 °C for 24 h. After cooling to 70 °C, hydrazine monohydrate (9.00 mL, 0.185 mol) was added to the reaction mixture dropwise and stirred for a further 72 h. On cooling to ambient temperature, the mixture was acidified with an aqueous solution of 6 M hydrochloric acid. The resultant precipitate was collected by vacuum filtration and washed with water (3 × 100 mL) and diethyl ether (3 × 100 mL) before drying under high vacuum to afford 2-fluoro-5-[(4''-oxo-3''*H*-phthalazin-1''-yl)methyl]benzoic acid (**137**) as a pale pink solid (4.31 g, 100%). Mp 251–252 °C. Spectroscopic data were consistent with the literature.⁷⁸ δ_{H} (500 MHz, DMSO-*d*₆) 4.34 (2H, s, 1'-H₂), 7.21 (1H, dd, *J* 8.5, 2.0 Hz, 3-H), 7.53–7.58 (1H, m, 4-H), 7.78–7.84 (2H, m, 6-H and 6''-H), 7.89 (1H, td, *J* 8.0, 1.5 Hz, 7''-

H), 7.96 (1H, d, J 8.0 Hz, 8''-H), 8.26 (1H, dd, J 8.0, 1.5 Hz, 5''-H), 12.50 (1H, s, NH); δ_C (126 MHz, DMSO- d_6) 36.3 (CH₂), 116.9 (d, $^2J_{CF}$ 22.6 Hz, CH), 119.3 (d, $^2J_{CF}$ 10.9 Hz, C), 125.4 (CH), 126.0 (CH), 127.9 (C), 129.1 (C), 131.5 (CH), 131.7 (CH), 133.5 (CH), 134.2 (d, $^4J_{CF}$ 3.7 Hz, C), 134.7 (d, $^3J_{CF}$ 8.7 Hz, CH), 144.8 (C), 159.3 (C), 159.8 (d, $^1J_{CF}$ 255.5 Hz, C), 164.8 (d, $^4J_{CF}$ 2.8 Hz, C); m/z (CI) 299.0828 (MH⁺. C₁₆H₁₂FN₂O₃ requires 299.0832), 287 (10%), 255 (21), 147 (7), 127 (31), 113 (18).

tert-Butyl

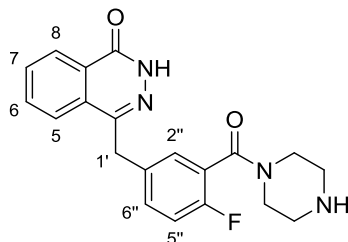
4-{2'-fluoro-5'-[(4'''-oxo-3'''H-phthalazin-1'''-yl)methyl]benzoyl}piperazine-1-carboxylate (138)⁷⁸



To a solution of 2-fluoro-5-[(4''-oxo-3''H-phthalazin-1''-yl)methyl]benzoic acid (**137**) (1.10 g, 3.68 mmol) in *N,N*-dimethylformamide (50 mL) was added triethylamine (0.769 mL, 5.52 mmol) followed by *O*-benzotriazole-*N,N,N',N'*-tetramethyluroniumhexafluorophosphate (1.50 g, 4.05 mmol). The reaction mixture was stirred at ambient temperature for 1 h, after which *tert*-butyl piperazine-1-carboxylate (0.687 g, 3.68 mmol) was added. The solution was heated to 50 °C and stirred for 48 h. The reaction mixture was washed with an aqueous saturated solution of sodium bicarbonate (30 mL) and the product extracted with ethyl acetate (3 × 30 mL). The organic layers were washed with an aqueous solution of 5% lithium chloride (60 mL) and brine (60 mL). The combined organic layers were dried (MgSO₄), filtered and concentrated *in vacuo* to give the crude product. Purification by flash column chromatography eluting with 5% methanol in dichloromethane gave *tert*-butyl 4-{2'-fluoro-5'-[(4'''-oxo 3'''H-phthalazin-1'''-yl)methyl]benzoyl}piperazine-1-carboxylate (**138**) as a pale yellow solid (1.23 g, 72%). Mp 215–216 °C (lit.⁷⁸ 214–216 °C); δ_H (400 MHz, CDCl₃) 1.47 (9H, s, O^tBu), 3.27 (2H, br s, NCH₂), 3.38 (2H, t, J 4.8 Hz, NCH₂), 3.51 (2H, br s, NCH₂), 3.75 (2H, br s, NCH₂), 4.27 (2H, s, 1''-H₂), 7.04 (1H, t, J 9.2 Hz, 3'-H), 7.27–7.37 (2H, m, 4'-H and 6'-H), 7.68–7.79 (3H, m, 6'''-H, 7'''-H and 8'''-H), 8.44–8.48 (1H, m, 5'''-H), 9.69 (1H, s, NH); δ_C (101 MHz, CDCl₃) 28.4 (3 × CH₃), 37.7 (CH₂), 42.0 (2 × CH₂), 46.9 (2 × CH₂), 80.4 (C), 116.2 (d, $^2J_{CF}$ 22.3 Hz, CH), 123.9 (d, $^2J_{CF}$ 17.3 Hz, C), 125.1 (CH), 127.2 (CH), 128.3 (C), 129.2 (d, $^3J_{CF}$ 3.5 Hz, CH), 129.5 (C), 131.6 (d, $^3J_{CF}$ 8.3 Hz, CH), 131.7 (CH),

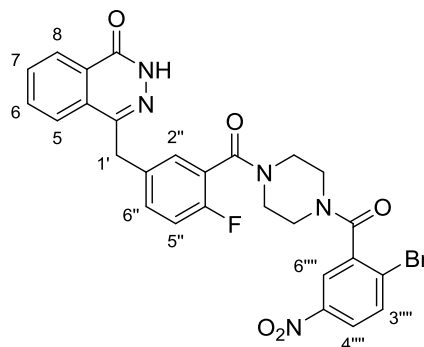
133.7 (CH), 134.3 (d, $^4J_{CF}$ 3.8 Hz, C), 145.6 (C), 154.5 (C), 157.0 (d, $^1J_{CF}$ 247.8 Hz, C), 160.4 (C), 165.1 (C); m/z (EI) 466.2018 (M^+ . $C_{25}H_{27}FN_4O_4$ requires 466.2016), 393 (12%), 366 (38), 281 (100), 254 (33), 196 (13), 166 (40), 91 (90).

4-[4''-Fluoro-3''-(piperazine-1'''-carbonyl)benzyl]-2H-phthalazin-1-one (131)⁷⁸



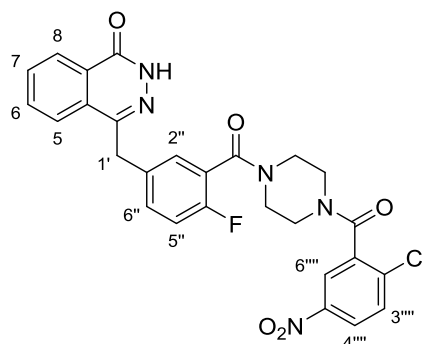
To a suspension of *tert*-butyl 4-{2'-fluoro-5'-[(4'''-oxo-3''''H-phthalazin-1''''-yl)methyl]benzoyl}piperazine-1-carboxylate (**138**) (0.278 g, 0.60 mmol) in ethanol (8 mL) was added an aqueous solution of 6 M hydrochloric (16 mL), and the resultant reaction mixture stirred vigorously at ambient temperature for 18 h. The ethanol was removed *in vacuo* and the aqueous layer made alkaline by the dropwise addition of an aqueous solution of 4 M sodium hydroxide. The solution was extracted with dichloromethane (3×20 mL) and the combined organic layers were dried ($MgSO_4$), filtered and concentrated *in vacuo*. Purification by trituration using a 1:1 diethyl ether/petroleum ether mixture gave 4-[4''-fluoro-3''-(piperazine-1'''-carbonyl)benzyl]-2H-phthalazin-1-one (**131**) as a white solid (0.150 g, 68%). Mp 193–195 °C. Spectroscopic data were consistent with the literature.⁷⁸ δ_H (400 MHz, $CDCl_3$) 2.07 (1H, br s, NH), 2.81 (2H, br s, NCH_2), 2.95 (2H, t, J 4.4 Hz, NCH_2), 3.28 (2H, br s, NCH_2), 3.77 (2H, br s, NCH_2), 4.29 (2H, s, 1'- H_2), 7.02 (1H, t, J 8.8 Hz, 5''-H), 7.26–7.37 (2H, m, 2''-H and 6''-H), 7.70–7.80 (3H, m, 5-H, 6-H and 7-H), 8.45–8.50 (1H, m, 8-H), 11.46 (1H, br s, NH); δ_C (101 MHz, $CDCl_3$) 37.7 (CH_2), 43.1 (CH_2), 45.7 (CH_2), 46.2 (CH_2), 48.2 (CH_2), 116.1 (d, $^2J_{CF}$ 22.1 Hz, CH), 124.3 (d, $^2J_{CF}$ 18.2 Hz, C), 125.1 (CH), 127.1 (CH), 128.3 (C), 129.1 (d, $^3J_{CF}$ 3.7 Hz, CH), 129.6 (C), 131.2 (d, $^3J_{CF}$ 8.1 Hz, CH), 131.6 (CH), 133.6 (CH), 134.2 (d, $^4J_{CF}$ 3.1 Hz, C), 145.6 (C), 157.0 (C, d, $^1J_{CF}$ 247.6 Hz), 160.8 (C), 165.0 (C); m/z (EI) 366.1486 (M^+ . $C_{20}H_{19}FN_4O_2$ requires 366.1492), 325 (13%), 298 (27), 281 (100), 254 (29), 85 (17).

4-{3''-[4'''-(2''''-bromo-5''''-nitrobenzoyl)piperazine-1'''-carbonyl]-4''-fluorobenzyl}-2*H*-phthalazin-1-one (139)



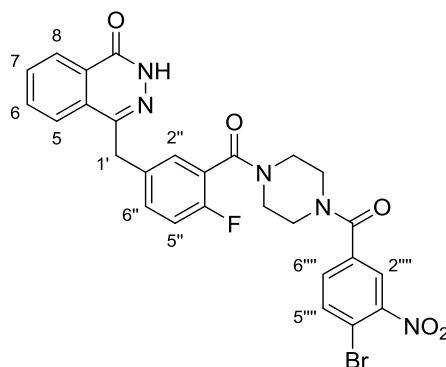
The reaction was carried out according to the previously described procedure for *tert*-butyl 4-{2'-fluoro-5'-[(4'''-oxo-3'''H-phthalazin-1'''-yl)methyl]benzoyl}piperazine-1-carboxylate (**138**) using 4-[4''-fluoro-3''-(piperazine-1'''-carbonyl)benzyl]-2*H*-phthalazin-1-one (**131**) (0.11 g, 0.22 mmol) and 2-bromo-5-nitrobenzoic acid (0.050 g, 0.20 mmol). This gave 4-{3''-[4'''-(2''''-bromo-5''''-nitrobenzoyl)piperazine-1'''-carbonyl]-4''-fluorobenzyl}-2*H*-phthalazin-1-one (**139**) as a white solid (0.061 g, 52%). Mp 137–140 °C; ν_{\max} (neat)/cm⁻¹ 3204 (NH), 2970 (CH), 1777 (CO), 1643 (CO), 1437, 1263, 1007, 739; δ_{H} (400 MHz, CDCl₃) 3.25–3.45 (8H, m, 4 × CH₂), 4.37 (2H, s, 1'-H₂), 6.99 (1H, t, *J* 8.6 Hz, 5''-H), 7.34–7.37 (3H, m, 2''-H, 6''-H and 3'''-H), 7.71–7.79 (3H, m, 5-H, 6-H and 7-H), 8.12 (1H, dd, *J* 8.6, 2.5 Hz, 4'''-H), 8.15 (1H, br s, 6'''-H), 8.44–8.48 (1H, m, 8-H), 11.49 (1H, s, NH); δ_{C} (101 MHz, CDCl₃) 37.7 (CH₂), 41.7 (CH₂), 42.1 (CH₂), 46.6 (CH₂), 47.2 (CH₂), 116.3 (d, ²*J*_{CF} 22.2 Hz, CH), 123.0 (CH), 123.3 (d ²*J*_{CF} 18.0 Hz, C), 124.9 (CH), 125.2 (CH), 126.5 (C), 127.3 (CH), 128.3 (C), 129.3 (d, ³*J*_{CF} 3.7 Hz, CH), 129.5 (C), 131.7 (CH), 131.9 (d, ³*J*_{CF} 8.1 Hz, CH), 133.8 (CH), 134.3 (CH), 134.5 (d, ⁴*J*_{CF} 3.2 Hz, C), 138.8 (C), 145.5 (C), 147.4 (C), 158.0 (d, ¹*J*_{CF} 248.0 Hz, C), 160.5 (C), 165.0 (C), 165.6 (C); *m/z* (ESI) 616.0588 (MNa⁺. C₂₇H₂₁⁷⁹BrFN₅NaO₅ requires 616.0602).

4-{3''-[4'''-(2''''-chloro-5''''-nitrobenzoyl)piperazine-1'''-carbonyl]-4''-fluorobenzyl}-2*H*-phthalazin-1-one (140)



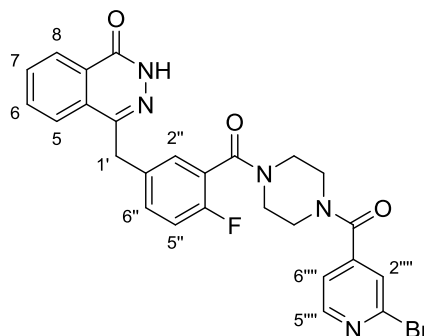
The reaction was carried out according to the previously described procedure for *tert*-butyl 4-{2'-fluoro-5'-[(4'''-oxo-3'''H-phthalazin-1'''-yl)methyl]benzoyl}piperazine-1-carboxylate (**138**) using 4-[4''-fluoro-3''-(piperazine-1'''-carbonyl)benzyl]-2*H*-phthalazin-1-one (**131**) (0.092 g, 0.25 mmol) and 2-chloro-5-nitrobenzoic acid (0.044 g, 0.22 mmol). This gave 4-{3''-[4'''-(2''''-chloro-5''''-nitrobenzoyl)piperazine-1'''-carbonyl]-4''-fluorobenzyl}-2*H*-phthalazin-1-one (**140**) as a yellow solid (0.052 g, 42%). Mp 139–141 °C; ν_{\max} (neat)/ cm^{-1} 3457 (NH), 2970 (CH), 1728 (CO), 1636 (CO), 1437, 1229, 909, 806; The compound exists as a 1.2:1 mixture of rotamers. Data for the major rotamer: δ_{H} (400 MHz, CDCl_3) 3.66–4.11 (8H, m, $4 \times \text{NCH}_2$), 4.32 (2H, s, 1'-H₂), 7.08 (1H, t, J 8.6 Hz, 5''-H), 7.35–7.36 (2H, m, 2''-H and 6''-H), 7.64 (1H, d, J 8.6 Hz, 3'''-H), 7.73–7.79 (3H, m, 5-H, 6-H and 7-H), 8.21–8.25 (2H, m, 4'''-H and 6'''-H), 8.45–8.49 (1H, m, 8-H), 11.41 (1H, s, NH); δ_{C} (101 MHz, CDCl_3) 37.7 (CH_2), 42.1 ($2 \times \text{CH}_2$), 47.1 ($2 \times \text{CH}_2$), 116.3 (d, $^2J_{\text{CF}}$ 22.6 Hz, CH), 123.3 (CH), 124.9 (CH), 125.2 (d, $^2J_{\text{CF}}$ 18.2 Hz, C), 127.2 (CH), 128.3 (CH), 129.3 (d, $^3J_{\text{CF}}$ 3.9 Hz, CH), 129.5 (C), 131.1 (CH), 131.7 (CH), 132.0 (d, $^3J_{\text{CF}}$ 8.3 Hz, CH), 133.7 (CH), 134.6 (C), 135.6 (d, $^4J_{\text{CF}}$ 3.3 Hz, C), 136.6 (C), 137.2 (C), 145.5 (C), 146.8 (C), 158.3 (d $^1J_{\text{CF}}$ 248.9 Hz, C), 160.8 (C), 164.7 (C), 165.2 (C); m/z (ESI) 572.1083 (MNa^+ . $\text{C}_{27}\text{H}_{21}^{35}\text{ClFN}_5\text{NaO}_5$ requires 572.1107).

4-{3''-[4'''-(4''''-Bromo-3''''-nitrobenzoyl)piperazine-1'''-carbonyl]-4''-fluorobenzyl}-2H-phthalazin-1-one (142)



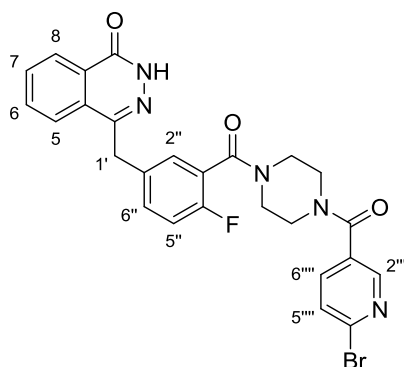
The reaction was carried out according to the previously described procedure for *tert*-butyl 4-{2'-fluoro-5'-[(4'''-oxo-3'''*H*-phthalazin-1'''-yl)methyl]benzoyl}piperazine-1-carboxylate (**138**) using 4-[4''-fluoro-3''-(piperazine-1'''-carbonyl)benzyl]-2*H*-phthalazin-1-one (**131**) (0.081 g, 0.22 mmol) and 4-bromo-3-nitrobenzoic acid (0.050 g, 0.20 mmol). This gave 4-{3''-[4'''-(4''''-bromo-3''''-nitrobenzoyl)piperazine-1'''-carbonyl]-4''-fluorobenzyl}-2*H*-phthalazin-1-one (**142**) as a white solid (0.067 g, 56%). Mp 122–126 °C; ν_{\max} (neat)/cm⁻¹ 3215 (NH), 2900 (CH), 1638 (CO), 1539, 1433, 1352, 1010, 731; The compound exists as a 1.5:1 mixture of rotamers. Data for the major rotamer: δ_{H} (400 MHz, CDCl₃) 3.38–3.99 (8H, m, 4 × NCH₂), 4.30 (2H, s, 1'-H₂), 7.01–7.06 (1H, m, 5''-H), 7.34–7.36 (2H, m, 2''-H and 6''-H), 7.72–7.80 (4H, m, ArH), 8.12 (1H, d, *J* 8.6 Hz, ArH), 8.20 (1H, s, 2'''-H), 8.44–8.45 (1H, m, 8-H), 11.43 (1H, s, NH); δ_{C} (101 MHz, CDCl₃) 37.6 (CH₂), 41.9 (2 × CH₂), 47.5 (2 × CH₂), 108.6 (CH), 116.2 (d ²*J*_{CF} 21.8 Hz, CH), 120.8 (CH), 123.3 (d, ²*J*_{CF} 17.4 Hz, C), 125.0 (CH), 125.8 (CH), 128.2 (C), 129.4 (d, ³*J*_{CF} 3.1 Hz, CH), 129.5 (C), 131.7 (CH), 132.0 (d, ³*J*_{CF} 7.9 Hz, CH), 133.7 (CH), 134.5 (d, ⁴*J*_{CF} 3.6 Hz, C), 135.6 (CH), 137.9 (C), 143.3 (C), 145.5 (C), 152.7 (C), 158.2 (d ¹*J*_{CF} 248.1 Hz, C), 160.8 (C), 165.2 (C), 166.8 (C); *m/z* (ESI) 616.0583 (MNa⁺. C₂₇H₂₁⁷⁹BrFN₅NaO₅ requires 616.0602).

4-{4''-Fluoro-3''-[4'''-(3''''-bromonicotinoyl)piperazine-1'''-carbonyl]-4''-fluorobenzyl}-2H-phthalazin-1-one (144)



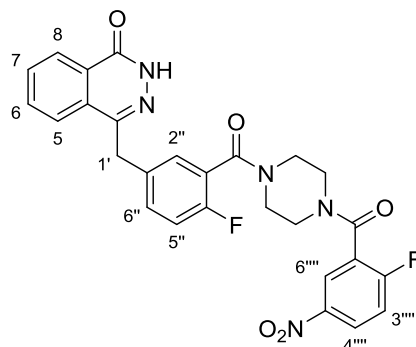
The reaction was carried out according to the previously described procedure for *tert*-butyl 4-{2'-fluoro-5'-[(4'''-oxo-3'''*H*-phthalazin-1'''-yl)methyl]benzoyl}piperazine-1-carboxylate (**138**) using 4-[4''-fluoro-3''-(piperazine-1'''-carbonyl)benzyl]-2*H*-phthalazin-1-one (**131**) (0.14 g, 0.39 mmol) and 2-bromo-4-pyridinecarboxylic acid (0.050 g, 0.35 mmol). This gave 4-{4''-fluoro-3''-[4'''-(3''''-bromonicotinoyl)piperazine-1'''-carbonyl]-4''-fluorobenzyl}-2*H*-phthalazin-1-one (**144**) as a yellow solid (0.074 g, 42%). Mp 130–133 °C; ν_{\max} (neat)/ cm^{-1} 3194 (NH), 2970 (CH), 1726 (CO), 1638 (CO), 1433, 1366, 1229; δ_{H} (400 MHz, CDCl_3) 3.31–3.46 (4H, m, $2 \times \text{NCH}_2$), 3.74–3.86 (4H, m, $2 \times \text{NCH}_2$), 4.31 (2H, s, 1'-H₂), 7.02–7.08 (1H, m, 5''-H), 7.25 (1H, br s, 2'''-H), 7.35–7.38 (2H, m, 2''-H and 6''-H), 7.47–7.51 (1H, m, 6'''-H), 7.73–7.78 (3H, m, 5-H, 6-H and 7-H), 8.41–8.49 (2H, m, 8-H and 5''''-H), 11.36 (1H, br s, NH); δ_{C} (101 MHz, CDCl_3) 37.6 (CH₂), 41.9 (CH₂), 42.3 (CH₂), 46.8 (CH₂), 47.4 (CH₂), 116.2 (d, $^2J_{\text{CF}}$ 24.1 Hz, CH), 123.3 (d, $^2J_{\text{CF}}$ 17.6 Hz, C), 125.0 (CH), 125.7 (CH), 127.2 (CH), 128.2 (C), 129.3 (d, $^3J_{\text{CF}}$ 3.5 Hz, CH), 129.5 (C), 131.7 (CH), 132.0 (d, $^3J_{\text{CF}}$ 8.1 Hz, CH), 133.7 (CH), 134.5 (d, $^4J_{\text{CF}}$ 3.4 Hz, C), 142.9 (C), 145.3 (C), 145.5 (CH), 150.8 (CH), 156.0 (C), 158.0 (d, $^1J_{\text{CF}}$ 250.0 Hz, C), 160.8 (C), 165.3 (C), 166.3 (C); m/z (ESI) 572.0686 (MNa^+ . $\text{C}_{26}\text{H}_{21}^{79}\text{BrFN}_5\text{NaO}_3$ requires 572.0704).

4-{4''-Fluoro-3''-[4'''-(4''''-bromonicotinoyl)piperazine-1'''-carbonyl]-4''-fluorobenzyl}-2H-phthalazin-1-one (146)



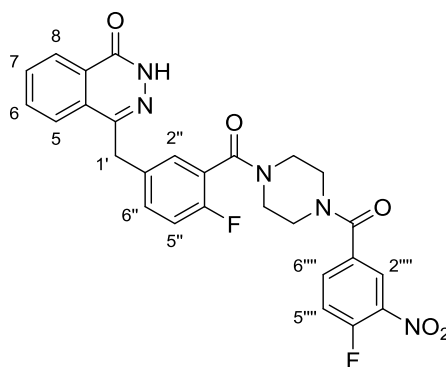
The reaction was carried out according to the previously described procedure for *tert*-butyl 4-{2'-fluoro-5'-[(4'''-oxo-3'''*H*-phthalazin-1'''-yl)methyl]benzoyl}piperazine-1-carboxylate (**138**) using 4-[4''-bromo-3''-(piperazine-1'''-carbonyl)benzyl]-2*H*-phthalazin-1-one (**131**) (0.10 g, 0.28 mmol) and 6-bromopyridine-3-carboxylic acid (0.050 g, 0.25 mmol). This gave 4-{4''-fluoro-3''-[4'''-(4''''-bromonicotinoyl)piperazine-1'''-carbonyl]-4''-fluorobenzyl}-2*H*-phthalazin-1-one (**146**) as a yellow solid (0.058 g, 41%). Mp 135–138 °C; ν_{\max} (neat)/ cm^{-1} 3025 (NH), 2970 (CH), 1730 (CO), 1600 (CO), 1428, 1228, 1002, 888; δ_{H} (400 MHz, CDCl_3) 3.33–3.80 (8H, m, $4 \times \text{NCH}_2$), 4.30 (2H, s, 1'- H_2), 7.02–7.08 (1H, m, 5''-H), 7.34–7.36 (2H, m, 2''-H and 6''-H), 7.56–7.64 (2H, m, 5'''-H and 6'''-H), 7.71–7.73 (1H, m, 5-H), 7.75–7.80 (2H, m, 6-H and 7-H), 8.43 (1H, s, 2''''-H), 8.46–8.48 (1H, m, 8-H), 11.07 (1H, s, NH); δ_{C} (101 MHz, CDCl_3) 37.8 (CH_2), 42.2 ($2 \times \text{CH}_2$), 47.2 ($2 \times \text{CH}_2$), 116.2 (d, $^2J_{\text{CF}}$ 22.7 Hz, CH), 123.3 (d, $^2J_{\text{CF}}$ 17.6 Hz, C), 125.0 (CH), 127.2 (CH), 128.3 (C), 128.4 (CH), 129.4 (d, $^3J_{\text{CF}}$ 3.2 Hz, CH), 129.5 (C), 130.0 (C), 131.7 (CH), 132.0 (d, $^3J_{\text{CF}}$ 8.1 Hz, CH), 133.7 (CH), 134.5 (d, $^4J_{\text{CF}}$ 3.6 Hz, C), 137.6 (CH), 143.9 (C), 145.5 (CH), 148.4 (C), 158.2 (d, $^1J_{\text{CF}}$ 250.0 Hz, C), 160.6 (C), 165.2 (C), 167.0 (C); m/z (ESI) 572.0731 (MNa^+ . $\text{C}_{26}\text{H}_{21}^{79}\text{BrFN}_5\text{NaO}_3$ requires 572.0704).

4-{3''-[4'''-(2''''-Fluoro-5''''-nitrobenzoyl)piperazine-1''''-carbonyl]-4''-fluorobenzyl}-2*H*-phthalazin-1-one (141)



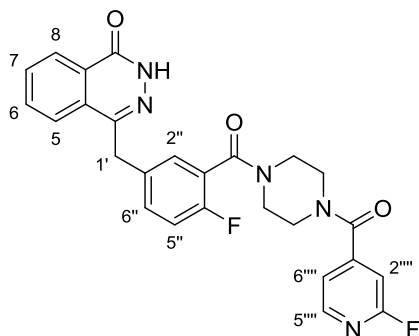
The reaction was carried out according to the previously described procedure for *tert*-butyl 4-{2'-fluoro-5'-[(4'''-oxo-3'''*H*-phthalazin-1''''-yl)methyl]benzoyl}piperazine-1-carboxylate (**138**) using 4-[4''-fluoro-3''-(piperazine-1''''-carbonyl)benzyl]-2*H*-phthalazin-1-one (**131**) (0.050 g, 0.14 mmol) and 2-fluoro-5-nitrobenzoic acid (0.028 g, 0.14 mmol). This gave 4-{3''-[4'''-(2''''-fluoro-5''''-nitrobenzoyl)piperazine-1''''-carbonyl]-4''-fluorobenzyl}-2*H*-phthalazin-1-one (**141**) as a yellow solid (0.042 g, 55%). Mp 140–142 °C; ν_{\max} (neat)/ cm^{-1} 3400 (NH), 2980 (CH), 1782 (CO), 1643 (CO), 1437, 1259, 1170, 1008; The compound exists as a 1.2:1 mixture of rotamers. Data for the major rotamer: δ_{H} (400 MHz, CDCl_3) 3.34–3.42 (8H, m, $4 \times \text{NCH}_2$), 4.31 (2H, s, 1- H_2), 7.08 (1H, t, J 8.6 Hz, 5''-H), 7.35–7.37 (3H, m, 2''-H, 6''-H and 3''''-H), 7.75–7.79 (3H, m, 4''''-H and $2 \times \text{ArH}$), 8.34–8.37 (2H, m, 6''''-H and ArH), 8.46 (1H, td, J 7.2, 1.6 Hz, 8-H), 10.88 (1H, s, NH); δ_{C} (101 MHz, CDCl_3) 37.7 (CH_2), 41.7 (CH_2), 42.1 (CH_2), 46.8 (CH_2), 47.3 (CH_2), 116.2 (d, $^2J_{\text{CF}}$ 22.4 Hz, CH), 117.3 (d, $^2J_{\text{CF}}$ 15.6 Hz, CH), 123.4 (d, $^2J_{\text{CF}}$ 17.6 Hz, C), 125.0 (d, $^3J_{\text{CF}}$ 7.9 Hz, CH), 125.8 (CH), 127.2 (d, $^3J_{\text{CF}}$ 2.6 Hz, CH), 127.4 (CH), 128.3 (C), 129.3 (d, $^3J_{\text{CF}}$ 3.2 Hz, CH), 129.5 (C), 131.7 (CH), 132.0 (d, $^3J_{\text{CF}}$ 7.5 Hz, CH), 133.7 (CH), 134.5 (d, $^4J_{\text{CF}}$ 3.7 Hz, C), 144.7 (d, $^2J_{\text{CF}}$ 11.8 Hz, C), 145.5 (C), 158.2 (d, $^1J_{\text{CF}}$ 249.2 Hz, C), 160.5 (C), 162.6 (d, $^1J_{\text{CF}}$ 252.0 Hz, C), 162.7 (C), 162.8 (C), 165.2 (C); m/z (ESI) 556.1393 (MNa^+ . $\text{C}_{27}\text{H}_{21}\text{F}_2\text{N}_5\text{NaO}_5$ requires 556.1403).

4-{3''-[4'''-(4''''-Fluoro-3''''-nitrobenzoyl)piperazine-1'''-carbonyl]-4''-fluorobenzyl}-2H-phthalazin-1-one (143)



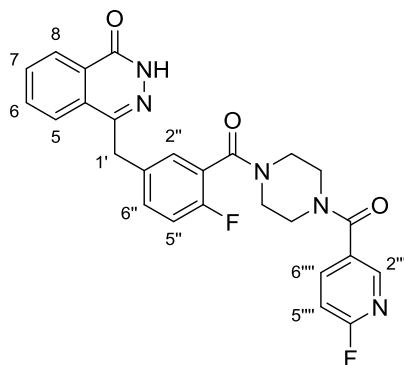
The reaction was carried out according to the previously described procedure for *tert*-butyl 4-{2'-fluoro-5'-[(4'''-oxo-3'''*H*-phthalazin-1'''-yl)methyl]benzoyl}piperazine-1-carboxylate (**138**) using 4-[4''-fluoro-3''-(piperazine-1'''-carbonyl)benzyl]-2*H*-phthalazin-1-one (**131**) (0.11 g, 0.30 mmol) and 4-fluoro-3-nitrobenzoic acid (0.050 g, 0.27 mmol). This gave 4-{3''-[4'''-(4''''-fluoro-3''''-nitrobenzoyl)piperazine-1'''-carbonyl]-4''-fluorobenzyl}-2*H*-phthalazin-1-one (**143**) as a yellow solid (0.069 g, 48%). Mp 143–146 °C; ν_{\max} (neat)/ cm^{-1} 2920 (NH), 2359 (CH), 1634 (CO), 1594, 1436, 1350, 1008, 811; δ_{H} (400 MHz, CDCl_3) 3.39–4.04 (8H, m, $4 \times \text{NCH}_2$), 4.30 (2H, s, 1'-H₂), 7.05–7.12 (1H, m, 5''-H), 7.35–7.38 (3H, m, 2''-H, 6''-H and 5''''-H), 7.71–7.80 (4H, m, 5-H, 6-H, 7-H and 6''''-H), 8.15 (1H, s, 2''''-H), 8.46 (1H, d, J 6.7 Hz, 8-H), 10.89 (1H, s, NH); δ_{C} (101 MHz, CDCl_3) 37.6 (CH_2), 42.0 ($2 \times \text{CH}_2$), 46.9 ($2 \times \text{CH}_2$), 116.2 (d, $^2J_{\text{CF}}$ 21.5 Hz, CH), 119.1 (d, $^2J_{\text{CF}}$ 21.4 Hz, CH), 123.3 (d, $^2J_{\text{CF}}$ 17.8 Hz, C), 125.0 (CH), 125.5 (d, $^3J_{\text{CF}}$ 2.4 Hz, CH), 127.2 (CH), 128.3 (C), 129.3 (d, $^3J_{\text{CF}}$ 2.8 Hz, CH), 129.5 (C), 131.7 (CH), 131.8 (d, $^4J_{\text{CF}}$ 4.7 Hz, C), 132.0 (d, $^3J_{\text{CF}}$ 8.1 Hz, CH), 133.7 (CH), 134.5 (d, $^4J_{\text{CF}}$ 2.8 Hz, C), 134.6 (CH), 137.2 (C), 145.5 (C), 157.3 (d, $^1J_{\text{CF}}$ 266.9 Hz, C), 158.0 (d, $^1J_{\text{CF}}$ 246.6 Hz, C), 160.5 (C), 165.2 (C), 167.0 (C); m/z (ESI) 556.1384 (MNa^+ . $\text{C}_{27}\text{H}_{21}\text{F}_2\text{N}_5\text{NaO}_5$ requires 556.1403).

4-{4''-Fluoro-3''-[4'''-(3''''-fluoronicotinoyl)piperazine-1'''-carbonyl]-4''-fluorobenzyl}-2H-phthalazin-1-one (145)



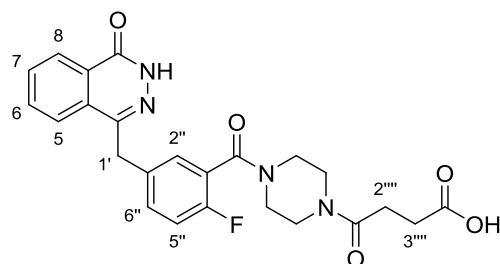
The reaction was carried out according to the previously described procedure for *tert*-butyl 4-{2'-fluoro-5'-[(4'''-oxo-3'''*H*-phthalazin-1'''-yl)methyl]benzoyl}piperazine-1-carboxylate (**138**) using 4-[4''-fluoro-3''-(piperazine-1'''-carbonyl)benzyl]-2*H*-phthalazin-1-one (**131**) (0.14 g, 0.39 mmol) and 2-fluoro-4-pyridinecarboxylic acid (0.050 g, 0.35 mmol). This gave 4-{4''-fluoro-3''-[4'''-(3''''-fluoronicotinoyl)piperazine-1'''-carbonyl]-4''-fluorobenzyl}-2*H*-phthalazin-1-one (**145**) as a yellow solid (0.074 g, 43%). Mp 128–134 °C; ν_{\max} (neat)/ cm^{-1} 3199 (NH), 2900 (CH), 1632 (CO), 1431, 1252, 1004, 727; δ_{H} (400 MHz, CDCl_3) 3.34–3.46 (4H, m, $2 \times \text{NCH}_2$), 3.75–3.88 (4H, m, $2 \times \text{NCH}_2$), 4.30 (2H, s, 1'-H₂), 6.93–7.08 (2H, m, 5''-H and 6''-H), 7.18 (1H, s, 2'''-H), 7.34–7.36 (2H, m, 2''-H and 6''-H), 7.73–7.78 (3H, m, 5-H, 6-H and 7-H), 8.29–8.34 (1H, m, 5''''-H), 8.46–8.48 (1H, m, 8-H), 11.29 (1H, s, NH); δ_{C} (101 MHz, CDCl_3) 37.6 (CH₂), 41.7 (CH₂), 42.3 (CH₂), 47.0 (CH₂), 47.5 (CH₂), 107.8 (d, $^2J_{\text{CF}}$ 36.7 Hz, CH), 116.3 (d, $^2J_{\text{CF}}$ 21.9 Hz, CH), 119.0 (d, $^4J_{\text{CF}}$ 4.3 Hz, CH), 123.3 (d, $^2J_{\text{CF}}$ 17.5 Hz, C), 125.0 (CH), 127.2 (CH), 128.3 (C), 129.3 (d, $^3J_{\text{CF}}$ 3.5 Hz, CH), 129.5 (C), 131.7 (CH), 132.0 (d, $^3J_{\text{CF}}$ 7.8 Hz, CH), 133.7 (CH), 134.6 (d, $^3J_{\text{CF}}$ 3.5 Hz, C), 145.5 (C), 148.2 (C), 148.8 (d, $^3J_{\text{CF}}$ 14.9 Hz, CH), 158.2 (d, $^1J_{\text{CF}}$ 250.0 Hz, C), 160.8 (C), 164.9 (d, $^1J_{\text{CF}}$ 245.6 Hz, C), 165.1 (C), 166.5 (C); m/z (ESI) 512.1487 (MNa⁺. C₂₆H₂₁F₂N₅NaO₃ requires 512.1505).

4-{4''-Fluoro-3''-[4''''-(4''''-fluoronicotinoyl)piperazine-1''''-carbonyl]-4''-fluorobenzyl}-2H-phthalazin-1-one (147)



The reaction was carried out according to the previously described procedure for *tert*-butyl 4-{2'-fluoro-5'-[(4''''-oxo-3''''*H*-phthalazin-1''''-yl)methyl]benzoyl}piperazine-1-carboxylate (**138**) using 4-[4''-fluoro-3''-(piperazine-1''''-carbonyl)benzyl]-2*H*-phthalazin-1-one (**131**) (0.114 g, 0.310 mmol) and 6-fluoropyridine-3-carboxylic acid (0.0400 g, 0.280 mmol). This gave 4-{4''-fluoro-3''-[4''''-(4''''-fluoronicotinoyl)piperazine-1''''-carbonyl]-4''-fluorobenzyl}-2*H*-phthalazin-1-one (**147**) as a white solid (0.0660 g, 48%). Mp 141–145 °C; ν_{\max} (neat)/cm⁻¹ 3227 (NH), 2866 (CH), 1637 (CO), 1612 (CO), 1435, 1288, 1011, 729; δ_{H} (400 MHz, CDCl₃) 3.38–3.82 (8H, m, 4 × NCH₂), 4.31 (2H, s, 1'-H₂), 7.00–7.07 (2H, m, 5''-H and 5''''-H), 7.33–7.35 (2H, m, 2''-H and 6''-H), 7.71–7.79 (3H, m, 5-H, 6-H and 7-H), 7.91 (1H, td, *J* 8.2, 2.2 Hz, 6''''-H), 8.32 (1H, br s, 2''''-H), 8.46–8.48 (1H, m, 8-H), 11.55 (1H, s, NH); δ_{C} (101 MHz, CDCl₃) 37.7 (CH₂), 42.1 (2 × CH₂), 47.0 (2 × CH₂), 110.0 (d, ²*J*_{CF} 36.1 Hz, CH), 116.2 (d, ²*J*_{CF} 23.3 Hz, CH), 123.4 (d, ²*J*_{CF} 18.8 Hz, C), 125.0 (CH), 127.2 (C), 128.3 (C), 128.9 (d, ⁴*J*_{CF} 4.7 Hz, C), 129.3 (d, ³*J*_{CF} 3.9 Hz, CH), 129.5 (C), 131.6 (CH), 131.9 (d ³*J*_{CF} 8.5 Hz, CH), 133.7 (CH), 134.5 (d, ⁴*J*_{CF} 3.4 Hz, C), 140.9 (d ³*J*_{CF} 8.7 Hz, CH), 145.5 (CH), 146.8 (d ³*J*_{CF} 15.5 Hz, CH), 158.2 (d ¹*J*_{CF} 250.0 Hz, C), 160.9 (C), 165.2 (C), 165.3 (d ¹*J*_{CF} 244.6 Hz, C), 167.0 (C); *m/z* (EI) 512.1487 (MNa⁺. C₂₆H₂₁F₂N₅NaO₃ requires 512.1505)

4-{3''-[4'''-(1''''-oxo-4''''-butanoic acid)-piperazine-1'''-carbonyl]-4''-fluorobenzyl}-2H-phthalazin-1-one (149)



4-[4''-Fluoro-3''-(piperazine-1'''-carbonyl)benzyl]-2H-phthalazin-1-one (**131**) (0.030 g, 0.080 mmol) and succinic anhydride (0.016 g, 0.16 mmol) were dissolved in acetonitrile (2 mL). 4-(Dimethylamino)pyridine (0.0010 g, 0.0080 mmol) was added and the mixture stirred for 24 hours at 80 °C. The solvent was removed *in vacuo* and the reaction mixture was diluted with a saturated aqueous solution of sodium bicarbonate (10 mL) and was washed with ethyl acetate (3 × 10 mL). The aqueous layer was acidified with an aqueous solution of 1 M hydrochloric acid and the product extracted with ethyl acetate (3 × 10 mL). The organic layers were combined, washed with brine (30 mL), dried (MgSO₄), filtered and concentrated *in vacuo*. Purification by flash column chromatography eluting with 10% methanol and 0.1% acetic acid in dichloromethane gave 4-{3''-[4'''-(1''''-oxo-4''''-butanoic acid)-piperazine-1'''-carbonyl]-4''-fluorobenzyl}-2H-phthalazin-1-one (**149**) as a white foam (0.037 g, 72%). Mp 200–205 °C; ν_{\max} (neat)/cm⁻¹ 3169 (NH/OH), 2922 (CH), 1782 (CO), 1636 (CO), 1439, 1247, 842; δ_{H} (400 MHz, CD₃OD) 2.57–2.61 (3H, m, 2''''-H₂ and 3''''-HH), 2.70 (1H, t, *J* 6.7 Hz, 3''''-HH), 3.27 (1H, br s, NCHH), 3.36 (1H, br s, NCHH), 3.51 (2H, t, *J* 5.0 Hz, NCH₂), 3.65–3.68 (2H, m, NCH₂), 3.73 (1H, t, *J* 5.0 Hz, NCHH), 3.81 (1H, t, *J* 5.0 Hz, NCHH), 4.38 (2H, s, 1'-H₂), 7.15 (1H, t, *J* 8.9 Hz, 5''-H), 7.37–7.39 (1H, m, 2''-H), 7.46–7.49 (1H, m, 6''-H), 7.82 (1H, t, *J* 7.7 Hz, 7-H), 7.87 (1H, t, *J* 7.7 Hz, 6-H), 7.94 (1H, m, 5-H), 8.36 (1H, d, *J* 7.7 Hz, 8-H); δ_{C} (101 MHz, CD₃OD) 27.5 (CH₂), 29.3 (CH₂), 36.8 (CH₂), 40.9 (CH₂), 41.8 (CH₂), 44.6 (CH₂), 46.5 (CH₂), 115.8 (d, ²*J*_{CF} 21.8 Hz, CH), 123.3 (d ²*J*_{CF} 18.5 Hz, C), 125.4 (CH), 126.1 (CH), 127.8 (C), 128.7 (d, ³*J*_{CF} 3.6 Hz, CH), 128.5 (C), 131.4 (CH), 132.0 (d, ³*J*_{CF} 8.1 Hz, CH), 133.6 (CH), 135.0 (d, ⁴*J*_{CF} 3.5 Hz, C), 146.3 (C), 158.2 (d, ¹*J*_{CF} 248.0 Hz, C), 160.9 (C), 165.9 (C), 166.0 (C), 171.6 (C); *m/z* (ESI) 489.1563 (MNa⁺. C₂₄H₂₃FN₄NaO₅ requires 489.1545).

6.5 Radioiododeboronation experimental

General experimental for radioiodination of aryl boronic acids with [125 I]NaI

Reductant free [125 I]NaI was purchased from Perkin Elmer (product number NEZ033H005MC) with a specific radioactivity of 643.8 GBq/mg in 0.1 M NaOH (pH 12–14) aqueous solution. All radiochemical yields were determined by radio-HPLC analysis of the crude product. Radiochemical yield refers to the amount of radioactive iodide converted into the desired product. Radioactivity yield refers to the isolated yield of radioactive product after purification.

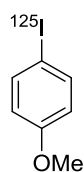
Analytical radio-HPLC method for determination of radioiodide incorporation

Analytical HPLC was performed with a Dionex Ultimate 3000 HPLC system equipped with a Flowstar LB 513 NaI scintillation detector and a DAD-3000 UV detector using a Synergi 4 μ m Hydro-RP 80 Å column (150 \times 4.6 mm) with 10 mm guard cartridge, UV 254 nm and flow 1 mL/min. The mobile phase for the analysis of substrates was water/acetonitrile. Analysis of the reaction mixture (to assess radioiodide incorporation) used a gradient profile of water and acetonitrile, as shown below.

Time (mins)	%MeCN
0–20	10–95
20–24	95
24–25	95–10
25–30	10

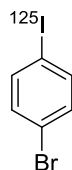
Co-elution with the UV signal from the 127 I-compound was used to confirm identity of the 125 I-product from each reaction described.

General method A for radioiodination: 4-[¹²⁵I]Iodoanisole (21)



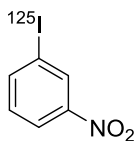
To a solution of *N*-chlorosuccinimide (0.50 mg, 3.9 μ mol) in dimethylcarbonate (0.1 mL) was added a 4–6 MBq solution of [¹²⁵I]NaI in water (0.01 mL). A solution of 4-methoxybenzeneboronic acid (0.60 mg, 3.9 μ mol) and Ph₃PAuNTf₂ (3.0 mg, 2.0 μ mol) in dimethylcarbonate (0.1 mL) was added and the reaction mixture heated to 90 °C for 20 minutes. The reaction mixture was then removed by syringe and diluted with a 1:1 mixture of acetonitrile and water (0.5 mL). Analysis of this solution by analytical radio-HPLC showed a radiochemical yield of 100%.

4-Bromo-[¹²⁵I]iodobenzene (154)



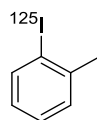
The reaction was carried out using 4-bromobenzeneboronic acid (0.60 mg, 3.0 μ mol) as described in general method A, except that the reaction was complete in 10 minutes. Analysis by radio-HPLC gave a radiochemical yield of 97%.

3-Nitro-[¹²⁵I]iodobenzene (155)



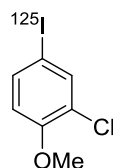
The reaction was carried out using 3-nitrobenzeneboronic acid (0.6 mg, 3.6 μ mol) as described in general procedure A. Analysis by radio-HPLC gave a radiochemical yield of 100%.

[¹²⁵I]Iodo-2-methylbenzene (156)



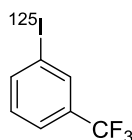
The reaction was carried out using 2-methylbenzeneboronic acid (0.60 mg, 4.4 μ mol) as described in general procedure A, except that the reaction was complete in 10 minutes. Analysis by radio-HPLC gave a radiochemical yield of 92%.

2-Chloro-4-[¹²⁵I]iodoanisole (157)



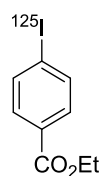
The reaction was carried out using 3-chloro-4-methoxybenzeneboronic acid (0.60 mg, 3.2 μ mol) as described in general procedure A. Analysis by radio-HPLC gave a radiochemical yield of 95%.

3-Trifluoromethyl-[¹²⁵I]iodobenzene (158)



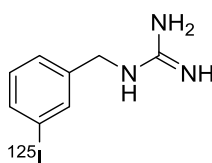
The reaction was carried out using 3-(trifluoromethyl)benzeneboronic acid (0.60 mg, 3.2 μ mol) as described in general procedure A, except that the reaction was heated to 80 °C for 30 minutes. Analysis by radio-HPLC gave a radiochemical yield of 94%.

Ethyl 4-[¹²⁵I]iodobenzoate (159)



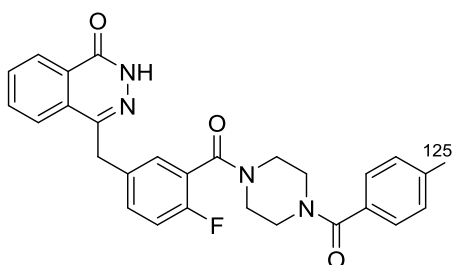
The reaction was carried out using 4-ethoxycarbonylbenzeneboronic acid (0.60 mg, 3.1 μ mol) as described in general procedure A, except that the reaction was heated to 80 °C for 30 minutes. Analysis by radio-HPLC gave a radiochemical yield of 100%.

N-(3-[¹²⁵I]iodobenzyl)guanidine (169)



The radio-iododeboronation reaction was carried out using {3-[2,3-bis(*tert*-butoxycarbonyl)guanidino]methylphenyl}boronic acid (**167**) (0.60 mg, 1.5 μ mol) as described in general procedure A, except that Ph₃PAuNTf₂ (2.3 mg, 1.5 μ mol) was used and the reaction was heated to 80 °C for 30 minutes. Analysis by radio-HPLC gave a radiochemical yield of 100% for *N*,*N*'-bis(*tert*-butoxycarbonyl)-*N*-3-[¹²⁵I]iodobenzylguanidine (**168**). Hydrochloric acid (0.2 mL) was added and the reaction mixture stirred at 90 °C for 20 minutes. Analysis by radio-HPLC gave a radiochemical yield of 97%.

4-{3'-[4''-(4'''-[¹²⁵I]iodobenzoyl)piperazine-1''-carbonyl]-4'-fluorobenzyl}-2*H*-phthalazin-1-one (120)



The reaction was carried out using 4-{3'-[4''-(benzoyl-4'''-boronic acid)piperazine-1''-carbonyl]-4'-fluorobenzyl}-2*H*-phthalazin-1-one (**162**) (0.60 mg, 1.2 μ mol) as described in general procedure A, except that Ph₃PAuNTf₂ (1.9 mg, 1.2 μ mol) was used and the

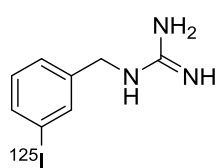
reaction was heated to 100 °C for 40 minutes. Analysis by radio-HPLC gave a radiochemical yield of 41%.

Semi-Preparative Radio-HPLC Method for Purification of *N*-(3-¹²⁵I)iodobenzyl)guanidine (169)

Semi-preparative HPLC was performed with a Dionex Ultimate 3000 HPLC system equipped with a Knauer Advanced Scientific Instruments Smartline UV Detector 2500, a photomultiplier tube (PMT) connected to a Lab Logic Flow-Count radiodetector and using a Synergi 4 µm Hydro-RP 80 Å column (150 × 10 mm, with 10 mm guard cartridge, UV 254 nm and flow 3 mL/min). A gradient profile of water and acetonitrile was used, as shown below.

Time (mins)	%MeCN
0–20	10–95
20–24	95
24–25	95–10
25–30	10

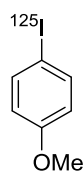
Synthesis and Purification of *N*-(3-¹²⁵I)iodobenzyl)guanidine (169)



To a solution of *N*-chlorosuccinimide (0.5 mg, 3.9 µmol, 1.0) in dimethylcarbonate (0.1 mL) was added a 10.16 MBq solution of [¹²⁵I]NaI in water (0.01 mL). A solution of {3-[2,3-bis(*tert*-butoxycarbonyl)guanidino]methylphenyl}boronic acid (0.6 mg, 1.5 µmol) and Ph₃PAuNTf₂ (2 mg, 1.5 µmol) in dimethylcarbonate (0.1 mL) was added and the reaction mixture heated to 80 °C for 30 minutes. Hydrochloric acid (0.2 mL) was added and the reaction was heated to 90 °C for 20 minutes. The mixture was diluted in a 1:1 mixture of acetonitrile and water (0.5 mL) and the crude product was purified by semi-preparative HPLC. The fraction containing *N*-(3-¹²⁵I)iodobenzyl)guanidine was evaporated to dryness, then reconstituted in 10.0% ethanol in 0.9% saline to afford *N*-(3-

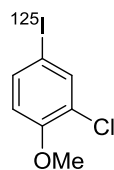
[¹²⁵I]iodobenzyl)guanidine (**169**) in 28% radioactivity yield (estimated using the measured radioactivity of the isolated product). The injected MIBG was below the UV detection limits and therefore the molar activity was calculated using the lowest concentration of *N*-(3-[¹²⁷I]iodobenzyl)guanidine which could be detected. Using this value, the molar activity was estimated to be greater than 2.73 GBq/μmol. The radiochemical purity of the final product was determined by analytical HPLC and was >98%. The identity of the product was confirmed by comparing the retention time of *N*-(3-[¹²⁵I]iodobenzyl)guanidine against the retention time *N*-(3-[¹²⁷I]iodobenzyl)guanidine.

General Method B for Radioiodination: 4-[¹²⁵I]Iodoanisole (**21**)



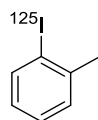
To a solution of *N*-chlorosuccinimide (1.8 mg, 13 μmol) in dimethylcarbonate (0.2 mL) was added a 4–6 MBq solution of [¹²⁵I]NaI in water (0.01 mL). After 20 minutes, a solution of 4-methoxybenzeneboronic acid (2.0 mg, 13 μmol) and potassium acetate (2.6 mg, 2.6 μmol) in dimethylcarbonate (0.2 mL) was added and the reaction mixture heated to 100 °C for 1.5 h. The reaction mixture was then removed by syringe and diluted with a 1:1 mixture of acetonitrile and water (0.5 mL). Analysis of this solution by analytical radio-HPLC showed a radiochemical yield of 93%.

2-Chloro-4-[¹²⁵I]iodoanisole (**157**)



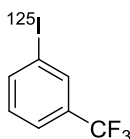
The reaction was carried out using 3-chloro-4-methoxybenzeneboronic acid (2.0 mg, 11 μmol) as described in general procedure B except that the reaction was complete after 2 h. Analysis by radio-HPLC gave a radiochemical yield of 95%.

[¹²⁵I]Iodo-2-methylbenzene (156)



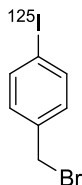
The reaction was carried out using 2-methylbenzeneboronic acid (2.0 mg, 9.0 μmol) as described in general procedure B except that the reaction was complete in 3 h. Analysis by radio-HPLC gave a radiochemical yield of 94%.

[¹²⁵I]Iodo-3-trifluoromethylbenzene (158)



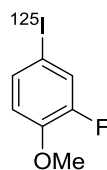
The reaction was carried out using 3-(trifluoromethyl)benzeneboronic acid (0.60 mg, 3.2 μmol) as described in general procedure B except that the reaction was complete in 3 h. Analysis by radio-HPLC gave a radiochemical yield of 61%.

4-[¹²⁵I]Iodobenzyl bromide (175)



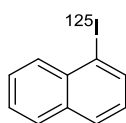
The reaction was carried out using 4-(bromomethyl)phenylboronic acid (2.0 mg, 6.8 μmol) as described in general procedure B except that the reaction was complete in 2.5 h. Analysis by radio-HPLC gave a radiochemical yield of 74%.

2-Fluoro-4-[¹²⁵I]iodoanisole (176)



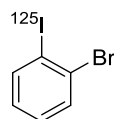
The reaction was carried out using 3-fluoro-4-methoxybenzeneboronic acid (2.0 mg, 12 μmol) as described in general procedure B except that the reaction was complete in 2.5 h. Analysis by radio-HPLC gave a radiochemical yield of 96%.

1-[¹²⁵I]iodonaphthalene (19)



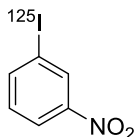
The reaction was carried out using naphthalene-1-boronic acid (2.0 mg, 8.0 μmol) as described in general procedure B except that the reaction was complete in 2.5 h. Analysis by radio-HPLC gave a radiochemical yield of 90%.

2-Bromo-[¹²⁵I]iodobenzene (177)



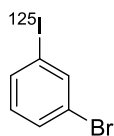
The reaction was carried out using 2-bromobenzeneboronic acid (2.0 mg, 7.0 μmol) as described in general procedure B except that the reaction was complete in 3 h. Analysis by radio-HPLC gave a radiochemical yield of 61%.

[¹²⁵I]iodo-3-nitrobenzene (155)



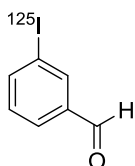
The reaction was carried out using 3-nitrobenzeneboronic acid (2.0 mg, 8.0 μmol) as described in general procedure B, except that acetonitrile (0.2 mL) was added and the reaction was complete after 2.5 h. Analysis by radio-HPLC gave a radiochemical yield of 92%.

3-Bromo-[¹²⁵I]iodobenzene (178)



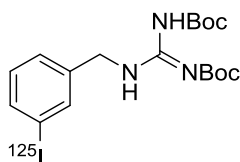
The reaction was carried out using 3-bromobenzeneboronic acid (2.0 mg, 7.0 μ mol) as described in general procedure B, except that acetonitrile (0.2 mL) was added and the reaction was complete after 3 h. Analysis by radio-HPLC gave a radiochemical yield of 72%.

3-[¹²⁵I]iodobenzaldehyde (179)



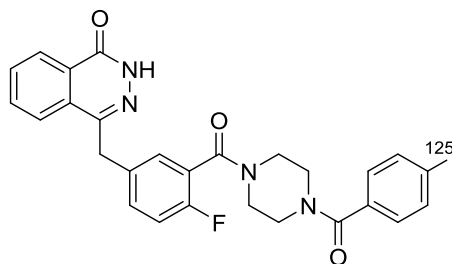
The reaction was carried out using 3-formylphenylboronic acid (2.0 mg, 9.0 μ mol) as described in general procedure B except that the reaction was complete in 3 h. Analysis by radio-HPLC gave a radiochemical yield of 15%.

N,N'-bis(*tert*-butoxycarbonyl)-*N''*-(3-[¹²⁵I]iodobenzyl)guanidine (168)



The reaction was carried out using {3-[2,3-bis(*tert*-butoxycarbonyl)guanidino]methylphenyl}boronic acid (**167**) (3.0 mg, 8.0 μ mol) as described in general procedure B, except that potassium acetate (0.4 mg, 4 μ mol) was added and the reaction was complete after 3.5 h. Analysis by radio-HPLC gave a radiochemical yield of 51%.

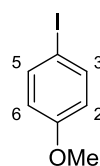
4-{3'-[4''-(4'''-[¹²⁵I]iodobenzoyl)piperazine-1''-carbonyl]-4'-fluorobenzyl}-2H-phthalazin-1-one (120)



The reaction was carried out using 4-{3'-[4''-(benzoyl-4'''-boronic acid)piperazine-1''-carbonyl]-4'-fluorobenzyl}-2H-phthalazin-1-one (**162**) (2 mg, 4 μ mol) as described in general procedure B, except that potassium acetate (0.4 mg, 4 μ mol) was added and the reaction was heated to 80 °C for 4 h. Analysis by radio-HPLC gave a radiochemical yield of 38%.

Experimental for ¹²⁷I compounds

4-Iodoanisole (21)¹⁰⁵

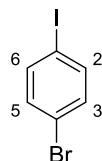


General procedure C: 4-Methoxybenzeneboronic acid (**153**) (0.050 g, 0.33 mmol) and *N*-iodosuccinimide (0.074 g, 0.33 mmol) were dissolved in dimethyl carbonate (1.5 mL) and Ph₃PAuNTf₂ (0.025 g, 0.017 mmol) was added. The mixture was stirred for 5 minutes at 90 °C. The crude mixture was passed through a silica plug and washed with 20:1 hexane/diethyl ether to give 4-iodoanisole (**21**) as a white solid (0.068 g, 88%). Mp 56–58 °C (lit.¹⁰⁵ 53–55 °C); δ_{H} (400 MHz, CDCl₃) 3.78 (3H, s, OCH₃), 6.68 (2H, d, *J* 6.8 Hz, 2-H and 6-H), 7.56 (2H, d, *J* 6.8 Hz, 3-H and 5-H); δ_{C} (101 MHz, CDCl₃) 55.5 (CH₃), 82.8 (C), 116.5 (2 \times CH), 138.3 (2 \times CH), 159.6 (C); *m/z* (EI) 234 (M⁺, 100%), 219 (29).

General procedure D: *N*-Chlorosuccinimide (0.044 g, 0.33 mmol) and sodium iodide (0.049 g, 0.33 mmol) were dissolved in dimethyl carbonate (1.5 mL) and stirred at room temperature for 10 minutes. 4-Methoxybenzeneboronic acid (**153**) (0.050 g, 0.33 mmol) and Ph₃PAuNTf₂ (0.025 g, 0.017 mmol) were added and the mixture was heated to 90 °C and stirred for 5 minutes. The crude mixture was passed through a silica plug and washed with 20:1 hexane/diethyl ether to give 4-iodoanisole (**21**) as a white solid (0.057 g, 74%).

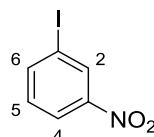
General procedure E: *N*-Chlorosuccinimide (0.029 g, 0.22 mmol) and sodium iodide (0.032 g, 0.22 mmol) were dissolved in dimethyl carbonate (1.5 mL) and stirred at room temperature for 10 minutes. 4-Methoxybenzeneboronic acid (**153**) (0.030 g, 0.20 mmol) and potassium acetate (0.002 g, 0.020 mmol) were added and the mixture stirred at 50 °C for 2 h. The crude mixture was passed through a silica plug and washed with 20:1 hexane/diethyl ether to give 4-iodoanisole (**21**) as a white solid (0.030 g, 65%).

4-Bromiodobenzene (154)¹⁰⁶



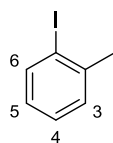
The reaction was carried out according to general procedure D using 4-bromobenzeneboronic acid (0.030 g, 0.15 mmol) and gave 4-bromiodobenzene (**154**) as a white solid (0.032 g, 75%). Mp 94–96 °C (lit.¹⁰⁶ 91–92 °C); δ_{H} (400 MHz, CDCl_3) 7.23 (2H, d, J 8.6 Hz, 2-H and 6-H), 7.54 (2H, d, J 8.6 Hz, 3-H and 5-H); δ_{C} (101 MHz, CDCl_3) 92.2 (C), 122.3 (C), 133.6 (2 \times CH), 139.2 (2 \times CH); m/z (EI) 282 (M^+ , 100%), 157 (35), 75 (40).

Iodo-3-nitrobenzene (155)¹⁰⁷



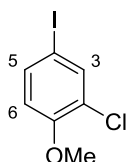
The reaction was carried out according to general procedure D using 3-nitrobenzeneboronic acid (0.015 g, 0.090 mmol) and gave iodo-3-nitrobenzene (**155**) as a yellow oil (0.010 g, 45%). Spectroscopic data were consistent with the literature.¹⁰⁷ δ_{H} (400 MHz, CDCl_3) 7.26 (1H, t, J 7.9 Hz, 5-H), 8.03 (1H, ddd, J 7.9, 1.9, 1.0 Hz, 6-H), 8.21 (1H, ddd, J 7.9, 1.9, 1.0 Hz, 4-H), 8.57 (1H, t, J 1.9 Hz, 2-H); δ_{C} (101 MHz, CDCl_3) 93.6 (C), 122.9 (CH), 130.8 (CH), 132.6 (CH), 143.6 (CH), 148.7 (C); m/z (EI) 249 (M^+ , 45%), 203 (20), 78 (80).

Iodo-2-methylbenzene (**156**)¹⁰⁸



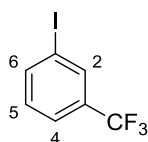
The reaction was carried out according to general procedure D using 2-methylbenzeneboronic acid (0.020 g, 0.10 mmol) and gave iodo-2-methylbenzene (**156**) as a yellow oil (0.011 g, 39 %). Spectroscopic data were consistent with the literature.¹⁰⁸ δ_{H} (400 MHz, CDCl_3) 2.44 (3H, s, 2- CH_3), 6.84–6.96 (1H, m, ArH), 7.23–7.25 (2H, m, ArH), 7.81 (1H, d, J 7.6 Hz, 6-H); δ_{C} (101 MHz, CDCl_3) 28.3 (CH_3), 101.3 (C), 127.5 (CH), 128.3 (CH), 129.9 (CH), 139.1 (CH), 141.5 (C); m/z (EI) 218 (M^+ , 48%), 234 (90).

2-Chloro-4-iodoanisole (**157**)¹⁰⁹



The reaction was carried out according to general procedure D using 3-chloro-4-methoxyphenylboronic acid (0.020 g, 0.11 mmol) and gave 2-chloro-4-iodoanisole (**157**) as a white solid (0.018 g, 62%). Mp 96–97 °C (lit.¹⁰⁹ 93–95 °C); δ_{H} (400 MHz, CDCl_3) 3.88 (3H, s, OCH_3), 6.68 (1H, d, J 8.6 Hz, 6-H), 7.51 (1H, dd, J 8.6, 2.2 Hz, 5-H), 7.65 (1H, d, J 2.2 Hz, 3-H); δ_{C} (101 MHz, CDCl_3) 56.3 (CH_3), 82.0 (C), 114.1 (CH), 123.9 (C), 136.7 (CH), 138.3 (CH), 155.2 (C); m/z (EI) 268 (M^+ , 100%), 253 (42), 225 (20).

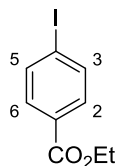
Iodo-3-trifluoromethylbenzene (**158**)¹¹⁰



The reaction was carried out according to general procedure D using 3-trifluoromethylbenzeneboronic acid (0.020 g, 0.11 mmol) and gave iodo-3-trifluoromethylbenzene (**158**) as a yellow oil (0.010 g, 33%).¹¹⁰ Spectroscopic data were consistent with the literature. δ_{H} (400 MHz, CDCl_3) 7.22 (1H, t, J 7.9 Hz, 5-H), 7.60 (1H, d, J 7.9 Hz, 4-H), 7.90 (1H, d, J 7.9 Hz, 6-H), 7.96 (1H, br s, 2-H); δ_{C} (101 MHz, CDCl_3) 94.0 (C), 124.6 (q, $^3J_{\text{CF}}$ 3.7 Hz, CH), 130.5 (CH), 132.8 (q, $^2J_{\text{CF}}$ 32.8 Hz, C), 134.4 (q, $^3J_{\text{CF}}$

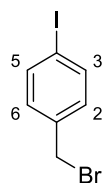
3.9 Hz, CH), 141.0 (q, $^4J_{\text{CF}}$ 1.1 Hz, CH) (signal for carbon directly attached to fluorine is not observed); m/z (EI) 272 (M^+ , 30%), 213 (60), 103 (25).

Ethyl 4-iodobenzoate (**159**)¹¹⁰



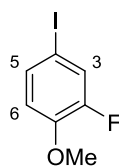
The reaction was carried out according to general procedure D using 4-ethoxycarbonylphenylboronic acid (0.020 g, 0.10 mmol) and gave ethyl 4-iodobenzoate (**159**) as a colourless oil (0.015 g, 54%). Spectroscopic data were consistent with the literature.¹¹⁰ δ_{H} (400 MHz, CDCl_3) 1.39 (3H, t, J 7.1 Hz, OCH_2CH_3), 4.36 (2H, q, J 7.1 Hz, OCH_2CH_3), 7.74 (2H, d, J 8.8 Hz, 3-H and 5-H), 7.80 (2H, d, J 8.8 Hz, 2-H and 6-H); δ_{C} (101 MHz, CDCl_3) 14.4 (CH_3), 61.4 (CH_2), 100.7 (C), 130.2 (C), 131.1 ($2 \times \text{CH}$), 137.9 ($2 \times \text{CH}$), 166.2 (C); m/z (EI) 276 (M^+ , 60%), 248 (30), 231 (90), 76 (50), 57 (55).

4-Iodobenzyl bromide (**175**)¹¹¹



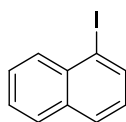
The reaction was carried out according to general procedure E using 4-(bromomethyl)phenylboronic acid (0.030 g, 0.14 mmol) and gave 4-iodobenzyl bromide (**175**) as a yellow solid (0.031 g, 75%). Mp 80–83 °C (lit.¹¹¹ 79–81 °C); δ_{H} (400 MHz, CDCl_3) 4.42 (2H, s, CH_2Br), 7.13 (2H, d, J 8.4 Hz, 2-H and 6-H), 7.67 (2H, d, J 8.4 Hz, 3-H and 5-H); δ_{C} (101 MHz, CDCl_3) 35.5 (CH_2), 94.1 (C), 130.8 ($2 \times \text{CH}$), 137.4 (C), 138.0 ($2 \times \text{CH}$); m/z (EI) 298 (M^+ , 20%), 217 (90), 84 (42).

2-Fluoro-4-iodoanisole (**176**)¹¹²



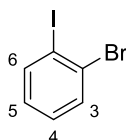
The reaction was carried out according to general procedure E using 3-fluoro-4-methoxybenzeneboronic acid (0.030 g, 0.18 mmol) and gave 2-fluoro-4-iodoanisole (**176**) as a white foam (0.032 g, 71%). Spectroscopic data were consistent with the literature.¹¹² δ_{H} (400 MHz, CDCl_3) 3.87 (3H, s, OCH_3), 6.71 (1H, t, J 8.4 Hz, 6-H), 7.36–7.40 (2H, m, 3-H and 5-H); δ_{C} (101 MHz, CDCl_3) 56.3 (CH_3), 80.9 (d, $^3J_{\text{CF}}$ 7.1 Hz, C), 115.2 (d, $^4J_{\text{CF}}$ 2.1 Hz, CH), 125.1 (d, $^2J_{\text{CF}}$ 20.4 Hz, CH), 133.3 (d, $^3J_{\text{CF}}$ 4.0 Hz, CH), 147.9 (d, $^2J_{\text{CF}}$ 10.3 Hz, C), 153.6 (d, $^1J_{\text{CF}}$ 251.2 Hz, C); m/z (EI) 252 (M^+ , 100%) 237 (41), 172 (25), 84 (45).

1-Iodonaphthalene (**19**)¹⁰⁷



The reaction was carried out according to general procedure E using naphthalene-1-boronic acid (0.030 g, 0.17 mmol) and gave 1-iodonaphthalene (**19**) as a yellow oil (0.019 g, 46%). Spectroscopic data were consistent with the literature.¹⁰⁷ δ_{H} (400 MHz, CDCl_3) 7.18 (1H, t, J 8.0 Hz, ArH), 7.52 (1H, td, J 8.0, 1.2 Hz, ArH), 7.57 (1H, td, J 8.0, 1.2 Hz, ArH), 7.77 (1H, d, J 8.0 Hz, ArH), 7.84 (1H, d, J 8.0 Hz, ArH), 8.09 (2H, d, J 8.0 Hz, ArH); δ_{C} (101 MHz, CDCl_3) 99.6 (C), 126.7 (CH), 126.9 (CH), 127.7 (CH), 128.6 (CH), 129.0 (CH), 132.1 (CH), 134.1 (C), 134.4 (C), 137.4 (CH); m/z (EI) 254 (M^+ , 100%), 127 (61), 62 (30).

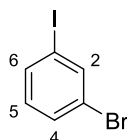
2-Bromiodobenzene (**177**)¹¹³



The reaction was carried out according to general procedure E using 2-bromobenzeneboronic acid (0.030 g, 0.15 mmol) and gave 2-bromiodobenzene (**177**) as a white foam (0.018 g, 43%). Spectroscopic data were consistent with the literature.¹¹³ δ_{H}

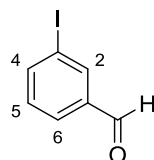
(400 MHz, CDCl₃) 7.00 (1H, td, *J* 7.8, 1.6 Hz, 5-H), 7.21 (1H, td, *J* 7.8, 1.6 Hz, 4-H), 7.63 (1H, dd, *J* 7.8, 1.6 Hz, 6-H), 7.87 (1H, dd, *J* 7.8, 1.6 Hz, 3-H); δ_{C} (101 MHz, CDCl₃) 101.1 (C), 128.4 (CH), 129.4 (CH), 132.8 (CH), 139.3 (C), 140.4 (CH); *m/z* (EI) 282 (M⁺, 15%), 84 (85), 66 (95).

3-Bromiodobenzene (**178**)¹¹⁴



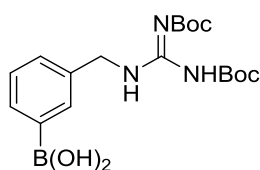
The reaction was carried out according to general procedure E using 3-bromobenzeneboronic acid (0.030 g, 0.15 mmol) and gave 3-bromiodobenzene (**178**) as a white foam (0.019 g, 45%). Spectroscopic data were consistent with the literature.¹¹⁴ δ_{H} (400 MHz, CDCl₃) 6.97 (1H, t, *J* 8.0 Hz, 5-H), 7.47 (1H, ddd, *J* 8.0, 1.7, 0.9 Hz, 6-H), 7.63 (1H, ddd, *J* 8.0, 1.7, 0.9 Hz, 4-H), 7.87 (1H, t, *J* 1.7 Hz, 2-H); δ_{C} (101 MHz, CDCl₃) 94.5 (C), 123.1 (C), 130.8 (CH), 131.3 (CH), 136.1 (CH), 139.7 (CH); *m/z* (EI) 284 (M⁺, 52%), 78 (80), 62 (95).

3-Iodobenzaldehyde (**179**)¹¹⁵



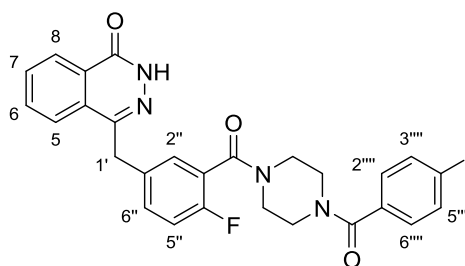
The reaction was carried out according to general procedure E using 3-formylphenylboronic acid (0.030 g, 0.20 mmol) and gave 3-iodobenzaldehyde as a yellow solid (0.030 g, 65%). Mp 59–61 °C (lit.¹¹⁵ 55–57 °C); δ_{H} (400 MHz, CDCl₃) 7.29 (1H, t, *J* 7.8 Hz, 5-H), 7.84 (1H, dt, *J* 7.8, 1.2 Hz, 4-H), 7.96 (1H, ddd, *J* 7.8, 1.6, 1.2 Hz, 6-H), 8.21 (1H, t, *J* 1.6 Hz, 2-H), 9.93 (1H, s, CHO); δ_{C} (101 MHz, CDCl₃) 94.6 (C), 128.9 (CH), 130.7 (CH), 138.0 (C), 138.4 (CH), 143.2 (CH), 190.7 (C); *m/z* (EI) 232 (M⁺, 100%), 77 (30), 51 (22).

{3-[2,3-Bis(*tert*-butoxycarbonyl)guanidino]methylphenyl}boronic acid (167)⁹⁶



N,N'-Bis(*tert*-butoxycarbonyl)-1*H*-pyrazole-1-carboxamide (**166**) (0.050 g, 0.16 mmol) and 3-(aminomethyl)benzeneboronic acid hydrochloride (**165**) (0.033 mg, 0.18 mmol) were dissolved in methanol (5 mL). Triethylamine (0.10 mL, 0.48 mmol) was added and the mixture stirred for 12 h at room temperature. The solvent was removed *in vacuo* and the crude material was purified by flash column chromatography, eluting with 50% ethyl acetate in petroleum ether to give {3-[2,3-bis(*tert*butoxycarbonyl)guanidino]methylphenyl}boronic acid (**167**) as a yellow solid (0.047 g, 75%). Mp 111–113 °C. Spectroscopic data were consistent with the literature.⁹⁶ δ_{H} (400 MHz, CD₃OD) 1.47 (9H, s, O^tBu), 1.50 (9H, s, O^tBu), 4.55 (2H, s, CH₂), 7.29–7.39 (2H, m, 2 × ArH), 7.53–7.75 (2H, m, 2 × ArH); δ_{C} (101 MHz, CD₃OD) 26.9 (3 × CH₃), 27.2 (3 × CH₃), 44.2 (CH₂), 79.1 (C), 83.2 (C), 127.6 (CH), 128.8 (d, ³*J*_{C-B} 50.2 Hz, CH), 132.6 (d, ²*J*_{C-B} 39.3 Hz, 2 × CH), 136.5 (CH), 152.8 (C), 156.1 (C), 163.2 (C) (signal for carbon directly attached to boron is not observed); *m/z* (ESI) 394 (MH⁺, 20%).

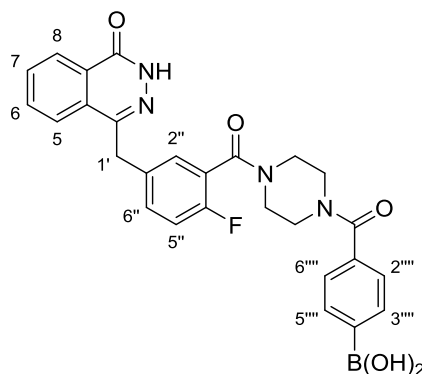
4-{3'-[4''-(4'''-iodobenzoyl)piperazine-1'''-carbonyl]-4''-fluorobenzyl}-2*H*-phthalazin-1-one (120)⁸⁵



The reaction was carried out according to the previously described procedure for *tert*-butyl 4-{2'-fluoro-5'-[(4'''-oxo-3'''H-phthalazin-1'''-yl)methyl]benzoyl}piperazine-1-carboxylate (**138**) using 4-[4''-fluoro-3''-(piperazine-1'''-carbonyl)benzyl]-2*H*-phthalazin-1-one (**131**) (0.30 g, 0.082 mmol) and 4-iodobenzoic acid (0.028 g, 0.074 mmol). This gave 4-[3'-[4''-(4'''-iodobenzoyl)piperazine-1'''-carbonyl]-4''-fluorobenzyl]-2*H*phthalazin-1-one (**120**) as a white foam (0.015 g, 34%). Spectroscopic data were consistent with the literature.⁸⁵ δ_{H} (400 MHz, CDCl₃) 3.14–4.02 (8H, m, 4 × NCH₂), 4.28 (2H, s, 1'-H₂), 7.04

(1H, t, J 7.8 Hz, 5''-H), 7.14 (2H, d, J 8.0 Hz, 3''''-H and 5''''-H), 7.29–7.37 (2H, m, 2''-H and 6''-H), 7.67–7.84 (5H, m, 5-H, 6-H, 7-H, 2''''-H and 6''''-H), 8.42–8.51 (1H, m, 8-H), 10.96 (1H, br s, NH); δ_c (101 MHz, CDCl₃) 37.7 (CH₂), 42.1 (2 × CH₂), 47.1 (2 × CH₂), 96.6 (C), 116.2 (d, $^2J_{CF}$ 21.7 Hz, CH), 123.6 (d, $^2J_{CF}$ 17.7 Hz, C), 125.0 (CH), 127.2 (CH), 128.4 (C), 128.9 (2 × CH), 129.3 (d, $^3J_{CF}$ 3.6 Hz, CH), 129.5 (C), 131.7 (CH), 131.9 (d, $^3J_{CF}$ 8.0 Hz, CH), 133.7 (CH), 134.4 (C), 134.6 (d, $^4J_{CF}$ 3.7 Hz, C), 137.9 (2 × CH), 145.5 (C), 157.1 (d, $^1J_{CF}$ 247.1 Hz, C), 160.4 (C), 165.2 (C), 169.7 (C); m/z (ESI) 619.0597 (MNa⁺. C₂₇H₂₂FIN₄NaO₃ requires 619.0613).

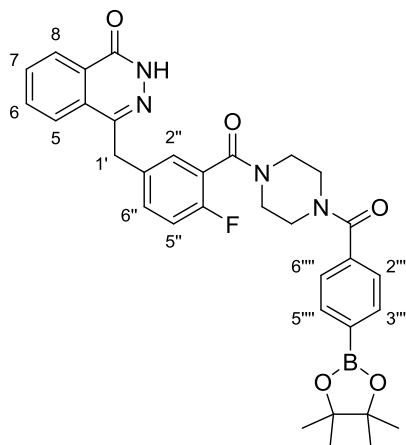
4-{3''-[4''-(Benzoyl-4''''-boronic acid)piperazine-1'''-carbonyl]-4''-fluorobenzyl}-2H-phthalazin-1-one (162)



The reaction was carried out according to the previously described procedure for *tert*-butyl 4-{2'-fluoro-5'-[(4''''-oxo-3''''H-phthalazin-1'''-yl)methyl]benzoyl}piperazine-1-carboxylate (**138**) using 4-[4''-fluoro-3''-(piperazine-1'''-carbonyl)benzyl]-2H-phthalazin-1-one (**131**) (0.11 g, 0.30 mmol) and 4-carboxyphenylboronic acid (**161**) (0.050, 0.30 mmol). This gave 4-{3''-[4''-(benzoyl-4''''-boronic acid)piperazine-1'''-carbonyl]-4''-fluorobenzyl}-2H-phthalazin-1-one (**162**) as a white solid (0.050 g, 33%). Mp 166–168 °C; ν_{max} (neat)/cm⁻¹ 3017 (NH), 2970 (CH), 1740 (CO), 1729 (CO), 1366, 1229, 1217; δ_H (400 MHz, CD₃OD) 3.46–3.82 (8H, m, 4 × NCH₂), 4.37 (2H, s, 1'-H₂), 6.84 (2H, d, J 7.5 Hz, 3''''-H and 5''''-H), 7.15 (1H, t, J 8.8 Hz, 5''-H), 7.31 (2H, d, J 7.5 Hz, 2''''-H and 6''''-H), 7.36 (1H, d, J 6.1 Hz, 6''-H), 7.45–7.50 (1H, m, 2''-H), 7.80 (1H, t, J 7.8 Hz, 7-H), 7.85 (1H, t, J 7.8 Hz, 6-H), 7.93 (1H, d, J 7.8 Hz, 5-H), 8.35 (1H, d, J 7.8 Hz, 8-H); δ_C (101 MHz, CD₃OD) 29.4 (2 × CH₂), 36.8 (CH₂), 41.7 (2 × CH₂), 114.9 (2 × CH), 115.8 (d, $^2J_{CF}$ 21.8 Hz, CH), 123.2 (d, $^2J_{CF}$ 17.1 Hz, C), 125.3 (C), 125.4 (CH), 126.1 (CH), 127.9 (C), 128.7 (d, $^3J_{CF}$ 3.8 Hz, CH), 129.1 (2 × CH), 129.5 (C), 131.4 (CH), 132.0 (d, $^3J_{CF}$ 8.0 Hz, CH), 133.6 (CH), 135.0 (d, $^4J_{CF}$ 3.8 Hz, C), 146.2 (C), 157.0 (d, $^1J_{CF}$ 247.2 Hz, C),

159.6 (C), 160.9 (C), 165.9 (C), 171.8 (C); m/z (ESI) 537.1718 (MNa^+ . $C_{27}H_{24}BFN_4NaO_5$ requires 537.1716).

4-{3''-[4'''-(Benzoyl-4''''-boronic acid pinacol ester)piperazine-1'''-carbonyl]-4''-fluorobenzyl}-2H-phthalazin-1-one (164)¹¹⁶



The reaction was carried out according to the previously described procedure for *tert*-butyl 4-{2'-fluoro-5'-[(4'''-oxo-3'''H-phthalazin-1'''-yl)methyl]benzoyl}piperazine-1-carboxylate (**138**) using 4-[4''-fluoro-3''-(piperazine-1'''-carbonyl)benzyl]-2H-phthalazin-1-one (**131**) (0.13 g, 0.35 mmol) and 4-carboxylphenylboronic acid pinacol ester (**163**) (0.80 g, 0.32 mmol). This gave 4-{3''-[4'''-(benzoyl-4''''-boronic acid pinacol ester)piperazine-1'''-carbonyl]-4''-fluorobenzyl}-2H-phthalazin-1-one (**164**) as a yellow solid (0.078 g, 50%). Mp 278–282 °C (lit.¹¹⁶ 288–291 °C); δ_H (400 MHz, $CDCl_3$) 1.35 (12H, s, 4 \times $OCCH_3$), 3.09–3.88 (8H, m, 4 \times NCH_2), 4.30 (2H, s, 1'- H_2), 7.03 (1H, br s, 5''-H), 7.33–7.42 (4H, m, 2''-H, 6''-H, 3''''-H and 5''''-H), 7.69–7.89 (5H, m, 5-H, 6-H, 7-H, 2''''-H and 6''''-H), 8.49 (1H, br s, 8-H), 11.25 (1H, br s, NH); δ_C (101 MHz, $CDCl_3$) 24.9 (4 \times CH_3), 37.7 (CH_2), 42.2 (2 \times CH_2), 47.1 (2 \times CH_2), 84.1 (2 \times C), 116.2 (d, $^2J_{CF}$ 21.5 Hz, CH), 123.6 (d, $^2J_{CF}$ 17.2 Hz, C), 125.0 (C), 126.2 (2 \times CH), 127.2 (CH), 128.3 (CH), 129.2 (d, $^3J_{CF}$ 3.2 Hz, CH), 129.5 (C), 131.6 (CH), 131.7 (d, $^3J_{CF}$ 7.8 Hz, CH), 133.7 (CH), 134.5 (d, $^4J_{CF}$ 3.3 Hz, C), 135.0 (2 \times CH), 137.5 (C), 145.5 (C), 158.2 (d, $^1J_{CF}$ 249.0 Hz, C), 160.7 (C), 165.2 (C), 170.5 (C) (signal for carbon directly attached to boron is not observed); m/z (ESI) 619.2483 (MNa^+ . $C_{33}H_{34}BFN_4NaO_5$ requires 619.2499).

7. References

- 1 S. L. Pimlott and A. Sutherland, *Chem. Soc. Rev.*, 2011, **40**, 149–162.
- 2 L. Zhu, K. Ploessl and H. F. Kung, *Science.*, 2013, **342**, 429–430.
- 3 M. J. Adam and D. S. Wilbur, *Chem. Soc. Rev.*, 2005, **34**, 153–163.
- 4 S. M. Ametamey, M. Honer and P. A. Schubiger, *Chem. Rev.*, 2008, **108**, 1501–1516.
- 5 S. Purser, P. R. Moore, S. Swallow and V. Gouverneur, *Chem. Soc. Rev.*, 2008, **37**, 320–330.
- 6 P. J. H. Scott, *Angew. Chem. Int. Ed.*, 2009, **48**, 6001–6004.
- 7 O. Jacobson, D. O. Kiesewetter and X. Chen, *Bioconjug. Chem.*, 2014, **26**, 1–18.
- 8 P. W. Miller, N. J. Long, R. Vilar and A. D. Gee, *Angew. Chem. Int. Ed.*, 2008, **47**, 8998–9033.
- 9 S. E. Snyder, L. Tluczek, D. M. Jewett, T. B. Nguyen, D. E. Kuhl and M. R. Kilbourn, *Nucl. Med. Biol.*, 1998, **25**, 751–754.
- 10 Y. Huang and R. Narendran, *J. Med. Chem.*, 2005, **48**, 5096–5099.
- 11 L. Samuelsson and B. Långström, *J. Label. Compd. Radiopharm.*, 2003, **46**, 263–272.
- 12 E. D. Hostetler, G. E. Terry and H. D. Burns, *J. Label. Compd. Radiopharm.*, 2005, **48**, 629–634.
- 13 S. Preshlock, M. Tredwell and V. Gouverneur, *Chem. Rev.*, 2016, **116**, 719–766.
- 14 D. O. Antuganov, M. P. Zykov, D. V Ryzhkova, T. A. Zykova, A. A. Vinal'ev, Y. O. Antuganova and O. P. Samburov, *Radiochemistry*, 2016, **58**, 649–653.
- 15 K. Hamacher, H. H. Coenen and G. Stocklin, *J. Nucl. Med.*, 1986, **27**, 235–239.
- 16 K. Hamacher and H. H. Coenen, *Appl. Radiat. Isot.*, 2006, **64**, 989–994.
- 17 L. Cai, S. Lu and V. W. Pike, *Eur. J. Org. Chem.*, 2008, **2008**, 2853–2873.
- 18 M.-R. Zhang, K. Kumata and K. Suzuki, *Tetrahedron Lett.*, 2007, **48**, 8632–8635.

- 19 M. U. Akbar, M. R. Ahmad, A. Shaheen and S. Mushtaq, *J. Radioanal. Nucl. Chem.*, 2016, **310**, 477–493.
- 20 S. L. Pimlott, L. Stevenson, D. J. Wyper and A. Sutherland, *Nucl. Med. Biol.*, 2008, **35**, 537–542.
- 21 A. A. Cant, S. Champion, R. Bhalla, S. L. Pimlott and A. Sutherland, *Angew. Chem. Int. Ed.*, 2013, **52**, 7829–7832.
- 22 J. Merrington and M. Bradley, *Chem. Commun.*, 2002, 140–141.
- 23 M. Caldarelli, I. R. Baxendale and S. V. Ley, *Green Chem.*, 2000, **2**, 43–46.
- 24 N. L. Sloan, S. K. Luthra, G. McRobbie, S. L. Pimlott and A. Sutherland, *Chem. Commun.*, 2017, **53**, 11008–11011.
- 25 H. Ito, R. Goto, M. Koyama, R. Kawashima, S. Ono, K. Sato and H. Fukuda, *Eur. J. Nucl. Med.*, 1996, **23**, 782–791.
- 26 K. Erlandsson, R. A. Bressan, R. S. Mulligan, R. N. Gunn, V. J. Cunningham, J. Owens, D. Wyper, P. J. Ell and L. S. Pilowsky, *Nucl. Med. Biol.*, 2003, **30**, 441–454.
- 27 M.-P. Kung, Z.-P. Zhuang, C. Hou and H. F. Kung, *J. Mol. Neurosci.*, 2004, **24**, 49–53.
- 28 W. C. Eckelman, M. R. Kilbourn and C. A. Mathis, *Nucl. Med. Biol.*, 2006, **33**, 449–451.
- 29 C. A. Lipinski, F. Lombardo, B. W. Dominy and P. J. Feeney, *Adv. Drug Deliv. Rev.*, 2001, **46**, 3–26.
- 30 S. D. Nelson, *Curr. Ther. Res.*, 2001, **62**, 885–899.
- 31 S. H. Isaacson, S. Fisher, F. Gupta, N. Hermanowicz, D. E. Kremens, M. F. Lew, K. Marek, R. Pahwa, D. S. Russell and J. Seibyl, *Expert Rev. Neurother.*, 2017, **17**, 219–225.
- 32 S. Colloby, J. Fenwick, *Arch. Neurol.*, 2004, **61**, 919–925.
- 33 S. D. Shorvon, *Epilepsia*, 2011, **52**, 1052–1057.
- 34 W. Löscher, H. Klitgaard, R. E. Twyman and D. Schmidt, *Nat. Rev. Drug Discov.*,

- 2013, **12**, 757.
- 35 D. M. Treiman, *Epilepsia*, 2001, **42**, 8–12.
- 36 M. Mantegazza, G. Curia, G. Biagini, D. S. Ragsdale and M. Avoli, *Lancet Neurol.*, 2010, **9**, 413–424.
- 37 C. E. Stafstrom, *Epilepsy Curr.*, 2007, **7**, 15–22.
- 38 S. M. Cain and T. P. Snutch, *Channels*, 2010, **4**, 475–482.
- 39 M. A. Rogawski, *Acta. Neurol. Scand. Suppl.*, 2015, **197**, 9–18.
- 40 S. Pati and A. V. Alexopoulos, *Cleve. Clin. J. Med.*, 2010, **77**, 457–467.
- 41 W. Löscher and C. Brandt, *Epilepsia*, 2009, **51**, 89–97.
- 42 S. Wiebe and N. Jette, *Nat. Rev. Neurol.*, 2012, **8**, 669–677.
- 43 W. L. Ramey, N. L. Martirosyan, C. M. Lieu, H. A. Hasham, G. M. Lemole and M. E. Weinand, *Clin. Neurol. Neurosurg.*, 2013, **115**, 2411–2418.
- 44 D. Spencer and K. Burchiel, *Epilepsy Res. Treat.*, 2012, **2012**, 382095.
- 45 Y. K. Kim, ; Dong, S. Lee, ; Sang, K. Lee, ; Chun, K. Chung, J.-K. Chung and M. C. Lee, *J. Nucl. Med.*, 2002, **43**, 1167–1174.
- 46 F. Lauritzen, N. C. de Lanerolle, T. S. W. Lee, D. D. Spencer, J. H. Kim, L. H. Bergersen and T. Eid, *Neurobiol. Dis.*, 2011, **41**, 577–584.
- 47 M. E. Morris and M. A. Felmler, *AAPS J.*, 2008, **10**, 311–321.
- 48 T. Fukao, G. Mitchell, J. O. Sass, T. Hori, K. Orii and Y. Aoyama, *J. Inherit. Metab. Dis.*, 2014, **37**, 541–551.
- 49 A. P. Halestrap and M. C. Wilson, *IUBMB Life*, 2011, **64**, 109–119.
- 50 F. Lauritzen, N. C. de Lanerolle, T. S. W. Lee, D. D. Spencer, J. H. Kim, L. H. Bergersen and T. Eid, *Neurobiol. Dis.*, 2011, **41**, 577–584.
- 51 F. Lauritzen, T. Eid and L. H. Bergersen, *Brain Struct. Funct.*, 2015, **220**, 1–12.
- 52 P. Sonveaux, F. Végran, T. Schroeder, M. C. Wergin, J. Verrax, Z. N. Rabbani, C. J. De Saedeleer, K. M. Kennedy, C. Diepart, B. F. Jordan, M. J. Kelley, B. Gallez, M.

- L. Wahl, O. Feron and M. W. Dewhirst, *J. Clin. Invest.*, 2008, **118**, 1–13.
- 53 J. S. Erlichman, A. Hewitt, T. L. Damon, M. Hart, J. Kuraszcz, A. Li and J. C. Leiter, *J. Neurosci.*, 2008, **28**, 4888–4896.
- 54 S. Gurrapu, S. K. Jonnalagadda, M. A. Alam, G. L. Nelson, M. G. Sneve, L. R. Drewes and V. R. Mereddy, *ACS Med. Chem. Lett.*, 2015, **6**, 558–561.
- 55 A. P. Halestrap, *Biochem. J.*, 1976, **156**, 193–207.
- 56 A. P. Halestrap and R. M. Denton, *Biochem. J.*, 1974, **138**, 313–316.
- 57 H. Wang, C. Yang, J. R. Doherty, W. R. Roush, J. L. Cleveland and T. D. Bannister, *J. Med. Chem.*, 2014, **57**, 7317–7324.
- 58 S. D. Guile, J. R. Bantick, D. R. Cheshire, M. E. Cooper, A. M. Davis, D. K. Donald, R. Evans, C. Eyssade, D. D. Ferguson, S. Hill, R. Hutchinson, A. H. Ingall, L. P. Kingston, I. Martin, B. P. Martin, R. T. Mohammed, C. Murray, M. W. D. Perry, R. H. Reynolds, P. V. Thorne, D. J. Wilkinson and J. Withnall, *Bioorg. Med. Chem. Lett.*, 2006, **16**, 2260–2265.
- 59 M. J. Ovens, C. Manoharan, M. C. Wilson, C. M. Murray and A. P. Halestrap, *Biochem. J.*, 2010, **431**, 217–225.
- 60 M. J. Ovens, A. J. Davies, M. C. Wilson, C. M. Murray and A. P. Halestrap, *Biochem. J.*, 2010, **425**, 523–530.
- 61 S. D. Guile, J. R. Bantick, M. E. Cooper, D. K. Donald, C. Eyssade, A. H. Ingall, R. J. Lewis, B. P. Martin, R. T. Mohammed, T. J. Potter, R. H. Reynolds, S. A. St-Gallay and A. D. Wright, *J. Med. Chem.*, 2007, **50**, 254–263.
- 62 C. M. Murray, R. Hutchinson, J. R. Bantick, G. P. Belfield, A. D. Benjamin, D. Brazma, R. V. Bundick, I. D. Cook, R. I. Craggs, S. Edwards, L. R. Evans, R. Harrison, E. Holness, A. P. Jackson, C. G. Jackson, L. P. Kingston, M. W. D. Perry, A. R. J. Ross, P. A. Rugman, S. S. Sidhu, M. Sullivan, D. A. Taylor-Fishwick, P. C. Walker, Y. M. Whitehead, D. J. Wilkinson, A. Wright and D. K. Donald, *Nat. Chem. Biol.*, 2005, **1**, 371–376.
- 63 J. Bantick, M. Cooper, M. Perry, P. Thorne, 2001, US6300334
- 64 H. Ogura, M. Sakaguchi and K. Takeda, *Chem. Pharm. Bull.*, 1972, **20**, 404–408.

- 65 L. Stevenson, A. A. S. Tavares, A. Brunet, F. I. McGonagle, D. Dewar, S. L. Pimlott and A. Sutherland, *Bioorg. Med. Chem. Lett.*, 2010, **20**, 954–957.
- 66 I. M. Lagoja, C. Pannecouque, A. Van Aerschot, M. Witvrouw, Z. Debyser, J. Balzarini, P. Herdewijn and E. De Clercq, *J. Med. Chem.*, 2003, **46**, 1546–1553.
- 67 A. A. S. Tavares, J. Lewsey, D. Dewar and S. L. Pimlott, *Nucl. Med. Biol.*, 2012, **39**, 127–135.
- 68 P. Jolliet-Riant and J. P. Tillement, *Fundam. Clin. Pharmacol.*, 1999, **13**, 16–26.
- 69 R. N. Waterhouse, *Mol. Imaging Biol.*, 2003, **5**, 376–389.
- 70 A. Leo, C. Hansch and D. Elkins, *Chem. Rev.*, 1971, **71**, 525–616.
- 71 C. Pidgeon, S. Ong, H. Liu, X. Qiu, M. Pidgeon, A. H. Dantzig, J. Munroe, W. J. Homback, J. S. Kasher, L. Glunz and T. Szczerba, *J. Med. Chem.*, 1995, **38**, 590–594.
- 72 C. Y. Yang, S. J. Cai, H. Liu and C. Pidgeon, *Adv. Drug Deliv. Rev.*, 1997, **23**, 229–256.
- 73 B. P. Martin, M. E. Cooper, D. K. Donald and S. D. Guile, *Tetrahedron Lett.*, 2006, **47**, 7635–7639.
- 74 Z. Wang, F. Wang, T. Tang and C. Guo, *Front. Med.*, 2012, **6**, 156–164.
- 75 A. N. Weaver and E. S. Yang, *Front. Oncol.*, 2013, **3**, 1–11.
- 76 L. T. Gien and H. J. Mackay, *J. Oncol.*, 2010, 151750.
- 77 D. V. Ferraris, *J. Med. Chem.*, 2010, **53**, 4561–4584.
- 78 K. A. Menear, C. Adcock, R. Boulter, X. Cockcroft, L. Copsey, A. Cranston, K. J. Dillon, J. Drzewiecki, S. Garman, S. Gomez, H. Javaid, F. Kerrigan, C. Knights, A. Lau, V. M. Loh, I. T. W. Matthews, S. Moore, M. J. O. Connor, G. C. M. Smith and N. M. B. Martin, *J. Med. Chem.*, 2008, **51**, 6581–6591.
- 79 S. Mabuchi, T. Sugiyama and T. Kimura, *J. Gynecol. Oncol.*, 2016, **27**, e31.
- 80 E. D. Deeks, *Drugs*, 2015, **75**, 231–240.
- 81 R. Plummer, C. Jones, M. Middleton, R. Wilson, J. Evans, A. Olsen, N. Curtin, A.

- Boddy, P. Mchugh, D. Newell, A. Harris, P. Johnson, H. Steinfeldt, R. Dewji, D. Wang and L. Robson, *J. Clin. Oncol.*, 2009, **14**, 7917–7923.
- 82 O. A. Khan, M. Gore, P. Lorigan, J. Stone, A. Greystoke, W. Burke, J. Carmichael, A. J. Watson, G. McGown, M. Thorncroft, G. P. Margison, R. Califano, J. Larkin, S. Wellman and M. R. Middleton, *Br. J. Cancer*, 2011, **104**, 750–755.
- 83 A. Galia, A. E. Calogero, R. Condorelli, F. Fraggetta, A. La Corte, F. Ridolfo, P. Bosco, R. Castiglione and M. Salemi, *Eur. J. Histochem.*, 2012, **56**, 45–48.
- 84 Z. Tu, W. Chu, J. Zhang, C. S. Dence, M. J. Welch and R. H. Mach, *Nucl. Med. Biol.*, 2005, **32**, 437–443.
- 85 F. Zmuda, G. Malviya, A. Blair, M. Boyd, A. J. Chalmers, A. Sutherland and S. L. Pimlott, *J. Med. Chem.*, 2015, **58**, 8683–8693.
- 86 F. Zmuda, A. Blair, M. C. Liuzzi, G. Malviya, A. J. Chalmers, D. Lewis, A. Sutherland and S. L. Pimlott, *J. Med. Chem.*, 2018, **61**, 4103–4114.
- 87 G. Carlucci, B. Carney, C. Brand, S. Kossatz, C. P. Irwin, S. D. Carlin, E. J. Keliher, W. Weber and T. Reiner, *Mol. Imaging Biol.*, 2015, **17**, 848–855.
- 88 C. Pascali, S. K. Luthra, V. W. Pike, G. W. Price, R. G. Ahier, S. P. Hume, R. Myers, L. Manjil and J. E. Cremer, *Appl. Radiat. Isot.*, 1990, **41**, 477–482.
- 89 T. Reiner, E. J. Keliher, S. Earley, B. Marinelli, R. Weissleder, *Angew. Chem. Int. Ed.*, 2011, **50**, 1922–1925.
- 90 J. H. J. Hoeijmakers, *N. Engl. J. Med.*, 2009, **361**, 1475–1485.
- 91 J. He, C. Yang and Z. Miao, *Acta. Pharmacol. Sin.*, 2010, **31**, 1172–1180.
- 92 K. A. Menear, C. Adcock, R. Boulter, X. Cockcroft, L. Copsey, A. Cranston, K. J. Dillon, J. Drzewiecki, S. Garman, S. Gomez, H. Javaid, F. Kerrigan, C. Knights, A. Lau, V. M. Loh, I. T. W. Matthews, S. Moore, M. J. O'Connor, G. C. M. Smith and N. M. B. Martin, *J. Med. Chem.*, 2008, **51**, 6581–6591.
- 93 T. Reiner, S. Earley, A. Turetsky and R. Weissleder, *ChemBioChem*, 2010, **11**, 2374–2377.
- 94 M. Tredwell, S. M. Preshlock, N. J. Taylor, S. Gruber, M. Huiban, J. Passchier, J.

- Mercier, C. Génicot and V. Gouverneur, *Angew. Chem. Int. Ed.*, 2014, **53**, 7751–7755.
- 95 C. Thiebes, G. K. S. Prakash, N. A. Petasis and G. A. Olah, *Synlett*, 1998, 141–142.
- 96 P. Zhang, R. Zhuang, Z. Guo, X. Su, X. Chen and X. Zhang, *Chem. Eur. J.*, 2016, **22**, 16783–16786.
- 97 G. Barker, S. Webster, D. G. Johnson, R. Curley, M. Andrews, P. C. Young, S. A. MacGregor and A. L. Lee, *J. Org. Chem.*, 2015, **80**, 9807–9816.
- 98 D. V. Partyka, M. Zeller, A. D. Hunter and T. G. Gray, *Angew. Chem. Int. Ed.*, 2006, **45**, 8188–8191.
- 99 N. Mézailles, L. Ricard and F. Gagosz, *Org. Lett.*, 2005, **7**, 4133–4136.
- 100 C. M. Alder, J. D. Hayler, R. K. Henderson, A. M. Redman, L. Shukla, L. E. Shuster and H. F. Sneddon, *Green Chem.*, 2016, **18**, 3879–3890.
- 101 S. Webster, K. M. O'Rourke, C. Fletcher, S. L. Pimlott, A. Sutherland and A. L. Lee, *Chem. Eur. J.*, 2018, **24**, 937–943.
- 102 H. Zhang, *Eur. J. Nucl. Med. Mol. Imaging.*, 2014, **46**, 220–231.
- 103 G. A. Molander and L. N. Cavalcanti, *J. Org. Chem.*, 2011, **76**, 7195–7203.
- 104 L. Niu, H. Zhang, H. Yang and H. Fu, *Synlett*, 2014, **25**, 995–1000.
- 105 M. E. Trusova, E. A. Krasnokutskaya, P. S. Postnikov, Y. Choi, K. W. Chi and V. D. Filimonov, *Synthesis*, 2011, 2154–2158.
- 106 G. M. K. E. B. Merkushev, N. D. Simakhinam, *Synthesis*, 1980, 486–487.
- 107 X. H. Liu, J. Leng, S. J. Jia, J. H. Hao, F. Zhang, H. L. Qin and C. P. Zhang, *J. Fluor. Chem.*, 2016, **189**, 59–67.
- 108 G. J. P. Perry, J. M. Quibell, A. Panigrahi and I. Larrosa, *J. Am. Chem. Soc.*, 2017, **139**, 11527–11536.
- 109 W. M. Ned D. Heindel, H. Donald Burns, *Synthesis*, 1980, 572–573.
- 110 W. Liu, X. Yang, Y. Gao and C. J. Li, *J. Am. Chem. Soc.*, 2017, **139**, 8621–8627.

- 111 S. Y. Cheung, H. F. Chow, T. Ngai and X. Wei, *Chem. Eur. J.*, 2009, **15**, 2278–2288.
- 112 Y. Malysheva, S. Combes, A. Fedorov, P. Knochel and A. Gavryushin, *Synlett*, 2012, **23**, 1205–1208.
- 113 J. N. Moorthy, K. Senapati and S. Kumar, *J. Org. Chem.*, 2009, **74**, 6287–6290.
- 114 M. Jiang, H. Yang, Y. Jin, L. Ou, H. Fu, *Synlett*, 2018, **29**, 1572–1577.
- 115 V. D. Filimonov, N. I. Semenischeva, E. A. Krasnokutskaya, Y. H. Ho and K. W. Chi, *Synthesis*, 2008, 401–404.
- 116 D. Zhou, W. Chu, T. Voller and J. A. Katzenellenbogen, *Tetrahedron Lett.*, 2018, **59**, 1963–1967.

8. Appendix

8.1 Radio-HPLC and UV/Vis HPLC chromatograms

The following chromatograms were obtained by analytical radio-HPLC (blue) of the reaction mixtures following radioiodination of the corresponding boronic acids. Overlays of the UV/Vis HPLC traces (black) of the unlabelled products are also shown.

